

SEISMIC STRENGTHENING OF A  
MID-RISE REINFORCED CONCRETE FRAME  
USING CFRPs: AN APPLICATION FROM REAL LIFE

A THESIS SUBMITTED TO  
THE GRADUATE SCHOOL OF NATURAL AND APPLIED SCIENCES  
OF  
MIDDLE EAST TECHNICAL UNIVERSITY

BY

MUSTAFA TÜMER TAN

IN PARTIAL FULFILLMENT OF THE REQUIREMENTS  
FOR  
THE DEGREE OF MASTER OF SCIENCE  
IN  
CIVIL ENGINEERING

MAY 2009

Approval of the thesis:

**SEISMIC STRENGTHENING OF A  
MID-RISE REINFORCED CONCRETE FRAME  
USING CFRPs: AN APPLICATION FROM REAL LIFE**

submitted by **MUSTAFA TÜMER TAN** in partial fulfillment of the requirements  
for the degree of **Master of Science in Civil Engineering Department, Middle  
East Technical University** by,

Prof. Dr. Canan Özgen \_\_\_\_\_  
Dean, Graduate School of Natural and Applied Sciences

Prof. Dr. Güney Özcebe \_\_\_\_\_  
Head of Department, Civil Engineering

Prof. Dr. Güney Özcebe \_\_\_\_\_  
Supervisor, Civil Engineering Dept., METU

Assoc. Prof. Dr. Barış Binici \_\_\_\_\_  
Co-Supervisor, Civil Engineering Dept., METU

**Examining Committee Members**

Assoc. Prof. Dr. Erdem Canbay \_\_\_\_\_  
Civil Engineering Dept., METU

Prof. Dr. Güney Özcebe \_\_\_\_\_  
Civil Engineering Dept., METU

Assoc. Prof. Dr. Barış Binici \_\_\_\_\_  
Civil Engineering Dept., METU

Assist. Prof. Dr. Özgür Kurç \_\_\_\_\_  
Civil Engineering Dept., METU

M.S. Joseph Kubin \_\_\_\_\_  
PROTA Bilgisayar

Date: \_\_\_\_\_ / 06 / 2009

**I hereby declare that all information in this document has been obtained and presented in accordance with academic rules and ethical conduct. I also declare that, as required by these rules and conduct, I have fully cited and referenced all material and results that are not original to this work.**

Name, Last name: Mustafa Tümer TAN

Signature:

## ABSTRACT

### SEISMIC STRENGTHENING OF A MID-RISE REINFORCED CONCRETE FRAME USING CFRPs: AN APPLICATION FROM REAL LIFE

Tan, Mustafa Tümer

M.S., Department Of Civil Engineering

Supervisor: Prof. Dr. Güney Özcebe

Co-Supervisor: Assoc. Prof. Dr. Barış Binici

May 2009, 162 pages

FRP retrofitting allows the utilization of brick infill walls as lateral load resisting elements. This practical retrofit scheme is a strong alternative to strengthen low to mid-rise deficient reinforced concrete (RC) structures in Turkey. The advantages of the FRP applications, to name a few, are the speed of construction and elimination of the need for building evacuation during construction. In this retrofit scheme, infill walls are adopted to the existing frame system by using FRP tension ties anchored the boundary frame using FRP dowels. Results of experiments have previously shown that FRP strengthened infill walls can enhance lateral load carrying capacity and reduce damage by limiting interstory drift deformations. In previous, analytical studies, a detailed mathematical model and a simplified version of the model for compression struts and tension ties was proposed and verified by comparing model estimations with test results.

In this study, an existing 9-storey deficient RC building located in Antakya was chosen to design and apply a hybrid strengthening scheme with FRPs and reduced number of shear walls. Linear elastic analysis procedure was utilized

(force based assessment technique) along with the rules of Mode Superposition Method for the retrofit design. FRP retrofit scheme was employed using the simplified model and design was conducted such that life safety performance criterion is satisfied employing elastic spectrum with 10% probability of exceedance in 50 years according to the Turkish Earthquake Code 2007. Further analytical studies are performed by using Modal Pushover and Nonlinear Time-History Analyses. At the end of these nonlinear analyses, performance check is performed according to Turkish Earthquake Code 2007, using the strains resulting from the sum of yield and plastic rotations at demand in the critical sections.

CFRP retrofitting works started at October 2008 and finished at December 2008 for the building mentioned in this study. Eccentric reinforced concrete shearwall installation is still being undertaken. All construction business is carried out without evacuation of the building occupants. This project is one of the first examples of its kind in Turkey.

Keywords: CFRP, Carbon Fiber Reinforced Polymers, Masonry Infill Walls, Reinforced Concrete Infill Walls, Mid-Rise Deficient Structures, Turkish Earthquake Code 2007, Modal Pushover Analysis, Nonlinear Time History Analysis, Linear Elastic Building Assessment

## ÖZ

### ORTA-KATLI BİR BETONARME BİNANIN LİFLİ KARBON POLİMERLERİ KULLANILARAK GÜÇLENDİRİLMESİ: GERÇEK HAYATTAN BİR UYGULAMA

Tan, Mustafa Tümer

Yüksek Lisans, İnşaat Mühendisliği Bölümü

Tez Yöneticisi: Prof. Dr. Güney Özcebe

Ortak Tez Yöneticisi: Doç. Dr. Barış Binici

Mayıs 2009, 162 sayfa

Lifli karbon polimerleri (LP) ile yapılan güçlendirme, tuğla dolgu duvarların da yapı içerisinde yanal yük taşıyıcı elemanlar olarak kullanılmasını sağlamaktadır. Bu pratik güçlendirme yöntemi, az-katlı ve orta-katlı yetersiz betonarme binaların depreme karşı güçlendirilmelerinde göz ardı edilmemesi gereken bir alternatiftir. LP ile yapılan güçlendirmelerin avantajları arasında imalat hızı ve yapı boşaltımına ihtiyaç bulunmaması sayılabilir. LP ile güçlendirilen dolgu duvarlar sisteme çekme ve basınç çubukları oluşturacak şekilde entegre edilir. Bu çekme ve basınç çubukları LP ankrajlar ile mevcut çerçeve sistemine tutturulur. Bu konuda daha önce yapılan deneyler, LP ile güçlendirilen tuğla dolgu duvarların sistem genelinde yanal yük kapasitesini artırdığını ve göreceli ötelenmeyi azaltarak hasarı önlediğini göstermiştir.

Daha önceki analitik çalışmalar sonucunda, çekme ve basınç çubukları için detaylı matematiksel modeller ve basitleştirilmiş tasarım modelleri oluşturulmuş ve bu modeller deney sonuçları ile karşılaştırılmıştır.

Bu çalışmada, Antakya’da bulunan 9 katlı mevcut bir betonarme bina seçilmiştir. LP ile güçlendirilmiş tuğla dolgu duvarlar ve sayıca azaltılmış dış merkezli betonarme perdeler kullanılarak karma bir güçlendirme uygulaması gerçekleştirilmiştir. LP ile güçlendirilmiş tuğla dolgu duvarlar, basitleştirilmiş tasarım formülleri kullanılarak modellenmiştir. 2007 Türk Deprem Yönetmeliği’ne göre 50 yılda %10 aşılma olasılığına sahip elastik spektrum kullanılarak mod birleştirme analizi gerçekleştirilmiştir. Can güvenliği performans kriterleri gözönüne alınarak kuvvet tabanlı doğrusal elastik bina değerlendirmesi yöntemi uygulanmıştır. Doğrusal elastik olmayan analitik çalışmalar çok modlu artımsal itme ve zaman tanım alanında hesaplar yapılarak gerçekleştirilmiştir. Doğrusal olmayan analizlerin sonucunda da yine 2007 Türk Deprem Yönetmeliği can güvenliği performans kriterlerine göre istem anındaki plastik dönmeler ve akma dönmelerinin toplamından yola çıkılarak kritik kesitler içindeki birim şekil değiştirmelere dayalı performans değerlendirmesi yapılmıştır.

Bu çalışmada özet olarak verilen güçlendirme projesi halihazırda uygulanma aşamasındadır. Ekim 2008’de başlayan güçlendirme çalışmalarının LP uygulama aşaması Aralık 2008 itibarı ile tamamlanmış olup halen dışardan perde duvar uygulama işlemleri devam etmektedir. Türkiye’de bir ilke imza atılan bu çalışma süresince bina sakinlerinin binayı boşaltmasına gerek kalmadan güçlendirme çalışmalarına devam edilmektedir.

Anahtar Kelimeler: LP, Lifli Karbon Polimerleri, Tuğla Dolgu Duvarlar, Betonarme Dolgu Duvarlar, Orta-Katlı Yetersiz Binalar, 2007 Türk Deprem Yönetmeliği, Çok Modlu Artımsal İtme Analizi, Zaman-Tanım alanında doğrusal olmayan analiz, Elastik Bina Değerlendirme Yöntemi

To my family

## **ACKNOWLEDGEMENTS**

This study was performed under the supervision of Prof. Dr. Güney Özcebe and co-supervision of Assoc. Prof. Dr. Barış Binici. I would like to express my sincere appreciation for their support, guidance, insights and great patience throughout the study. I am glad to get the chance of working with them in such a project.

Joseph Kubin is highly acknowledged for his tremendous tolerance as an employer, attitude as a friend and technical guidance as a very knowledgeable engineer. Also, Yasin Fahjan deserves thanks for the advices and friendship he provided.

Thanks go to Cihat Mazmanoğlu, Ali Hoca and Hakan Uslu for their unquestionably warm hospitality and complimentary helps.

My all friends; they really were at the right place at the right time when I needed.

And finally my family; their precious presence was always the real reason and motivation for me. Thank you very much.

This study was conducted under the financial support of NATO.

ARTYOL Engineering and YKS Companies are also acknowledged for their valuable support.

# TABLE OF CONTENTS

ABSTRACT .....	iv
ÖZ .....	vi
ACKNOWLEDGEMENTS .....	ix
TABLE OF CONTENTS .....	x
LIST OF TABLES .....	xiii
LIST OF FIGURES .....	xv
CHAPTERS	
1 INTRODUCTION	
1.1. GENERAL .....	1
1.2. PREVIOUS STUDIES .....	2
1.3. OBJECTIVE AND SCOPE .....	8
2 ANALYSIS AND ASSESSMENT PROCEDURES IN 2007 TURKISH EARTHQUAKE CODE	
2.1. INTRODUCTION .....	10
2.2. LINEAR ELASTIC ANALYSIS AND FORCE BASED ASSESSMENT PROCEDURE .....	10
2.2.1. Modelling Considerations for Linear Elastic Analysis .....	14
2.2.2. Equivalent Static Earthquake Load Analysis .....	14
2.2.3. Mode Superposition Analysis .....	16
2.2.4. Force Based Assessment Details .....	17
2.3. NONLINEAR ANALYSIS AND DISPLACEMENT BASED ASSESSMENT PROCEDURE .....	20
2.3.1. Modelling Considerations for Pushover Analysis According	

	to Turkish Earthquake Code .....	20
2.3.2.	Static Pushover Analysis.....	23
2.3.3.	Modal Pushover Analysis .....	24
2.3.4.	3D Nonlinear Time History Analysis.....	26
2.3.5.	Simplified Procedure for 3D Nonlinear Time History Analysis.....	28
2.3.6.	Earthquake Record Selection Criteria in Turkish Earthquake Code 2007 .....	30
2.3.7.	Turkish Earthquake Code 2007 Nonlinear Assessment Procedure .....	31
<b>3</b>	<b>CFRP MODELLING AND APPLICATION</b>	
3.1.	STRUCTURAL BEHAVIOR .....	36
3.2.	MATHEMATICAL MODEL.....	36
3.3.	TEC 2007 CONSIDERATIONS .....	41
3.5.	APPLICATION DETAILS .....	43
<b>4</b>	<b>ANALYZED STRUCTURE</b>	
4.1.	GENERAL INFORMATION ABOUT BUILDING AND STRUCTURAL SYSTEM.....	47
4.2.	EXISTING MATERIAL AND SOIL CONDITIONS.....	50
4.3.	MODELLING .....	51
4.4.	ANALYSIS AND ASSESSMENT OF BUILDING USING LINEAR ELASTIC METHOD .....	52
4.4.1.	Existing Building .....	52
4.4.2.	Retrofitting with Eccentric Reinforced Concrete Shearwalls and CFRP.....	54

4.5.	ANALYSIS AND ASSESSMENT OF THE BUILDING USING NONLINEAR MODAL PUSHOVER METHOD .....	59
4.5.1.	General .....	59
4.5.2.	Existing Building .....	60
4.5.3.	Retrofitted Building .....	80
4.6.	ANALYSIS AND ASSESSMENT OF THE BUILDING USING SIMPLIFIED NONLINEAR TIME HISTORY ANALYSIS .....	100
4.6.1.	Existing Building .....	100
4.6.1.	Retrofitted Building .....	122
5	SUMMARY AND CONCLUSION .....	140
	REFERENCES .....	144
	APPENDIX A .....	147
	APPENDIX B .....	149
	APPENDIX C .....	154
	APPENDIX D .....	157

## LIST OF TABLES

### TABLES

Table 2.1	Required seismic performance levels for design earthquakes .....	12
Table 2.2	Performance Criteria .....	18
Table 2.3	DCR Limit Ratios for Reinforced Concrete Ductile Beams.....	19
Table 2.4	DCR Limit Ratios for Reinforced Concrete Ductile Columns.....	19
Table 2.5	DCR Limit Ratios for Reinforced Concrete Ductile Walls .....	19
Table 2.6	DCR Limit Ratios for Strengthened Masonry Infill Walls.....	20
Table 2.7	Interstorey Drift Ratio Limits .....	20
Table 4.1	Storey and Section Information for the structure .....	49
Table 4.2	Elastic Modal Characteristics of Existing Building .....	53
Table 4.3	Modal Characteristics of Building Retrofitted with Reinforced Concrete Shearwalls and CFRP strengthened masonry infill walls.....	56
Table 4.4	Existing building: Capacity Curve for Mode 1 .....	61
Table 4.5	Existing building: Performance Point for Mode 1 .....	61
Table 4.6	Existing building: Capacity Curve for Mode 2 .....	62
Table 4.7	Existing building: Performance Point for Mode 2 .....	63
Table 4.8	Existing building: Performance Point for Mode 3 .....	63
Table 4.9	Existing building: Capacity Curve for Mode 3 .....	64
Table 4.10	Retrofitted building: Capacity Curve for Mode 1 .....	83
Table 4.11	Retrofitted building: Performance Point for Mode 1 .....	83
Table 4.12	Retrofitted building: Capacity Curve for Mode 2 .....	84
Table 4.13	Retrofitted building: Performance Point for Mode 2 .....	84
Table 4.14	Retrofitted building: Capacity Curve for Mode 3 .....	85
Table 4.15	Retrofitted building: Performance Point for Mode 3 .....	85
Table 4.16	Selected Earthquakes for Soil Class Z2 to be used in time history analysis .....	103
Table B.1	Example Calculation of Compression Strut and	

	Tension Tie Properties according to TEC 2007 .....	149
Table C.1	Quantity Take-off: CFRP strengthened wall D1X .....	154
Table C.2	Quantity Take-off: CFRP strengthened wall D2X .....	154
Table C.3	Quantity Take-off: CFRP strengthened wall D3X .....	155
Table C.4	Quantity Take-off: CFRP strengthened wall D1Y .....	155
Table C.5	Quantity Take-off: CFRP strengthened wall D2Y .....	156

## LIST OF FIGURES

### FIGURES

Figure 2.1	Generalized Flowchart for Linear Elastic Assessment Procedure ...	11
Figure 2.2	Damage Levels and Performance Boundaries for ductile members.....	13
Figure 2.3	TEC 2007 Spectra for different performance levels .....	15
Figure 2.4	Moment Rotation relationships suggested by TEC 2007.....	21
Figure 2.5	Bilinearization of Moment-Curvature diagram .....	22
Figure 2.6	Typical flowchart for modal pushover analysis .....	25
Figure 2.7	Obtaining load deformation relationship for each storey.....	29
Figure 2.8	Establishing 2D nonlinear model for time history analysis .....	30
Figure 2.9	Comparison of code spectrum with derived spectrum .....	31
Figure 2.10	Calculation of Inelastic Demand .....	33
Figure 3.1	Analytical Model of CFRP retrofitted Masonry Infill Wall .....	37
Figure 3.2	Masonry Infill Wall Parameters .....	37
Figure 3.3	Analytical and Simplified models for Compression and Tension ties .....	38
Figure 3.4	Axial Plastic Hinge representing the masonry infill wall retrofitted with CFRP .....	40
Figure 3.5	Application of CFRP on the masonry infill wall.....	43
Figure 3.6	Shop drawing for masonry infill wall .....	45
Figure 3.7	Frame anchor dowel and surface anchor details.....	45
Figure 3.8	Surface anchors.....	46
Figure 4.1	Earthquake Zones of Turkey (1996) .....	47
Figure 4.2	Existing State of the building Front and Rear View .....	48
Figure 4.3	Typical Floor Plan of the existing building .....	49
Figure 4.4	TEC 2007 Elastic Spectrum for Soil Type Z2.....	50
Figure 4.5	Solid Rendered Model of Existing Building.....	51
Figure 4.6	Analytical Model Of Existing Building .....	52

Figure 4.7	Existing Building X Direction Assessment Summary .....	53
Figure 4.8	Existing Building Y Direction Assessment Summary .....	54
Figure 4.9	Adding Eccentric Shearwall adjacent to existing frame .....	55
Figure 4.10	Typical Storey Plan, RC shearwalls are anchored from outside of the building.....	56
Figure 4.11	Assessment results for X Direction (Eccentric Shearwalls) .....	57
Figure 4.12	Assessment results for Y Direction (Eccentric Shearwalls) .....	57
Figure 4.13	Drift Ratio profile for Existing and Retrofitted building after elastic analysis.....	58
Figure 4.14	Existing Building: Deformed Shape and hinge formation.....	60
Figure 4.15	Existing Building: Performance Point Calculation for Mode 1 .....	62
Figure 4.16	Existing Building: Performance Point Calculation for Mode 2 .....	63
Figure 4.17	Existing Building: Performance Point Calculation for Mode 2 .....	64
Figure 4.18	Base Shear vs Roof Displacement curves for first three modes of existing building .....	65
Figure 4.19	Demand curves for first three modes of existing building.....	65
Figure 4.20	Existing Building: Concrete Strains for Basement Storey Columns.....	66
Figure 4.21	Existing Building: Steel Strains for Basement Storey Columns .....	66
Figure 4.22	Existing Building: Concrete Strains for Basement Storey Beams .....	67
Figure 4.23	Existing Building: Steel Strains for Basement Storey Beams .....	67
Figure 4.24	Existing Building: Concrete Strains for Ground Storey Columns .....	68
Figure 4.25	Existing Building: Concrete Strains for Ground Storey Beams .....	68
Figure 4.26	Existing Building: Steel Strains for Ground Storey Beams.....	69
Figure 4.27	Existing Building: Concrete Strains for 1st Storey Columns .....	69
Figure 4.28	Existing Building: Concrete Strains for 1st Storey Beams.....	70
Figure 4.29	Existing Building: Steel Strains for 1st Storey Beams.....	70
Figure 4.30	Existing Building: Concrete Strains for 2nd Storey Columns.....	71
Figure 4.31	Existing Building: Concrete Strains for 2nd Storey Beams .....	71
Figure 4.32	Existing Building: Steel Strains for 2nd Storey Beams .....	72
Figure 4.33	Existing Building: Concrete Strains for 3rd Storey Columns .....	72

Figure 4.34	Existing Building: Concrete Strains for 3rd Storey Beams .....	73
Figure 4.35	Existing Building: Steel Strains for 3rd Storey Beams .....	73
Figure 4.36	Existing Building: Concrete Strains for 4th Storey Columns .....	74
Figure 4.37	Existing Building: Concrete Strains for 4th Storey Beams .....	74
Figure 4.38	Existing Building: Steel Strains for 4th Storey Beams .....	75
Figure 4.39	Existing Building: Concrete Strains for 5th Storey Columns .....	75
Figure 4.40	Existing Building: Concrete Strains for 5th Storey Beams .....	76
Figure 4.41	Existing Building: Steel Strains for 5th Storey Beams .....	76
Figure 4.42	Existing Building: Concrete Strains for 6th Storey Columns .....	77
Figure 4.43	Existing Building: Concrete Strains for 6th Storey Beams .....	77
Figure 4.44	Existing Building: Steel Strains for 6th Storey Beams .....	78
Figure 4.45	Existing Building: Concrete Strains for 7th Storey Columns .....	78
Figure 4.46	Existing Building: Concrete Strains for 7th Storey Beams .....	79
Figure 4.47	Existing Building: Steel Strains for 7th Storey Beams .....	79
Figure 4.48	Existing Building: Drift Ratios .....	80
Figure 4.49	Retrofitted Building: Hinge Formation .....	81
Figure 4.50	Retrofitted Building: Masonry Infill frame in X direction .....	82
Figure 4.51	Retrofitted Building: Performance Point for Mode 1 .....	83
Figure 4.52	Retrofitted Building: Performance Point for Mode 2 .....	84
Figure 4.53	Retrofitted Building: Performance Point for Mode 3 .....	85
Figure 4.54	Base Shear vs Roof Displacement curves for first three modes of retrofitted building .....	86
Figure 4.55	Demand curves for first three modes of retrofitted building .....	86
Figure 4.56	Retrofitted Building: Concrete Strains for basement columns .....	87
Figure 4.57	Retrofitted Building: Steel Strains for basement beams .....	87
Figure 4.58	Retrofitted Building: Concrete strains for ground storey columns ..	88
Figure 4.59	Retrofitted Building: Steel strains for ground storey beams .....	88
Figure 4.60	Retrofitted Building: Concrete strains for 1st storey columns .....	89
Figure 4.61	Retrofitted Building: Steel strains for 1st storey beams .....	89
Figure 4.62	Retrofitted Building: Axial strains for 1st storey CFRP .....	90
Figure 4.63	Retrofitted Building: Concrete strains for 2nd storey columns .....	90

Figure 4.64	Retrofitted Building: Steel strains for 2nd storey beams .....	91
Figure 4.65	Retrofitted Building: Axial strains for 2nd storey CFRP .....	91
Figure 4.66	Retrofitted Building: Concrete strains for 3rd storey columns.....	92
Figure 4.67	Retrofitted Building: Steel strains for 3rd storey beams .....	92
Figure 4.68	Retrofitted Building: Axial strains for 3rd storey CFRP .....	93
Figure 4.69	Retrofitted Building: Concrete strains for 4th storey columns.....	93
Figure 4.70	Retrofitted Building: Steel strains for 4th storey beams .....	94
Figure 4.71	Retrofitted Building: Axial strains for 4th storey CFRP .....	94
Figure 4.72	Retrofitted Building: Concrete strains for 5th storey columns.....	95
Figure 4.73	Retrofitted Building: Steel strains for 5th storey beams .....	95
Figure 4.74	Retrofitted Building: Axial strains for 5th storey CFRP .....	96
Figure 4.75	Retrofitted Building: Concrete strains for 6th storey columns.....	96
Figure 4.76	Retrofitted Building: Steel strains for 6th storey beams .....	97
Figure 4.77	Retrofitted Building: Axial strains for 6th storey CFRP .....	97
Figure 4.78	Retrofitted Building: Concrete strains for 7th storey columns.....	98
Figure 4.79	Retrofitted Building: Steel strains for 7th storey beams .....	98
Figure 4.80	Retrofitted Building: Axial strains for 7th storey CFRP .....	99
Figure 4.81	Retrofitted Building: Drift Ratios .....	99
Figure 4.82	Storey capacity curves for existing building.....	101
Figure 4.83	2D model for nonlinear time history analysis and force-deformation input .....	102
Figure 4.84	Envelope drift ratio demand for existing building at each storey after time history analysis. ....	103
Figure 4.85	Concrete strains for basement storey columns .....	104
Figure 4.86	Steel strains for basement storey columns .....	104
Figure 4.87	Concrete strains for basement storey beams.....	105
Figure 4.88	Steel strains for basement storey beams .....	105
Figure 4.89	Concrete strains for ground storey columns .....	106
Figure 4.90	Steel strains for ground storey columns .....	106
Figure 4.91	Concrete strains for ground storey beams.....	107
Figure 4.92	Steel strains for ground storey beams .....	107

Figure 4.93	Concrete strains for 1st storey columns .....	108
Figure 4.94	Steel strains for 1st storey columns .....	108
Figure 4.95	Concrete strains for 1st storey beams.....	109
Figure 4.96	Steel strains for 1st storey beams .....	109
Figure 4.97	Concrete strains for 2nd storey columns.....	110
Figure 4.98	Steel strains for 2nd storey columns .....	110
Figure 4.99	Concrete strains for 2nd storey beams .....	111
Figure 4.100	Steel strains for 2nd storey beams.....	111
Figure 4.101	Concrete strains for 3rd storey columns .....	112
Figure 4.102	Steel strains for 3rd storey columns .....	112
Figure 4.103	Existing Building Concrete strains for 3rd storey beams .....	113
Figure 4.104	Existing Building Steel strains for 3rd storey beams.....	113
Figure 4.105	Existing Building Concrete strains for 4th storey columns .....	114
Figure 4.106	Existing Building Steel strains for 4th storey columns.....	114
Figure 4.107	Existing Building Concrete strains for 4th storey beams.....	115
Figure 4.108	Existing Building Steel strains for 4th storey beams .....	115
Figure 4.109	Existing Building Concrete strains for 5th storey columns .....	116
Figure 4.110	Existing Building Steel strains for 5th storey columns.....	116
Figure 4.111	Existing Building Concrete strains for 5th storey beams.....	117
Figure 4.112	Existing Building Steel strains for 5th storey beams .....	117
Figure 4.113	Existing Building Concrete strains for 6th storey columns .....	118
Figure 4.114	Existing Building Steel strains for 6th storey columns.....	118
Figure 4.115	Existing Building Concrete strains for 6th storey beams.....	119
Figure 4.116	Existing Building Steel strains for 6th storey beams .....	119
Figure 4.117	Existing Building Concrete strains for 7th storey columns .....	120
Figure 4.118	Existing Building Steel strains for 7th storey columns.....	120
Figure 4.119	Existing Building Concrete strains for 7th storey beams.....	121
Figure 4.120	Existing Building Steel strains for 7th storey beams .....	121
Figure 4.121	Storey capacity curves for retrofitted building .....	123
Figure 4.122	Envelope drift ratio demand for retrofitted building at each storey after time history analysis.....	124

Figure 4.123 Concrete strains for basement storey columns .....	124
Figure 4.124 Concrete strains for basement storey beams .....	125
Figure 4.125 Steel strains for basement storey beams .....	125
Figure 4.126 Concrete strains for ground storey columns .....	126
Figure 4.127 Concrete strains for ground storey beams .....	126
Figure 4.128 Steel strains for ground storey beams .....	127
Figure 4.129 Concrete strains for 1st storey columns .....	127
Figure 4.130 Concrete strains for 1st storey beams .....	128
Figure 4.131 Steel strains for 1st storey beams .....	128
Figure 4.132 Axial strains for 1st storey CFRP Walls .....	129
Figure 4.133 Concrete strains for 2nd storey columns .....	129
Figure 4.134 Concrete strains for 2nd storey beams .....	130
Figure 4.135 Steel strains for 2nd storey beams .....	130
Figure 4.136 Axial Strains for 2nd storey CFRP Walls .....	131
Figure 4.137 Concrete Strains for 3rd storey columns .....	131
Figure 4.138 Concrete Strains for 3rd storey beams .....	132
Figure 4.139 Steel Strains for 3rd storey beams .....	132
Figure 4.140 Axial Strains for 3rd storey CFRP Walls .....	133
Figure 4.141 Concrete Strains for 4th storey columns .....	133
Figure 4.142 Steel Strains for 4th storey beams .....	134
Figure 4.143 Axial Strains for 4th storey CFRP Walls .....	134
Figure 4.144 Concrete Strains for 5th storey columns .....	135
Figure 4.145 Steel Strains for 5th storey beams .....	135
Figure 4.146 Axial Strains for 5th storey CFRP Walls .....	136
Figure 4.147 Concrete Strains for 6th storey columns .....	136
Figure 4.148 Steel Strains for 6th storey beams .....	137
Figure 4.149 Axial Strains for 6th storey CFRP Walls .....	137
Figure 4.150 Concrete Strains for 7th storey columns .....	138
Figure 4.151 Steel Strains for 7th storey beams .....	138
Figure 4.152 Axial Strains for 7th storey CFRP Walls .....	139
Figure 5.1 Comparison of drift demands for different analysis	

	techniques for existing building .....	141
Figure 5.2	Comparison of drift demands for different analysis techniques for retrofitted building.....	142
Figure 5.4	Variation of drift ratio of ground storey with respect to time.....	143
Figure A.1	Stress-Strain Curve.....	148
Figure D.1	Corroded reinforcements inside the ground storey column .....	157
Figure D.2	Column repaired against corrosion.....	158
Figure D.3	CFRP Application on the masonry infill wall .....	159
Figure D.4	Foundation excavation for eccentric reinforced concrete shearwalls.....	160
Figure D.5	Production of eccentric reinforced concrete shearwalls.....	160
Figure D.6	Production of eccentric reinforced concrete shearwalls.....	161
Figure D.7	Production of eccentric reinforced concrete shearwalls.....	162

# CHAPTER 1

## INTRODUCTION

### 1.1. GENERAL

Strengthening of deficient structures is a main challenge both in structural engineering practice and in academic studies. This is because of the fact that the existing deficient structure contains many unknowns in terms of material quality and its distribution among members, existing reinforcement design, curtailment and detailing, previous damages, ductility level, proper modelling of load-bearing and non load-bearing members (both new and existing ones)

Besides these physical challenges, there are a limited number of efficient analysis and assessment techniques which are valid for mid-rise to high-rise structures, especially which suffer from higher modal contributions.

Another challenge come into scene in terms of economical considerations. Especially for residential buildings, there is a huge problem of evacuation and relocation of residents which drastically increases the cost of retrofit. Also, speed of construction is another parameter that needs to be taken into consideration, especially when the deficient building stock in Turkey and the need for quick action is considered.

Standard course of retrofitting includes installation of reinforced concrete infills and column jacketing where necessary in current construction practice in Turkey. Along with elastic analysis, this is an effective solution for low-rise ( $n < 8$ ) structures. However, for mid-rise and high-rise building stock, which constitutes approximately 10% of total building stock in Turkey, hybrid strengthening schemes such as CFRP and Reinforced Concrete patterns are a powerful candidates that should not be ignored.

## 1.2. PREVIOUS STUDIES

There were significant amount of experimental and analytical work conducted on retrofitting with reinforced concrete infills, behaviour and modelling of masonry infills and CFRP strengthened masonry infills. Other studies included below are on linear and nonlinear earthquake performance analyses and assessment techniques.

Canbay, Ersoy and Ozcebe (2003) [1] conducted lateral load tests on three-bay, two-storey 1/3 scale reinforced concrete frame specimens. They exposed the bare frame to damaging drift reversals up to drift ratio of 1.9% at first storey. After strengthening the frames with reinforced concrete infill walls installed at the middle bay, specimens were continued to be subjected to drift reversals again up to the same value of 1.6%. The aim was determine the distribution of lateral loads among existing nonductile frame members and newly added reinforced concrete infills. Specimens were prepared with all the deficiencies that majority of buildings in Turkey have such as low concrete strength, inadequate lateral stiffness, inadequate confinement and lap splices at the floor level. Bare frame resisted to a lateral load of 14 kN whereas strengthened frame could carry a lateral of 53 kN at the end of the test. It was measured that during the first cycles, 99% of the total lateral loads were being resisted by infill wall. Even, during the last cycles the ratio was 90%. Besides these, stiffness of the infilled frame was approximately 15 times greater than the stiffness of the bare frame.

Turk, Ersoy and Ozcebe [2] investigated the seismic behavior of damaged reinforced concrete frames rehabilitated by introducing cast in place reinforced concrete infills. One-bay, two storey reinforced concrete frames were prepared and tested under reverse-cyclic lateral loading until considerable damage occurred. Some of the test frames were detailed properly according to the current Turkish earthquake code whereas others were representing the common deficiencies observed in existing residential buildings. Damaged test frames were retrofitted with reinforced concrete infills and loaded laterally again under reverse-cyclic lateral loading. Test results yield that lateral strength and stiffness were significantly increased with the introduction of reinforced concrete infills. It was

also concluded that the damage level of the frame did not affect the behavior of infilled frame significantly provided that the infills are properly connected to the existing frame. Damaged frames were not repaired, however according to the study, the performance of these infilled frames were satisfactory. Authors observed that the presence of a lap splice in column longitudinal bars above the floor level was the most adverse factor that affected the infilled frame performance, especially when the lap length is small.

Reinforced concrete infills are verified to be very effective in seismic retrofit designs. Being thought only as gravity load producing members and being ignored in most elastic and inelastic analyses, researchers and engineers also concentrated their efforts on determining the positive and/or adverse effects masonry infill walls in seismic performance of reinforced concrete buildings. Analytical studies were also made to adopt a proper elastic and inelastic model for masonry infill walls.

Mehrabi, Shing, Schuller and Noland (1996) [3] studied the influence of masonry infill panels on the seismic performance of reinforced concrete frames. Two types of frames were considered in their study. One was designed for moderate wind loads and the other for strong earthquake forces. Twelve 1/2-scale, single-story, single-bay, frame specimens were tested. The parameters investigated included the strength of infill panels with respect to that of the bounding frame, the panel aspect ratio, the distribution of vertical loads, and the lateral-load history. It was found that infill panels significantly improved the performance of reinforced concrete frames. However, specimens with strong frames and strong panels exhibited a better performance than those with weak frames and weak panels in terms of the load resistance and energy-dissipation capability. It was also found that the lateral loads developed by the infilled frame specimens were always higher than that of the bare frame even for the least ductile specimen deforming up to a drift level of 2%.

Negro and Verzeletti (1996) [4] conducted experimental studies on 4-storey, 2 by 2-bay, 1/1 scaled reinforced concrete frames in European Association of Structural Mechanics Laboratories. Frame specimens were designed according to Eurocode 2 and Eurocode 8 provisions. One type of frames had masonry infill

walls at each storey whereas other type had no masonry infills. The last type of frame specimens had masonry infill walls except the first storey which causes a soft storey. Vibration frequencies, spectral accelerations, storey drifts, base shear forces, rotations at beams and columns and energy dissipation capacities were compared.

Proenca, Oliviera and J.P. Almeida [5] analyzed a pre-earthquake code designed 11-storey reinforced concrete hospital structure in Portuguese. This interesting study was about the seismic performance assessment block number 22. The building had strong facade and interior rubble stone containing masonry walls that were non-negligible. Masonry infill walls were modelled by diagonal compression struts. As a result of several nonlinear pushover and sensitivity analyses, they observed that a soft storey formation may exist at 3<sup>rd</sup> storey after the sudden failure of strong masonry infills. After the analytical models are refined to reflect the new situation, it was observed that the deformation demands were concentrated at the soft storey columns and beams. In contrast, reinforced concrete elements were kept practically undeformed without significant stresses. Only masonry elements above and below soft-storey were subjected to significant axial force increments, hence with a possibility of leading to another soft storey formation at the onset of the performance point. It was concluded that in the case of early reinforced concrete structures such as the example building in their study, either facade or partition walls have significant stiffening effects that greatly determines the early nonlinear stages. These infills can - and as was the case in the study – lead to a sudden drop of strength and stiffness which will severely affect the load resisting mechanism and damage pattern.

Sayın, Yıldızlar and Kaplan [6] conducted an analytical study in which they modelled masonry infilled walls as panels and diagonal compression struts between frame members in a 4 by 4-bay, 5-storey reinforced concrete regular building. They tried to focus on the positive and adverse effects of masonry infill presence and their location inside the building. It was observed that frames modelled with masonry exhibited a more rigid response to lateral loads than the bare frames. They also observed that masonry infills can cause torsional irregularities as well as shifts in center of gravity and rigidity in a symmetrical

structural system. They achieved similar results for panel and diagonal strut modelling.

The similar studies on the seismic performance of bare masonry infills as explained above led to further experimental and analytical studies which focused on using them effectively for retrofitting projects.

A joint experimental study [7] was carried out under the coordination of Middle East Technical University Structural Laboratory in order to determine the effect of Carbonfiber Reinforced Polymer (CFRP) retrofitting to lateral load behavior of reinforced concrete frames. In order to achieve this purpose, parallel tests were conducted in Middle East Technical University (METU), Kocaeli University – Boğaziçi University (KU-BU) and Istanbul Technical University (ITU). Two-storey, one-bay reinforced concrete frames were tested in different scales. Frames were designed to include the common deficiencies of the structures in Turkey. The arrangement of the CFRP layers, the amount of CFRP used, the anchorage of CFRP fabric to the wall and the frame elements were the major parameters investigated. Proper CFRP detailing schemes were developed to reduce the adverse effects of the common deficiencies. A cross-bracing (strut) type CFRP detailing was determined to be most effective and economical scheme among the other tested alternatives. In this pattern, CFRP strips were placed in two diagonal directions instead of fully covering the infill surface. Diagonal strips were anchored to the frame members and to the hollow clay tile infills. CFRP flag sheets are applied in the corners of the infill. Two dominant failure modes were identified. One of them was in the form of a combined pull-out and slip failure with the failure of CFRP anchors. This is followed by a load transfer to diagonal compression strut which then causes corner crushing in the infill. Second failure mode is caused by CFRP debonding from the infill surface. When this occurs, previously formed cracks start to widen and tie action is lost before a sliding shear failure occurs in the masonry infill wall. Tests have shown that anchor failure occurs at an effective diagonal FRP strain of about 0.002 when three CFRP anchors with a depth of about five times the hole diameter is used per corner on each side of the infill. the second failure mode marks the limiting strength of the strengthened infill. Beyond a strain level of about 0.006, FRP debonding took

place resulting in a sliding shear failure of the infill followed by a sudden drop of strength. These tests indicated that the infill walls contribute significantly to the lateral strength and stiffness of the reinforced concrete frames. By reinforcing the infill walls with CFRP composite sheets, the behaviour of the test specimens further improved in terms of strength, stiffness and the energy dissipation characteristics. In specimens with inadequate lap splices, confinement of lap splice regions of the columns with CFRP composite sheets in transverse direction delayed bond slip and significant energy dissipated through the hysteretic behaviour.

Binici and Ozcebe [8] carried out analytical studies in order to propose analysis guidelines for FRP strengthened masonry infill walls for use in seismic evaluation methods. For this purpose, they presented a diagonal compression-strut and tension-tie model to analytically represent the strengthened infill wall that is integrated to the boundary frame members. Authors analyzed a two-storey one-bay frame using plane stress elements to demonstrate the structural deformations and flow of stresses. The analysis results showed that when FRPs are bonded to the infill wall and tied to the boundary frame, it acts as a tension tie whose width is similar to the width of the provided CFRP sheet in the effectively anchored region. Trilinear stress-strain response models were proposed for the tension and compression truss members which represent the infill wall strengthened with CFRP. Authors conducted static inelastic analyses to verify the proposed models and they performed comparisons with test results. They observed good agreement between measured and estimated stiffness, strength and deformation capacity. Besides these, authors also worked on a case study of typical reinforced concrete frame with infill walls analyzed with and without upgrades. Substantial strength and deformation capacity increases were observed as a result of the applied retrofit design.

Binici et. al. [9] proposed a simplified analytical model for use in displacement based design of FRPs based on previous experimental and analytical studies explained above. The main reason for the need to develop a simplified model was that, most commercially available softwares can not handle softening region in force-deformation relationships for plastic hinges and link elements. And

also, it was indicated to be more practical to assume elasto-plastic relationships for inelastic elements as suggested by FEMA 356 [10] and TEC 2007 [11]. According to the simplified model, the initial stiffness of the FRP ties were taken equal to the stiffness of the FRP sheets neglecting the presence of hollow clay tile and plaster prior to cracking. At a tensile strength corresponding to an FRP strain of 0.003, plastic flow was assumed to take place up to a strain level of 0.006 at which complete strength deterioration occurs. For the infill strut, complete strength degradation was assumed to take place at a strain of 0.012. With these simplifications, additional conservatism was introduced in the model while preserving the accuracy of the original model. In the study, authors also used this simplified model in a displacement based FRP retrofit design example. Nonlinear static pushover analyses were performed in order to estimate displacement capacity of the building for the required evaluation techniques. Building was experiencing an overall drift ratio of 1.2%. Upon retrofit, the drift ratio was reduced to 0.8%. Based on these results, authors concluded that FRP retrofit scheme was successful in controlling drift deformations and reducing demands in columns.

Chopra and Goel [12] developed an improved pushover analysis procedure named as Modal Pushover Analysis (MPA) which can be regarded as a simple extension of the conventional single-mode pushover analysis to the multi-mode response. Method is based on structural dynamics theory. Basic idea behind the procedure was in fact proposed in earlier studies [13], [14]. Firstly, the procedure was applied to linearly elastic buildings and it was shown that the procedure is equivalent to well known response spectrum analysis. Then, the procedure was extended to estimate the seismic demands of inelastic systems. Earthquake induced demands for a 9-story SAC building were determined by MPA, nonlinear dynamic analysis and pushover analysis using uniform, “code” and multi-modal load patterns. The comparison of results indicated that pushover analysis for all patterns greatly underestimates the storey drift demands and lead to large errors in plastic hinge rotations. The MPA was more accurate than all pushover analyses in estimating floor displacements, story drifts, plastic hinge rotations and plastic hinge locations. MPA results were also shown to be weakly dependent on ground

motion intensity based on the results obtained from El Centro ground motion scaled by factors varying from 0.25 to 3. It was concluded that by including the contributions of a sufficient number of modes (two or three), the height-wise distribution of responses estimated by MPA is generally similar to the „exact“ results from nonlinear dynamic analysis.

Fahjan [15] discussed basic methodologies and criteria for selecting strong ground motion time histories in his study. The time domain scaling procedure was utilized to scale the available real records to match the proposed elastic design spectrum given in TEC 2007 for different seismic regions and soil types. In this method, the difference between the response spectrum of scaled record and the target spectrum is tried to be minimized by using least squares method. Using the Pacific Earthquake Engineering Research Center (PEER) database, he classified acceleration-time records according to the soil types in Turkish Earthquake Code. These classified records are scaled by time domain scaling procedure between the period interval of  $T_A = 0.01$  and  $T_B = 5$  seconds. Considering the Turkish Earthquake Code criteria for selecting acceleration-time records, ten best fitting real records were selected for each soil type. Earthquake magnitude, focal mechanism and site conditions were taken into account.

### **1.3. OBJECTIVE AND SCOPE**

This study mainly focuses on retrofitting a real life mid-rise reinforced concrete frame building with a hybrid scheme. Hybrid scheme comprises of masonry infill walls retrofitted with CFRPs and eccentric reinforced concrete shearwalls. Behavior before and after retrofit scheme is investigated. Besides these, retrofit scheme is analyzed and assessed using different analysis and assessment techniques and results are compared.

Analysis and assessment procedures explained in current Turkish Earthquake Code For Buildings (TEC 2007) are used throughout the study. Because of the procedural complexity and high computational demand, Incremental Response Spectrum Analysis (IRSA) [16] method is kept out of

scope. Modal Pushover Analysis proposed by Chopra [12] and nonlinear time history analyses as described by TEC 2007 are utilised. Assessment after modal pushover and time history analysis was also conducted according to TEC 2007 provisions.

This thesis is composed of five main chapters and four appendices. Brief contents are given as follows:

Chapter 1 Statement of the problem and literature survey on reinforced concrete infills, masonry infills and analysis procedures

Chapter 2 Brief introduction and description of the available analysis and assessment procedures in 2007 Turkish Earthquake Code.

Chapter 3 Explanation of CFRP mathematical model, modelling considerations for CFRP strips, application details criteria located in 2007 Turkish Earthquake Code.

Chapter 4 Seismic assessment of the 9-storey case study building with linear elastic and nonlinear procedures using different retrofit schemes and presentation of results.

Chapter 5 A brief summary, discussions and conclusions

## **CHAPTER 2**

### **ANALYSIS AND ASSESSMENT METHODS IN 2007 TURKISH EARTHQUAKE CODE**

#### **2.1. INTRODUCTION**

Turkish Earthquake Code (TEC) 2007 [1] suggests linear and non-linear analysis methods for assessment of existing buildings. A complete chapter is devoted inside the code for this purpose. Analysis and assessment methods mentioned in TEC 2007 are:

- Linear Elastic Analysis and Force Based Assessment
  - Equivalent Static Load Method
  - Mode Superposition
- Non-Linear Analysis and Displacement Based Assessment
  - Static Pushover (with invariant load distribution)
  - Multi Mode Pushover (IRSA Method) [2],
  - Time-History Analysis

#### **2.2. LINEAR ELASTIC ANALYSIS AND FORCE BASED ASSESSMENT PROCEDURE**

Linear elastic assessment procedure simply depends on comparing earthquake force demands on members with member capacities. At first, a linear elastic analysis of the existing building is performed. Then, member capacities and demands are calculated. Member capacities are compared with the demands and a Demand/Capacity Ratio (DCR) is calculated for each member. These DCR values are compared with the limit values provided by the code. At last, a global performance evaluation is performed by counting failing members. Typical flowchart of operations are given in Figure 2.1.

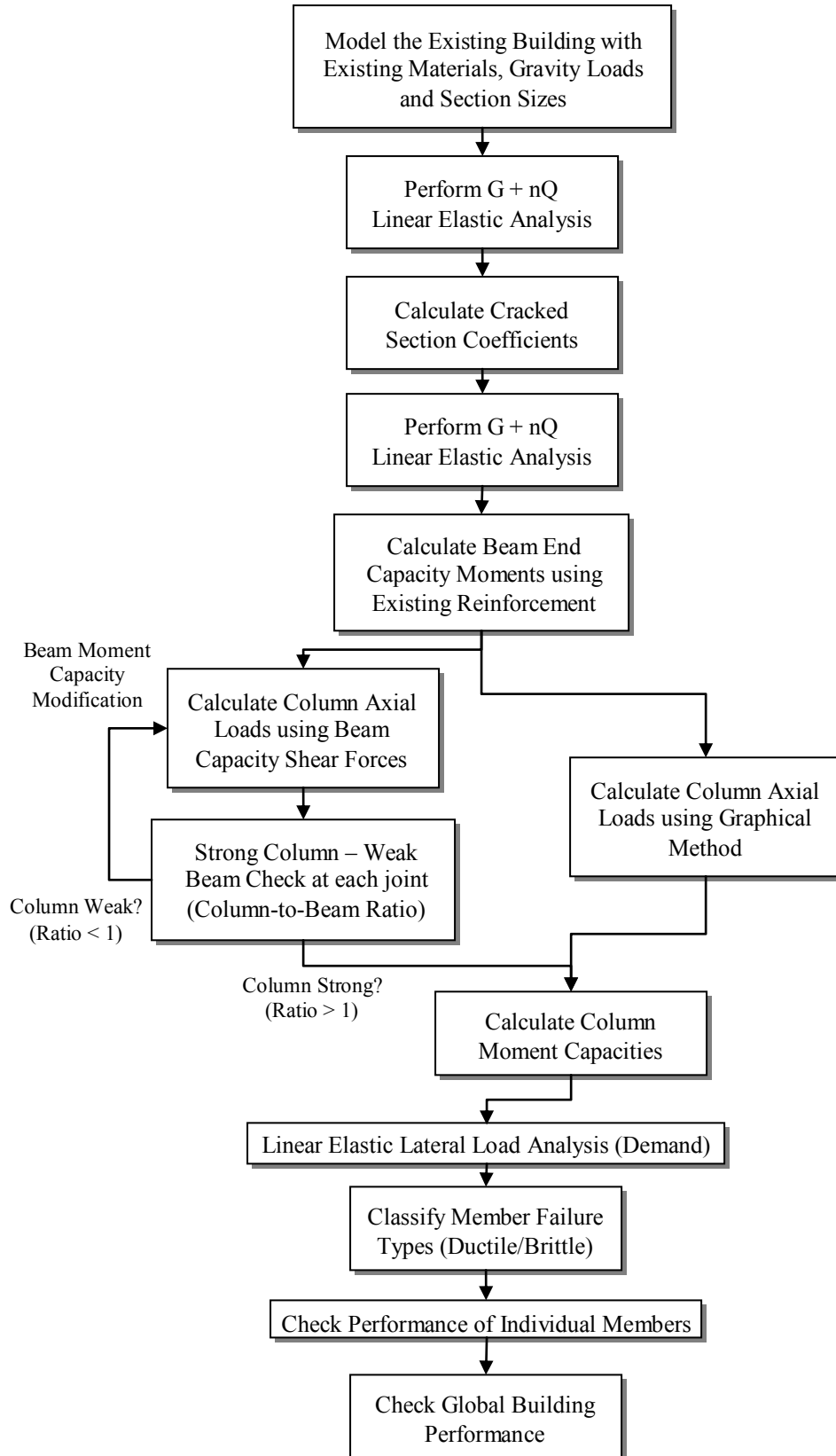


Figure 2.1 : Generalized flowchart for linear elastic assessment procedure

One or multiple performance levels must be defined for the building. TEC 2007 foresees specific performance levels for buildings with different purpose of occupation. Limit values for critical sections and the building is governed by performance level. Code spectrum is also scaled according to the selected performance level. Table 2.1 summarizes these performance levels.

Table 2.1: Required seismic performance levels for design earthquakes

Building Type	Probability of Exceedence		
	% 50 in 50 years	% 10 in 50 years	% 2 in 50 years
<b>Buildings for Immediate Use just after EQ:</b> Hospitals, Medical Installments, emergency facilities, communication and energy installations, transportation stations, city, municipality and official governmental buildings, disaster management HQs etc.	-	IO	LS
<b>Densely crowded buildings with long occupancy durations:</b> Schools, Dormitories, pansions, military facilities, Prison buildings, museums, etc..	-	IO	LS
<b>Densely crowded buildings with short occupancy durations:</b> Cinema, theater, concert halls, culture and convention centers, sports facilities.	IO	LS	-
<b>Buildings with Dangerous Storages:</b> Buildings used as a storage facility for toxic, flammable and explosive materials.	-	IO	CP
<b>Other Buildings:</b> Buildings outside the above classification. (Residentials, office buildings, hotels, touristic facilities, industrial buildings, etc.)	-	LS	-

Where,

IO: Immediate Occupancy, LS: Life Safety and CP: Collapse Prevention

Since the example building is a residential building, it must satisfy the “Life Safety (LS)” criteria under an earthquake having a 10% probability of exceedence in 50 years. Performance levels for ductile members are given in Figure 2.2.

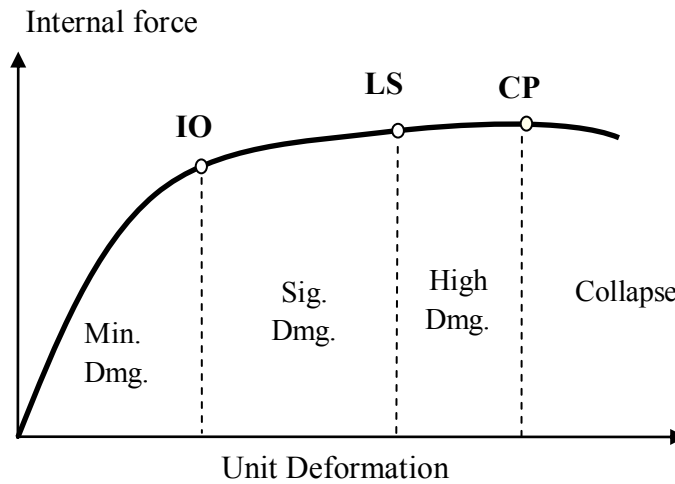


Figure 2.2: Damage Levels and Performance Boundaries for ductile members

In elastic analyses, no ductility assumption is made for the structure at the beginning. That means, the “Force Reduction Factor ( Global R )” is taken as 1 (i.e. the building is analysed under unreduced elastic loads). Depending on the performance level defined for the target building, different probability of exceedence values are used for the elastic spectrum. Design Elastic Spectrum, which is identified by 10% probability of exceedence in 50 years, is multiplied by 1.5 for 2% probability of exceedence (severe earthquake) and divided by 2 for a 50% probability of exceedence in 50 years. Additionally, building importance factor is ignored in calculations (i.e.  $I = 1$ ). No additional eccentricities are considered ( $e = 0$ ). The earthquake loads are always applied at the center of mass without additional torsion.

### 2.2.1. Modelling Considerations for Linear Elastic Analysis

TEC 2007 suggests general valid modelling techniques for 3-dimensional modelling. Rigid zones, rigid diaphragms, use of frame and shell members with 3-dimensional valid formulations are all provisioned by the code.

The earthquake performance of the structure is assessed under the combined effect of vertical and earthquake loads. A vertical load analysis (consisting of imposed and dead loads) is carried out with uncracked sections. Cracked section property modifications are done according to the axial load levels found at the end of this analysis. (Equation 2.1)

$$\begin{aligned} & \text{for beams} && (EI)_c = 0.4(EI)_o \\ & \text{for columns and walls} && \frac{N_D}{A_c f_{cm}} \leq 0.10 \Rightarrow (EI)_c = 0.4(EI)_o \\ & && \frac{N_D}{A_c f_{cm}} \geq 0.40 \Rightarrow (EI)_c = 0.8(EI)_o \end{aligned} \quad (2.1)$$

Where;

- $N_D$  : Axial Load under G+nQ loading
- $A_c$  : Gross Section Area
- $f_{cm}$  : Existing concrete characteristic compressive strength
- $E$  : Modulus of Elasticity
- $I$  : Uncracked moment of Inertia

For intermediate values, cracked section properties can be found by interpolation. Vertical load analysis is repeated by newly found cracked sections. Earthquake analysis is also done by these cracked section properties.

### 2.2.2. Equivalent Static Earthquake Load Analysis

Equivalent static load method is the common method used in practice. First two period of the structure is utilised in calculation of the spectral acceleration. The special assumptions mentioned in above paragraphs are valid. However, there

are certain limitations in the application of this method. For buildings exceeding 25 m in height and 8 storeys, this load calculation method can not be used. Moreover, if the “Floor Torsion Coefficient” is greater than 1.4, this method is invalid. The building studied in this thesis does not fulfill the requirements for an equivalent static load calculation. Total lateral load acting on the structure is determined by Equation 2.2.

$$V_t = \lambda \frac{W \cdot A(T_1)}{R(T_1)} \geq 0.1 A_0 I W \quad (2.2)$$

W is the total weight of the building. Dead loads and a portion of live loads are combined to calculate the total weight. “Live load participation factor” is given by the code depending on the type of the structure. Building importance factor (I) and seismic load reduction factor (R) are taken as 1.  $A_0$  is effective ground acceleration coefficient varying between 0.4 and 0.1 depending on the seismic zone. Total load calculated by Equation 2.2 is further multiplied by  $\lambda$ .  $\lambda$  can be taken as 0.85 for structures having more than 2 storeys, 1 for others.  $A(T_1)$  can be calculated by Equation 2.3.

$$A(T) = A_o I S(T) \quad (2.3)$$

$S(T)$  is the spectrum coefficient and it depends on site conditions and building natural period of vibration.

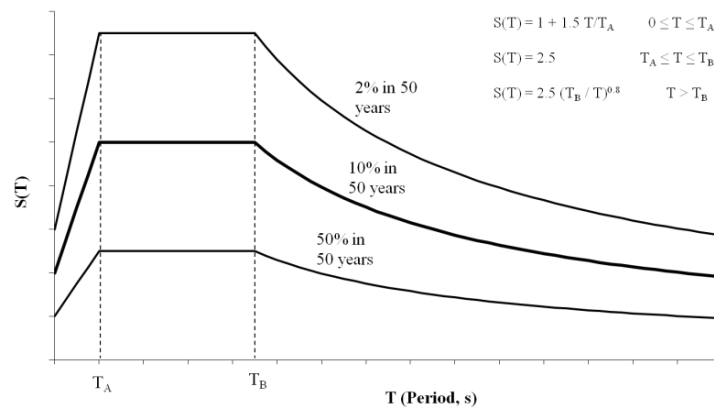


Figure 2.3: TEC 2007 spectra for different performance levels

Seismic load distribution along the storey levels are performed as explained by the following equations:

$$V_t = \Delta F_N + \sum_{i=1}^N F_i \quad (2.4)$$

$$\Delta F_N = 0.0075 N V_t \quad (2.5)$$

$$F_i = (V_t - \Delta F_N) \frac{w_i H_i}{\sum_{j=1}^N w_j H_j} \quad (2.6)$$

### 2.2.3. Mode Superposition Analysis

In order to use linear elastic method of assessment for the buildings that have higher modal contributions, TEC 2007 suggests to calculate the lateral loads by mode superposition analysis. Buildings that have more than 8 storeys or higher than 25 m (except basements) goes into this category. Also, buildings with torsional irregularity coefficients greater than 1.4 at any storey must be analyzed with mode superposition method of analysis. This method is based on the combination of maximum contributions obtained from each separate vibration mode. Sufficient number of vibration modes should be taken into consideration that is the sum of effective mass participating ratios should be greater than 90% of the total mass of the building for each direction. This criterion is summarized in the equations 2.7, 2.8 and 2.9. Maximum contributions of response quantities are combined with either Square Root of Sum of Squares (SRSS) or Complete Quadratic Combination (CQC). For any two natural vibration modes  $T_m$  and  $T_n$  ( $T_m < T_n$ ), if  $T_m / T_n > 0.8$ , SRSS method can not be used.

$$\sum_{n=1}^Y M_{xn} = \sum_{n=1}^Y \frac{\{\sum_{i=1}^N (m_i \phi_{xin})\}^2}{M_n} \geq 0.9 \sum_{i=1}^N m_i \quad (2.7)$$

$$\sum_{n=1}^Y M_{yn} = \sum_{n=1}^Y \frac{\{\sum_{i=1}^N (m_i \phi_{yin})\}^2}{M_n} \geq 0.9 \sum_{i=1}^N m_i \quad (2.8)$$

$$M_n = \sum_{i=1}^N (m_i \phi_{xin}^2 + m_i \phi_{yin}^2 + m_{\phi_i} \phi_{\phi_{in}}^2) \quad (2.9)$$

#### 2.2.4. Force Based Assessment Details

TEC 2007 proposes a force based assessment procedure to use with elastic analysis methods. Assessment technique depends on the determination of Demand/Capacity Ratios (DCR) for each member in the structure.

Reinforced concrete members are classified as “Ductile” if mode of failure is flexure. They are classified as “Brittle” if the failure is due to shear or axial load. At the critical sections of each beam, column and wall member, the “capacity shear” forces are calculated. This shear force is calculated from flexural capacities of the sections. Characteristic strength of concrete and steel (determined in site survey) will be used directly in capacity calculations. However, these capacities will be multiplied by the “level of information coefficients ( $\leq 1$ )” in order to take the uncertainties due to insufficient information. Capacity shear forces are calculated with the shear resistance specified in TS500 [17].

For ductile sections, DCR is found by Equation 2.10

$$r = \frac{M_E}{M_R - M_D} = \frac{\text{EQ Moment}}{\text{Residual Moment Capacity}} \quad (2.10)$$

where  $M_R$  is the capacity moment,  $M_D$  is the moment calculated from the vertical load analysis.

For brittle sections, DCR is found by Equation (2.11)

$$r = \frac{V_E}{V_R} = \frac{\text{Capacity Shear Force}}{\text{Shear Resistance}} \quad (2.11)$$

After the performance criteria are determined, the member DCR are compared with the code specified tables for the specified performance level. For instance, for the Life Safety Performance Level, the number of beams in “High Damage” region should not exceed the 30% of the total in compatible direction in any storey. For columns, the shear force carried by “High Damage” columns should not exceed the 20% of total shear in compatible direction in any storey. These criteria are summarized in Table 2.2. Limit values for DCR values for different member types are given in Table 2.3 – 2.7.

Table 2.2: Performance Criteria

	<b>Immediate Occupancy</b>	<b>Life Safety</b>	<b>Collapse Prevention</b>	<b>Collapse</b>
<b>Damage in Structural Members</b>	None	Minor	Important amount damaged.	Some of load carrying members collapsed.
<b>Damage in non-structural members</b>	Minor	May be damaged. Infill walls do not collapse.	Damaged. Some of infill walls collapse.	Big majority collapse.
<b>Permanent Deformations</b>	None	Minor	Present	Significantly present
<b>Columns and Shearwalls</b>	All in minimum damage region. (< IO)	All in Min. Damage or Significant Damage Region. (< IO or <LS)	All < LS	Building must be retrofitted.
<b>Beams</b>	IO < (at most 10%) < LS	LS < (at most 30%) < CP	At most 20% > CP	
<b>Ratio of shear force carried by insufficient columns</b>		V <sub>t</sub> (High Damage) (LS < (at most 20%) < CP) Top storey 40%	V <sub>t</sub> (Collapse Region) < 20%	

Table 2.3: DCR Limit Ratios for Reinforced Concrete Ductile Beams

Ductile Beams			Damage Level		
$\frac{\rho - \rho'}{\rho_b}$	Confinement	$\frac{V_e}{b_w d f_{cm}}$	IO	LS	CP
$\leq 0.0$	Yes	$\leq 0.65$	3	7	10
$\leq 0.0$	Yes	$\geq 1.30$	2.5	5	8
$\geq 0.5$	Yes	$\leq 0.65$	3	5	7
$\geq 0.5$	Yes	$\geq 1.30$	2.5	4	5
$\leq 0.0$	No	$\leq 0.65$	2.5	4	6
$\leq 0.0$	No	$\geq 1.30$	2	3	5
$\geq 0.5$	No	$\leq 0.65$	2	3	5
$\geq 0.5$	No	$\geq 1.30$	1.5	2.5	4

Table 2.4: DCR Limit Ratios for Reinforced Concrete Ductile Columns

Ductile Beams			Damage Level		
$\frac{N_K}{A_c f_{cm}}$	Confinement	$\frac{V_e}{b_w d f_{cm}}$	IO	LS	CP
$\leq 0.1$	Yes	$\leq 0.65$	3	6	8
$\leq 0.1$	Yes	$\geq 1.30$	2.5	5	6
$\geq 0.4$ and $\leq 0.7$	Yes	$\leq 0.65$	2	4	6
$\geq 0.4$ and $\leq 0.7$	Yes	$\geq 1.30$	1.5	2.5	3.5
$\leq 0.1$	No	$\leq 0.65$	2	3.5	5
$\leq 0.1$	No	$\geq 1.30$	1.5	2.5	3.5
$\geq 0.4$ and $\leq 0.7$	No	$\leq 0.65$	1.5	2	3
$\geq 0.4$ and $\leq 0.7$	No	$\geq 1.30$	1	1.5	2
$\geq 0.7$	-	-	1	1	1

Table 2.5: DCR Limit Ratios for Reinforced Concrete Ductile Walls

Ductile Walls	Damage Level		
Confinement	IO	LS	CP
YES	3	6	8
NO	2	4	6

Table 2.6: DCR Limit Ratios for Strengthened Masonry Infill Walls

$L_{infill}/h_{infill}$ 0.5 – 2.0	Damage Level		
	IO	LS	CP
Demand/Capacity Ratio (DCR)	1	2	-
Interstorey Drift Ratio	0.0015	0.0035	-

Table 2.7: Interstorey Drift Ratio Limits

Interstorey Drift Ratio	Damage Level		
	IO	LS	CP
$\Delta_i / h_i$	0.01	0.03	0.04

### 2.3. NONLINEAR ANALYSIS AND DISPLACEMENT BASED ASSESSMENT PROCEDURE

Elastic methods of assessment can not consider post yielding behaviour such as redistribution. More importantly, order of plastic hinge formation and failure mechanisms can not be observed. Moreover, hysteretic behaviour of material and sections can also be considered in nonlinear analyses. Similarly, Oguz [18] states in her thesis that, “Elastic methods can predict elastic capacity of structure and indicate where the first yielding will occur, however they do not predict failure mechanisms and account for the redistribution of forces that will take place as the yielding progresses.”

TEC2007 suggests static and modal pushover analyses as well as time-history method as nonlinear methods.

#### 2.3.1 Modelling Considerations for Pushover Analysis According To Turkish Earthquake Code

A 3-dimensional model that represents the fundamental static and dynamic properties of the building must be created. Cracked section properties must be

calculated as explained for the linear elastic analyses. Rigid zones and vertical loads must be assigned properly. As it is known, rigid zones have significant effect on structural stiffness and hence, building codes make rigid zone modelling compulsory. As also being valid for linear elastic analysis, any accidental eccentricity is not considered ( $e=1$ ). All lateral loads are directly assigned to mass center. However, if there are additional torsional moments due to dominant mode shape, these should be applied as a part of the load pattern. As-built material characteristic strengths are used.

All critical sections are assigned plastic hinges. For the beam sections, M3 hinges are used. Column and wall sections involve axial load interaction, hence they require preparation of 3-dimensional interaction surface as well as moment-curvature relations for two directions. Thus they are assigned PMM hinges. If there are frame members that only carry tension or compression such as retrofitted masonry walls, struts, etc, only axial load hinges are used. Two plastic hinges are used for each end of beams and columns, whereas axial hinges are assigned to the midspan of the related members if available.

TEC 2007 suggests the use of a confined concrete model and a steel model that can represent strain hardening. Modified Kent and Park Model and steel model is given in Appendix A.

TEC 2007 suggests the use of elastic-perfectly plastic or strain hardened moment-rotation relationship to be used in analysis. Figure 2.4 illustrates the moment-rotation relationships.

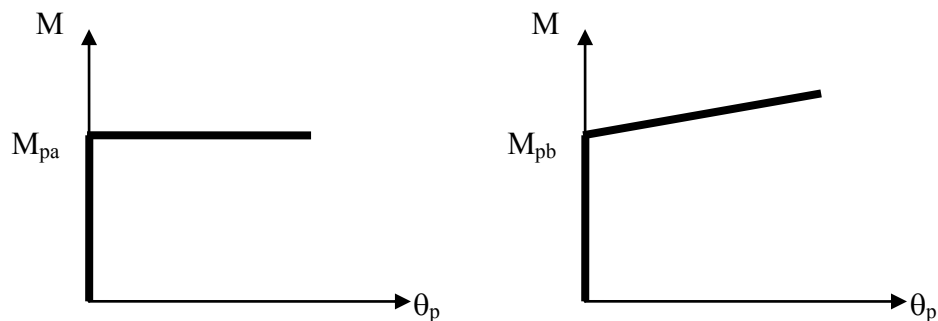


Figure 2.4: Moment Rotation relationships suggested by TEC 2007

In order to obtain yield and ultimate moment and curvature values, diagrams must be converted into bi-linear form. Steps for converting moment curvature diagram into a bilinear form are as follows:

- Ultimate curvature ( $\phi_u$ ) and ultimate moment ( $M_u$ ) is found from the moment curvature diagram.
- First yield of tension steel ( $\epsilon_y = f_y / E_s$ ) or the point where concrete extreme fiber reaches a strain of 0.002 can be regarded as yield point ( $\phi_y, M_y$ ).
- Yield point is further modified by  $M_n/M_y$  factor where  $M_n$  is the moment at which the steel tension strain reaches 0.015 or concrete extreme fiber strain reaches to 0.004, whichever first occurs.

Figure 2.5 explains the procedure schematically.

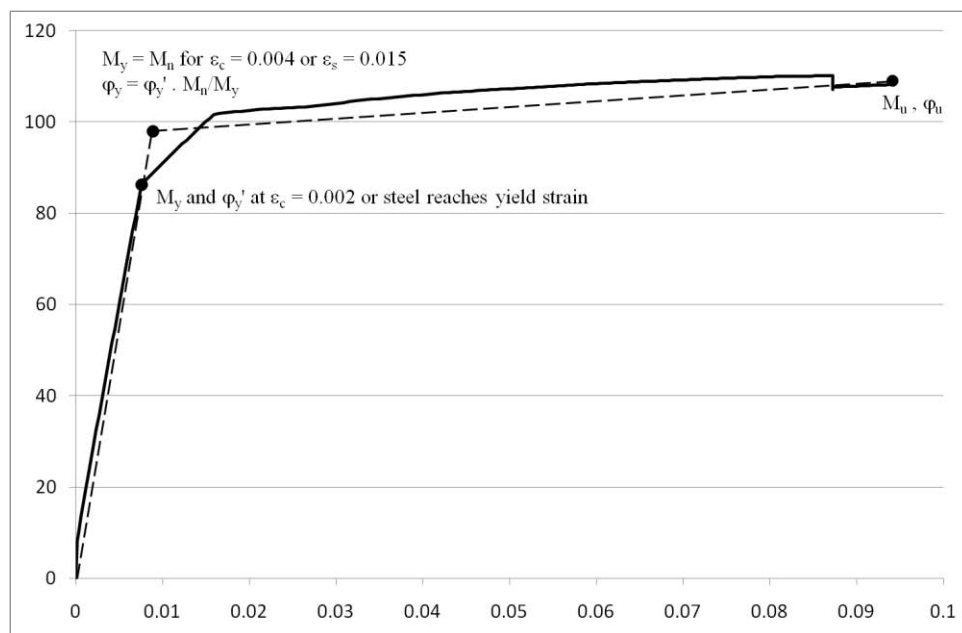


Figure 2.5 : Bilinearization of Moment-Curvature diagram

Moment-Curvature values must be converted into Moment-Rotation pairs in order to use in the analysis softwares. Equations 2.12 can be used to convert curvature values into rotation.

$$\theta_u = (\phi_u - \phi_y) \cdot L_p + \theta_y \quad (2.12)$$

Where,

$\phi_y$  = Yield curvature

$\phi_u$  = Ultimate curvature

$L_p$  = Plastic hinge length of section =  $h / 2$

$L_n$  = Clear Length of Member

$\theta_y$  = Yield Rotation

$\theta_u$  = Ultimate Rotation

Interaction curves are defined for different angles for the section. Other interaction curves can be obtained by Equation 2.13

$$\left( \frac{M_{ux}}{M_{uxo}} \right)^{\frac{\log 0.5}{\log \beta}} + \left( \frac{M_{uy}}{M_{uyo}} \right)^{\frac{\log 0.5}{\log \beta}} = 1 \quad (2.13)$$

Where

$M_{uxo}$  = Uniaxial flexural strength about x-axis

$M_{uyo}$  = Uniaxial flexural strength about y-axis

$M_{ux}$  = Component of biaxial flexural strength on the x-axis at required inclination

$M_{uy}$  = Component of biaxial flexural strength on the y-axis at required inclination

$\beta$  = parameter dictating the shape of interaction surface

### 2.3.2 Static Pushover Analysis

Pushover analysis, in summary, is a step by step procedure in which the lateral loads are applied in certain increments. Each frame element is assigned plastic hinges at their critical sections. As the lateral load increases, these plastic hinges start to activate. Building is “pushed” until a mechanism is obtained or a monitored target displacement is reached. Results, however, are dependent on the lateral load pattern selected. TEC 2007 suggests the use of load pattern associated with dominant elastic mode consistent with the direction of analysis. Distribution

of loads are calculated by multiplication of dominant mode shape  $\phi_n$  with mass of the storey. Calculated loads are assigned to the mass center along two orthogonal directions and about the Z axis. One of the critical assumptions made in the analysis is that the load distribution does not change with plastic hinge formations. There are several adaptive methods [13], [14] in which equivalent lateral loads are calculated at each step using the mode shapes based on instantaneous stiffness matrix and corresponding elastic pseudo-accelerations. Before lateral pushover analysis, a gravity analysis is conducted and the final conditions of this gravity analysis are taken as the initial conditions for lateral pushover analysis. It is worth to note that, in some very weak beam systems, there may be occurrences of beam hinge yieldings due to gravity loading. These preformed hinges must also be considered in lateral pushover analysis. According to the author's experiences in Turkey, this situation is quite frequent.

Turkish Earthquake Code allows the use of static pushover analysis if,

- Building height is less than 25 m above the ground level (except basements)
- Number of storeys is less than 8 (except basements)
- Torsional irregularity coefficient is less than 1.4
- Effective mass participation ratio for the dominant to be used in analysis is greater than or equal to 70%.

### **2.3.3 Modal Pushover Analysis**

Modal Pushover Analysis (MPA) was developed by Chopra and Goel [12]. The main aim was to keep conceptual simplicity and computational attractiveness of pushover procedures with invariant force distribution while providing superior accuracy in estimating seismic demands on buildings.

The MPA was first developed for linearly elastic buildings and it was shown that the procedure is equivalent to well known response spectrum analysis. Method was then enhanced to cover inelastic systems with certain assumptions and approximations. A typical flowchart of operations is given in Figure 2.6

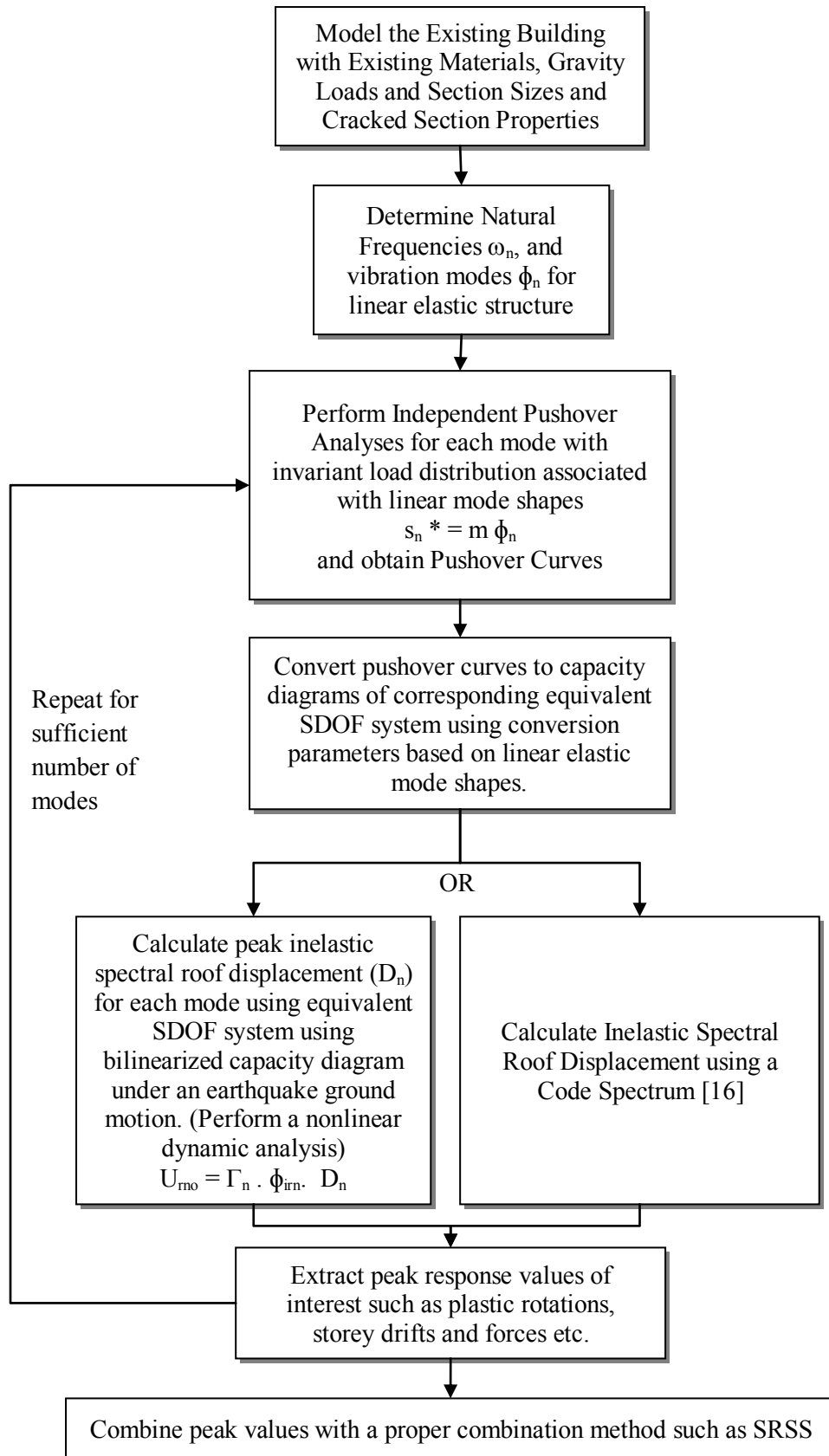


Figure 2.6 : Typical flowchart for Modal Pushover Analysis

One of the assumptions in this method is neglecting coupling effect that may arise between the modal coordinates as the yielding progresses in the structure, i.e., pushover analyses are run independently in each mode by neglecting the effect of other modes in the plastic hinge formation. Another limitation is to use superposition for an inelastic system since superposition is valid for elastic systems. Also, combination method used to combine the peak responses also includes its own approximations.

#### **2.3.4 3D Nonlinear Time History Analysis**

In order to examine the exact nonlinear behavior of building structures, nonlinear time history analysis has to be carried out. In this method, the structure is subjected to real ground motion records. This makes the analysis method quite different from all other approximate analysis methods since the inertial forces are directly determined from these ground motions. Response quantities of the building such as deformations and forces are calculated as a function of time, considering the dynamic properties of the building.

In SAP2000, the nonlinear time-history analysis can be carried out as follows:

- The model representing the building structure is created, vertical loads (dead load and live load), member properties and member nonlinear behaviors are defined and assigned to the model.
- Floor masses are assigned.
- Hinge properties are defined and these properties are assigned to the member ends considering end-offsets.
- The ground motion record is defined as a function of acceleration versus time.
- An initial loading is applied to the model like it is done in the pushover analyses to represent the initial case. This case must be composed of the dead loads and reduced live loads.

The analysis and the time history parameters are defined in order to perform a nonlinear time history analysis. In “time history type” option, the

“direct-integration” time-history analysis solves equations for the entire structure at each time step while “modal” time-history analysis uses the method of mode superposition. In this study, direct integration method is used for the analyses.

The total time of the analysis is the number of output time steps multiplied by the output time-step size. The results are saved at time is equal to zero and at the given subsequent output time steps; although during the analysis intermediate results are computed at every time step of every applied-load time-history function.

For the damping calculations, there are three options in SAP2000. These are; “direct specification”, “specifying modal damping by period” and “specifying damping by frequency” options. In “direct specification” option, the damping values are entered considering mass and stiffness proportional coefficients. In “specify modal damping by period” option, the damping values with the first and second periods are assigned. Using these values, the program calculates the mass proportional and stiffness proportional coefficients. “specify modal damping by frequency” has the same interface but this time frequency values instead of periods are assigned. In the analyses of the analytical models “specify modal damping by period” option is used

In addition to these, the nonlinear parameters must be entered to the program. “Maximum total steps” is the maximum number of steps allowed in the analysis. It may include saved steps as well as the intermediate sub steps, whose results are not saved. “Maximum null steps” is the total number of the null steps that occur during the nonlinear solution procedure when a frame hinge is trying to unload and iteration does not converge and a smaller step size is attempted. “Maximum iterations per step iteration” is used to make sure that equilibrium is achieved at each step of the analysis and the “iteration convergence tolerance” is used to make sure that equilibrium is achieved at each step of the analysis.

The analysis stops at every output time step, and at every time step where one of the input time-history function is defined. In addition, an upper limit on the step size used for integration may be set. “maximum substep size” used for this option while the “minimum substep size” is used when the nonlinear iteration cannot converge within the specified maximum number of iterations.

### 2.3.5 Simplified Procedure for 3D Nonlinear Time History Analysis

Performing a 3D nonlinear time history analysis for a 3-dimensional frame is quite time consuming. Moreover, since structure is subject to cyclic accelerations, solution usually has difficulty to converge which leads to an iterative process. That iterative process is composed of “Modify the input – Run the analysis” steps which makes the intrinsic nature of the analysis more time consuming. In this study, time history analysis was utilized only for determining the demand drifts, not internal forces or plastic rotations.

Procedure consists of following steps:

- Create identical 3D models for the building. In each model, restrain the joints of a separate storey level. Each restrained level should be carrying the dead load of remaining upper storeys.
- Apply static X and Y unit loads to the diaphragm node above the restrained storey level for each model.
- Run static pushover analyses using the unit loads defined. Obtain static pushover curves for each storey from different models. (i.e. pushover curve for Storey 1 comes from model 1, storey 2 comes from model 2 etc.). This is explained in Figure 2.7
- Using the static pushover curves (i.e. load-deformation relationship in the direction of considered DOF), create a lumped 2D model of the building.
- In 2D model, assign storey masses and rotational inertias of the storeys to the nodes. Define “multilinear plastic (takeda)” links between the nodes.
- Each link will be assigned the force deformation relationship obtained from the static pushover analyses. See Figure 2.8 for illustration.
- Define the earthquake functions and perform nonlinear time history analysis.

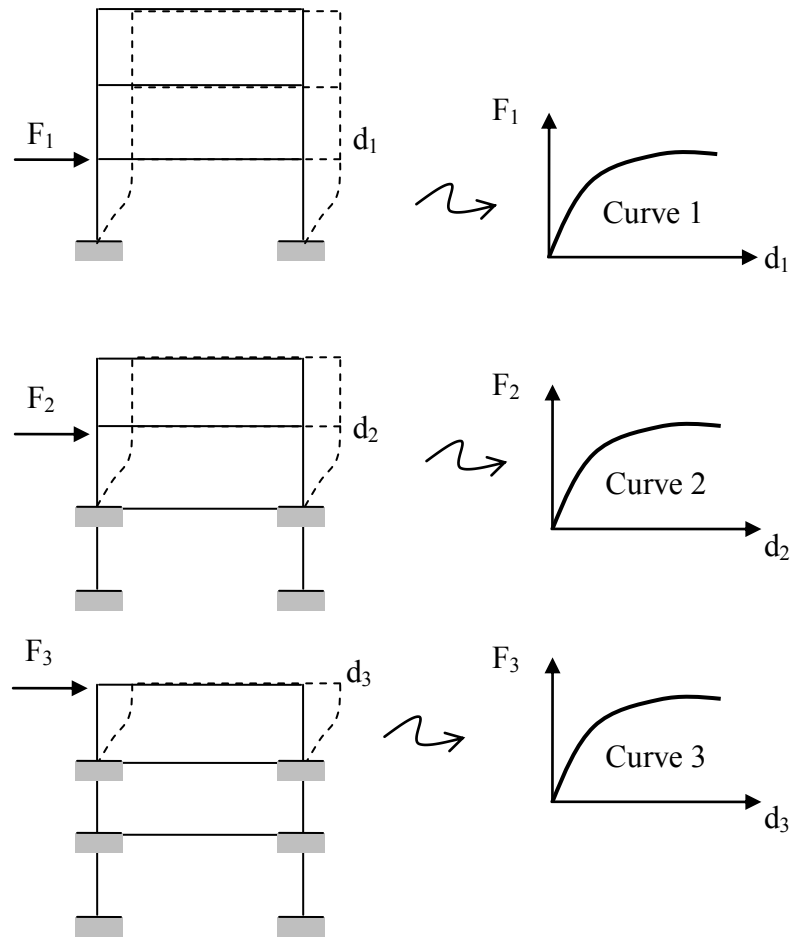


Figure 2.7 : Obtaining load deformation relationship for each storey

- List the node deformation results for each output time step. Find the maximum interstorey drifts for each storey node. Take the average or envelope of the drift demands for each separate earthquake case.
- Using the demand drifts, go back to static pushover models and extract the plastic rotations and internal forces related with the step which corresponds to the obtained demand.
- Merge frame and hinge member results and perform member by member assessment.

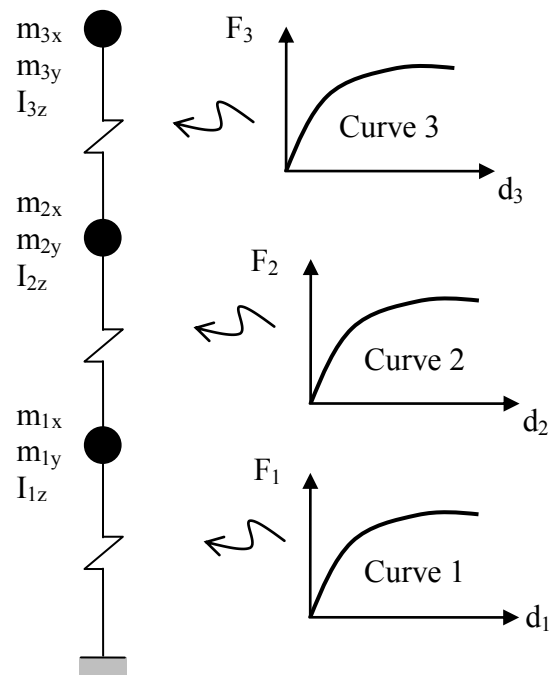


Figure 2.8 : Establishing 2D nonlinear model for time history analysis

### 2.3.6 Earthquake Record Selection Criteria in Turkish Earthquake Code 2007

Synthetic or adjusted accelerograms can be used in time history analyses according to TEC 2007. Criteria for selected records can be summarized as follows:

- At least three records will be used. Maximum values for responses must be used for 3 earthquakes. Average values can be used if 7 earthquakes are used.
- Strong motion duration can not be longer than 5 times 1st period of vibration or 15 seconds.
- Average spectral acceleration value corresponding to  $T=0$  can not be less than  $A_0g$  value defined in TEC2007.

- Average spectral acceleration values produced from the synthetic records for 5% damping ratio will not be less than 90% of the elastic design spectrum for periods between  $0.2T_1$  and  $2T_1$ .

In this study, selection of earthquakes was done according to Fahjan [15] However, scaling factors were modified by comparing the spectral acceleration value of derived 5% SDOF spectrum with the code spectrum for the period of structure. This is illustrated in Figure ??

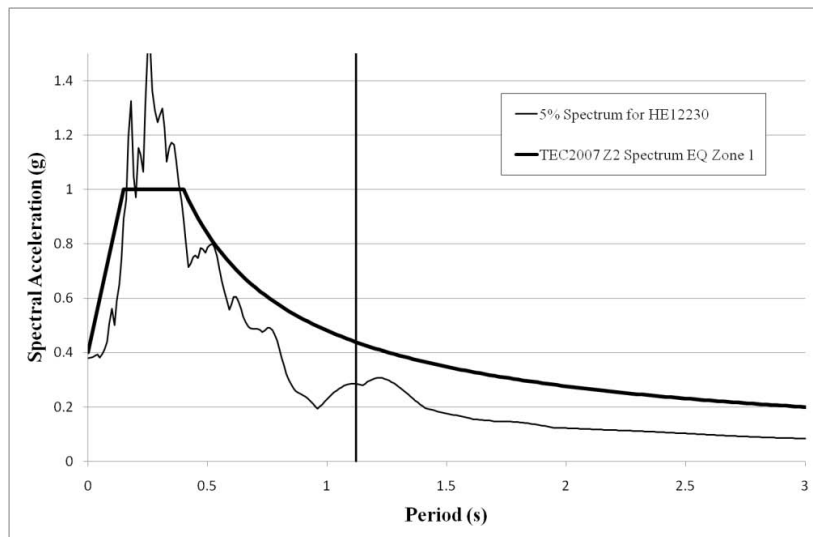


Figure 2.9: Comparison of code spectrum with derived spectrum

### 2.3.7 Turkish Earthquake Code 2007 Nonlinear Assessment Procedure

Pushover analysis yields a Roof Displacement-Base Shear curve which is also known as Capacity Curve. If a modal pushover analysis is done, there will be more than one capacity curves, i.e. for each mode. This curve can represent the nonlinear behaviour of the building under any ground motions with assumptions and approximations involved. The major task after the pushover analysis to

estimate the seismic demand, be it by a specific ground motion or a code spectrum for a definite performance level. In the literature, there are several methods proposed (ATC-40, FEMA 356). The method explained in this study is consistent with the TEC 2007 requirements.

The capacity curve obtained at the end of the pushover analysis is in Force (V) and Displacement ( $\Delta$ ) coordinates. This curve must be transformed into Spectral Acceleration ( $S_a$ ) and Spectral Displacement ( $S_d$ ) coordinates. These conversions are explained in the following equations.

Conversion for Capacity Curve Force Values can be done by using Equation 2.14

$$S_a = \frac{V}{m \cdot \alpha_1} \quad (2.14)$$

Displacement values are transformed into spectral displacement by equation 2.15

$$S_d = \Delta \cdot \Gamma_1 \cdot \phi_{r1} \quad (2.15)$$

Code spectra are generally given in  $S_a - T$  coordinates. In order to convert T into spectral displacement, equation 2.16 can be used

$$S_d = \frac{g \cdot S_a \cdot T^2}{4 \cdot \pi^2} \quad (2.16)$$

Where,

$\Gamma_1$  = Modal participation ratio

$\phi_{r1}$  = roof Displacement for the dominant mode considered

m = Total Mass

$\alpha_1$  = Modal Mass participation ratio for the first mode

Figure 2.10 illustrates the calculation of  $S_{de}$  by using  $S_{ae}$ .

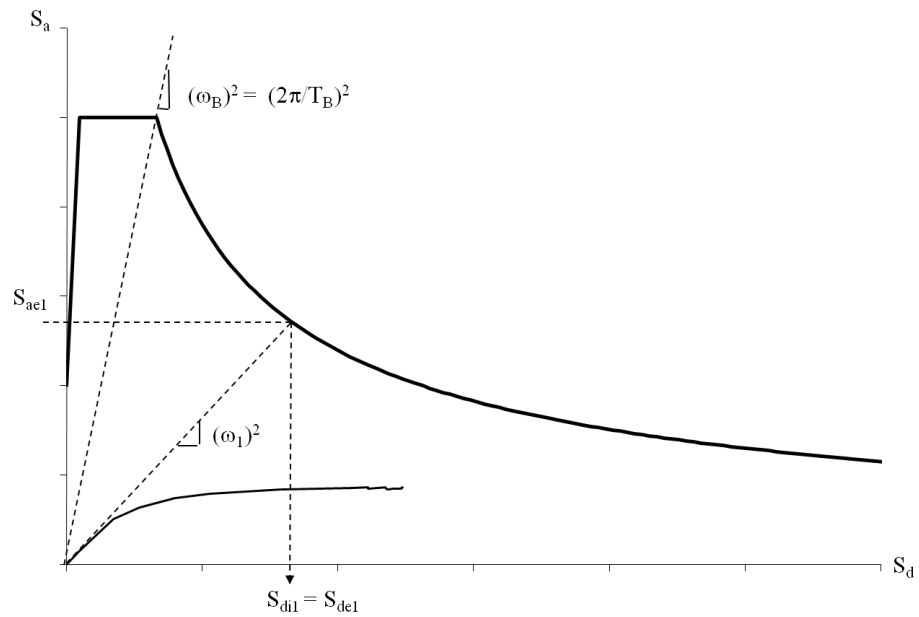


Figure 2.10: Calculation of Inelastic demand

If the period of natural vibration for the selected direction is greater than the corner period of the spectrum inelastic spectral displacement can be accepted as equal to elastic spectral displacement.

If the period value is smaller than the corner period then an iterative approach is used to obtain the inelastic spectral displacement demand.

After the target displacement is calculated as explained above, the response quantities such as member forces, plastic rotations, displacements are extracted from results database. Similar to the elastic assessment procedure, ductility check of the member is performed first. The shear force ( $V_e$ ) values directly obtained at target displacement is compared with TS500 shear capacities ( $V_r = V_c + V_w$ ).

If the member is ductile (i.e.  $V_r > V_e$ ), the performance check is done by using the concrete and steel strains inside the section. For different performance levels, different strain limits are available.

Minimum Damage limits for ductile sections are stated by equation 2.17.  $\epsilon_{cu}$  is the strain at the extreme concrete fiber whereas  $\epsilon_s$  is the strain at steel.

$$(\varepsilon_{cu})_{IO} = 0.0035 ; (\varepsilon_s)_{IO} = 0.01 \quad (2.17)$$

Life Safety (LS) limits for ductile sections are given by equation 2.18.  $\varepsilon_{cg}$  is the strain at the concrete fiber at the top of confined region surrounded by links.  $\varepsilon_s$  is the strain value at steel.  $\rho_s$  is volumetric ratio of transverse reinforcement required by section 3.2.8 of TEC 2007.  $\rho_{sm}$  is the existing volumetric ratio of transverse reinforcement in the section.

$$(\varepsilon_{cg})_{LS} = 0.0035 + 0.01 (\rho_s / \rho_{sm}) \leq 0.0135 ; (\varepsilon_s)_{LS} = 0.04 \quad (2.18)$$

Collapse prevention limits are given by equation 2.19. Notation is same as the ones given for life safety limits.

$$(\varepsilon_{cg})_{CP} = 0.004 + 0.014 (\rho_s / \rho_{sm}) \leq 0.018 ; (\varepsilon_s)_{CP} = 0.06 \quad (2.19)$$

In order to obtain strain values inside the section, total curvature must be calculated. Analysis software yields plastic rotation at demand displacement. Plastic curvature ( $\varphi_p$ ) is calculated by equation 2.20

$$\varphi_p = \frac{\theta_p}{L_p} \quad (2.20)$$

Total curvature ( $\varphi_t$ ) is the sum of yield curvature and plastic curvature. Yield curvature is known since the section analysis should have been done before.

$$\varphi_t = \varphi_y + \varphi_p \quad (2.21)$$

Strain at the extreme fiber can be calculated by equation 2.22.  $c$  is the depth of neutral axis measured from the top of the section.

$$\varepsilon_{cu} = \varphi_t \cdot c \quad (2.22)$$

Global performance check needs to be done after member performance determination. Table 2.2 summarizes the performance criteria for global evaluation.

## **CHAPTER 3**

### **CFRP MODELLING AND APPLICATION**

#### **3.1. STRUCTURAL BEHAVIOR**

Experimental [7] and analytical studies [8] revealed that when a reinforced concrete frame with masonry infill wall is subjected to lateral loads, the infill wall acts as a diagonal strut while the infill is separated from the frame at the opposite side. Applying CFRP retrofit scheme reduces the inter-storey deformations by acting as tension ties. Diagonal FRPs are bonded on the infill wall surface. These FRPs are then tied to the framing members using FRP anchors in order to realize this tension tie formation. These tension ties contribute to load carrying capacity and the lateral stiffness of the existing reinforced concrete frame structure. Moreover, in addition to the tension ties, compression strut provide additional strength and stiffness along the infill diagonal.

#### **3.2. MATHEMATICAL MODEL**

CFRP strengthened masonry infill walls can be modelled by using a compression strut –tension tie model as shown in Figure 3.1. These ties need to be assigned sectional properties in order to be used in linear and nonlinear analyses.

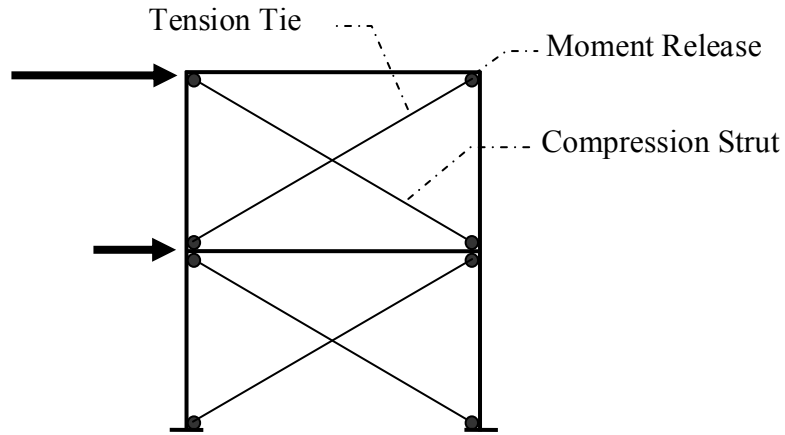


Figure 3.1: Analytical Model of CFRP retrofitted Masonry Infill Wall

Physical illustration of a masonry infill wall is given in Figure 3.2

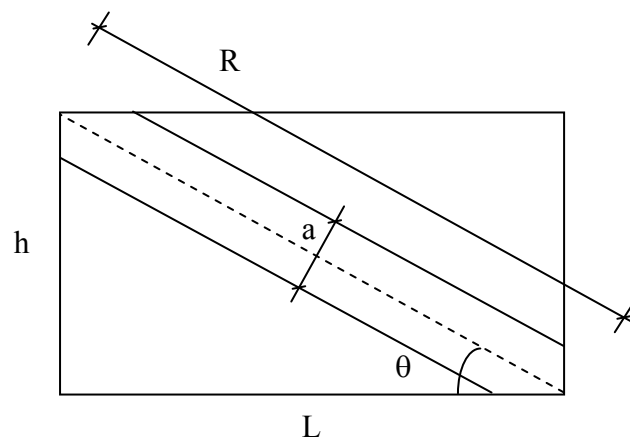


Figure 3.2: Masonry Infill Wall Parameters

A trilinear stress-strain curve was proposed for tension ties by Binici et. al. [9]. Compression tie model is also a trilinear model. Analytical and simplified models proposed by Binici and Ozcebe and Ozcelik [9] is given in Figure 3.3

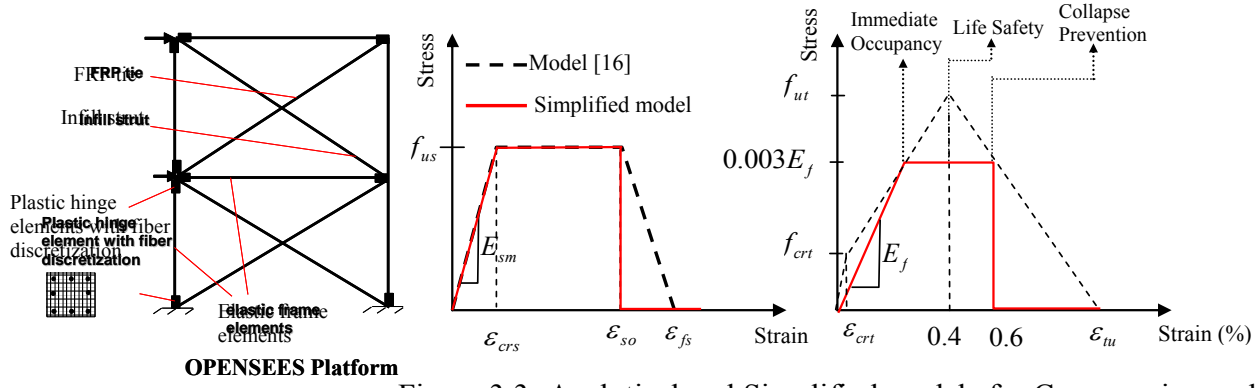


Figure 3.3: Analytical and Simplified models for Compression and Tension ties.

According to this analytical model, area of the composite tension can be calculated by Equation 3.1

$$A_{tie} = w_f \cdot t_{tie} \quad (3.1)$$

$w_f$  is the width of provided CFRP.  $t_{tie}$  can be calculated by Equation 3.2

$$t_{tie} = t_f + t_p + t_{in} \quad (3.2)$$

where  $t_f$ ,  $t_p$  and  $t_{in}$  are the thicknesses for fiber, plaster and infill respectively. Cracking stress of the tie ( $f_{crt}$ ) can be found by Equation 3.3.

$$f_{crt} = \frac{V_{crt}}{A_{tie}} \quad (3.3)$$

$$V_{crt} = f_{pt} w_f \left( (t_{in} + t_p) + \frac{E_f}{E_m} t_f \right) \quad (3.4)$$

$f_{pt}$  is the tensile strength of the plaster.  $E_f$  and  $E_m$  are elasticity modulus for FRP and mortar. Tensile capacity  $V_{ut}$  and the tensile strength  $f_{ut}$  can be calculated by using Equations 3.5 and 3.6.

$$V_{ut} = \varepsilon_{f,eff} w_f t_f E_f \quad (3.5)$$

$$f_{ut} = \frac{V_{ut}}{A_{ie}} \quad (3.6)$$

Area of compression strut is given by Equation 3.7

$$A_{st} = w_s t_{st} \quad (3.7)$$

$$t_{st} = t_p + t_{in} \quad (3.8)$$

$$w_s = \frac{(1-\alpha)\alpha h}{\cos \theta} \quad (3.9)$$

Where h is the height of the infill,  $\theta$  is strut inclination angle and  $\alpha$  is dimensionless parameter to account for frame infill contact length.  $\alpha$  is given by Equation 3.10. Schematic representation of parameters are given in Figure 3.2.

$$\alpha = \sqrt{\frac{2(M_{pj} + 0.2M_{pc})}{h^2 t_{st} f_{mc}}} \quad (3.10)$$

$M_{pj}$  is the minimum of the moment capacities of the column or the beam,  $M_{pc}$  is the moment capacity of the column.  $f_{mc}$  is the compressive strength of the infill and plaster composite. Ultimate strength ( $V_{us}$ ) of diagonal compressive strength is minimum of sliding shear ( $V_{ss}$ ) or corner crushing ( $V_{cc}$ ) capacities. Calculation of these capacities are given in Equations 3.12 and 3.13.

$$V_{us} = \min(V_{ss}, V_{cc}) \quad (3.11)$$

$$V_{ss} = f_{mv} L t_{st} \quad (3.12)$$

$$V_{cc} = 250 t_{st} f_{mc} \quad (3.13)$$

Ultimate strength is given by,

$$f_{us} = \frac{V_{us}}{A_{st}} \quad (3.14)$$

In Equation 3.12,  $f_{mw}$  is the shear strength of the mortar/plaster and  $L$  is the width of the infill wall.  $f_{mc}$  is the corner crushing strength and  $E_{sm}$  is the elasticity modulus of the infill material.

$$f_{mc} = \frac{f_{in}t_{in} + f_m t_p}{t_{st}} \quad (3.15)$$

$$E_{sm} = \frac{E_{in}t_{in} + E_m t_p}{t_{st}} \quad (3.16)$$

A sample nonlinear axial hinge is given in Figure 3.4. Details of the calculation both for linear and nonlinear properties in given in Appendix B.

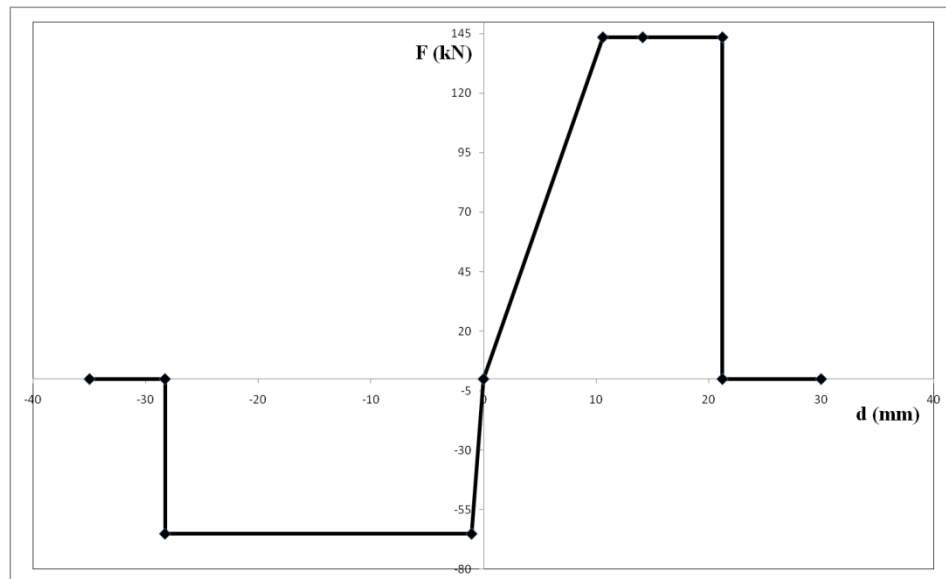


Figure 3.4: Axial Plastic Hinge representing the masonry infill wall retrofitted with CFRP

It should be noted that, during modelling, this P hinges should be assigned just at the middle of the strut members.

### 3.3. TEC 2007 CONSIDERATIONS

According to the TEC 2007 provisions, the masonry infill walls with  $0.5 \leq Length / Height \leq 2$  can be retrofitted with CFRP. Formation of the compression strut inside the existing frame is vital and adequate anchorage must be provided to achieve this.

TEC 2007 [1] proposes Equation 3.17 to calculate the Tension Capacity of diagonal tension tie. When carefully investigated it is also the tensile strength suggested by the mentioned simplified design model.

$$T_f = 0.003 E_f w_f t_f \quad (3.17)$$

Axial stiffness ( $k_t$ ) of the diagonal tension strut is calculated by Equation 3.18

$$k_t = \frac{E_f w_f t_f}{r_{wall}} \quad (3.18)$$

where  $E_f$ ,  $w_f$  and  $t_f$  are Modulus of Elasticity (230000 MPa), width and thickness (0.16 mm single layer) of the CFRP strip respectively.  $r_{wall}$  denotes the diagonal length of the masonry infill wall.  $w_f$  cannot be greater than the value calculated for the compression strut by Equation 3.19

$$a_{wall} = 0.175 (\lambda_{wall} h_k)^{-0.4} r_{wall} \quad (3.19)$$

where  $a_{wall}$  is diagonal compression strut width,  $h_k$  is the column dimension.  $\lambda_{wall}$  is calculated by Equation 3.20.

$$\lambda_{wall} = \left[ \frac{E_{wall} t_{wall} \sin 2\theta}{4E_c I_k h_{wall}} \right]^{\frac{1}{4}} \quad (3.20)$$

$E_{wall}$  and  $E_c$  are the moduli of elasticity for masonry infill and existing reinforced concrete frame respectively.  $I_k$  is the moment of inertia of the column and  $\theta$  is the horizontal angle of the diagonal.

Axial stiffness of the compression strut is calculated by Equation 3.21

$$k_{wall} = \frac{a_{wall} t_{wall} E_{wall}}{r_{wall}} \quad (3.21)$$

According to TEC 2007, shear strength of the compression or tension strut is the horizontal component of compressive or tensile strength of the diagonal strut.

For the compression strut, Shear capacity is given by the Equation 3.22

$$V_{wall} = A_{wall} (\tau_{wall} + f_{yd} \rho_{sh}) \leq 0.22 A_{wall} f_{wall} \quad (3.22)$$

$\tau_{wall}$  is the shear strength of retrofitted infill.  $A_{wall}$  is the horizontal section area for the wall. If the masonry infill is retrofitted with mesh reinforcement, then,  $f_{yd}$  is the yield strength of the mesh steel.  $\rho_{sh}$  is the ratio of the transverse reinforcement area to wall section area.

Turkish Earthquake Code suggests following material properties to be used in calculations

Hollow Brick

$$E_{wall} = 1000 \text{ Mpa} ; f_{wall} = 1 \text{ MPa} ; \tau_{wall} = 0.15 \text{ Mpa} \quad (3.23)$$

Solid Clay Brick

$$E_{wall} = 1000 \text{ Mpa} ; f_{wall} = 2 \text{ MPa} ; \tau_{wall} = 0.25 \text{ Mpa} \quad (3.24)$$

Light Concrete Block

$$E_{wall} = 1000 \text{ Mpa} ; f_{wall} = 1.5 \text{ MPa} ; \tau_{wall} = 0.20 \text{ Mpa} \quad (3.25)$$

### 3.5. APPLICATION DETAILS

As it was stated previously, FRP retrofit scheme is used to reduce inter-storey deformation demands by using CFRPs to act as tension ties. To achieve this purpose, diagonal CFRPs bonded on the infill wall are tied to the framing members using FRP anchors as shown in Figure 3.5. Embedded fan type FRP anchors formed by rolling FRP sheets are connected in the corner region in order to achieve efficient use of FRP materials. To eliminate premature debonding of FRP from the plaster surface anchor dowels are used along the thickness of the infill wall.

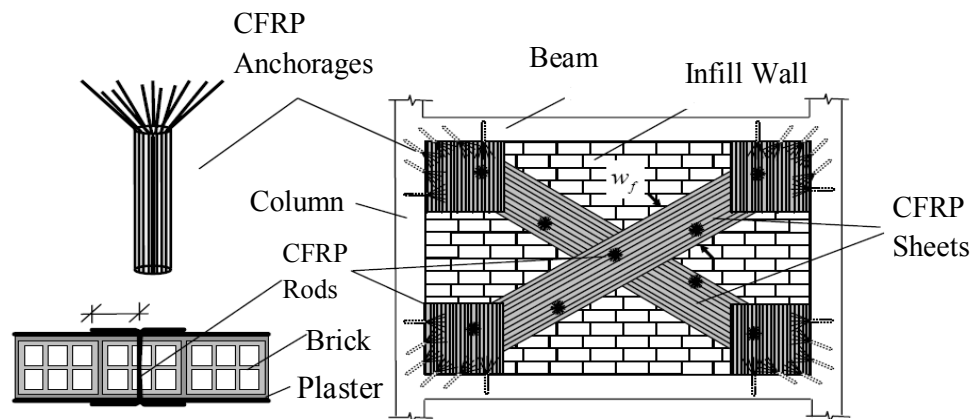


Figure 3.5: Application of CFRP on the masonry infill wall.

Turkish Earthquake Code requires some constructive conditions for the application of CFRPs.

- Walls which have a H/L aspect ratio between 0.5 and 2 can be retrofitted using CFRPs
- In order for the effective load transfer to realize between tension tie and the frame members, there should be at least a 30 mm spacing between outer faces of frame members and the masonry infill surface.

- CFRP square flag sheets having a width of at least  $1.5w_f$  should be used at the corners in order to distribute the stresses evenly at the anchor region.
- CFRP application should be done for each face of the masonry infill. Surface anchors must be used through the thickness of the infill in order to tie two separate CFRP sheet on two separate face.
- Surface anchors must be spaced at least 600 mm from each other. Surface anchors should not be closer than 150 mm to the CFRP strip edge.
- Load transfer between CFRP strip and frame members are done with CFRP dowels. CFRP strips are saturated with epoxy and rolled around a silicon stick. Anchor ends are shaped as fan.
- A anchor drill which is clean for dust is prepared inside the frame members. This anchor socket is injected with epoxy and CFRP anchors are placed inside the anchor socket. CFRP strip width used for anchor production should not be less than 100 mm. Diameter of the anchor holes should not be less then 10 mm, while they should be drilled at least up to 150 mm depth. An anchor dowell prepared this way can carry a tension load up to 20 kN or the tensile capacity of the LP anchor strip rolled around silicon.

A typical shop drawing prepared for the CFRP retrofit project of the case study building in this study is given in Figure 3.6, Figure 3.7 and Figure 3.8

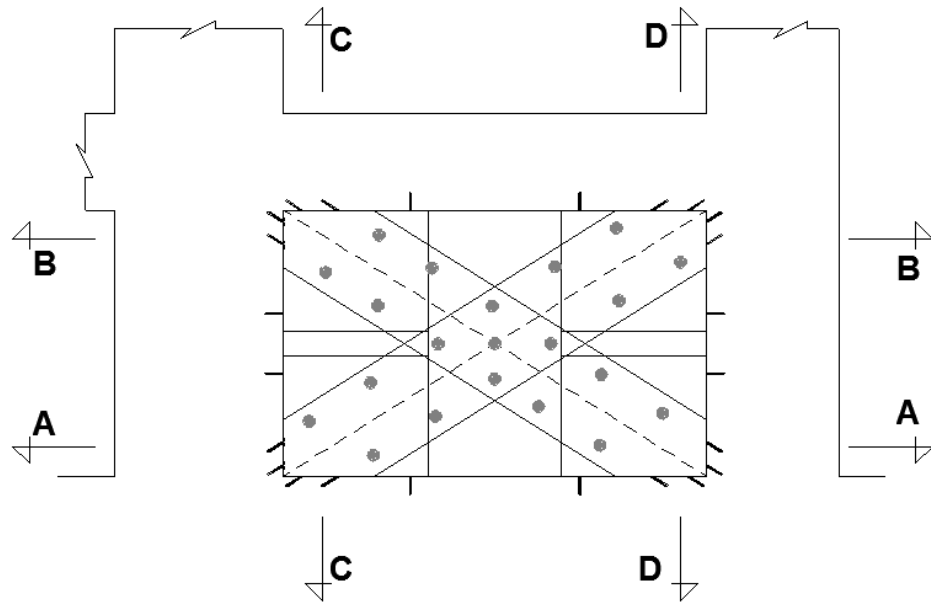


Figure 3.6: Shop drawing for masonry infill wall

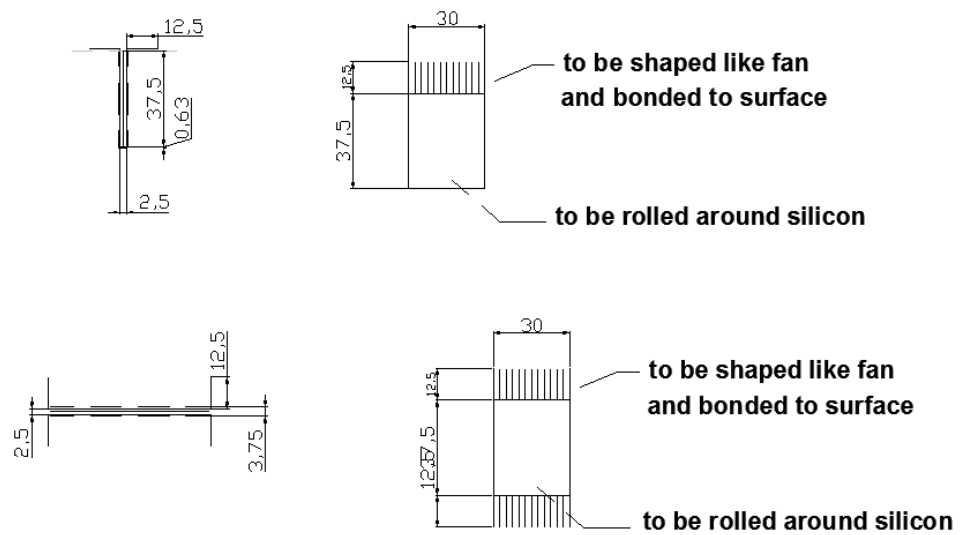


Figure 3.7: Frame anchor dowel and surface anchor details

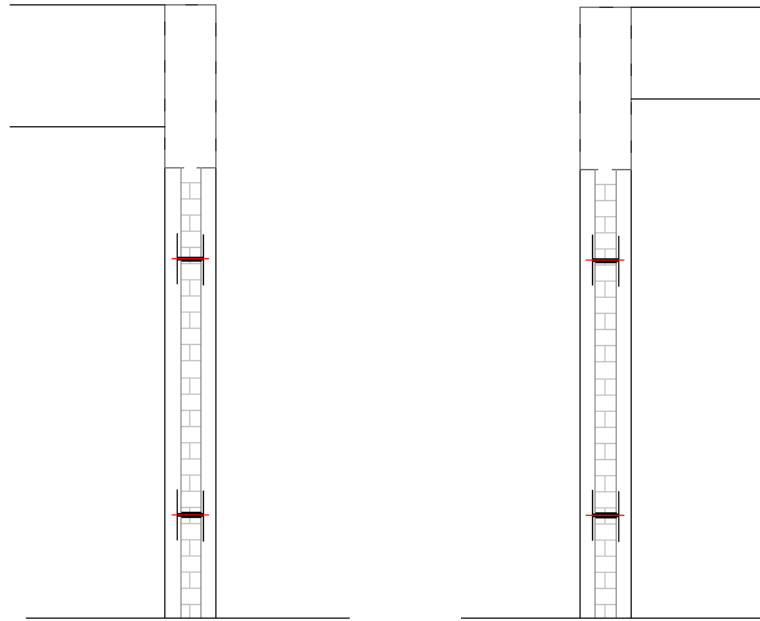
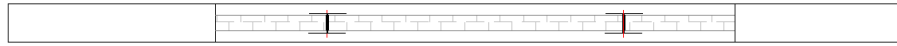


Figure 3.8: Surface anchors

# CHAPTER 4

## ANALYZED STRUCTURE

### 4.1. GENERAL INFORMATION ABOUT BUILDING AND STRUCTURAL SYSTEM

The building named “Antakya Municipality A2 Block”, is located in Sümer Mahallesi, Antakya. Construction year is 1974. According to TEC 2007, city of Antakya is located in Earthquake Zone 1, which corresponds to a effective Ground Acceleration Coefficient of  $A_0 = 0.4$ . Earthquake zone and location of the building is given in Figure 4.1.

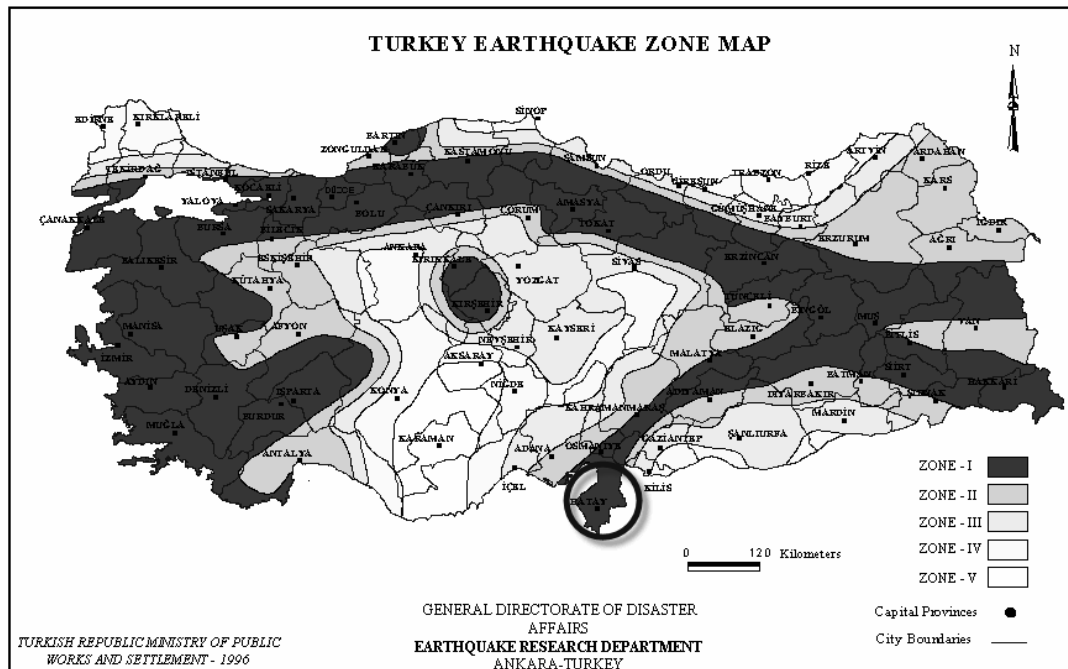


Figure 4.1: Earthquake Zones of Turkey (1996)

As the building is used for residential purposes, the importance factor is given as 1 ( $I = 1$ ) by the code. However, this importance factor is ignored in the assessment procedure according to the code.

Structural system is composed of reinforced concrete frames. There are no shearwall members which should have a  $1 / 7$  thickness over length ratio according to TEC 2007. Building has 9 typical storeys with one ground floor. Views from the building is given in Figure 4.2. Storey and member section information is summarized in Table 4.1. The building has a total height of 28.8 m. Typical floor plan is given in Figure 4.3.



Figure 4.2: Existing State of the building Front and Rear View

Table 4.1: Storey and Section Information for the structure

Storey	Height (m)	Floor Area (m <sup>2</sup> )	Column Dimensions	Beam Dimensions
Basement	3.6	415	25x50 25x60 25x90 25x120 25x140	25x80 25x120
Ground	4.8	415	“	25x80 25x120
1	3	415	“	25x60 25x80 25x100
2	3	415	“	“
3	3	415	“	“
4	3	415	“	25x60 25x80
5	3	415	“	“
6	3	415	“	“
7	3	415	“	“
8	3	415	“	“

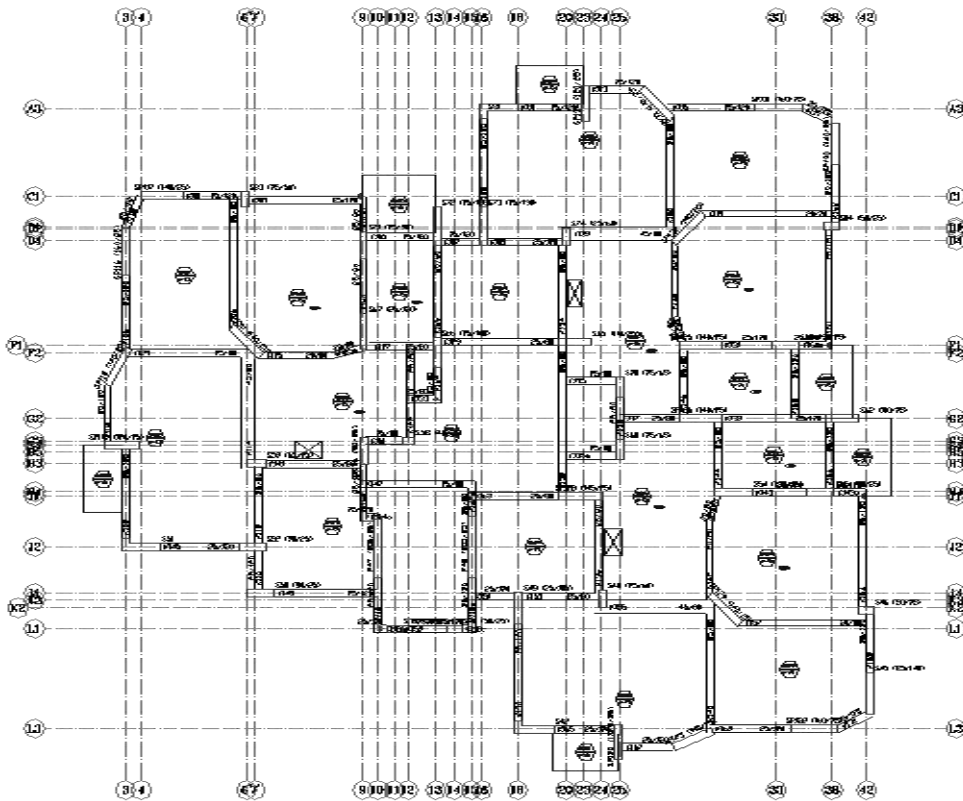


Figure 4.3: Typical Floor Plan of the existing building

## 4.2. EXISTING MATERIAL AND SOIL CONDITIONS

A detailed site survey has been conducted to determine the existing state of the structure. According to this survey, the concrete compressive strength was determined as  $f_{ck} = 10$  MPa. The reinforcement steel used in concrete sections is S220 Plain Bar. There are incidents of corrosion especially at basement and ground floor. The survey results show that the on-site reinforcement amount are in 99% compliance with the blueprints of the buildings. Typical stirrup layout in columns and beams is  $\phi 8/20/25$  with a clear cover of 25 mm. There is no confinement in support regions. Thus, the stirrup layout is clearly inadequate for the current TEC 2007 detailing provisions and sufficient energy dissipation and deformation capacity at critical regions. Building satisfies the “detailed level of information” criteria explained in TEC 2007.

Geotechnical investigations reveal that the soil beneath the structure can be classified as Z2. Spectrum corner periods are  $T_A=0.15$  sec and  $T_B=0.40$  sec. Turkish Earthquake Code Spectrum for Z2 is given in Figure 4.4.

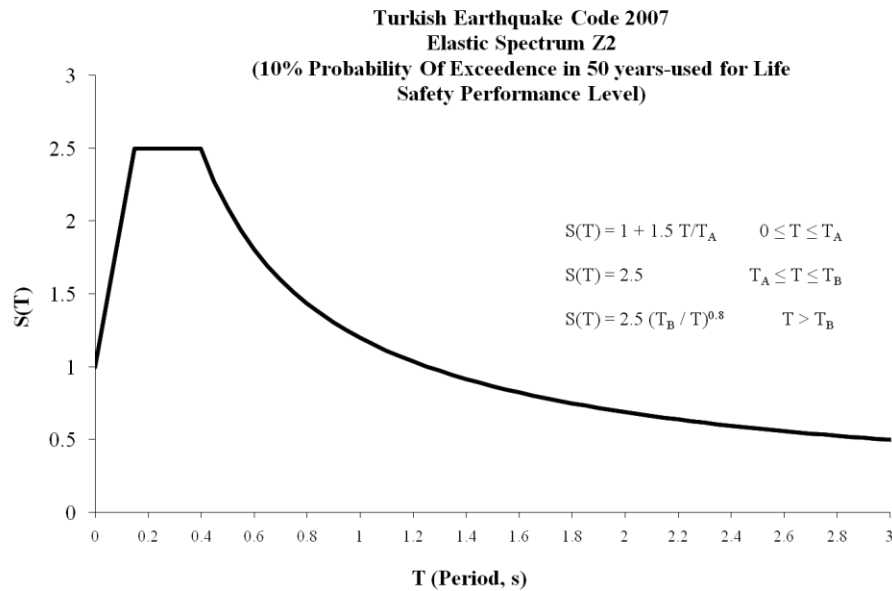


Figure 4.4: TEC 2007 Elastic Spectrum for Soil Type Z2

### 4.3. MODELLING

Three dimensional finite element model of the building was created by using frame elements for beams and columns. Shearwalls (both in existing and retrofitted buildings) were also modelled by frame elements defined at their midpoints. Slab loads were decomposed onto the beams using yield line theory. Rigid diaphragms were utilized at each storey level. At each beam-column intersection, rigid end-offsets were introduced. The building was assumed to be fixed at foundation level, thus, no elastic soil springs were assigned to foundation nodes. Figure 4.5 and 4.6 shows the 3D solid and analytical model of the existing building.

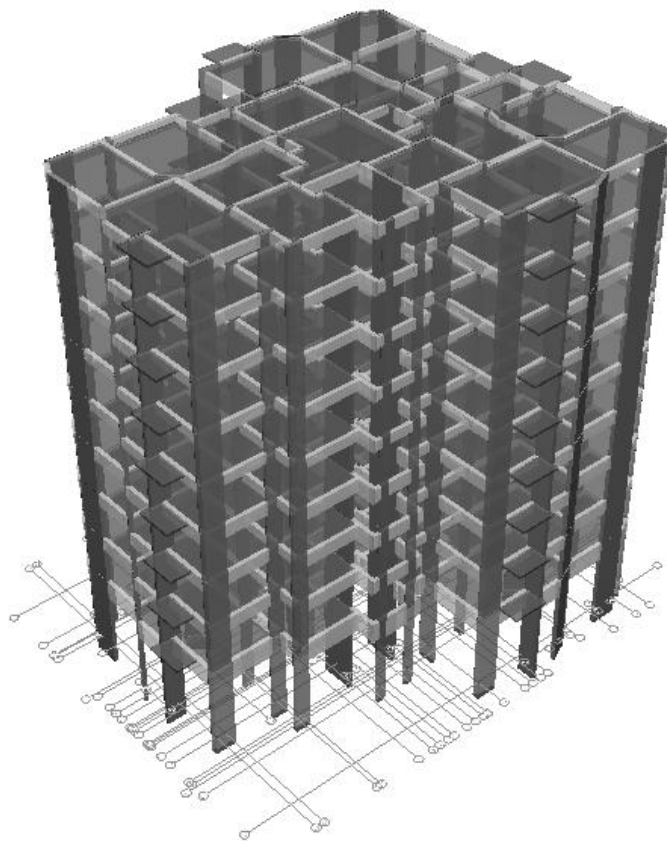


Figure 4.5: Solid Rendered Model of Existing Building

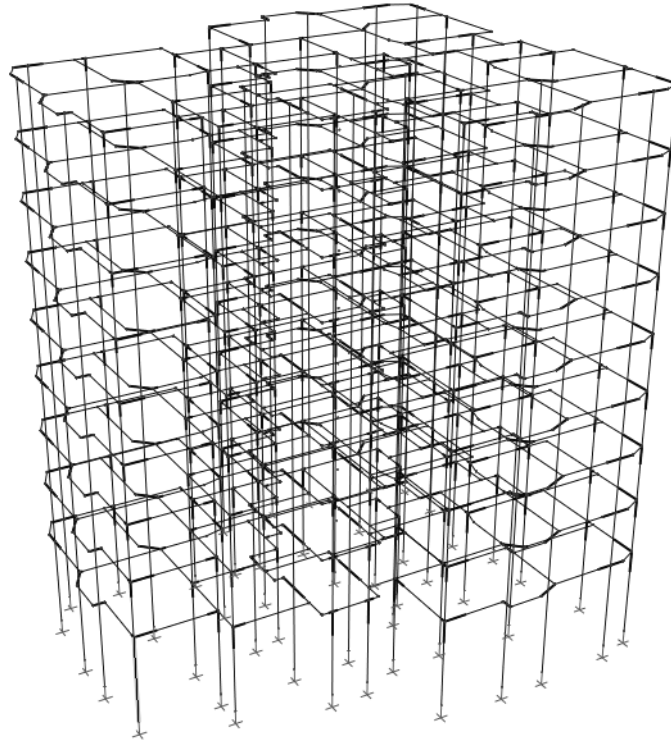


Figure 4.6: Analytical Model Of Existing Building

CFRP strengthened masonry infill walls were modelled by using a compression strut –tension tie model details of which was thoroughly explained in Chapter 3.

#### **4.4. ANALYSIS AND ASSESSMENT OF THE BUILDING USING LINEAR ELASTIC METHOD**

##### **4.4.1 Existing Building**

Elastic method of analysis was performed with mode superposition. Modal analysis results are tabulated in Table 4.2.

Table 4.2: Elastic Modal Characteristics of Existing Building

Mode	Period (sec)	%Mass – Ux	%Mass – Uy	%Mass – Rz
1	1.12	0.7	66.2	4.3
2	0.97	70.3	1.1	0.2
3	0.79	0.5	4.3	67.4
4	0.33	0.1	13.5	0.9
5	0.29	14.5	0.1	0.02
6	0.25	0.05	0.7	12.7
7	0.16	0.03	3.4	0.3
8	0.14	3.65	0.02	0
9	0.13	0.01	0.2	2.9
10	0.10	0.01	1.4	0.1

Force based assessment technique was applied. Details of the linear elastic assessment technique was explained in Chapter 2. DCR values for each member were calculated and compared with the limit values in Tables 2.3, 2.4, 2.5, 2.6, 2.7 and 2.8. Damage Levels of members were determined and the performance criteria were checked against the member damage levels. Bar charts summarizing the assessment results are presented in Figure 4.7 and Figure 4.8.

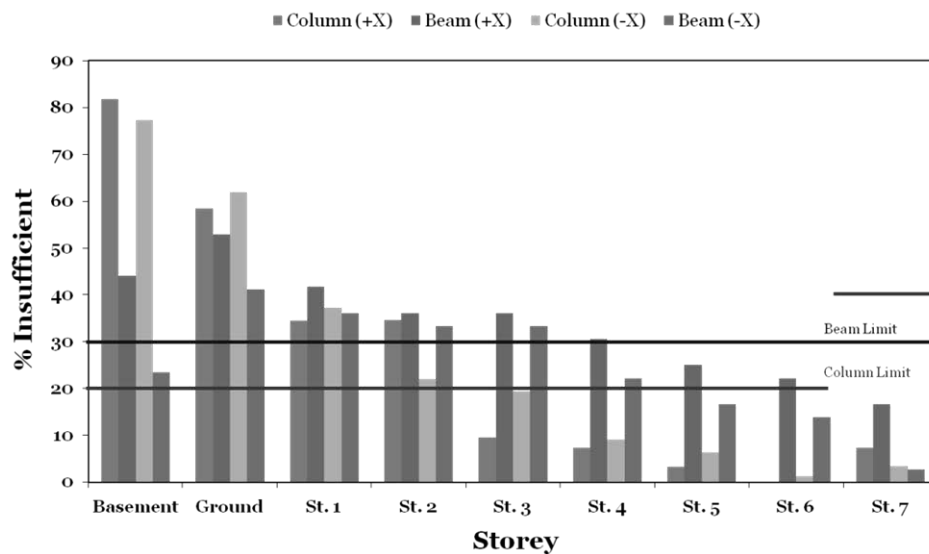


Figure 4.7: Existing Building X Direction Assessment Summary

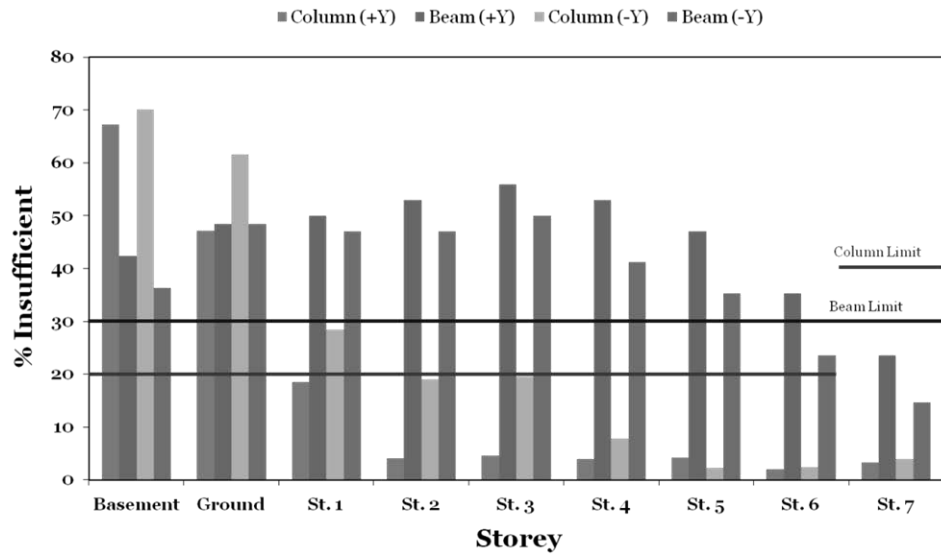


Figure 4.8: Existing Building Y Direction Assessment Summary

At the ground floor, the ratio of shear force carried by columns in high damage region over the storey shear forces become as high as 70%. Beams in X and Y direction in high damage region comprises a percentage as high as 70% of total number of beams in that direction for the investigated storey. Maximum interstorey drift ratio is 0.009 which satisfies the Life Safety (LS) performance. However, vertical and horizontal load carrying members do not satisfy the LS performance. Building must be strengthened and carried up to at least LS performance level under priorily mentioned design spectrum.

#### 4.4.2 Retrofitting with Eccentric Reinforced Concrete Shearwalls and CFRP

Utilizing CFRP infill walls instead of in-plane RC shearwalls, speeds up the construction and decreases the construction work needed. However, still the outer walls need to cast in place between the existing frames. Scaffolding still needs to be supported outside and some rooms of the flats will be evacuated. CFRP usage inside does not need any evacuation or laborous construction work. In order to isolate the construction work totally outside the building with a

comparably priced alternative, it was decided to use eccentric RC walls anchored to the existing frame and slab system from outside of the building. Details of the application is given in Figure 4.9.

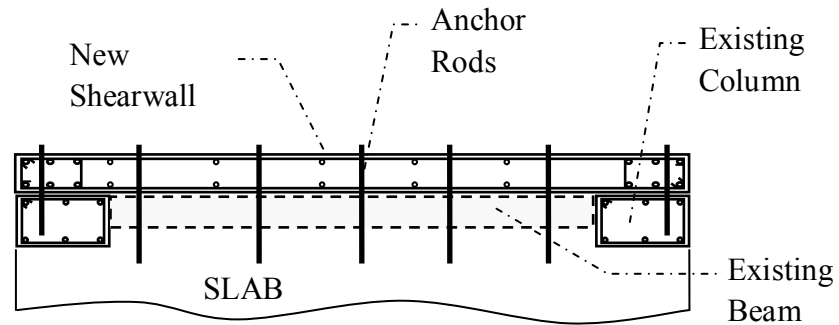


Figure 4.9: Adding Eccentric Shearwall adjacent to existing frame

In this pattern, 30 cm thick reinforced concrete shearwalls were installed outside the building. Some of the masonry infill walls were selected inside the building to be retrofitted with CFRP. Because of the architectural restrictions, shearwalls in X direction were half of the Y direction walls. The stiffness distribution was tried to be balanced by installing more CFRP retrofitted masonry infill walls in X direction. The storey plan is given in Figure 4.10.

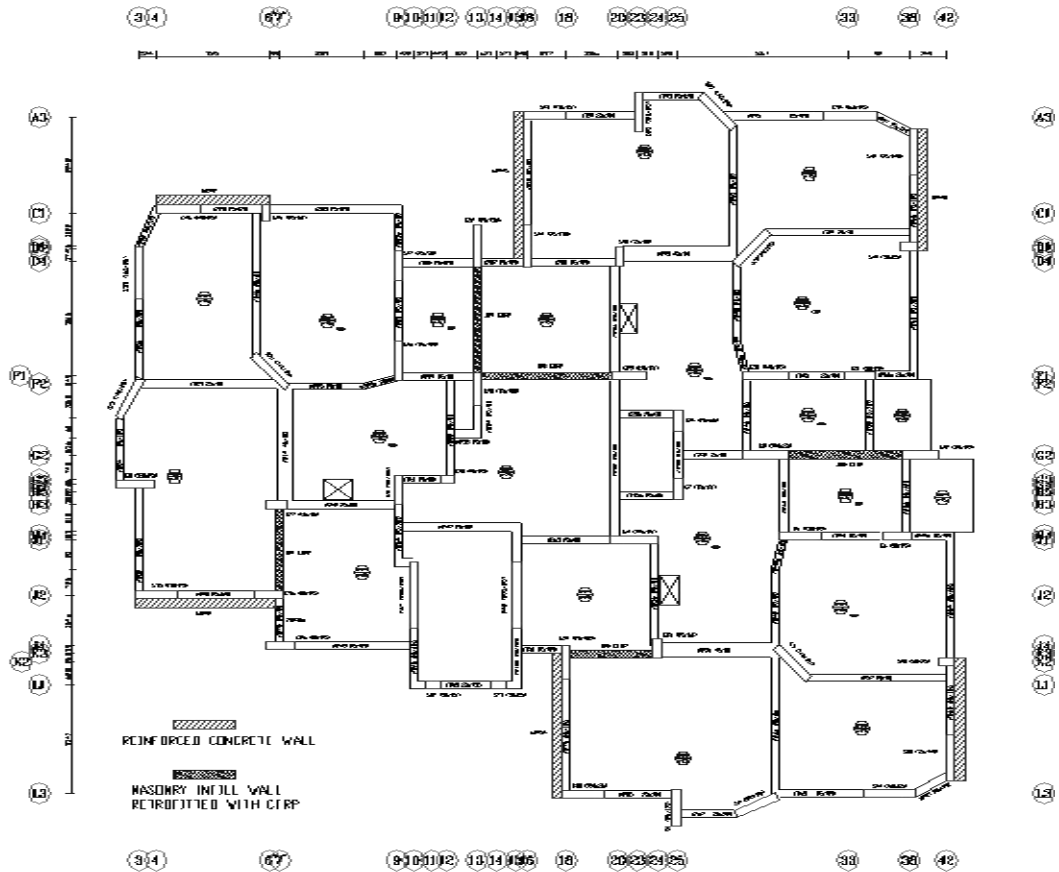


Figure 4.10: Typical Storey Plan, RC shearwalls are anchored from outside of the building

Modal characteristics of the building after this pattern is given in Table 4.3.

Table 4.3: Modal Characteristics of Building Retrofitted with Reinforced Concrete Shearwalls and CFRP strengthened masonry infill walls

Mode	Period (sec)	%Mass – Ux	%Mass – Uy	%Mass – Rz
1	0.82	0.90	40.00	23.30
2	0.74	47.7	9.90	6.19
3	0.66	15.1	14.88	29.57
4	0.15	1.64	7.21	10.44
5	0.14	12.48	7.26	0.55
6	0.13	6.34	5.97	6.96
7	0.06	2.72	0.94	5.3
8	0.06	4.13	3.21	0.18
9	0.05	1.93	3.69	5.66
10	0.04	0.11	0.12	5.85

Assessment results are presented in Figure 4.11 and Figure 4.12. This scheme satisfies the Life Safety Performance Level.

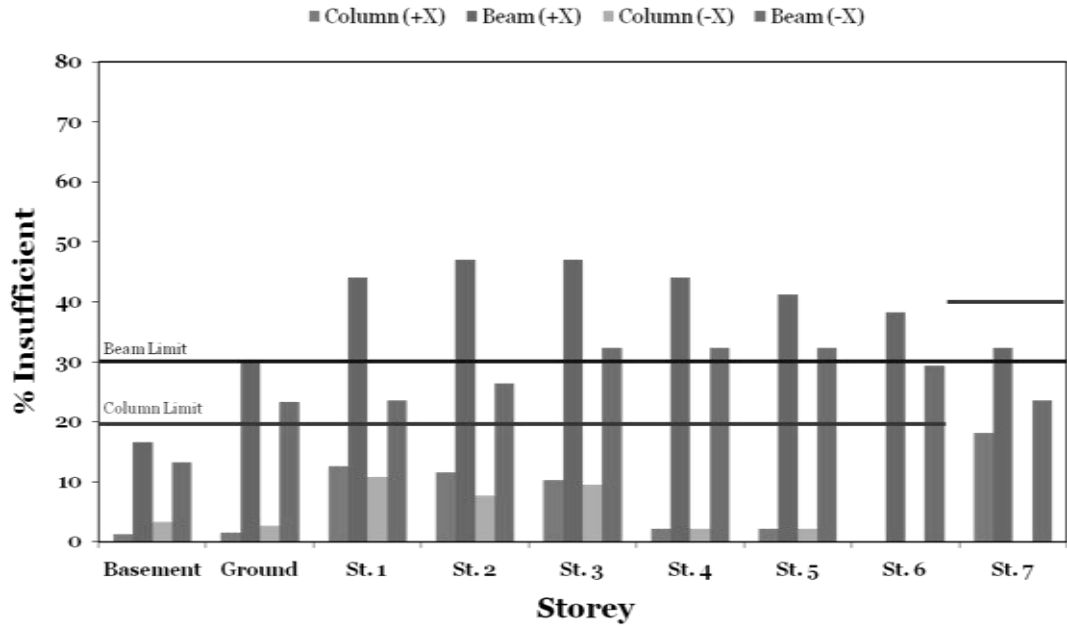


Figure 4.11: Assessment results for X Direction (Eccentric Shearwalls)

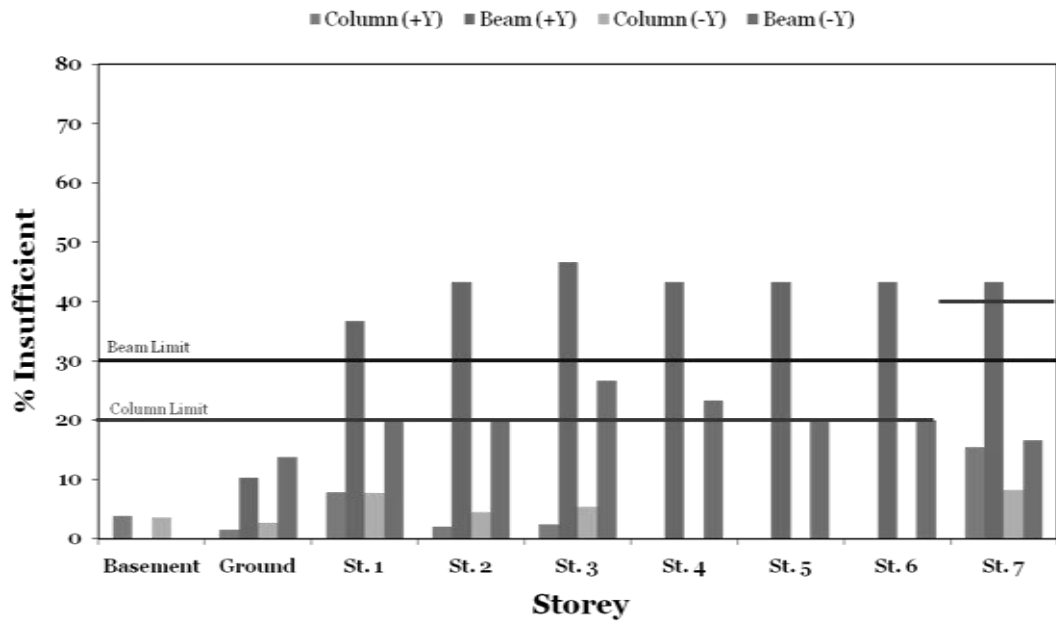


Figure 4.12: Assessment results for Y Direction (Eccentric Shearwalls)

Figure 4.13 illustrates the drift ratios obtained after elastic analysis for existing and retrofitted building. Drift ratios satisfy the code-given limits for Life Safety performance level and the drift limit for retrofitted masonry infill walls. The reduction of the drift ratio is also observed.

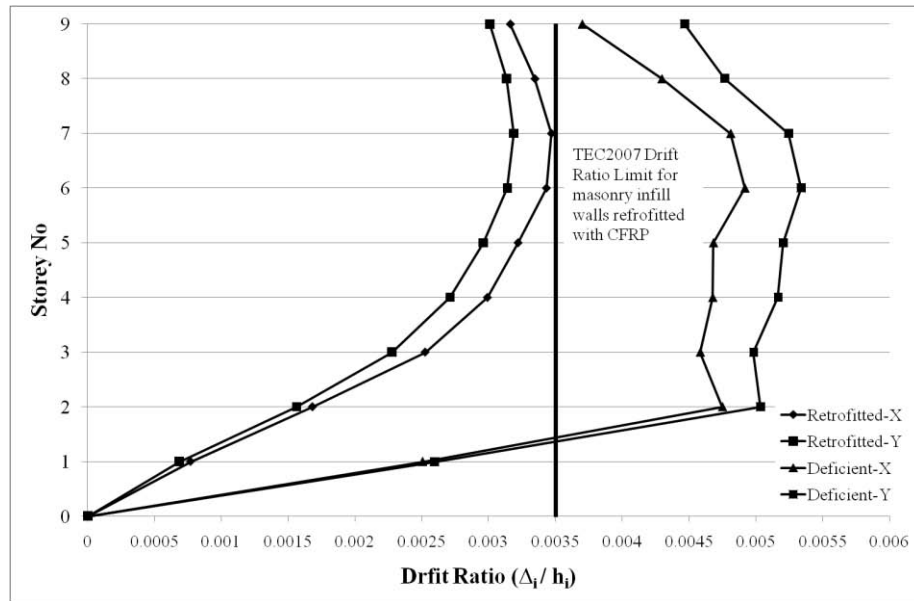


Figure 4.13: Drift Ratio profile for Existing and Retrofitted building after elastic analysis

Retrofit scheme is successful in reducing the demands in columns and walls. Global building performance values are well beyond the code limits. Although the code limits for beams were 30% for life safety criteria, a limit of 50% was used to assess beams. Brittle failure was not observed in beams and columns.

## **4.5. ANALYSIS AND ASSESSMENT OF THE BUILDING USING NONLINEAR MODAL PUSHOVER METHOD**

### **4.5.1 General**

For nonlinear analysis, formation of an elastic model is not adequate. Nonlinear coupled PMM (for columns and walls) and uncoupled MM (for beams) plastic hinges must be assigned to each ductile frame member. These plastic hinges are used at each critical section. Since plastic hinges can not be assigned to shell elements, shearwalls are also modelled by using frame elements. Calculation of moment plastic hinges are explained section 2.3.1. CFRP tension and compression struts are assigned axial hinges at their midspan. Force-deformation relationship for axial hinge is calculated using simplified model explained in Section 3.2. An example derivation of axial plastic hinge is presented in Section 3.4.2. Also, as explained in Chapter 3, CFRP strengthened masonry walls are modelled by tension tie – compression strut analogy.

First three modes of were used both for existing and retrofitted structure in modal pushover analysis. Modal characteristics for existing and retrofitted building are presented in Table 4.2 and 4.3 respectively. Analyses were conducted using SAP2000 v10 and Probina Orion v15.1 software packages. A detailed flowchart for modal pushover analysis is given in Figure 2.6. Typical steps for completing the modal pushover analysis and assessment task can be summarized as:

1. Nonlinear analytical model is prepared.
2. Eigenvalue analysis is performed to obtain vibration modes.
3. Separate nonlinear static analysis cases are created in SAP2000 to handle separate pushover analyses which have the load pattern associated with the selected first three modes.
4. Capacity curve for different pushover cases are obtained. Monitored displacement is selected to be along the DOF which has the highest modal mass participation factor for the related mode.

5. Capacity curves are normalized using the modal participation factor, modal amplitude and modal mass participation factor as explained in Section 2.3.5.
6. Demands for three modal capacity curves are obtained and plastic rotations, internal forces and displacements are extracted from analysis database.
7. All demand quantities are combined using SRSS. It should be noted that the SRSS method yields a loss in sign of the extracted quantities.
8. Member-by-member assessment is performed.

#### 4.5.2 Existing Building

Capacity and demand curves for three modes after the analysis of existing building is given in Figures 4.15 – 4.19. Capacity and demand curves are tabulated in Tables 4.4 – 4.9. Deformed shape and hinge formation is presented in Figure 4.14

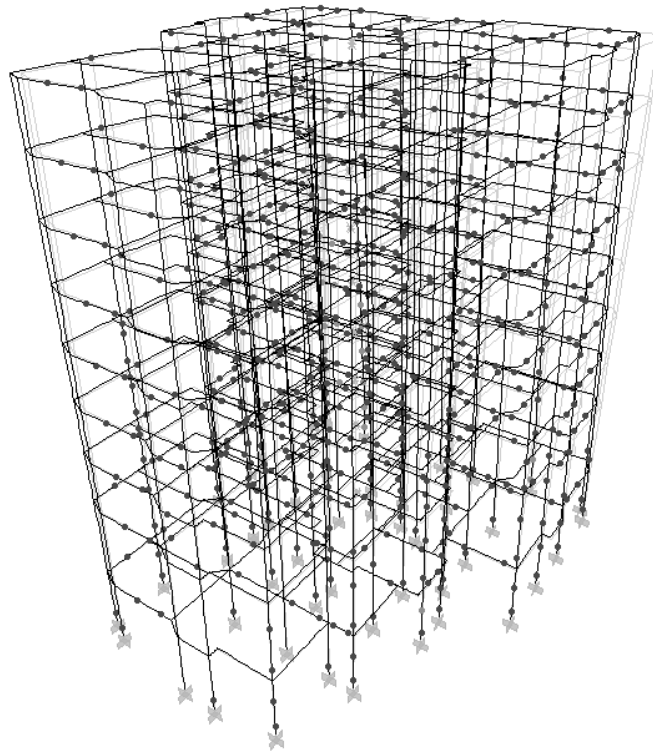


Figure 4.14: Existing Building: Deformed Shape and hinge formation.

Table 4.4: Existing building: Capacity Curve for Mode 1

<b>Roof Disp. (mm)</b>	<b>Base Shear (kN)</b>	<b>S<sub>d</sub></b>	<b>S<sub>a</sub> (g)</b>
0	0	0	0
0.972821	44.411	0.798222	0.00147
45.635172	2911.244	37.4447	0.09633
79.355951	3937.212	65.11337	0.130278
119.332147	4557.639	97.91475	0.150807
149.024749	4812.04	122.2782	0.159225
209.613892	5109.727	171.993	0.169075
268.63561	5292.783	220.4216	0.175133
289.144827	5335.03	237.2499	0.17653
350.037553	5449.174	287.2138	0.180307
386.17647	5499.834	316.8666	0.181984
448.508925	5585.465	368.0118	0.184817
484.462989	5625.657	397.5129	0.186147

Table 4.5: Existing building: Performance Point for Mode 1

<b>Γ</b>	172.37 kNs <sup>2</sup>	<b>W</b>	44443.5 kN
<b>φ</b>	69.34 mm	<b>α</b>	0.68
<b>Γ.φ</b>	11952.14	<b>W.α</b>	30221.58 kN
<b>Performance Point</b>			
<b>S<sub>d</sub></b>	154 mm (from graph)		
<b>Γ.φ</b>	1.218735 mm		
<b>d</b>	187.6852 mm		

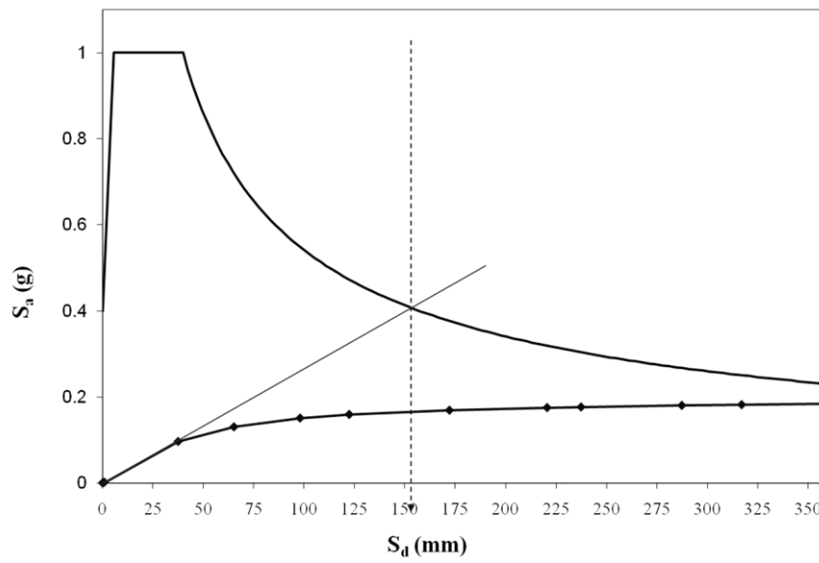


Figure 4.15: Existing Building: Performance Point Calculation for Mode 1

Table 4.6: Existing building: Capacity Curve for Mode 2

<b>Roof Disp. (mm)</b>	<b>Base Shear (kN)</b>	<b>S<sub>d</sub></b>	<b>S<sub>a</sub> (g)</b>
0	0	0	0
0.785757	204.159	0.578063	0.005966
37.615441	4355.364	27.6728	0.12727
55.894993	5226.59	41.12064	0.152728
80.555405	5809.438	59.26273	0.16976
132.712945	6372.539	97.63382	0.186215
193.001999	6736.186	141.9871	0.196841
255.565188	6966.156	188.0133	0.203561
319.353426	7121.15	234.9409	0.20809
382.621727	7237.38	281.4859	0.211486
442.793295	7323.667	325.7527	0.214008
502.67874	7390.468	369.809	0.21596
563.279357	7446.992	414.3915	0.217612
622.667881	7494.451	458.0822	0.218998
641.424854	7505.815	471.8813	0.21933

Table 4.7: Existing building: Performance Point for Mode 2

$\Gamma$	183.44 kNs <sup>2</sup>	<b>W</b>	44443.5 kN
$\phi$	72.67 mm	$\alpha$	0.77
$\Gamma.\phi$	13330.58	<b>W.<math>\alpha</math></b>	30221.58 kN
<b>Performance Point</b>			
$S_d$	110 mm (from graph)		
$\Gamma.\phi$	1.359 mm		
<b>d</b>	149.522 mm		

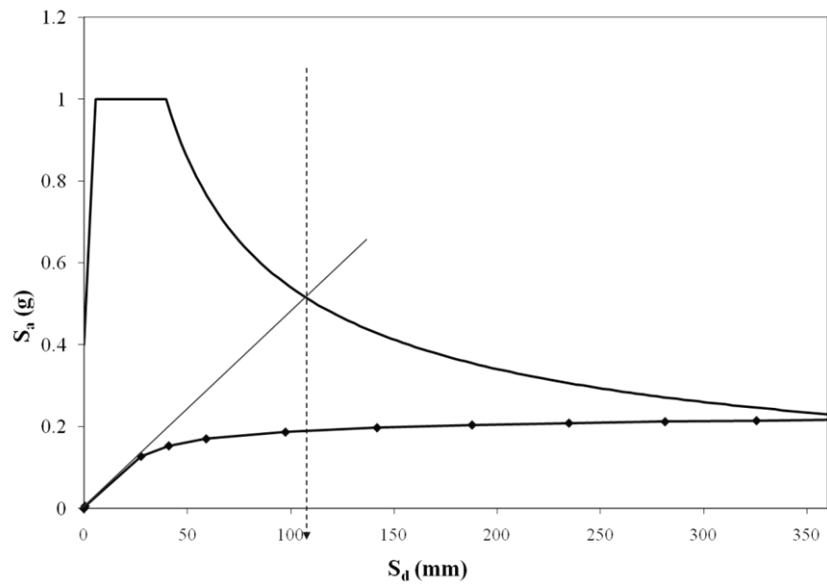


Figure 4.16: Existing Building: Performance Point Calculation for Mode 2

Table 4.8: Existing building: Performance Point for Mode 3

$\Gamma$	60.878 kNs <sup>2</sup>	<b>W</b>	44443.5 kN
$\phi$	23.28 mm	$\alpha$	0.086
$\Gamma.\phi$	1417.262	<b>W.<math>\alpha</math></b>	30221.58 kN
<b>Performance Point</b>			
$S_d$	87 mm (from graph)		
$\Gamma.\phi$	0.144 mm		
<b>d</b>	12.572 mm		

Table 4.9: Existing building: Capacity Curve for Mode 3

Roof Disp. (mm)	Base Shear (kN)	$S_d$	$S_a$ (g)
0	0	0	0
0.785757	204.159	0.578063	0.005966
37.615441	4355.364	27.6728	0.12727
55.894993	5226.59	41.12064	0.152728
80.555405	5809.438	59.26273	0.16976
132.712945	6372.539	97.63382	0.186215
193.001999	6736.186	141.9871	0.196841
255.565188	6966.156	188.0133	0.203561
319.353426	7121.15	234.9409	0.20809
382.621727	7237.38	281.4859	0.211486
442.793295	7323.667	325.7527	0.214008
502.67874	7390.468	369.809	0.21596
563.279357	7446.992	414.3915	0.217612
622.667881	7494.451	458.0822	0.218998
641.424854	7505.815	471.8813	0.21933

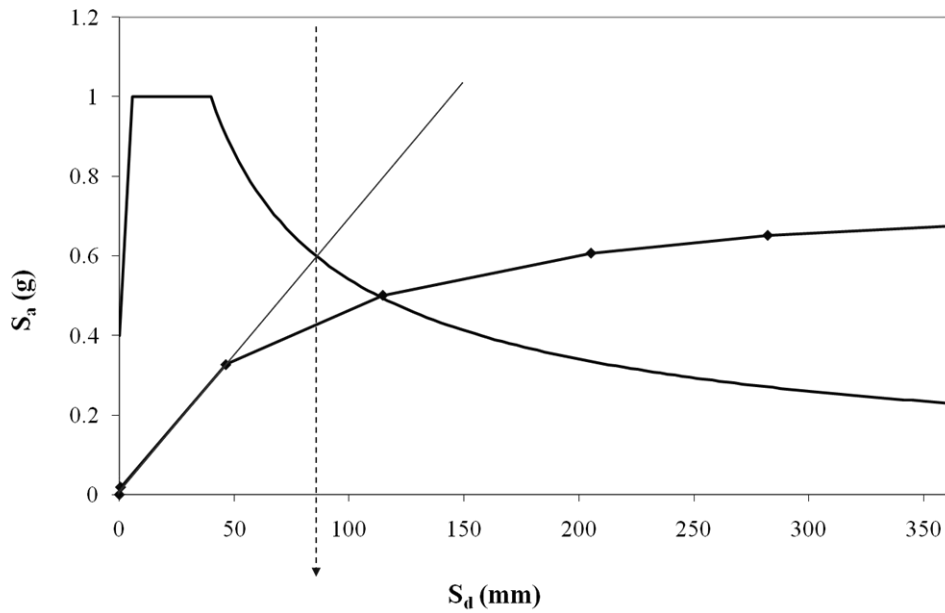


Figure 4.17: Existing Building: Performance Point Calculation for Mode 2

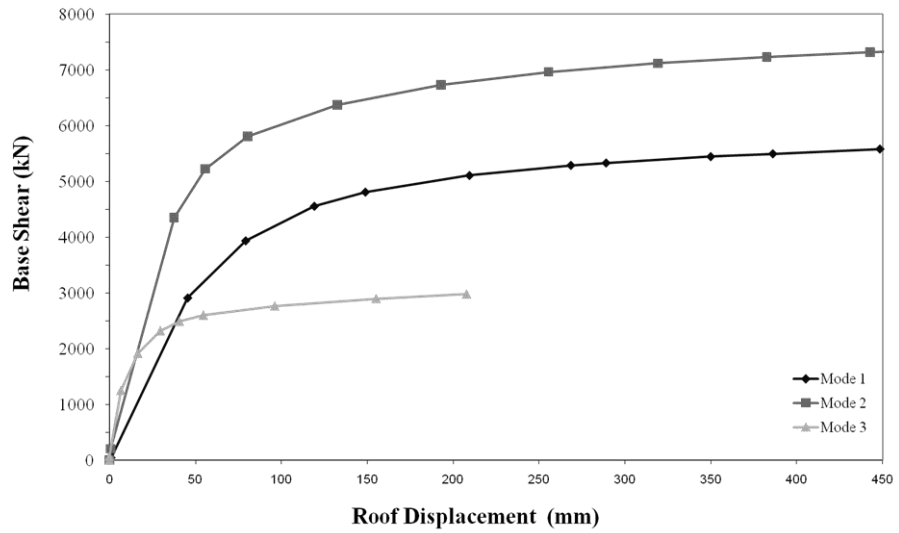


Figure 4.18: Base Shear vs Roof Displacement curves for first three modes of existing building.

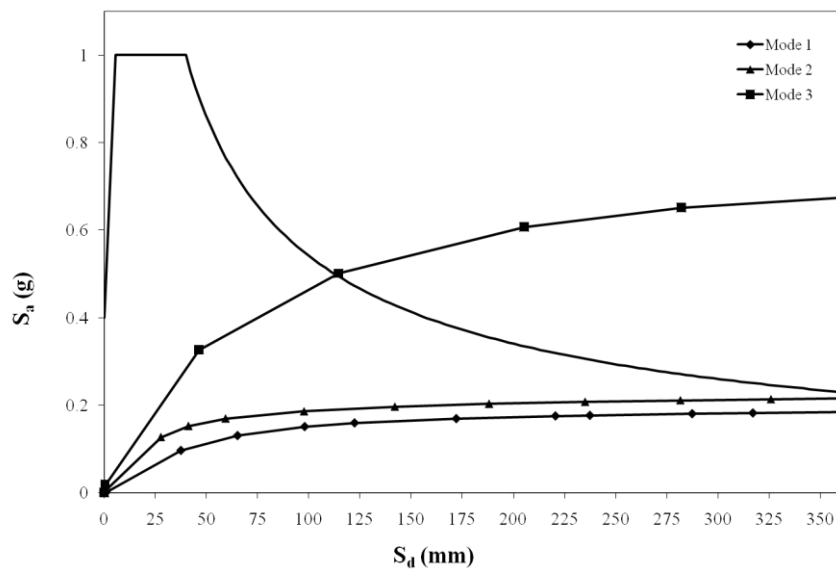


Figure 4.19: Demand curves for first three modes of existing building

Modal pushover assessment results for existing building is given in Figures 4.20 – 4.47.

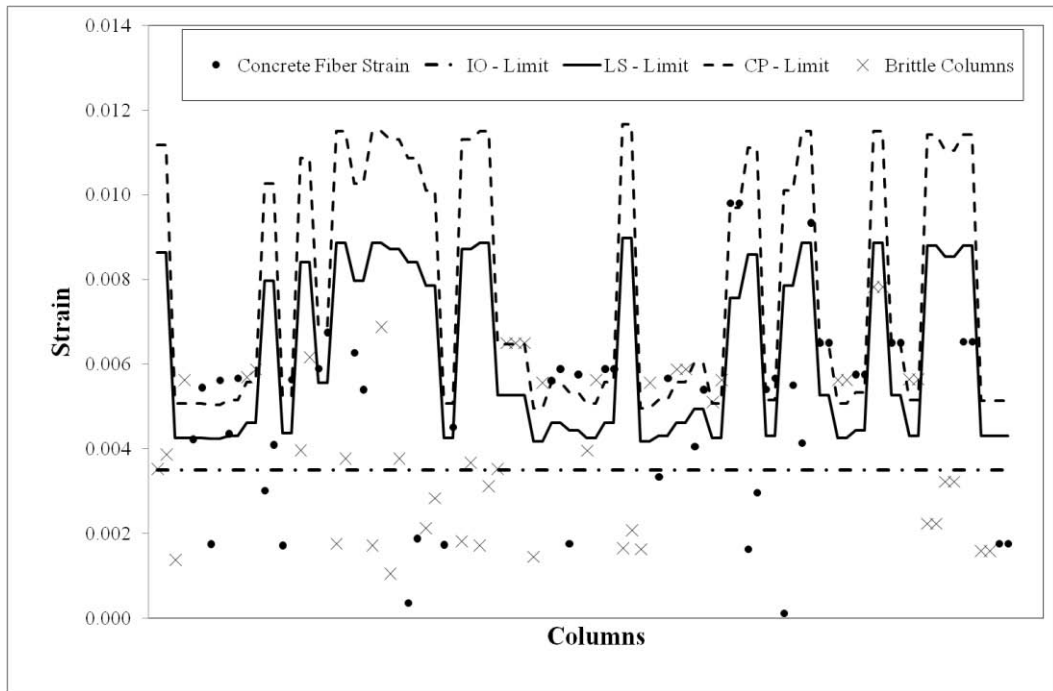


Figure 4.20: Existing Building: Concrete Strains for Basement Storey Columns

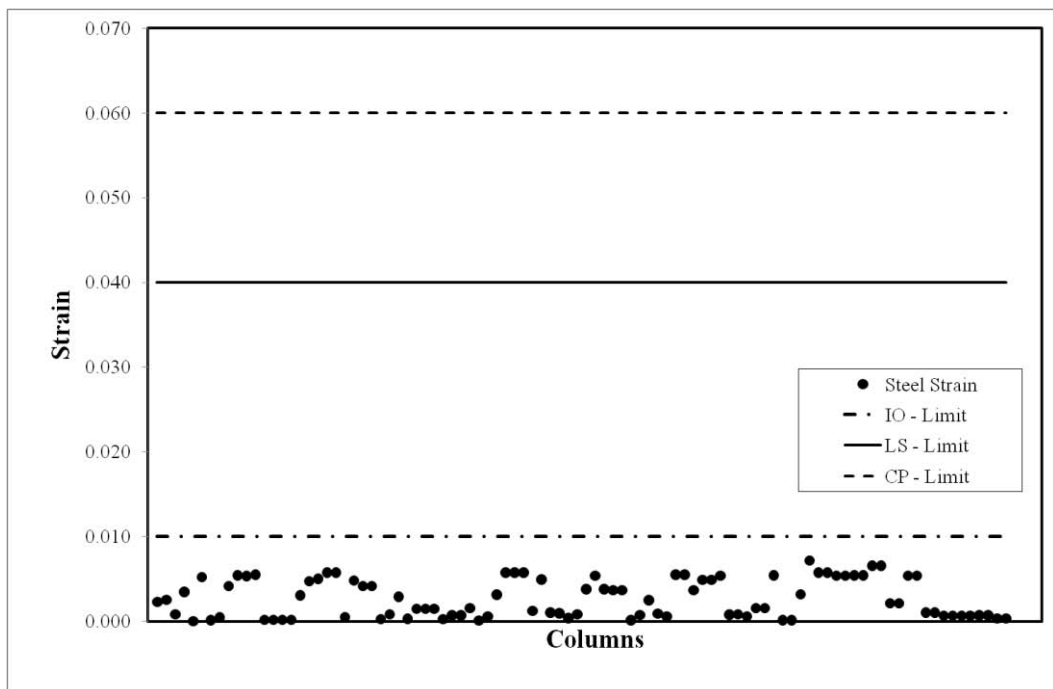


Figure 4.21: Existing Building: Steel Strains for Basement Storey Columns

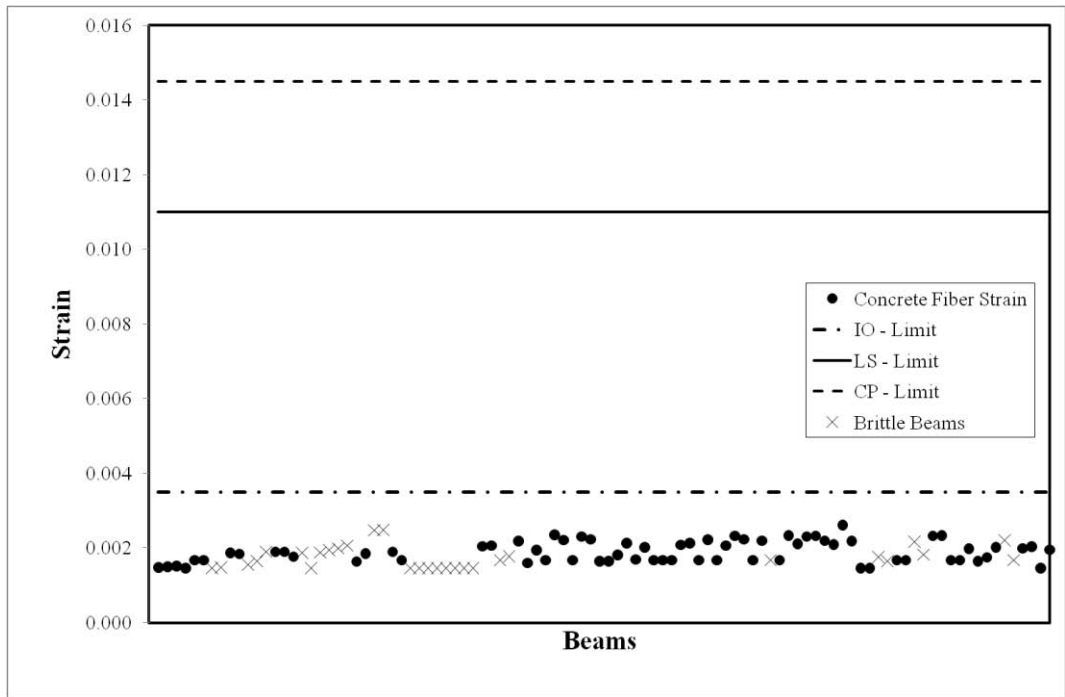


Figure 4.22: Existing Building: Concrete Strains for Basement Storey Beams

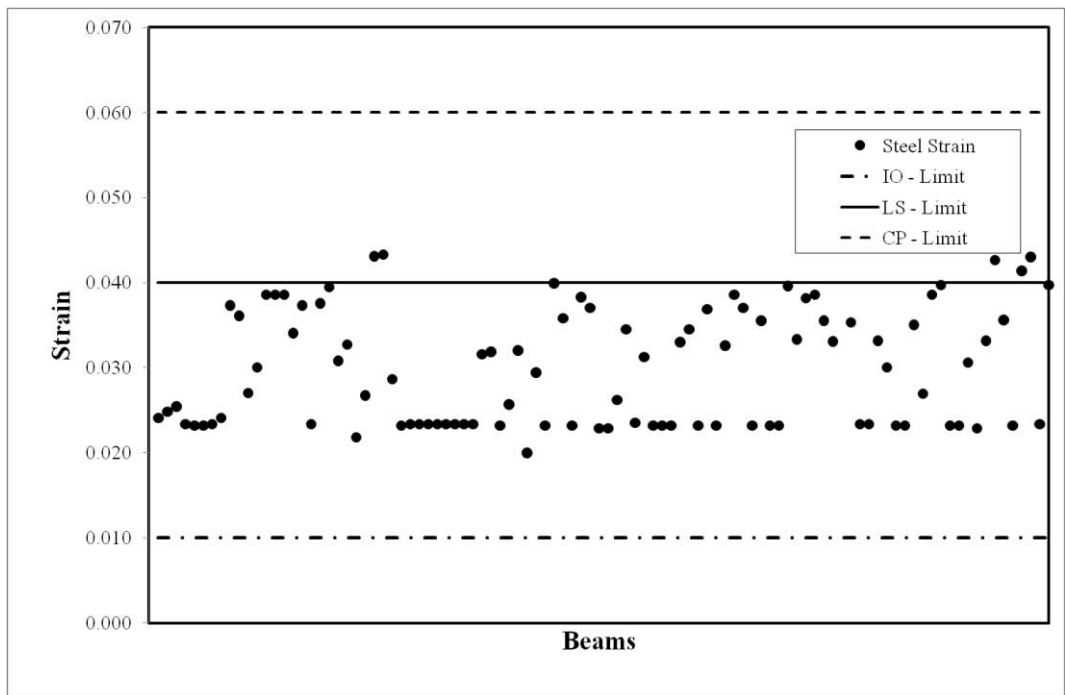


Figure 4.23: Existing Building: Steel Strains for Basement Storey Beams

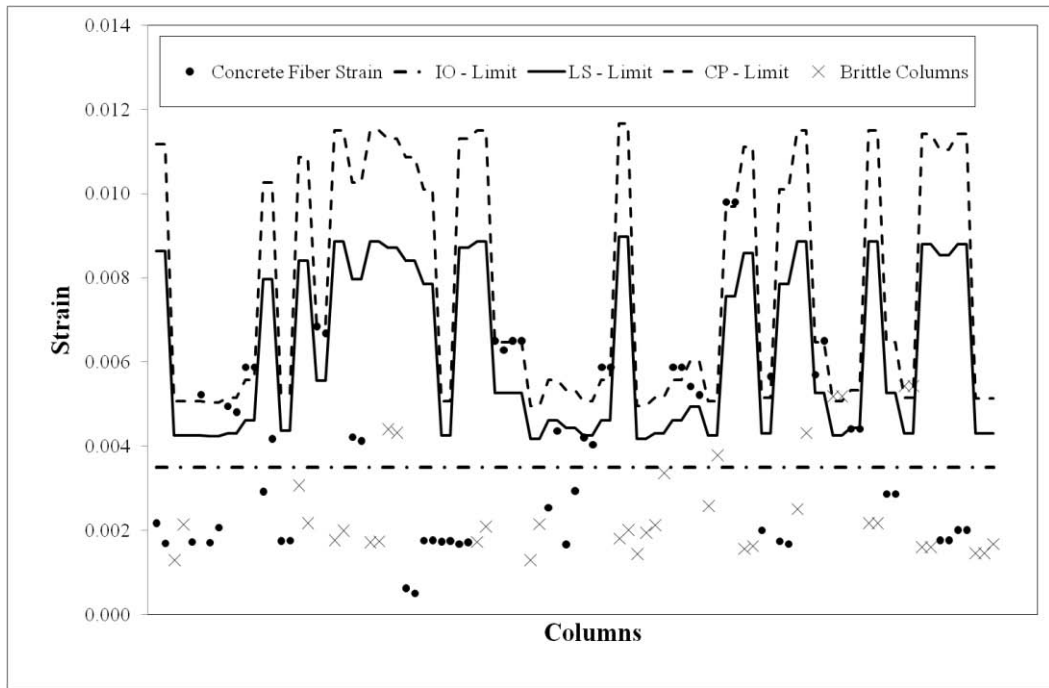


Figure 4.24: Existing Building: Concrete Strains for Ground Storey Columns

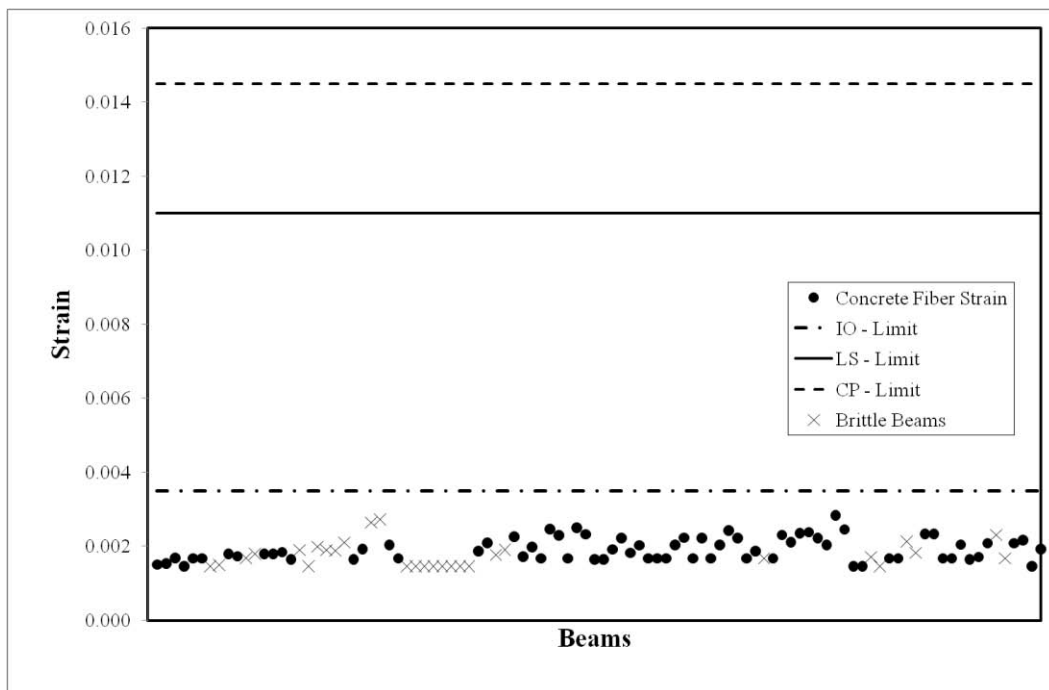


Figure 4.25: Existing Building: Concrete Strains for Ground Storey Beams

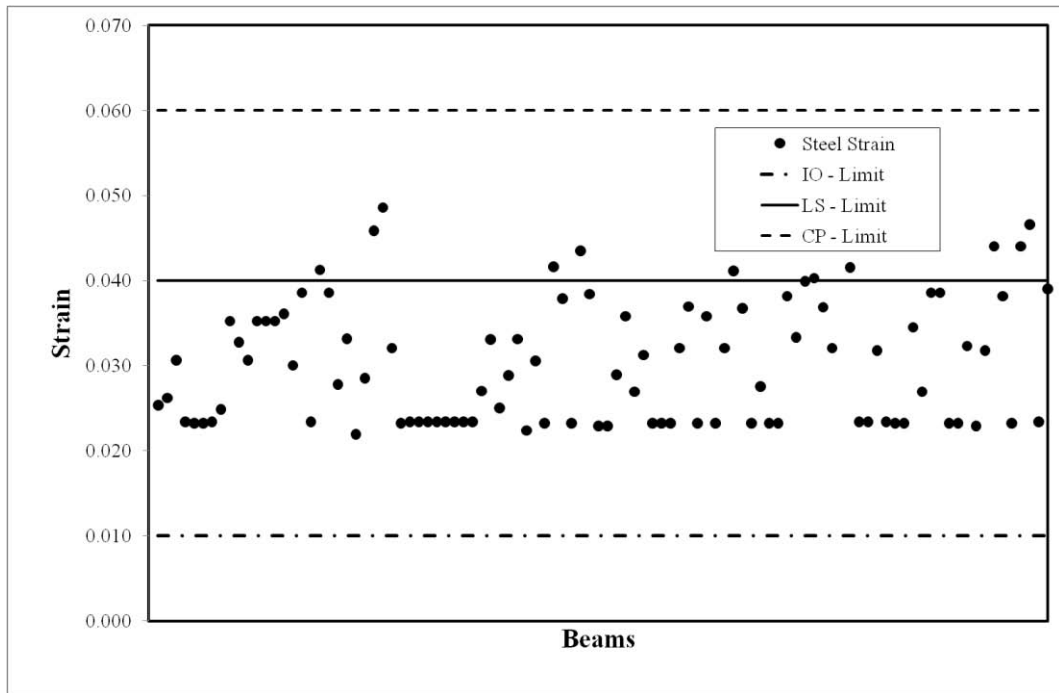


Figure 4.26: Existing Building: Steel Strains for Ground Storey Beams

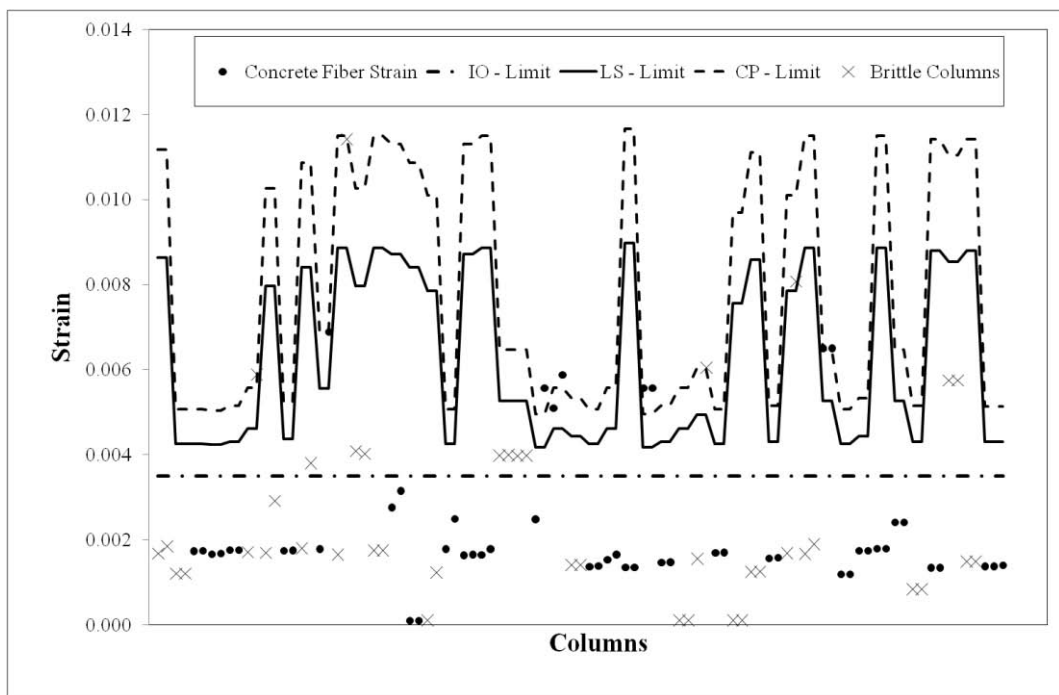


Figure 4.27: Existing Building: Concrete Strains for 1st Storey Columns

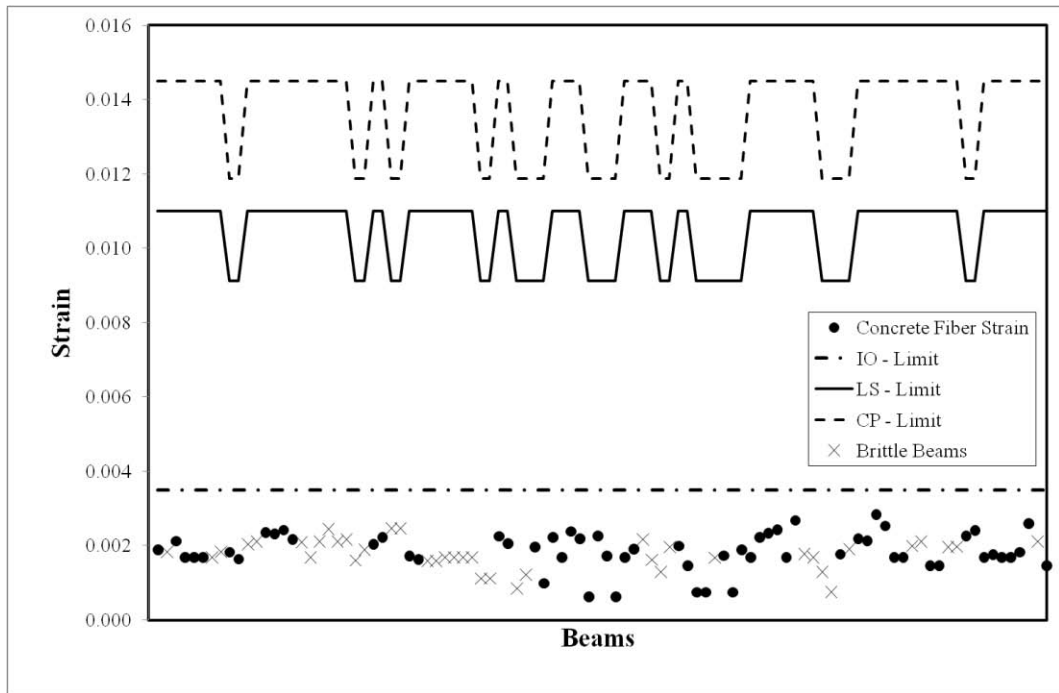


Figure 4.28: Existing Building: Concrete Strains for 1st Storey Beams

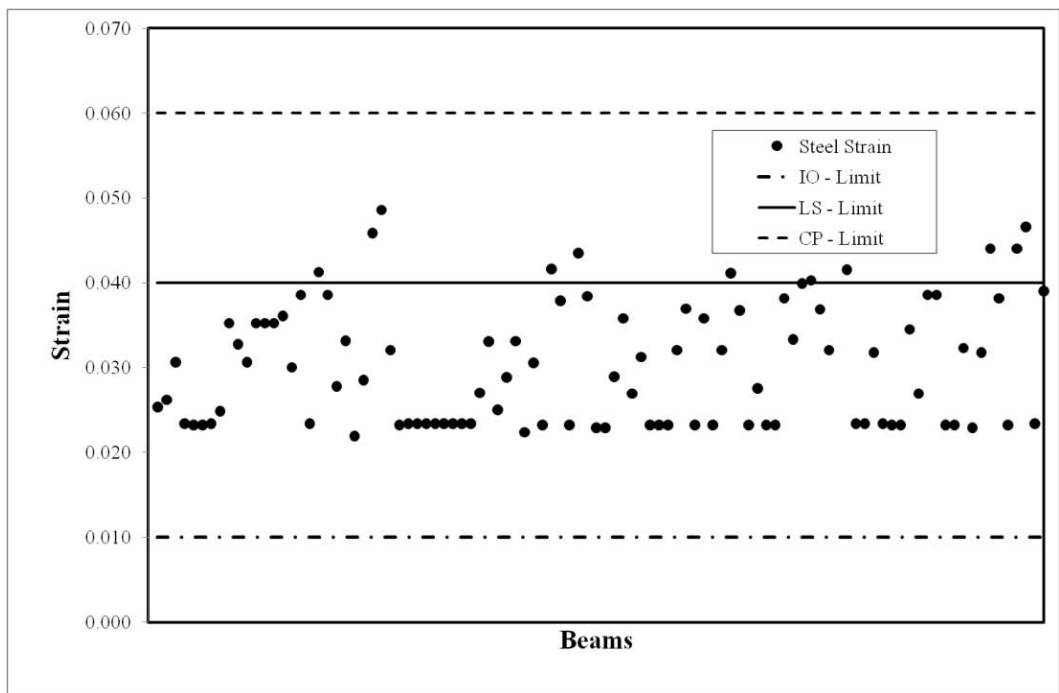


Figure 4.29: Existing Building: Steel Strains for 1st Storey Beams

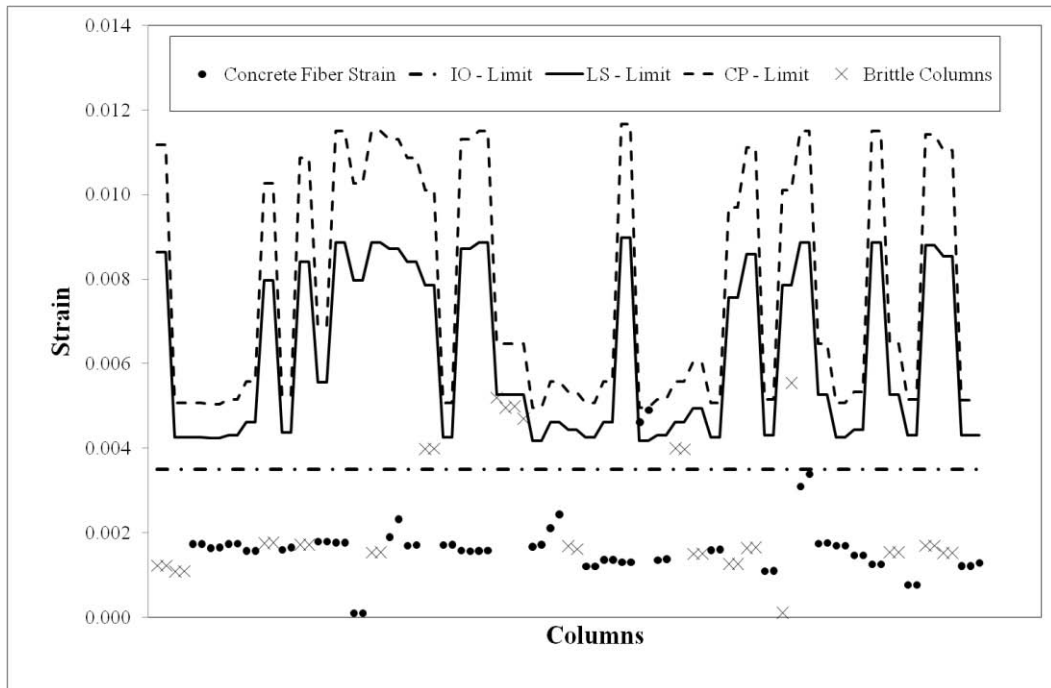


Figure 4.30: Existing Building: Concrete Strains for 2nd Storey Columns

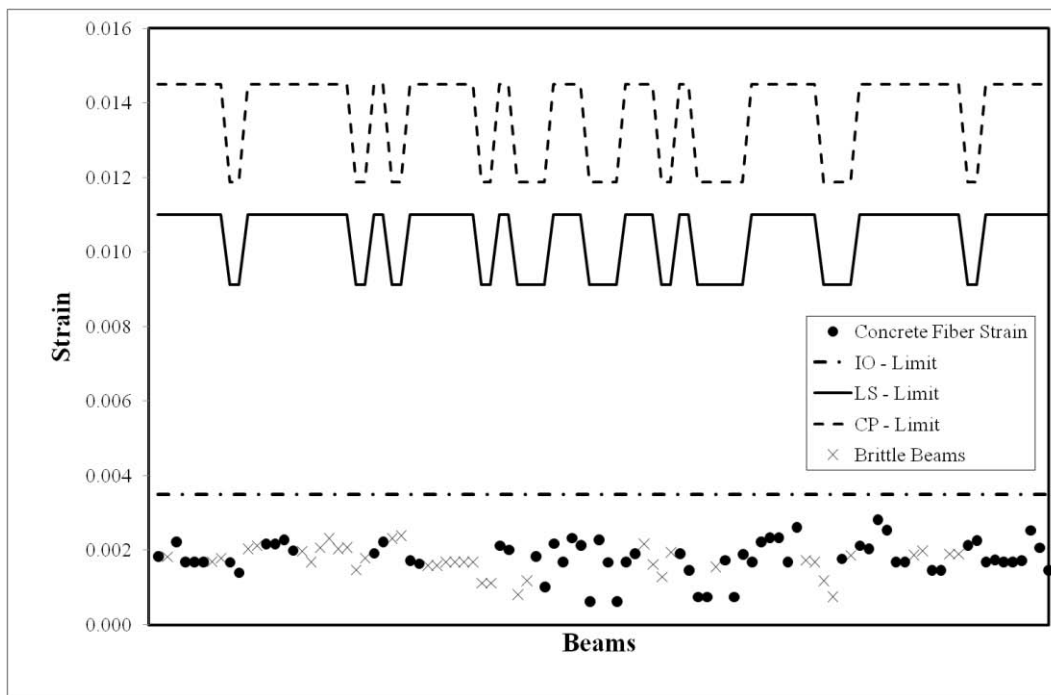


Figure 4.31: Existing Building: Concrete Strains for 2nd Storey Beams

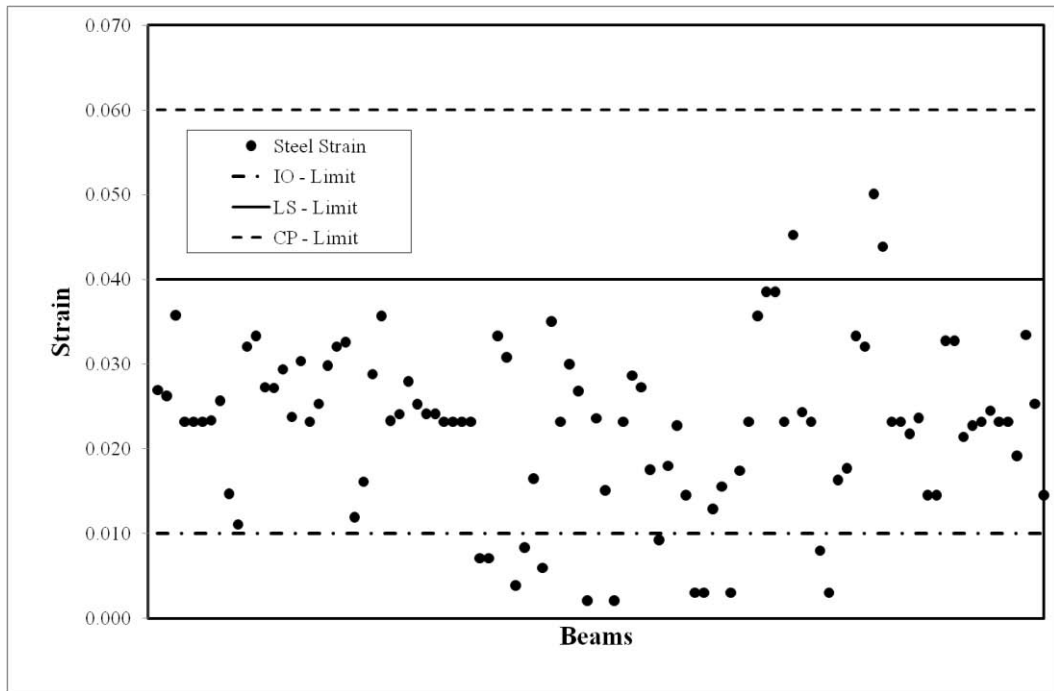


Figure 4.32: Existing Building: Steel Strains for 2nd Storey Beams

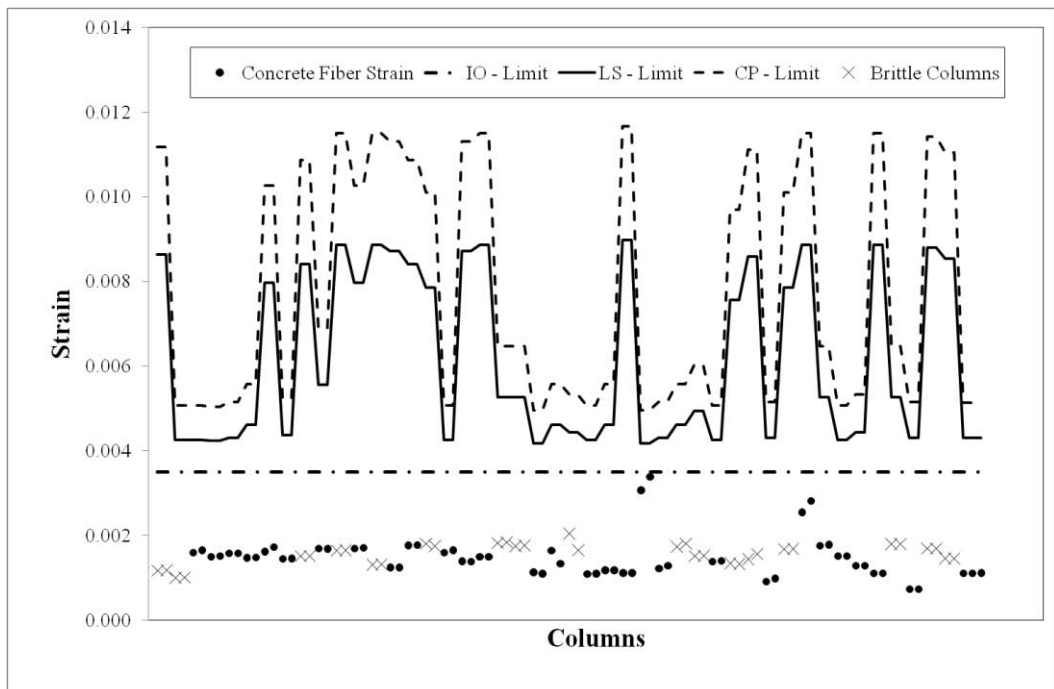


Figure 4.33: Existing Building: Concrete Strains for 3rd Storey Columns

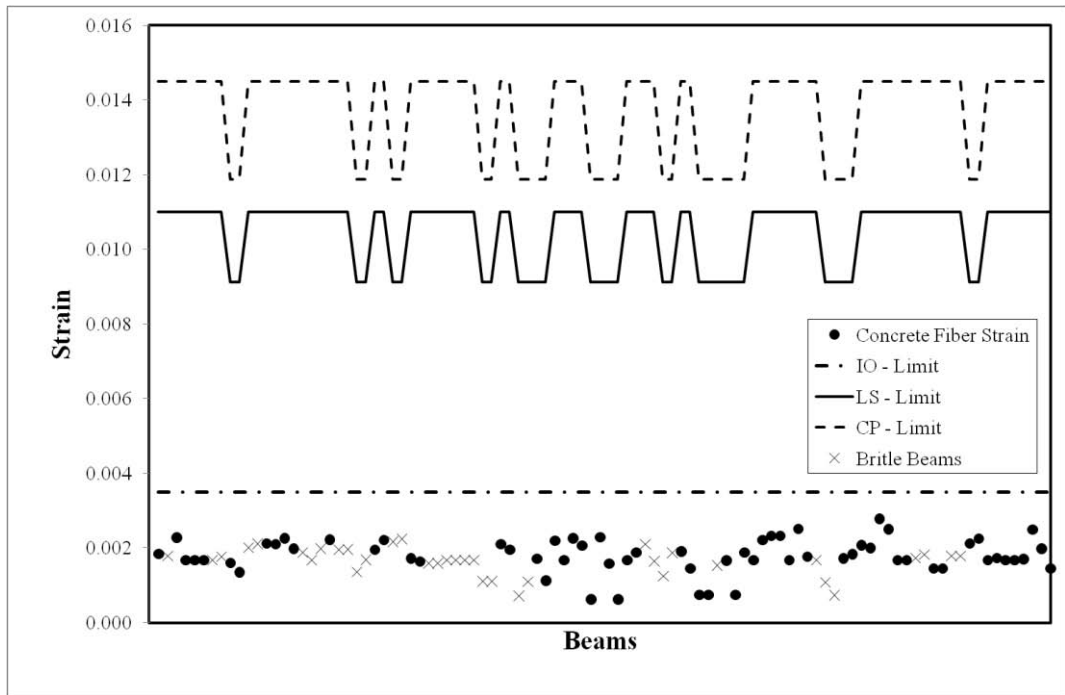


Figure 4.34: Existing Building: Concrete Strains for 3rd Storey Beams

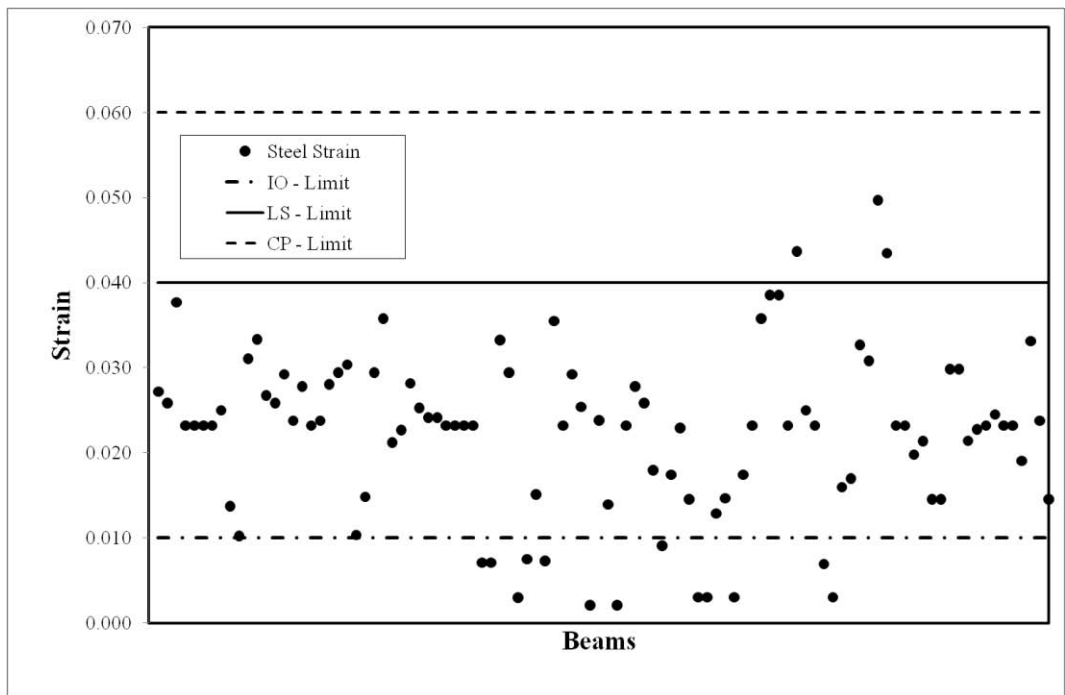


Figure 4.35: Existing Building: Steel Strains for 3rd Storey Beams

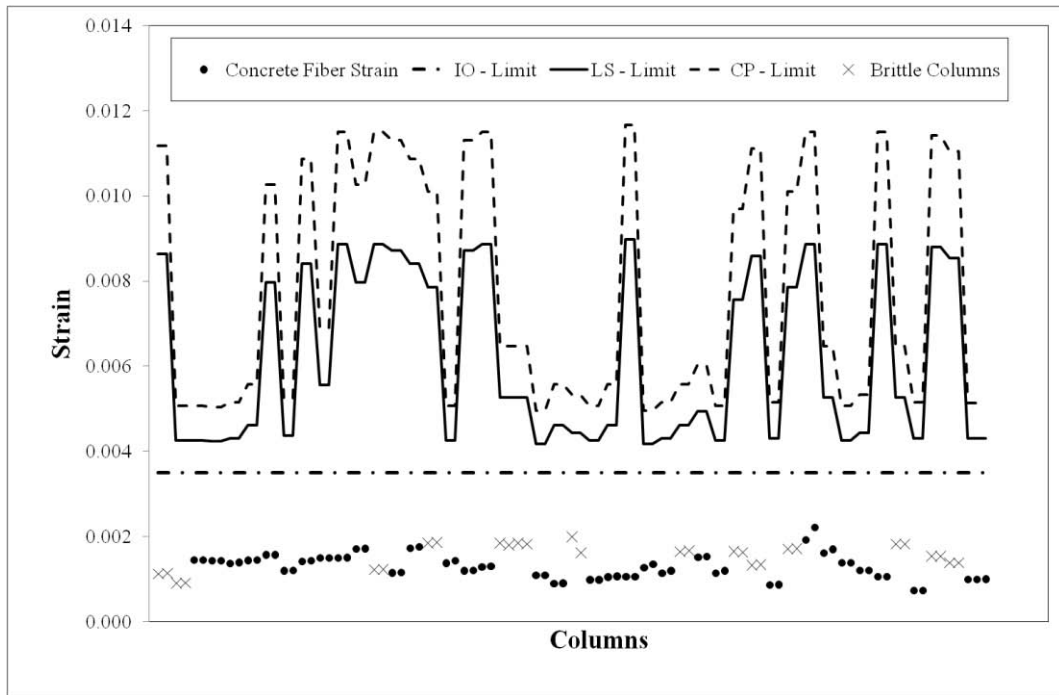


Figure 4.36: Existing Building: Concrete Strains for 4th Storey Columns

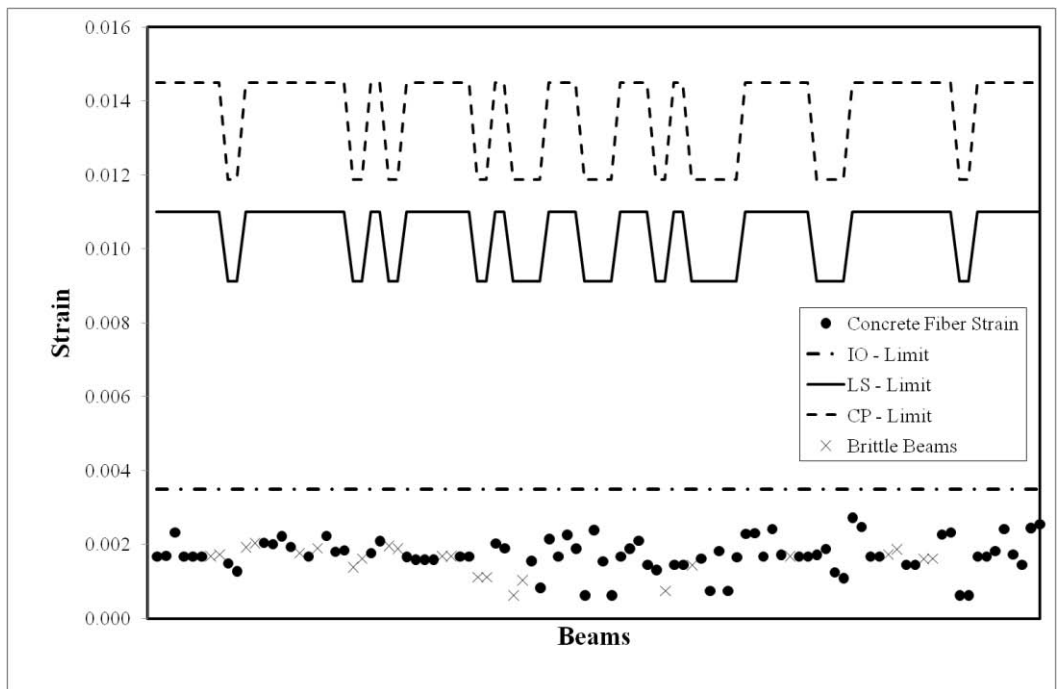


Figure 4.37: Existing Building: Concrete Strains for 4th Storey Beams

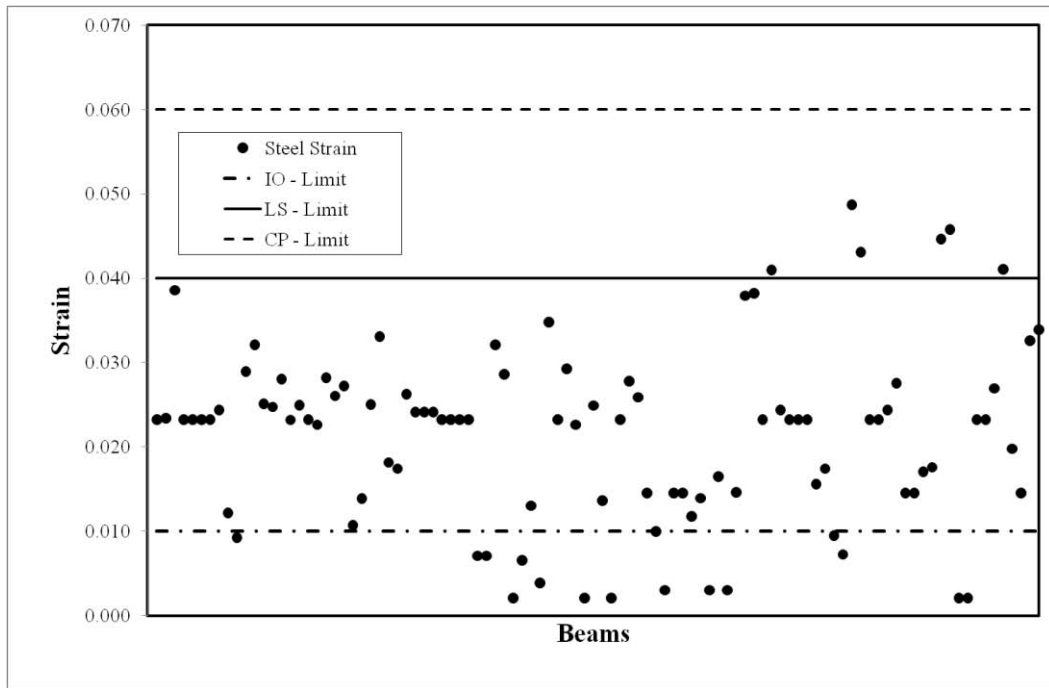


Figure 4.38: Existing Building: Steel Strains for 4th Storey Beams

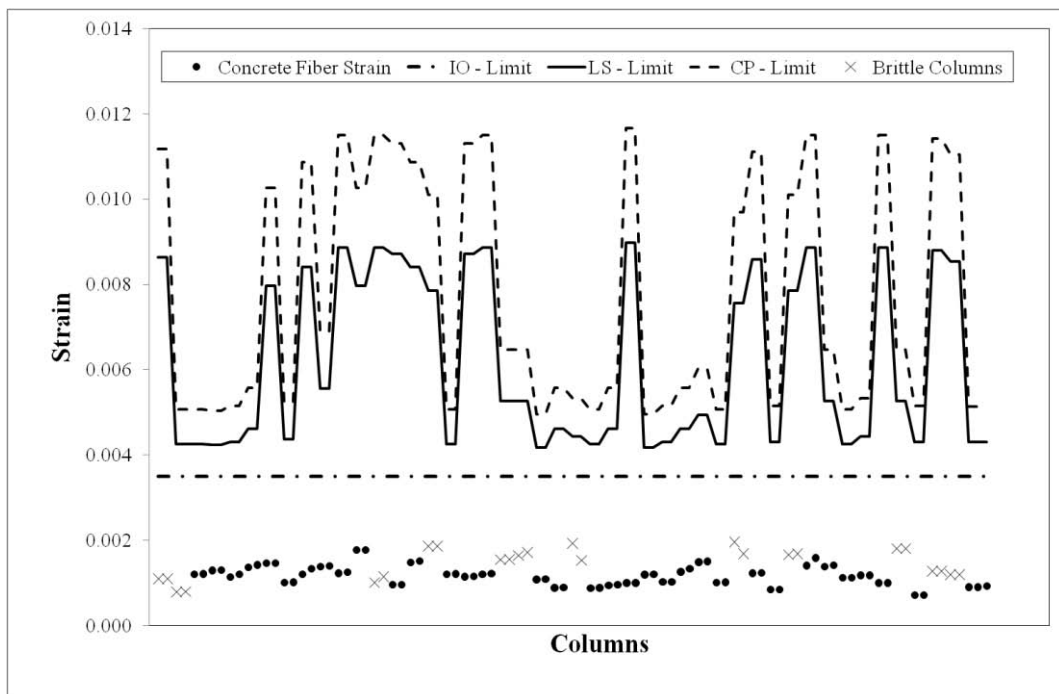


Figure 4.39: Existing Building: Concrete Strains for 5th Storey Columns

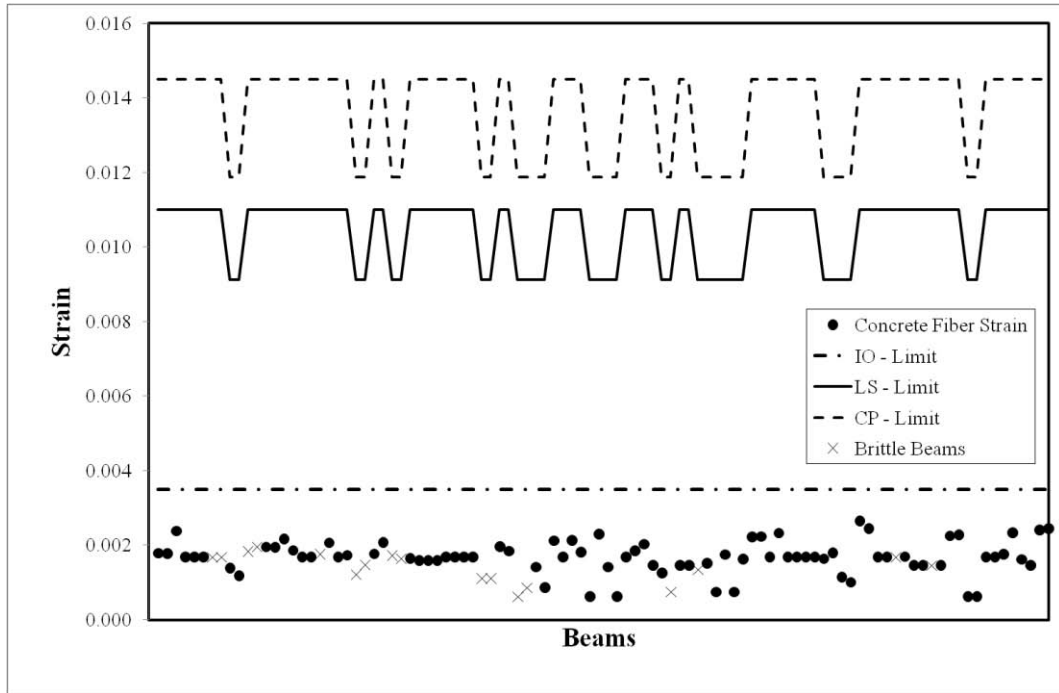


Figure 4.40: Existing Building: Concrete Strains for 5th Storey Beams

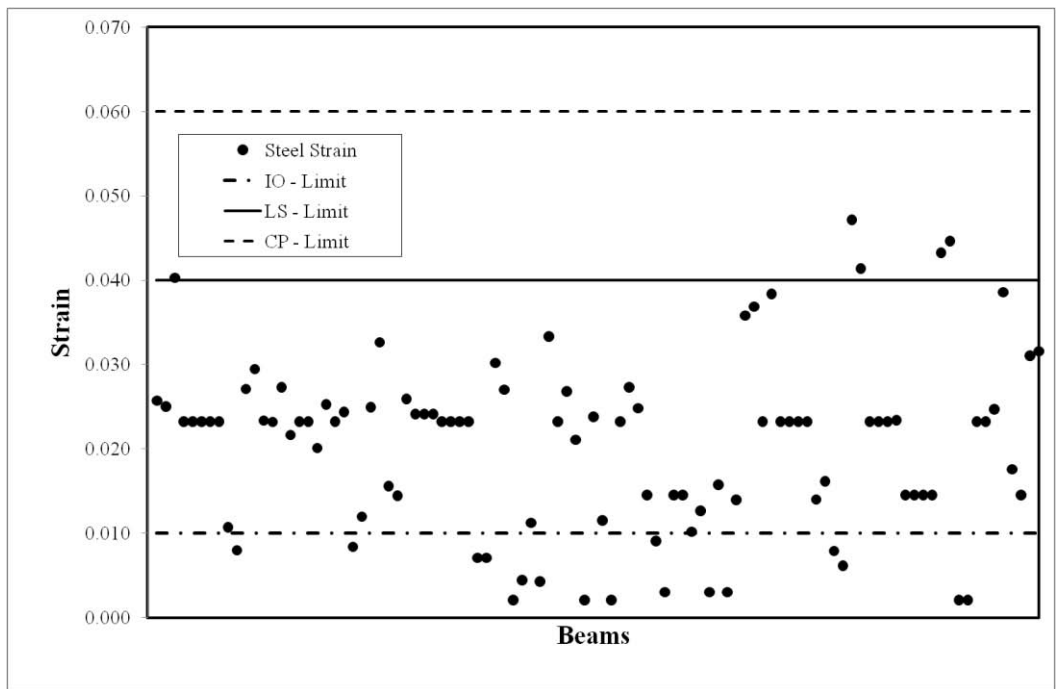


Figure 4.41: Existing Building: Steel Strains for 5th Storey Beams

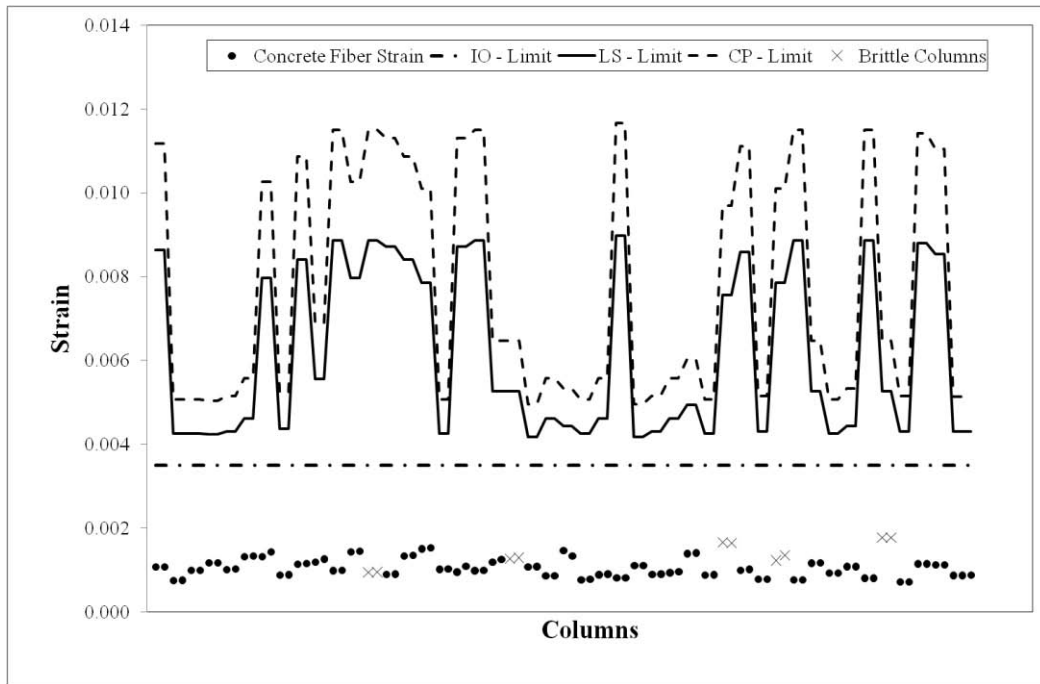


Figure 4.42: Existing Building: Concrete Strains for 6th Storey Columns

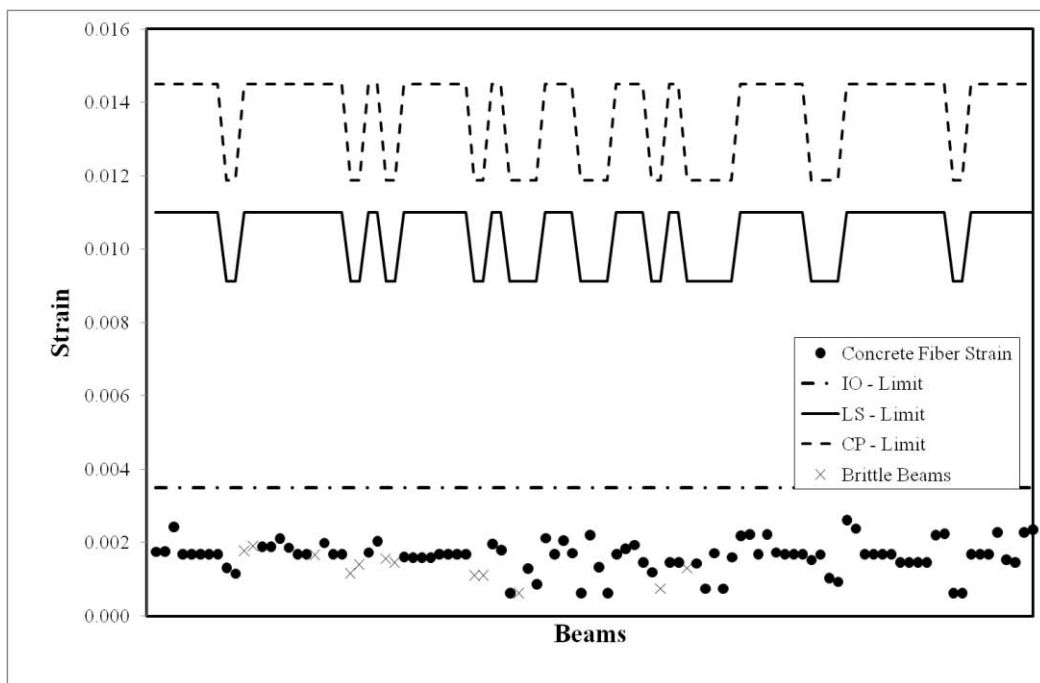


Figure 4.43: Existing Building: Concrete Strains for 6th Storey Beams

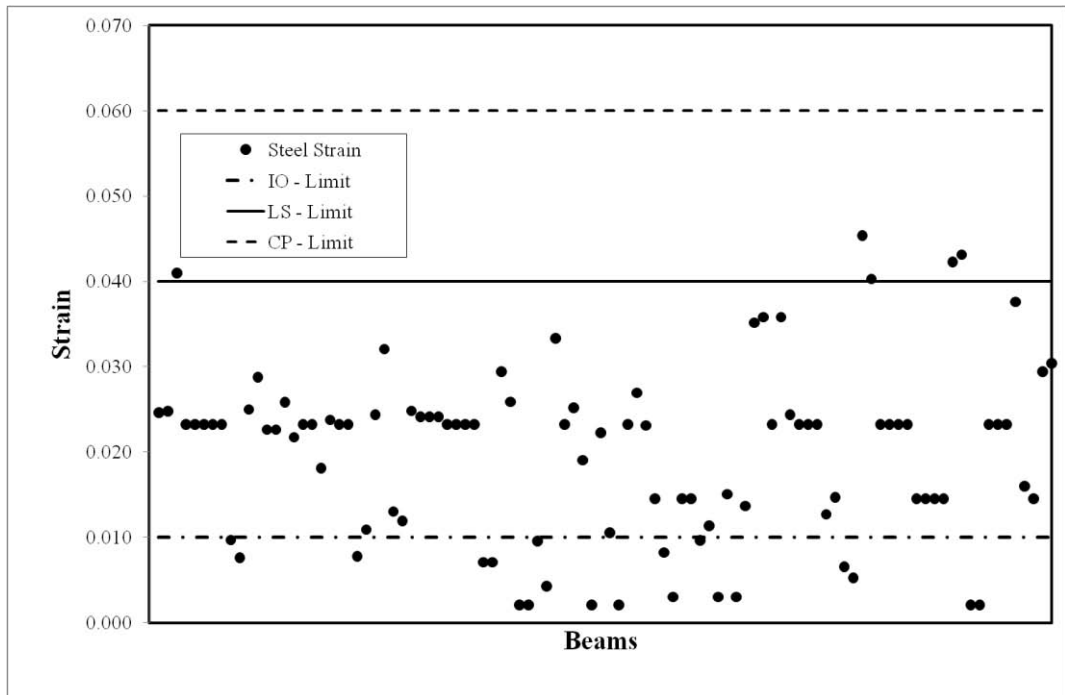


Figure 4.44: Existing Building: Steel Strains for 6th Storey Beams

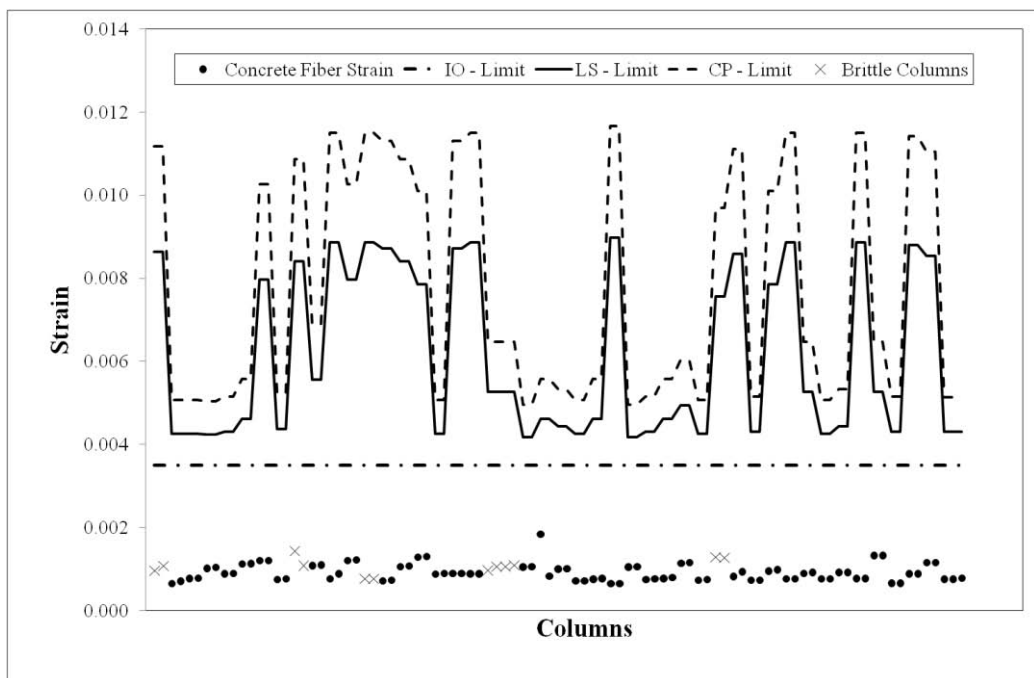


Figure 4.45: Existing Building: Concrete Strains for 7th Storey Columns

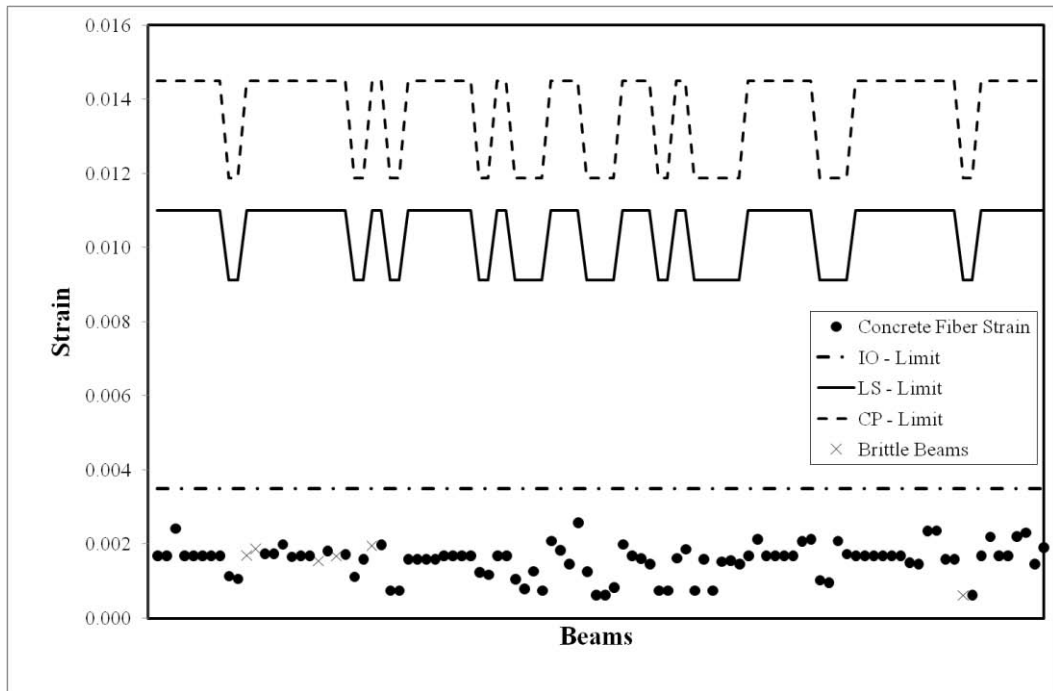


Figure 4.46: Existing Building: Concrete Strains for 7th Storey Beams

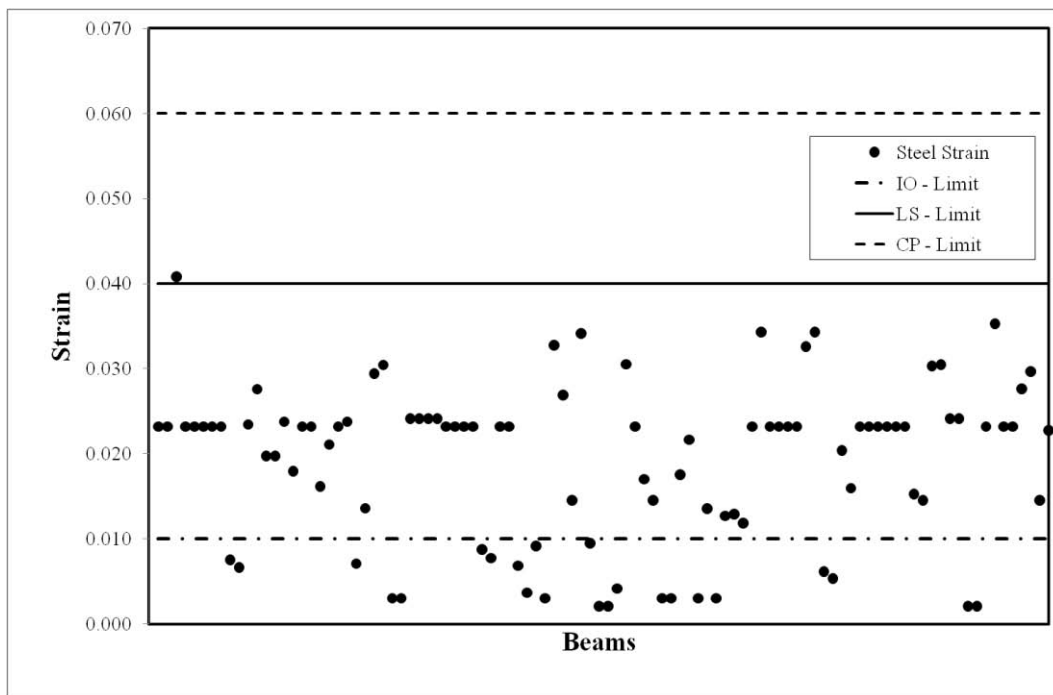


Figure 4.47: Existing Building: Steel Strains for 7th Storey Beams

Drift ratios for existing building is given in Figure 4.48.

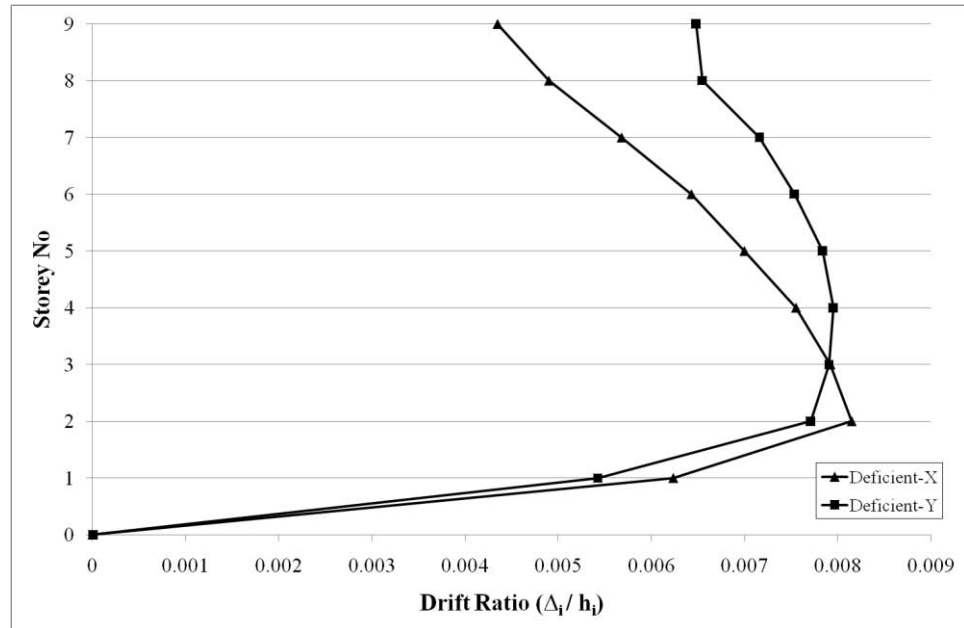


Figure 4.48: Existing Building: Drift Ratios

Existing building suffers from brittle column and beam failures. Brittle members are indicated with a very high concrete strain in the figures. Besides this, basement, ground and 1st storey ductile columns exceed life safety and collapse prevention limits as shown in the figures above. Largest interstorey drift ratio is observed in Ground storey, which is also the storey with the maximum height. It was also observed that hinge formation in columns is concentrated in basement, ground and 1st storeys.

### 4.5.3 Retrofitted Building

Modal pushover analysis is applied to same retrofit scheme explained in section 4.4.2. Same modelling and analysis rules apply like in previous section. Assessment results are tabulated in the following figures. Concrete, beam,

shearwall and CFRP retrofitted masonry infill wall strains are plotted and compared with the code-given limits.

Capacity and demand curves for three modes after the analysis of retrofitted building is given in Figures 4.51 – 4.55. Capacity and demand curves are tabulated in Tables 4.10 – 4.15. Deformed shape and hinge formation is presented in Figure 4.49.

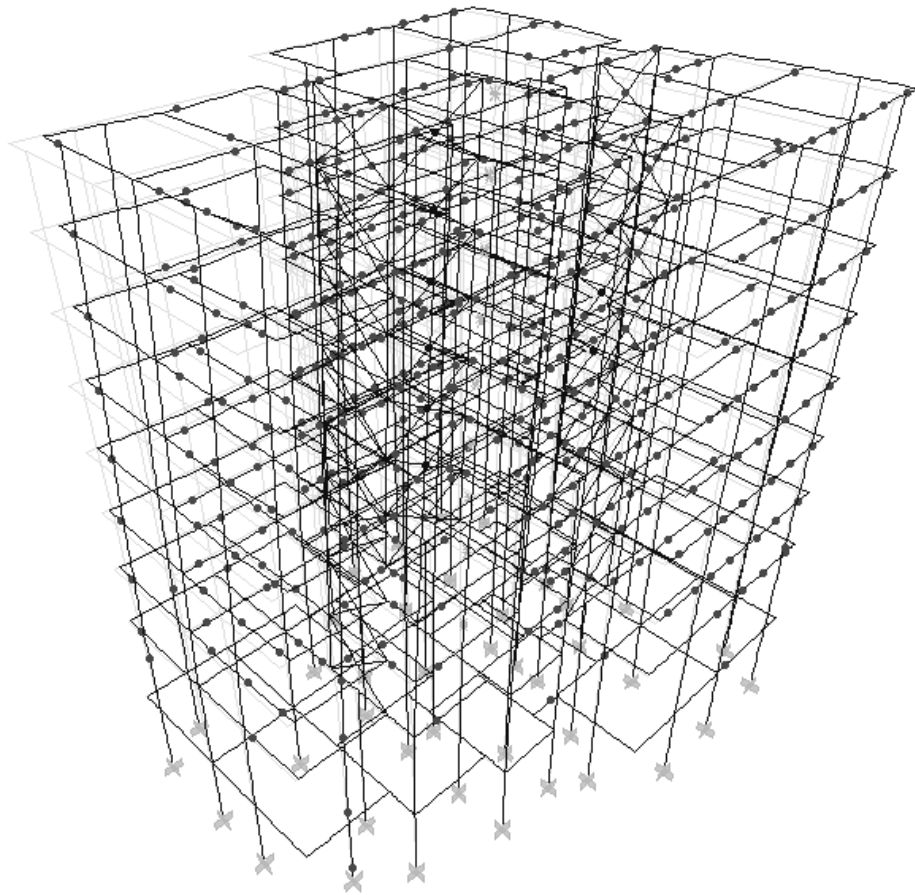


Figure 4.49: Retrofitted Building: Hinge Formation

Figure 4.50 presents a frame in X direction which contains a masonry infill wall strengthened with CFRP. As shown, it can be seen that CFRP masonry infill sits on reinforced concrete shearwall at lower storeys. Shearwall is modelled by T-frame (mid-pier) model. In the retrofitted building majority of the plastic hinges

appear to be formed at beam ends which is also preferable. In the figure axial hinge formation can also be seen tension ties and compression struts which define a CFRP masonry infill wall.

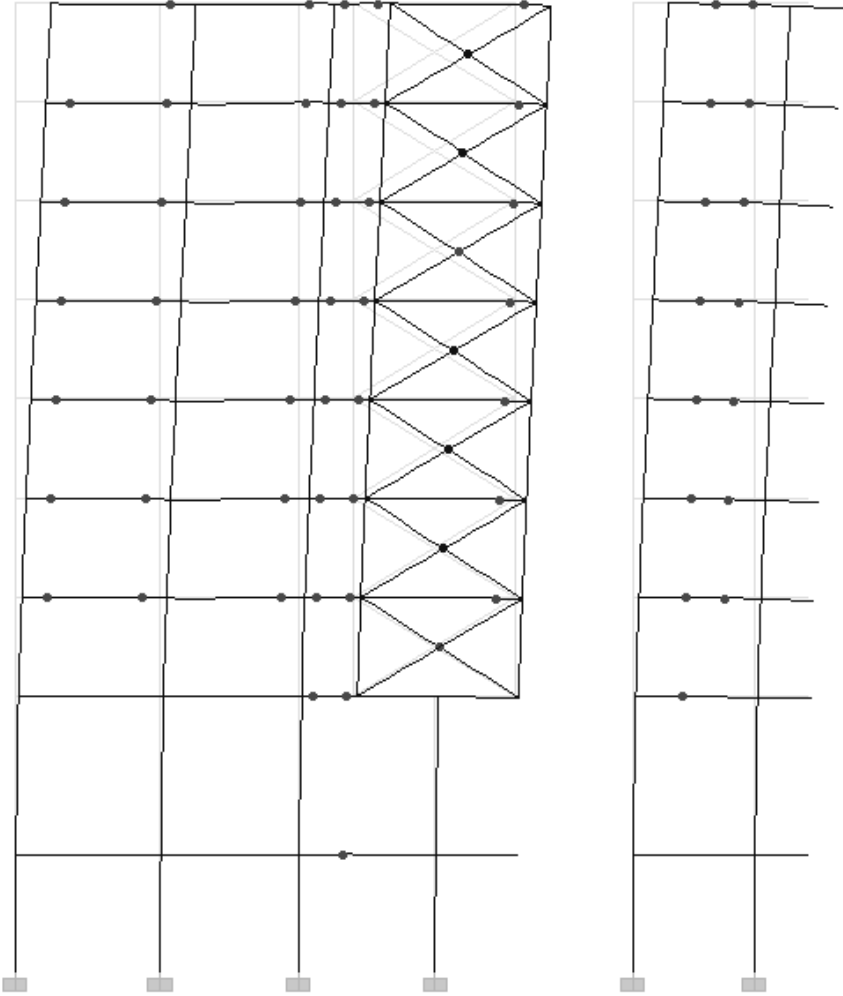


Figure 4.50: Retrofitted Building: Masonry Infill frame in X direction

Table 4.10: Retrofitted building: Capacity Curve for Mode 1

Roof Disp. (mm)	Base Shear (kN)	$S_d$	$S_a$ (g)
0	0	0	0
0.528687	135.752	3.69588	0.004081
28.198128	4458.954	197.124	0.13406
56.055785	6255.412	391.8679	0.188071
82.704372	7003.68	578.1596	0.210567
126.457439	7549.823	884.0232	0.226987
186.796057	7933.376	1305.831	0.238519
245.732008	8169.143	1717.833	0.245607
277.96405	8281.019	1943.157	0.248971

Table 4.11: Retrofitted building: Performance Point for Mode 1

$\Gamma$	58.447 kNs <sup>2</sup>	$W$	51970.3 kN
$\phi$	24.00 mm	$\alpha$	0.64
$\Gamma \cdot \phi$	1402.868	$W \cdot \alpha$	33260.99 kN
<b>Performance Point</b>			
$S_d$	350 mm (from graph)		
$\Gamma \cdot \phi$	0.14 mm		
$d$	50 mm		

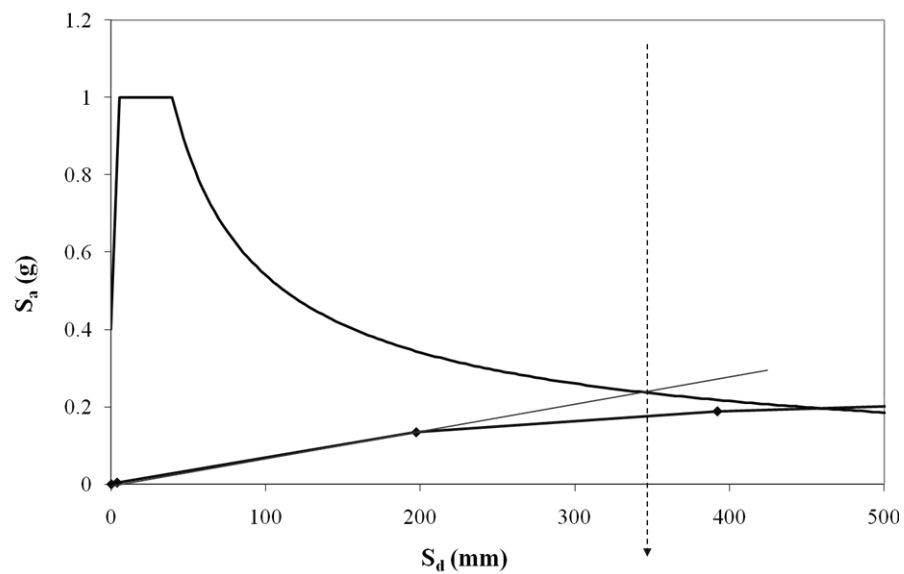


Figure 4.51: Retrofitted Building: Performance Point for Mode 1

Table 4.12: Retrofitted building: Capacity Curve for Mode 2

Roof Disp. (mm)	Base Shear (kN)	$S_d$	$S_a$ (g)
0	0	0	0
2.214477	493.762	15.63315	0.014845
30.061135	5510.29	212.2172	0.165668
46.399842	7018.308	327.5607	0.211007
66.737572	7923.543	471.1354	0.238223
105.081397	8672.489	741.8245	0.260741
165.977237	9253.102	1171.72	0.278197
201.488204	9458.88	1422.41	0.284384
264.448128	9724.862	1866.877	0.29238
323.821719	9942.502	2286.027	0.298924
389.369814	10152.4	2748.765	0.305234
406.179145	10203.357	2867.431	0.306766
422.091723	10238.866	2979.766	0.307834

Table 4.13: Retrofitted building: Performance Point for Mode 2

$\Gamma$	58.125 kNs <sup>2</sup>	$W$	51970.3 kN
$\phi$	23.9 mm	$\alpha$	0.64
$\Gamma.\phi$	1389.188	$W.\alpha$	33260.99 kN
<b>Performance Point</b>			
$S_d$	310 mm (from graph)		
$\Gamma.\phi$	0.14 mm		
$d$	34 mm		

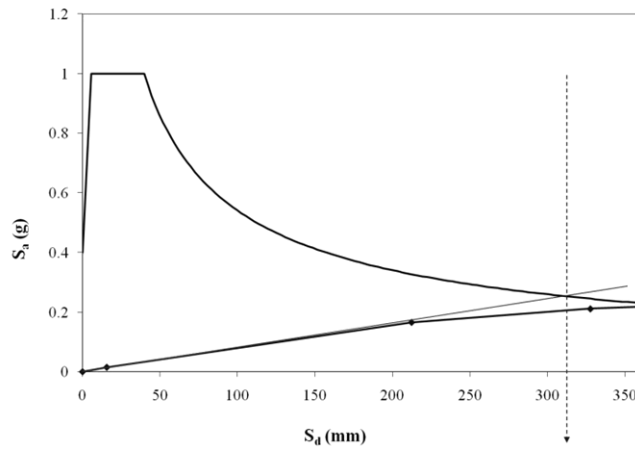


Figure 4.52: Retrofitted Building: Performance Point for Mode 2

Table 4.14: Retrofitted building: Capacity Curve for Mode 3

Roof Disp. (mm)	Base Shear (kN)	$S_d$	$S_a$ (g)
0	0	0	0
0.141295	29.109	28.60349	0.023338
4.278269	1024.65	866.0846	0.821503
13.610358	1780.665	2755.255	1.42763
19.976389	2132.211	4043.982	1.709479
21.211165	2223.176	4293.948	1.782409
22.658599	2285.122	4586.964	1.832074
82.026962	3013.138	16605.38	2.415753
141.786717	3359.464	28703.03	2.693417
201.145941	3640.535	40719.6	2.918763

Table 4.15: Retrofitted building: Performance Point for Mode 3

$\Gamma$	11.13 kNs <sup>2</sup>	$W$	51970.3 kN
$\phi$	4.35 mm	$\alpha$	0.024
$\Gamma.\phi$	48.44	$W.\alpha$	33260.99 kN
<b>Performance Point</b>			
$S_d$	290 mm (from graph)		
$\Gamma.\phi$	0.00494 mm		
$d$	1.5 mm		

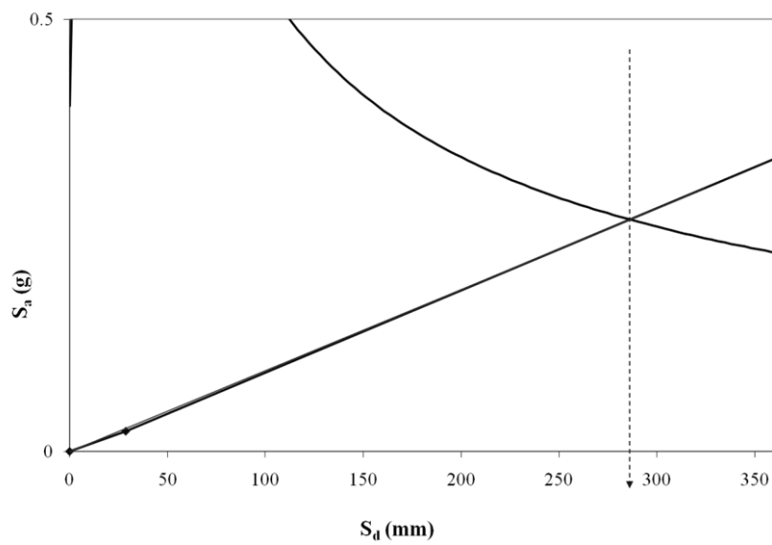


Figure 4.53: Retrofitted Building: Performance Point for Mode 3

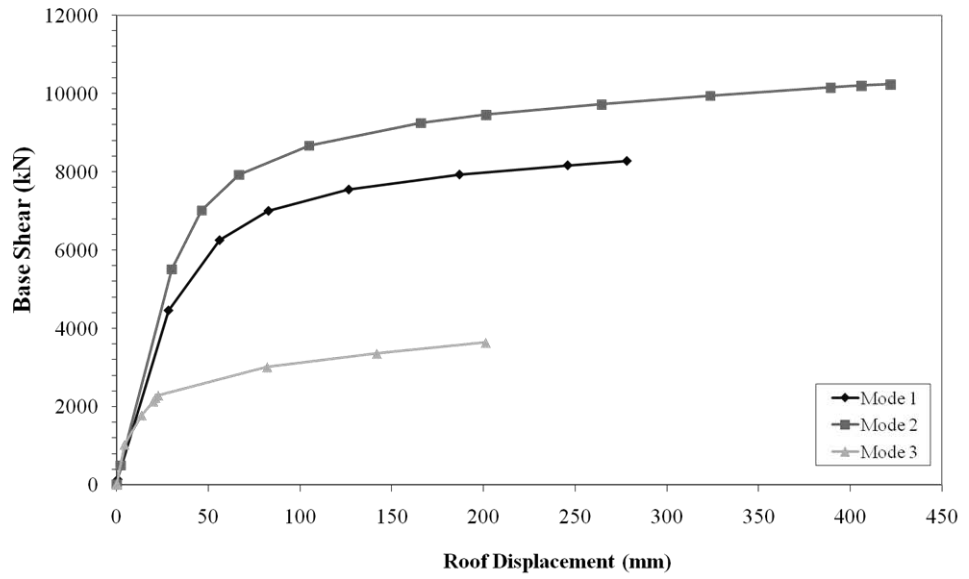


Figure 4.54: Base Shear vs Roof Displacement curves for first three modes of retrofitted building.

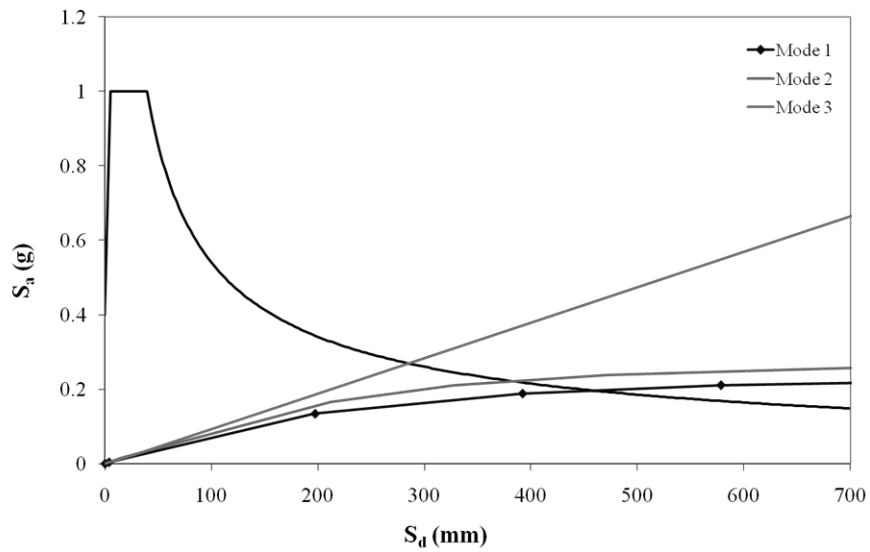


Figure 4.55: Demand curves for first three modes of retrofitted building

Modal pushover assessment results for existing building is given in Figures 4.56 – 4.80

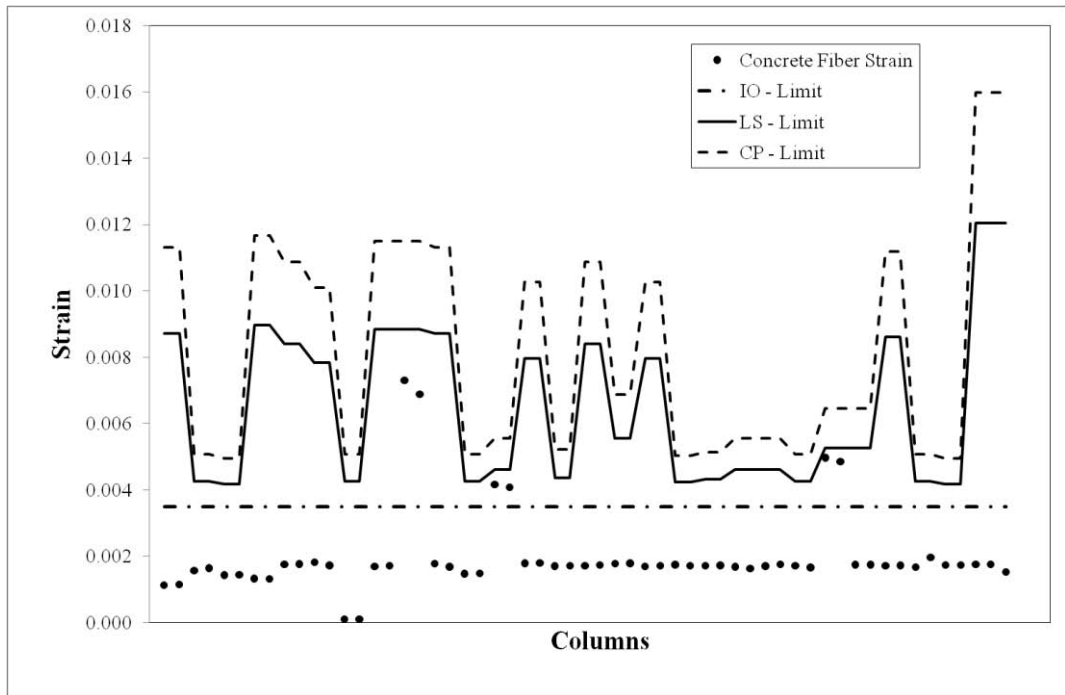


Figure 4.56: Retrofitted Building: Concrete Strains for basement columns

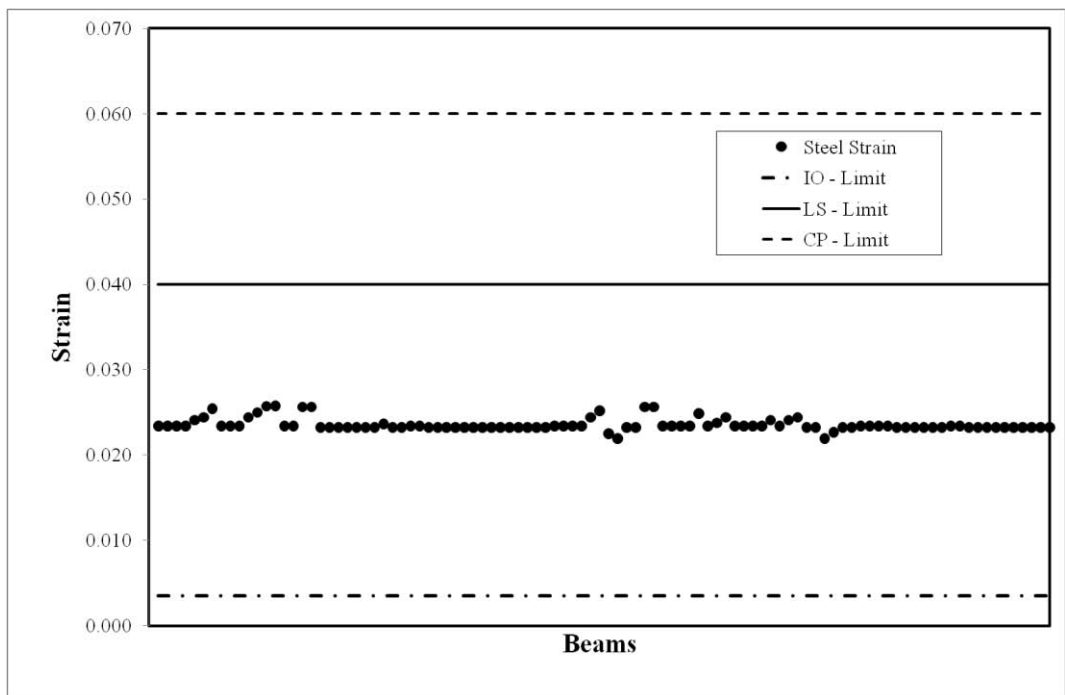


Figure 4.57: Retrofitted Building: Steel Strains for basement beams

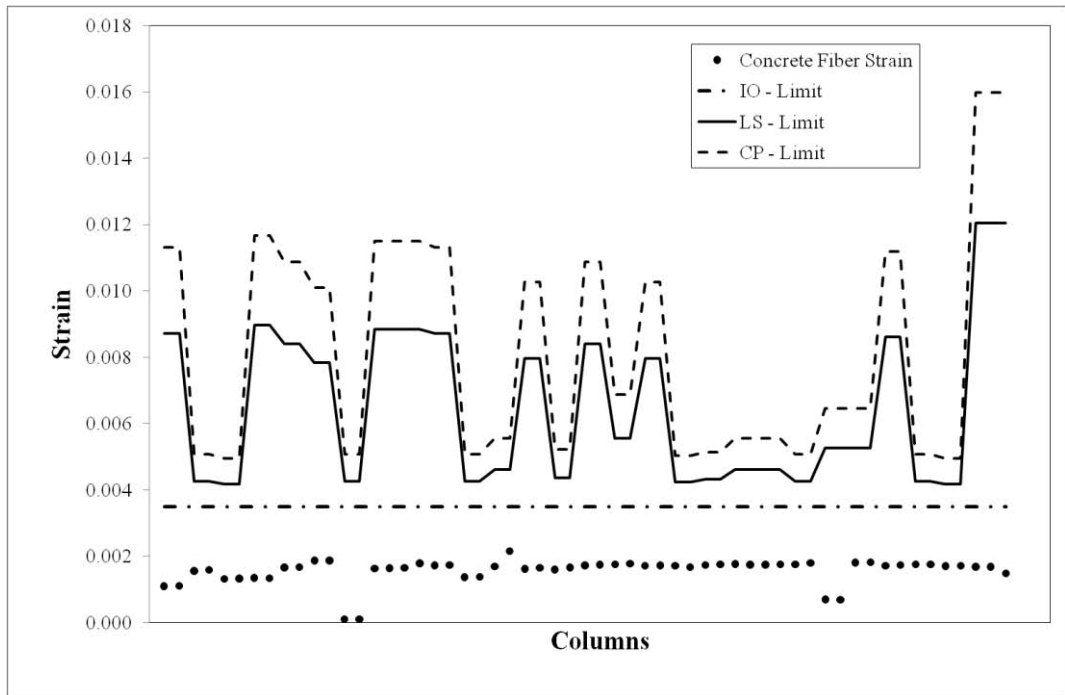


Figure 4.58: Retrofitted Building: Concrete strains for ground storey columns

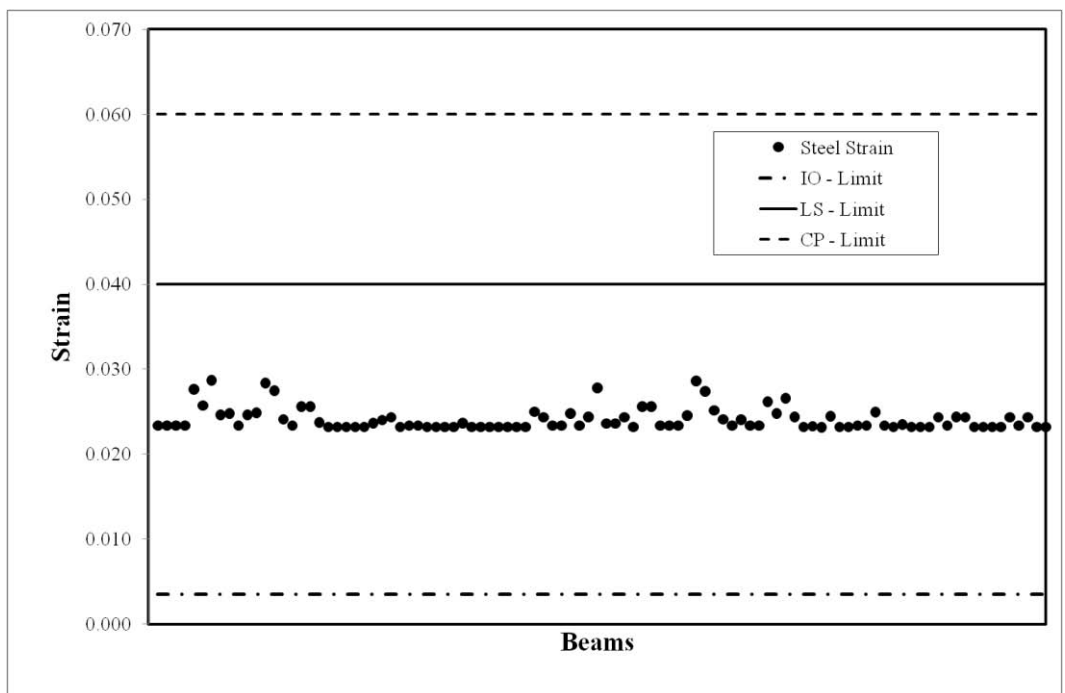


Figure 4.59: Retrofitted Building: Steel strains for ground storey beams

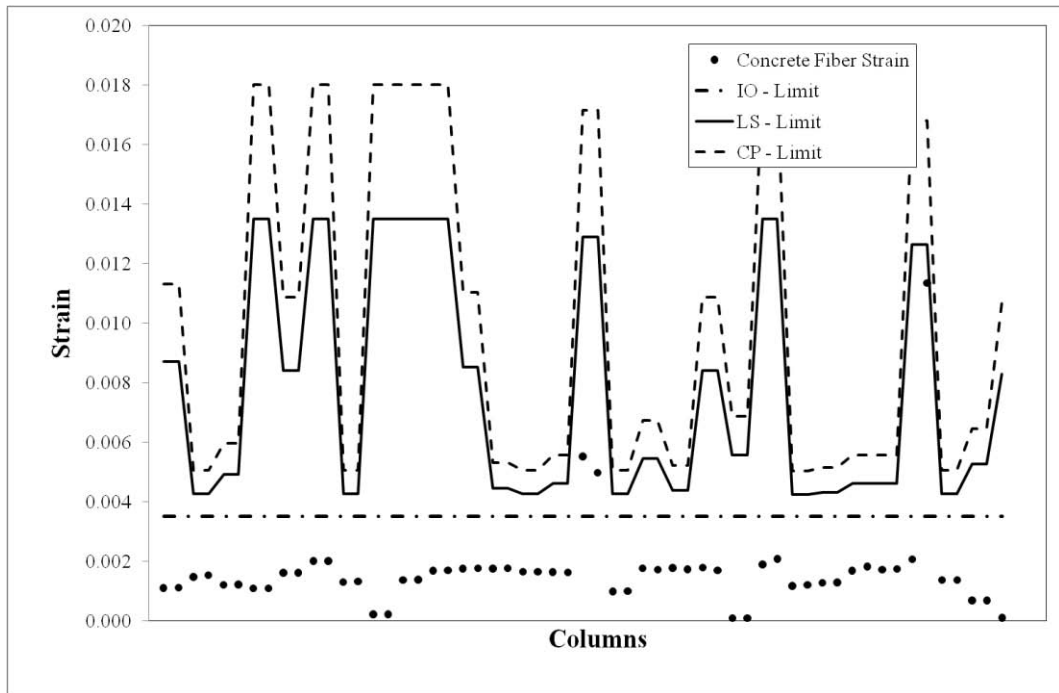


Figure 4.60: Retrofitted Building: Concrete strains for 1st storey columns

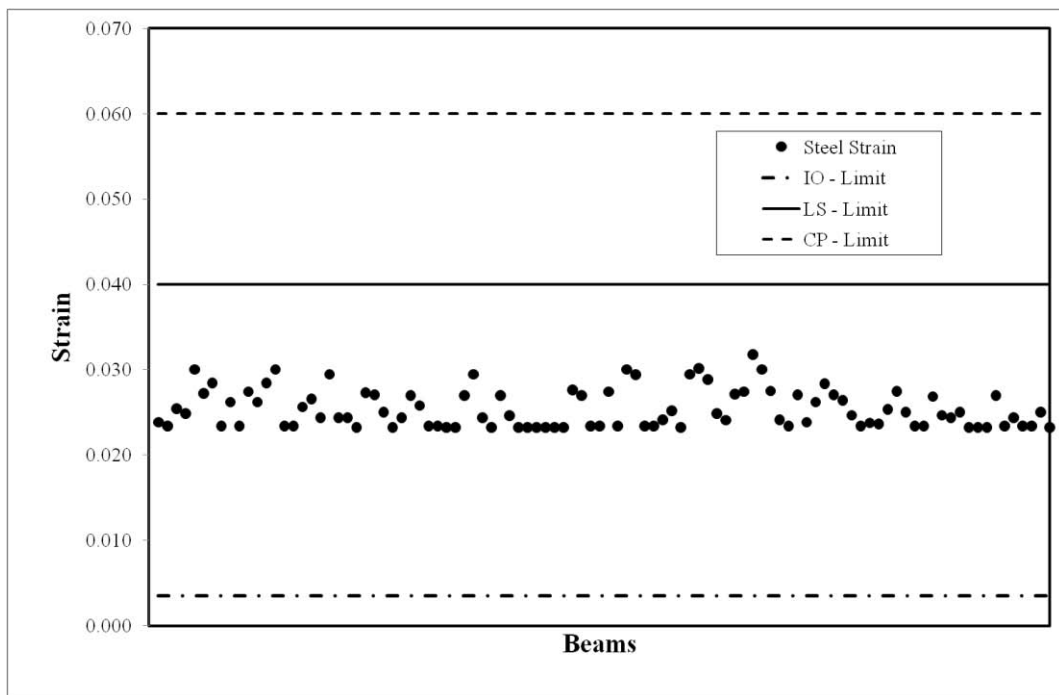


Figure 4.61: Retrofitted Building: Steel strains for 1st storey beams

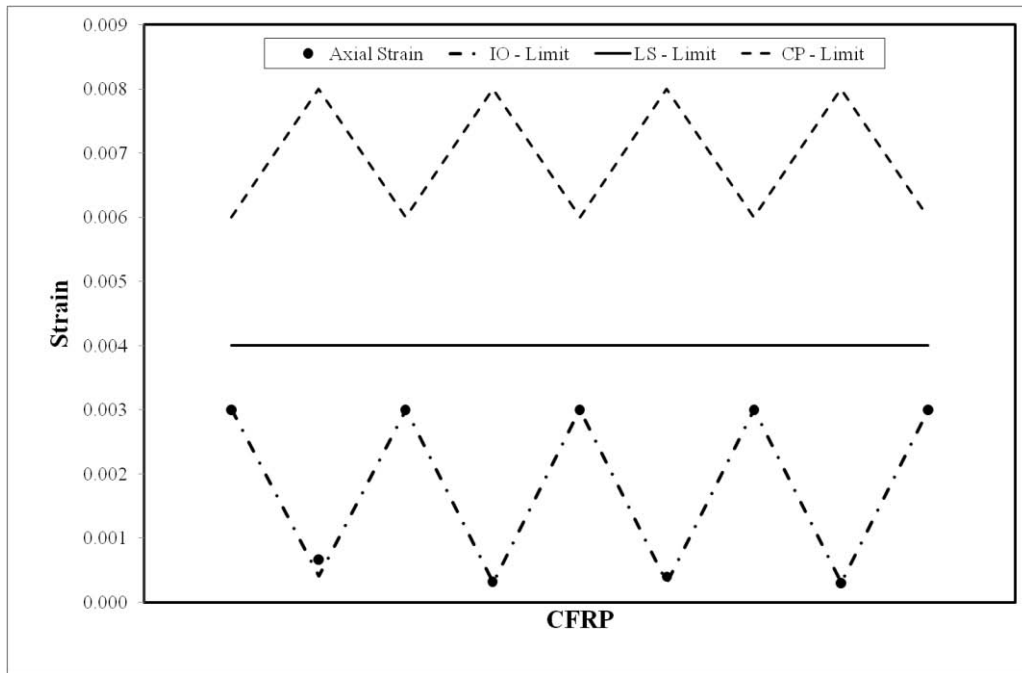


Figure 4.62: Retrofitted Building: Axial strains for 1st storey CFRP

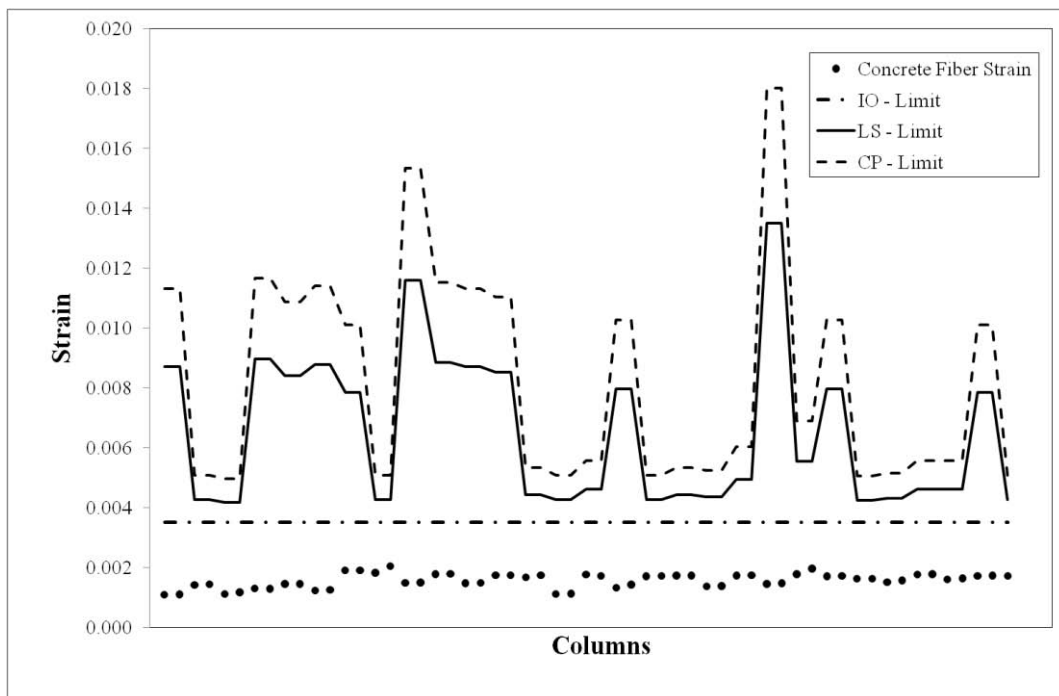


Figure 4.63: Retrofitted Building: Concrete strains for 2nd storey columns

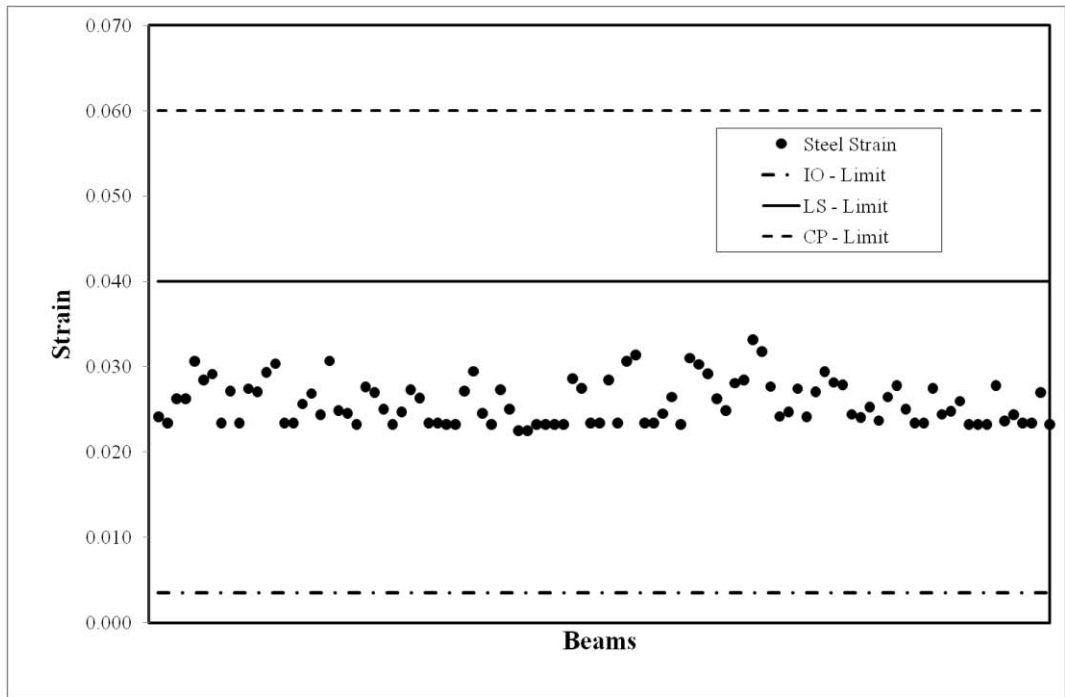


Figure 4.64: Retrofitted Building: Steel strains for 2nd storey beams

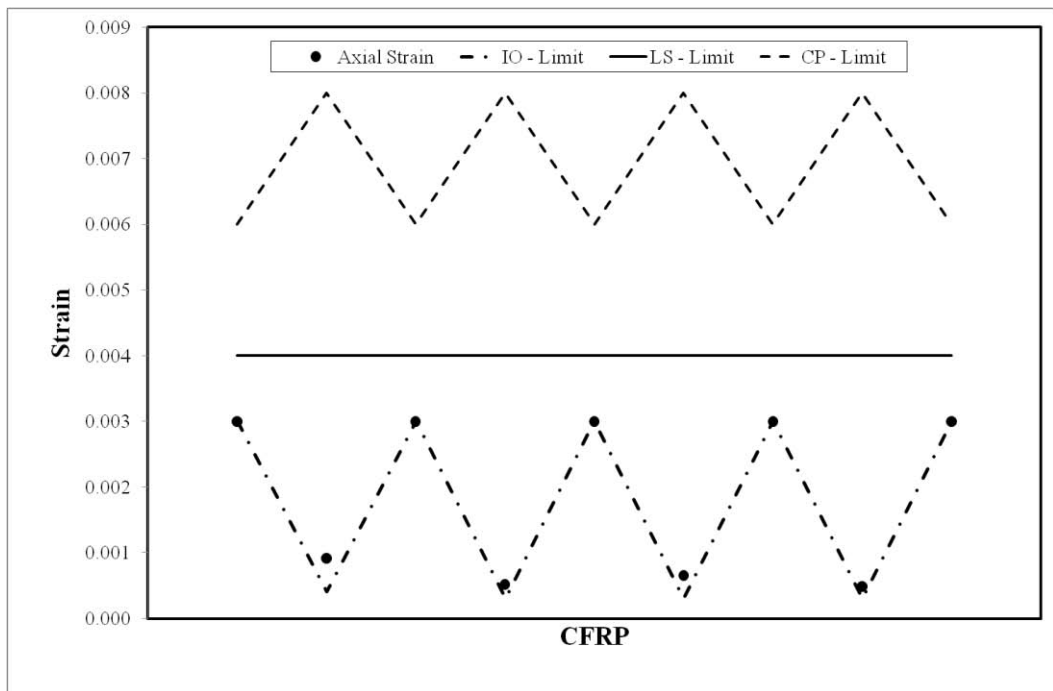


Figure 4.65: Retrofitted Building: Axial strains for 2nd storey CFRP

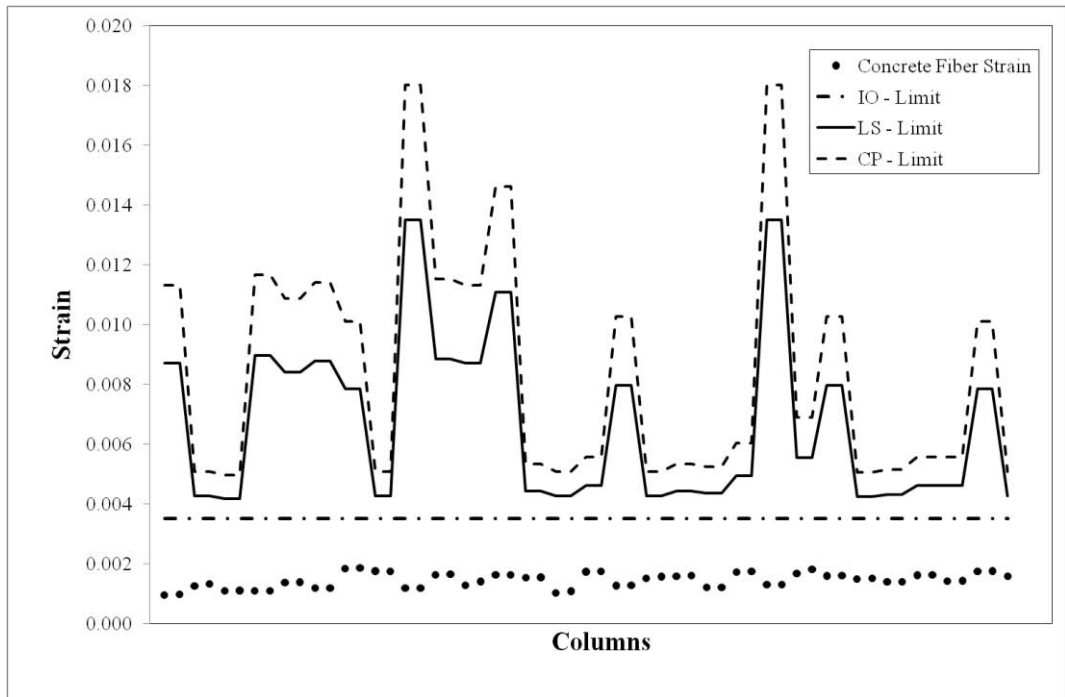


Figure 4.66: Retrofitted Building: Concrete strains for 3rd storey columns

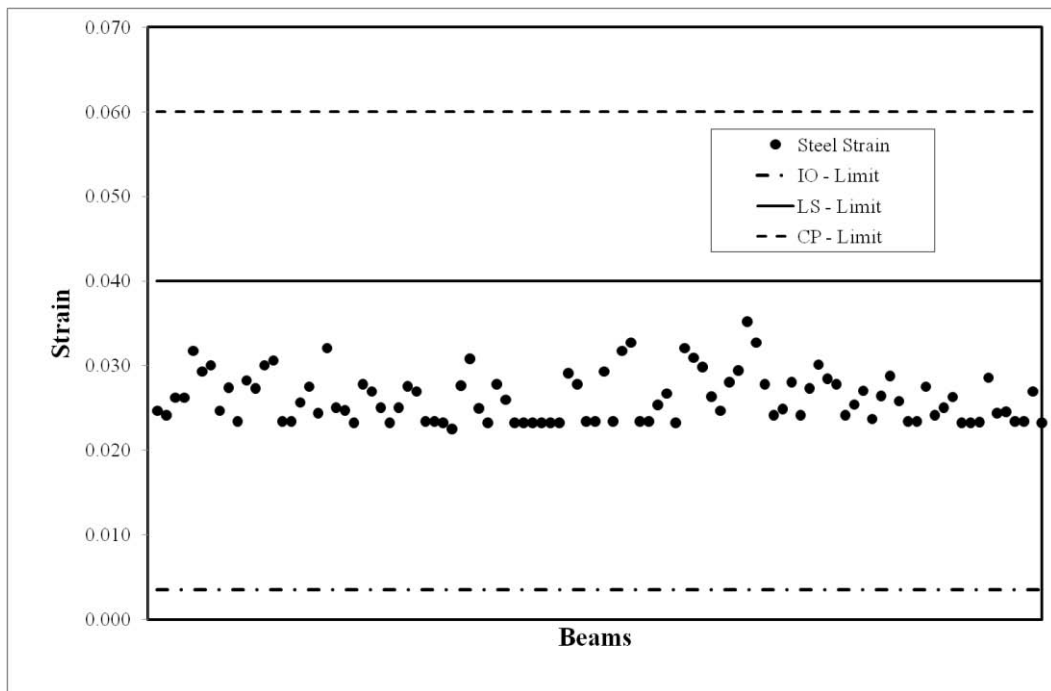


Figure 4.67: Retrofitted Building: Steel strains for 3rd storey beams

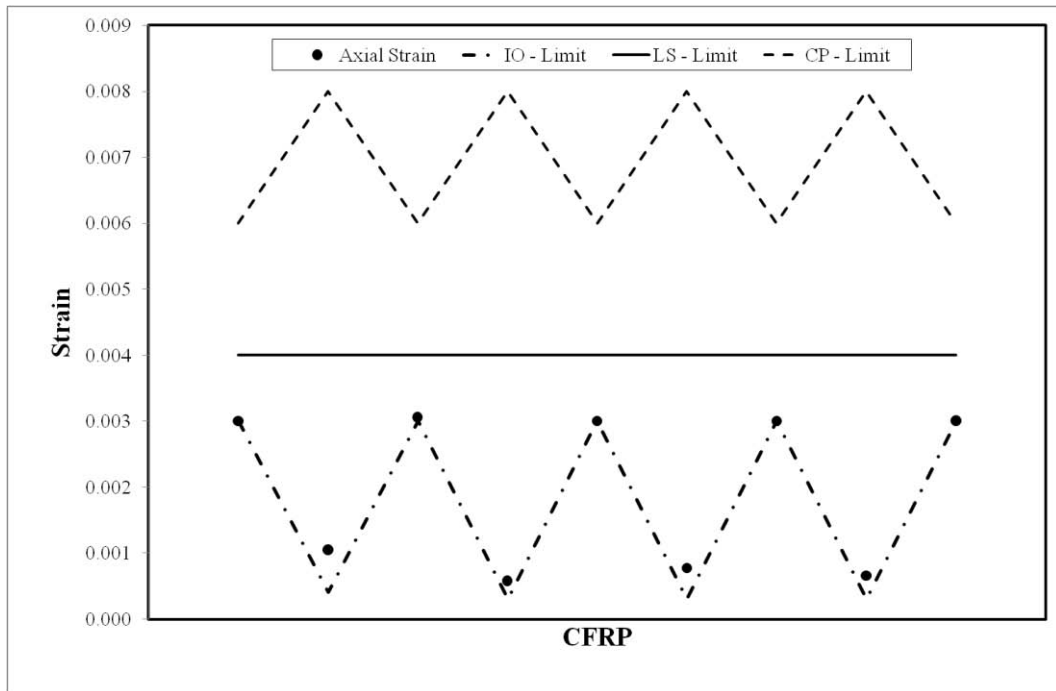


Figure 4.68: Retrofitted Building: Axial strains for 3rd storey CFRP

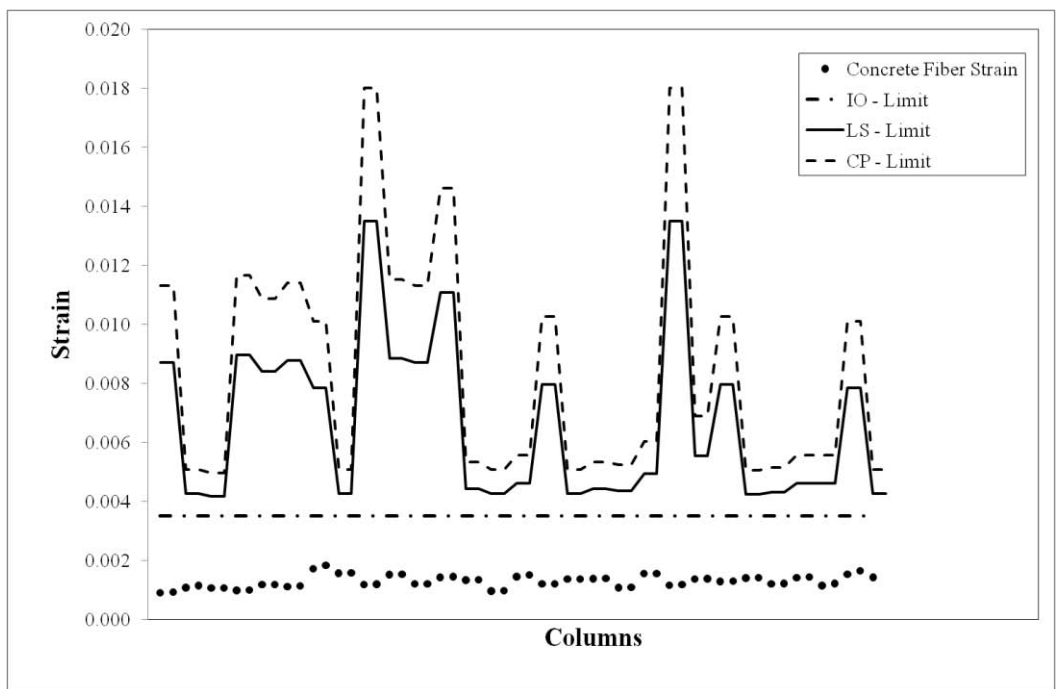


Figure 4.69: Retrofitted Building: Concrete strains for 4th storey columns

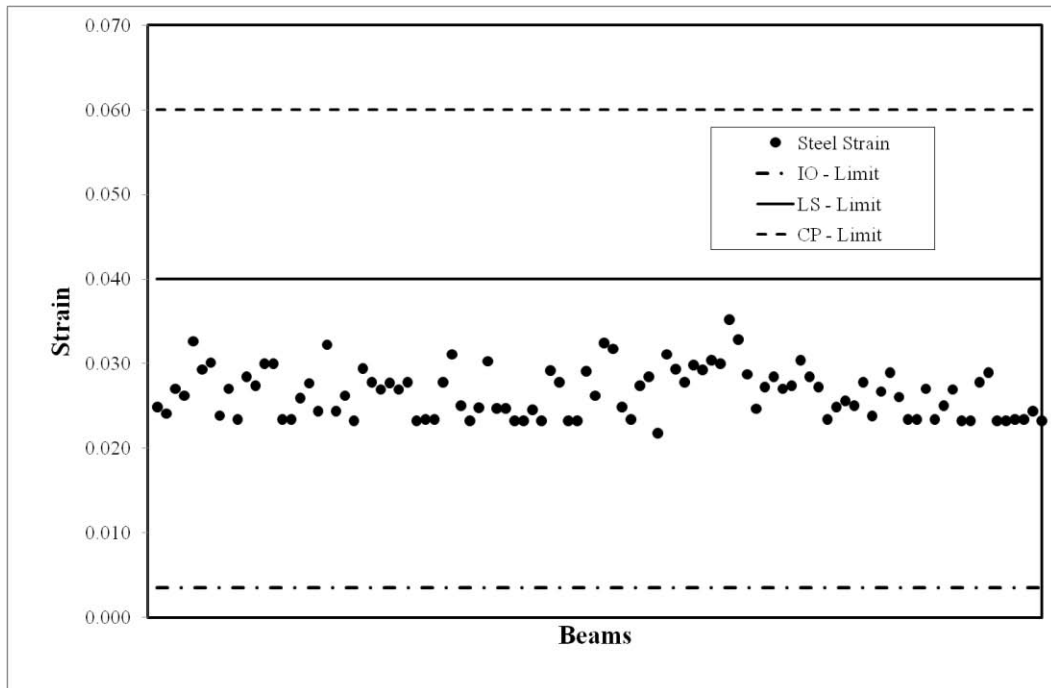


Figure 4.70: Retrofitted Building: Steel strains for 4th storey beams

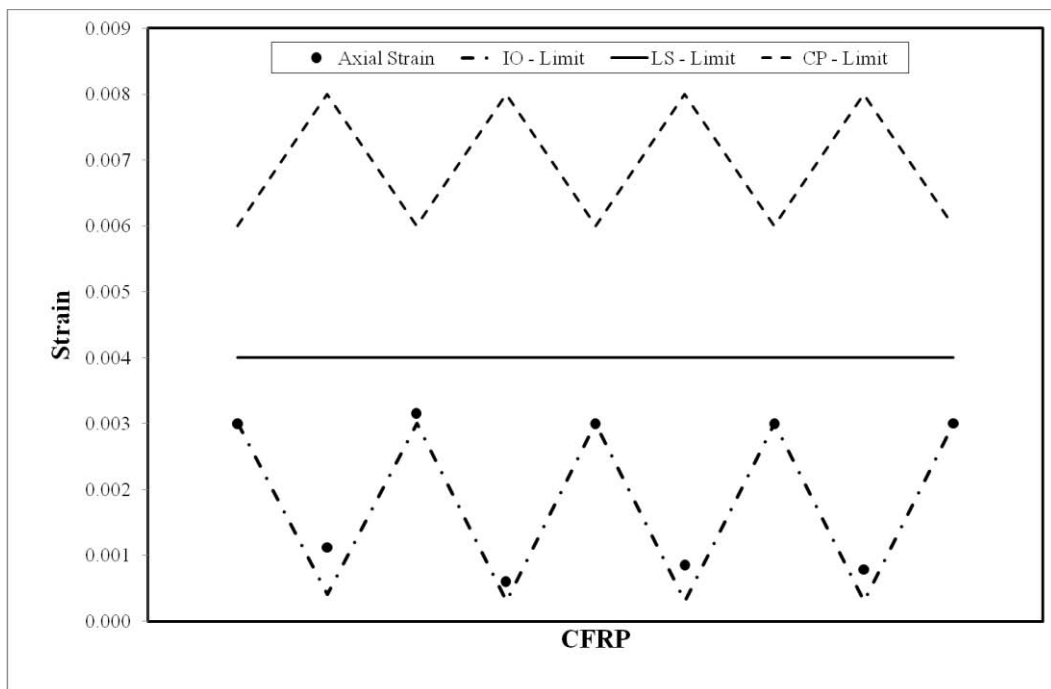


Figure 4.71: Retrofitted Building: Axial strains for 4th storey CFRP

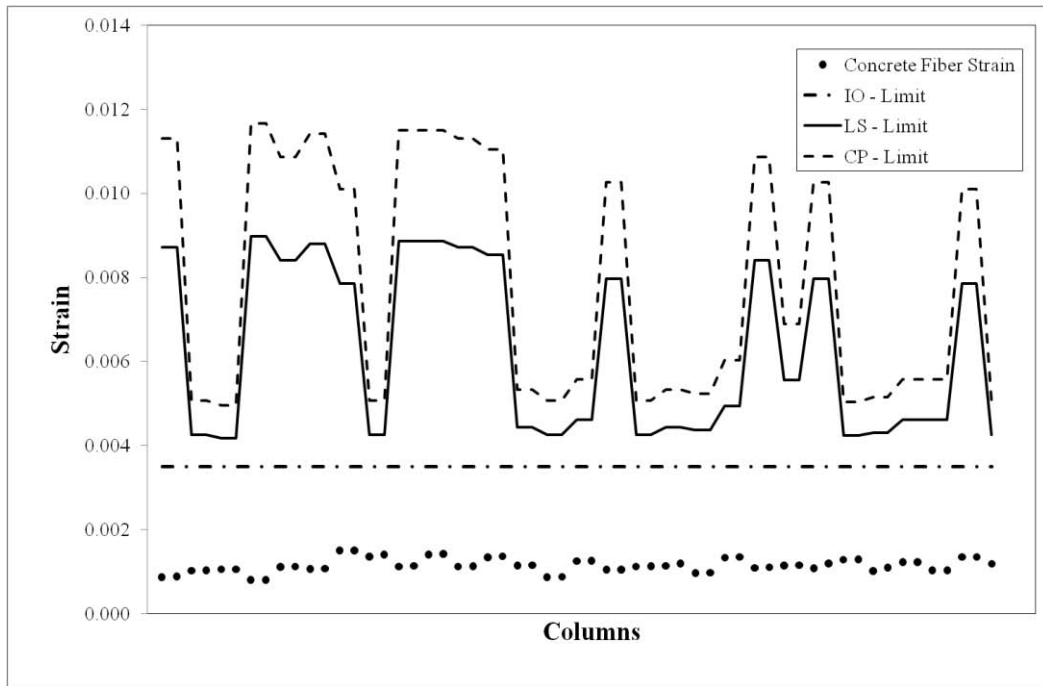


Figure 4.72: Retrofitted Building: Concrete strains for 5th storey columns

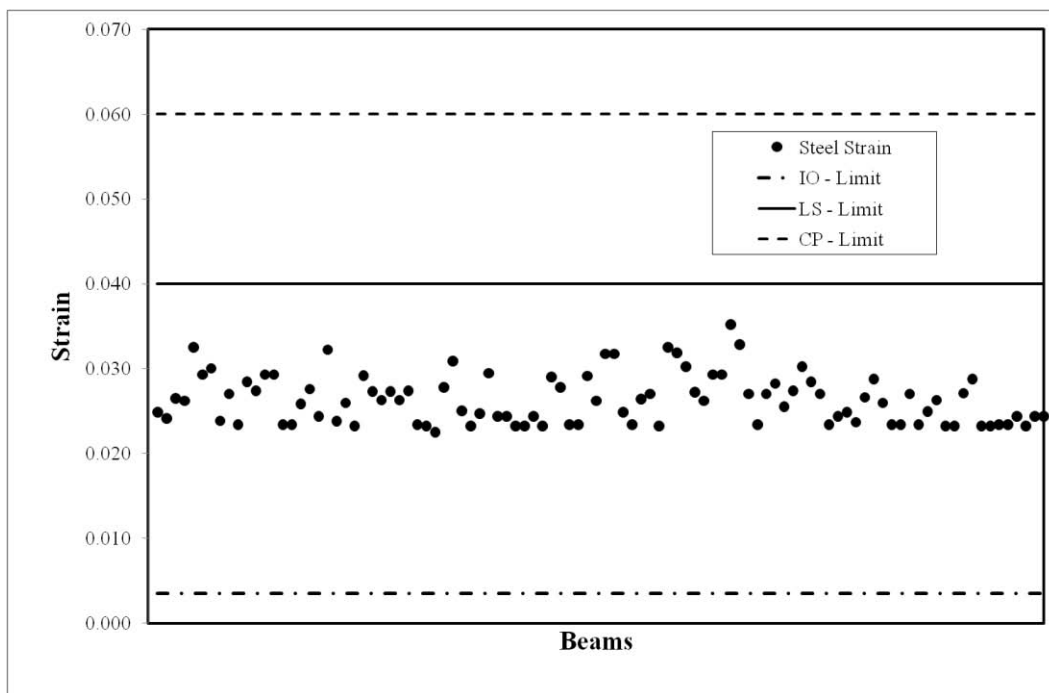


Figure 4.73: Retrofitted Building: Steel strains for 5th storey beams

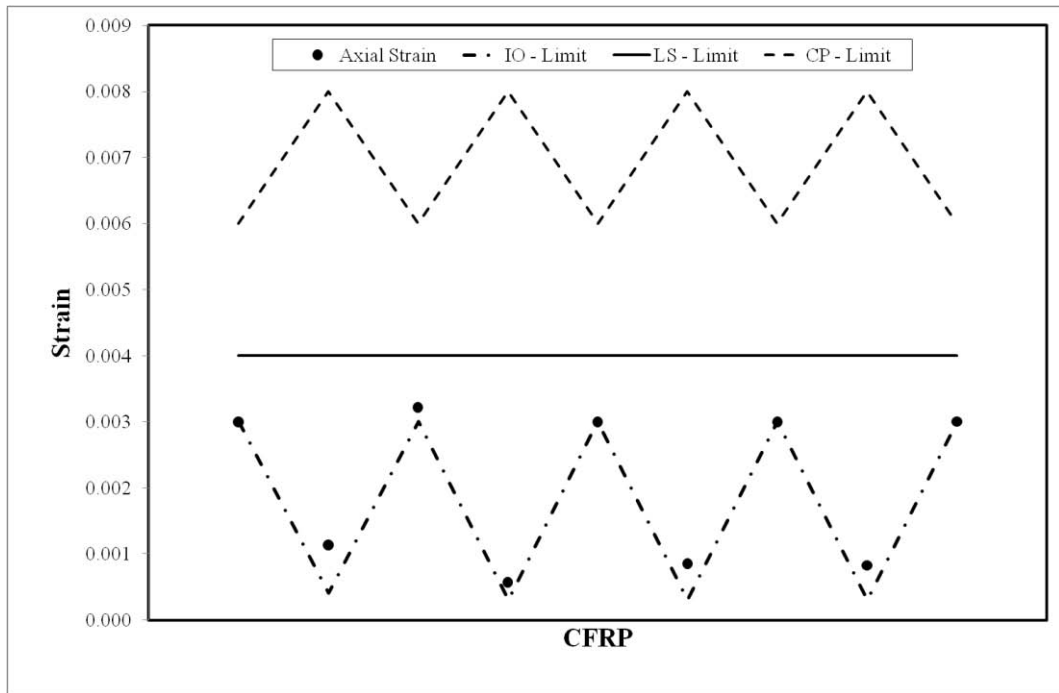


Figure 4.74: Retrofitted Building: Axial strains for 5th storey CFRP

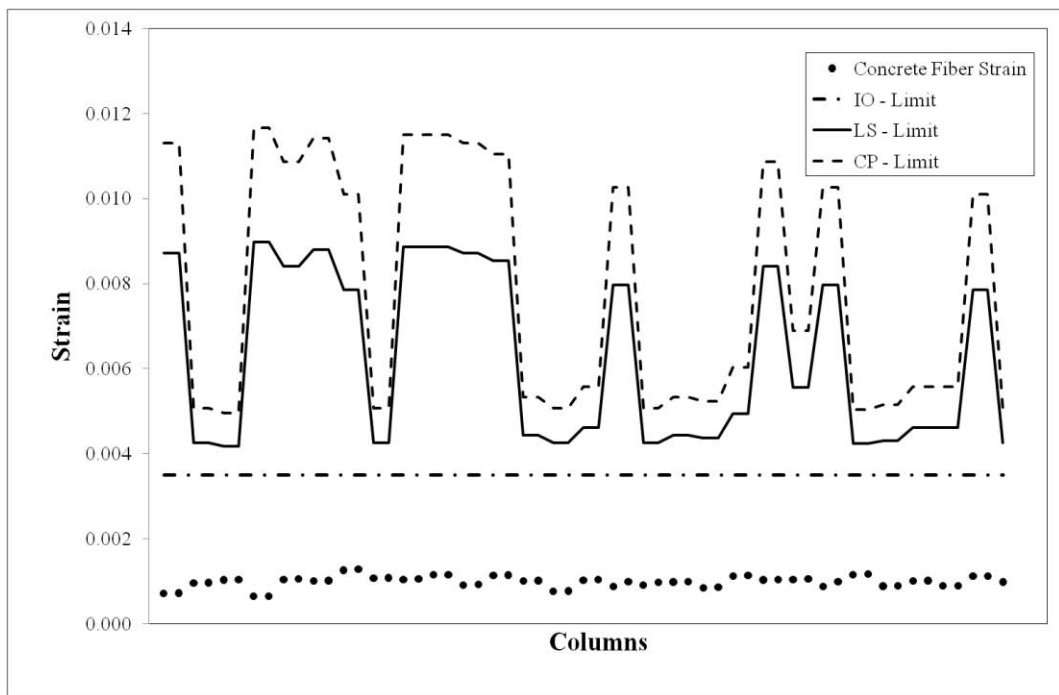


Figure 4.75: Retrofitted Building: Concrete strains for 6th storey columns

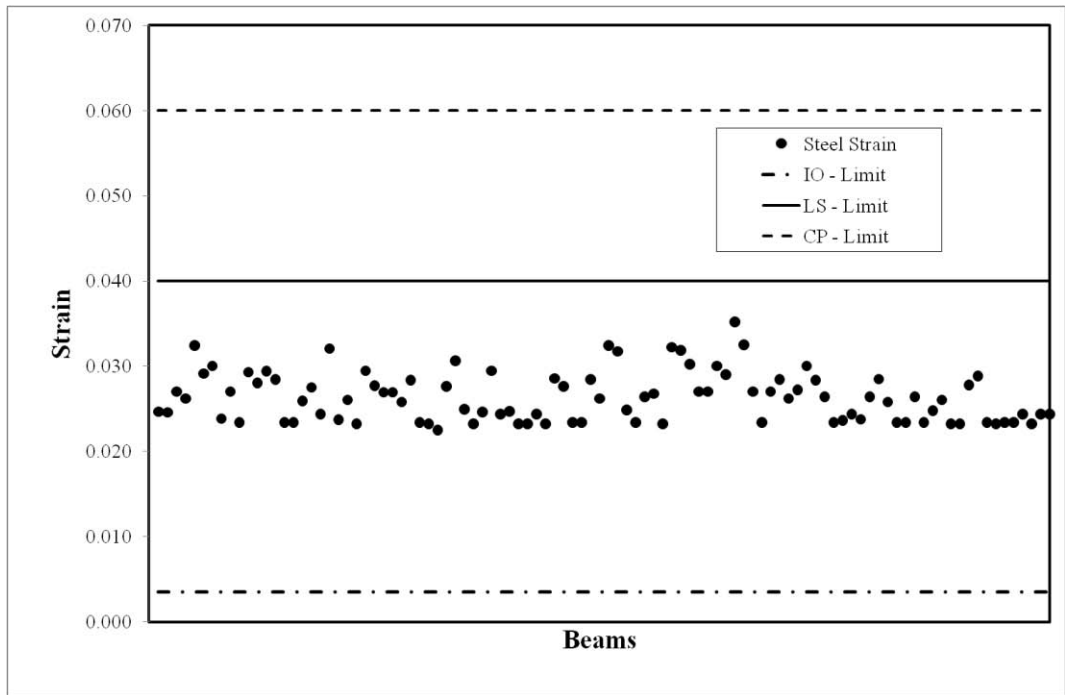


Figure 4.76: Retrofitted Building: Steel strains for 6th storey beams

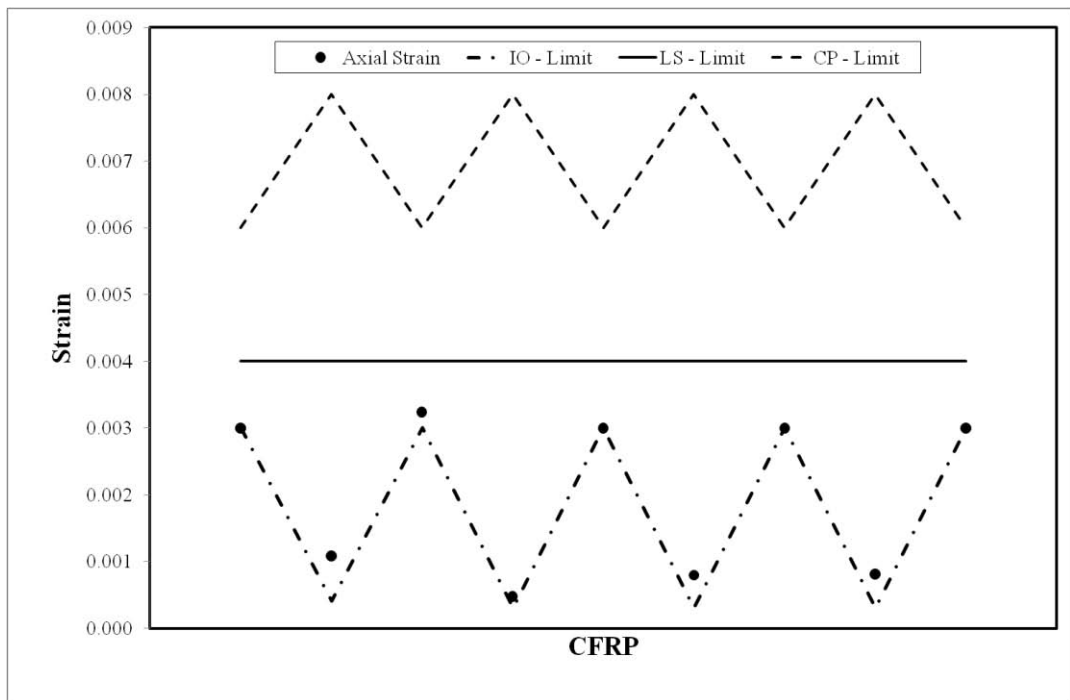


Figure 4.77: Retrofitted Building: Axial strains for 6th storey CFRP

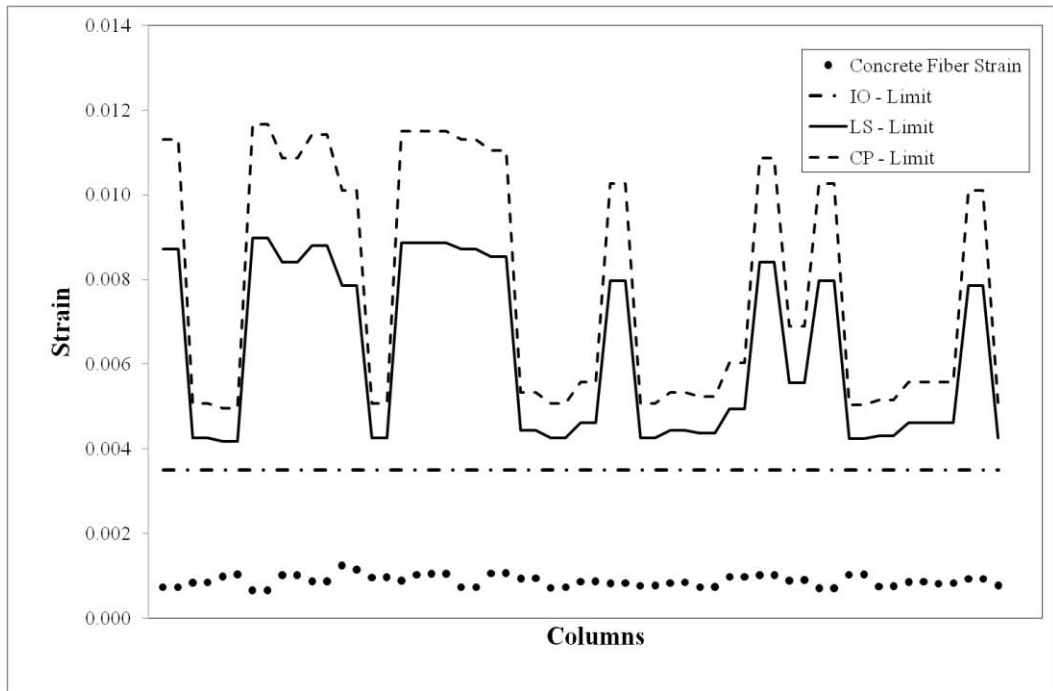


Figure 4.78: Retrofitted Building: Concrete strains for 7th storey columns

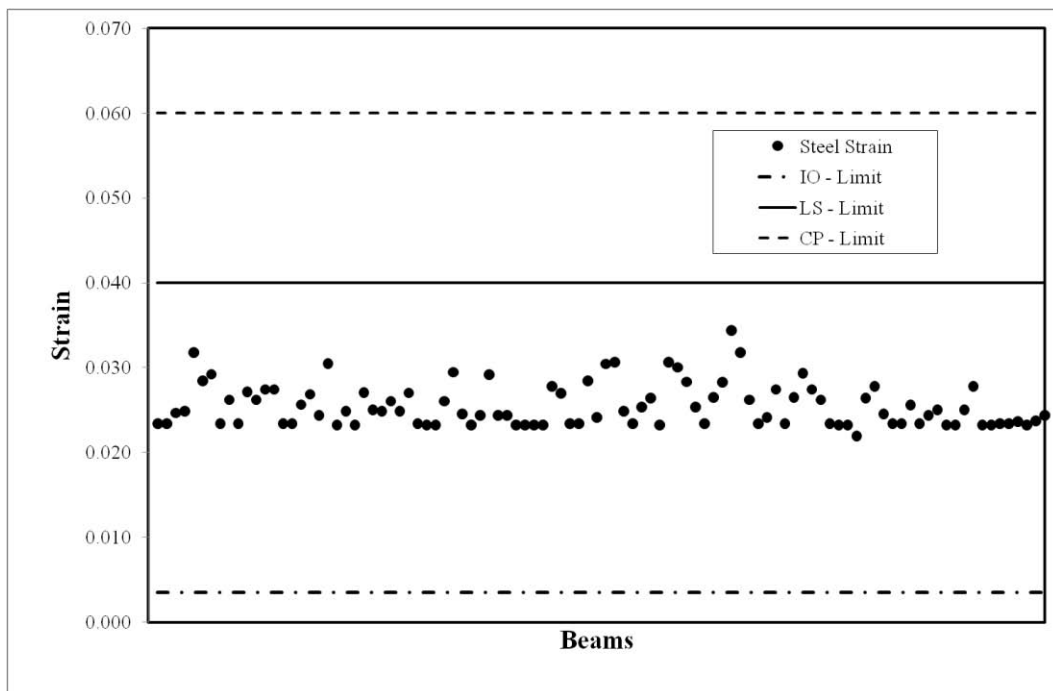


Figure 4.79: Retrofitted Building: Steel strains for 7th storey beams

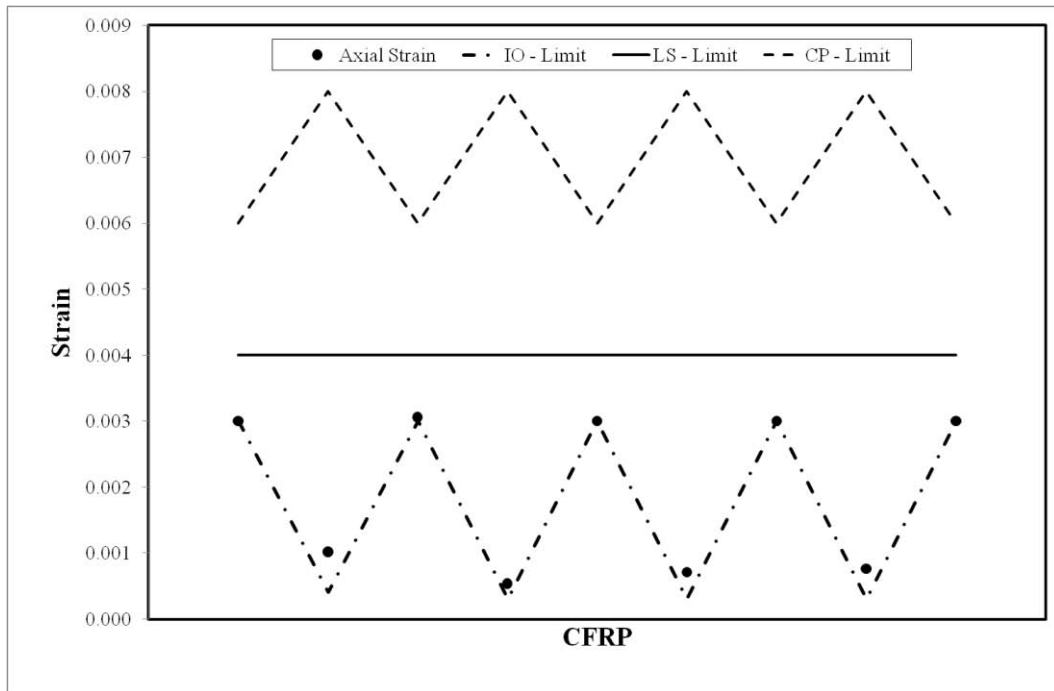


Figure 4.80: Retrofitted Building: Axial strains for 7th storey CFRP

Drift ratios for retrofitted building is given in Figure 4.81.

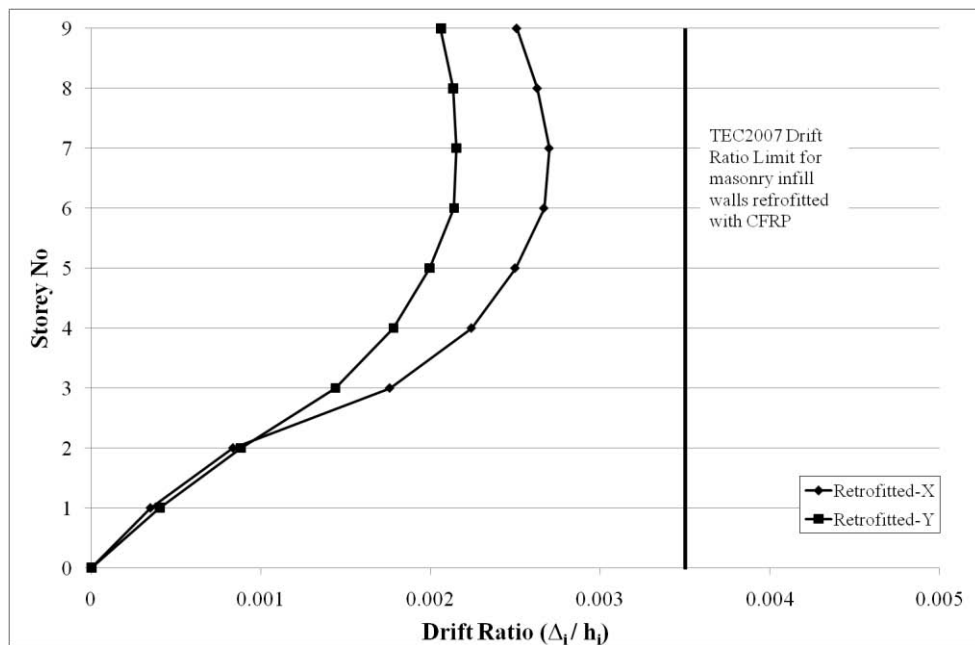


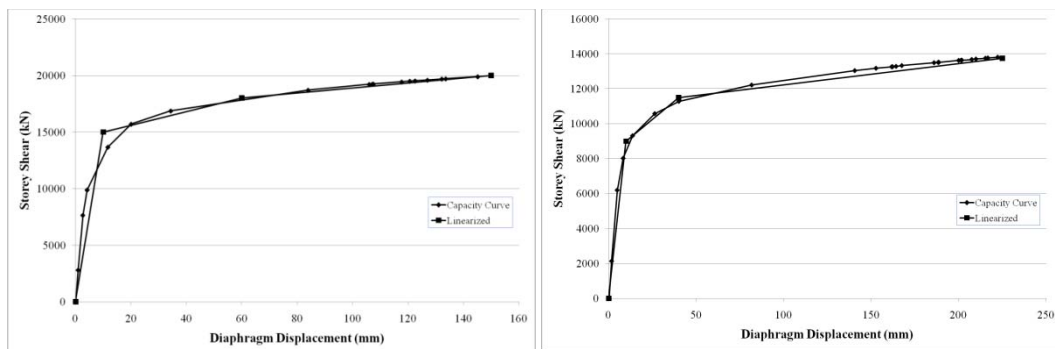
Figure 4.81: Retrofitted Building: Drift Ratios

Retrofit scheme eliminates the brittle failures occurring in existing structures. Column, beam and shearwall concrete strains in the critical sections remain under immediate occupancy limit. For the beams, we observe that the tension steel strains govern the performance behaviour. They usually remain under the life safety limit, indicating that all the beams perform well for life safety criteria. Newly added reinforced concrete shearwalls also satisfy immediate occupancy limits. Also, CFRP masonry walls do not gain strains over life safety limits. Turkish Earthquake code suggests a maximum drift ratio of 0.0035 for CFRP strengthened masonry walls. We observe that, interstorey drift ratios satisfy this condition. From the performance graphs of CFRPs, it can be implied that CFRP walls will provide us with a auxiliary lateral resistance under larger interstorey drifts. Same global performance conditions that applies to elastic analysis is valid for nonlinear analysis. Retrofitted scheme satisfy code-given criteria.

#### 4.6. ANALYSIS AND ASSESSMENT OF THE BUILDING USING SIMPLIFIED NONLINEAR TIME HISTORY ANALYSIS

##### 4.6.1 Existing Building

Details of the procedure is given in section 2.3.5. Capacity curves for each storey of the existing building is given in Figure 4.82.



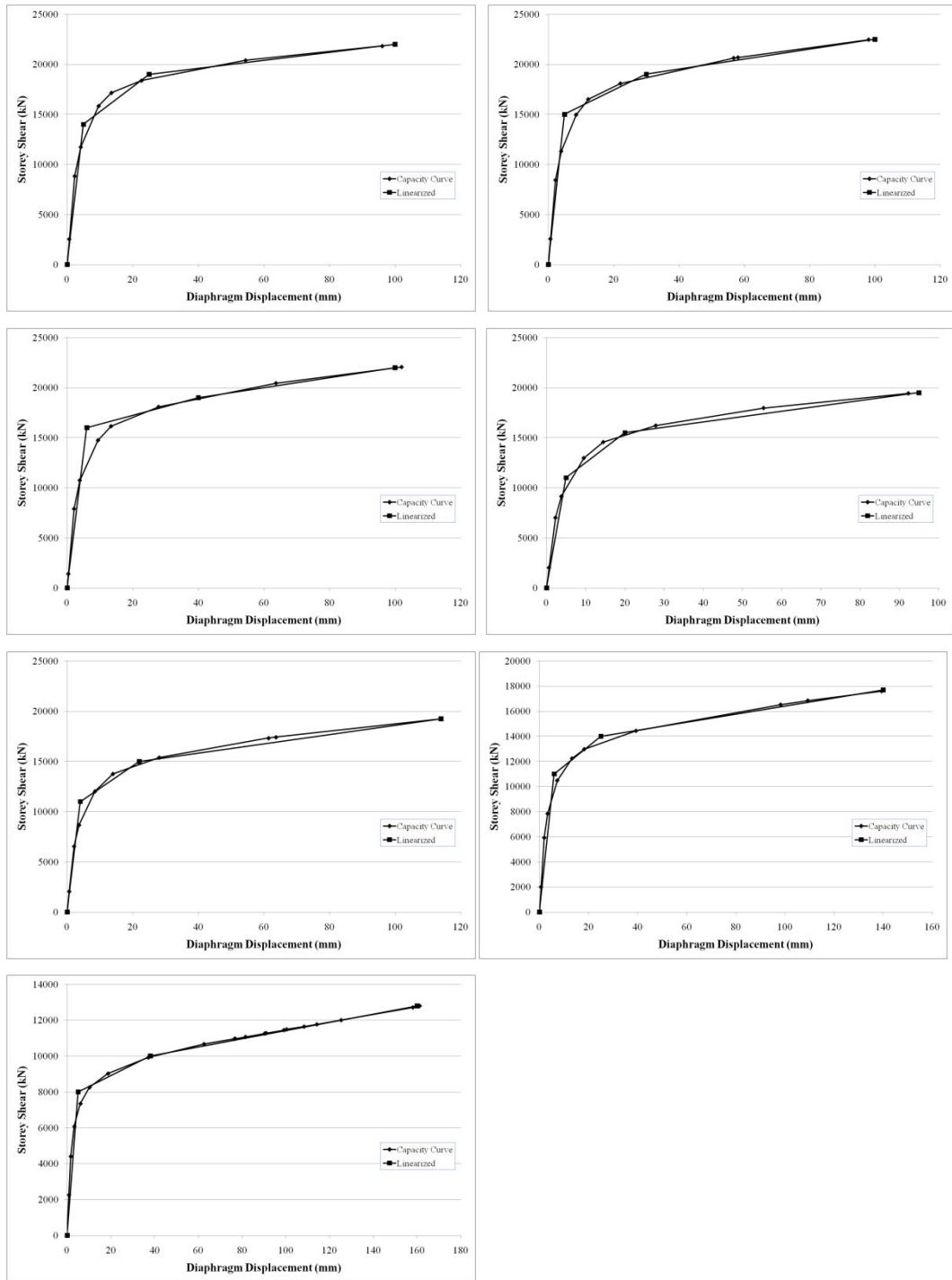


Figure 4.82: Storey capacity curves for existing building.

In SAP2000, “multilinear plastic link” elements are utilized and these capacity curves are used as force-deformation relationship. 2D nonlinear model and a typical interface for force-deformation input is shown in Figure 4.83.

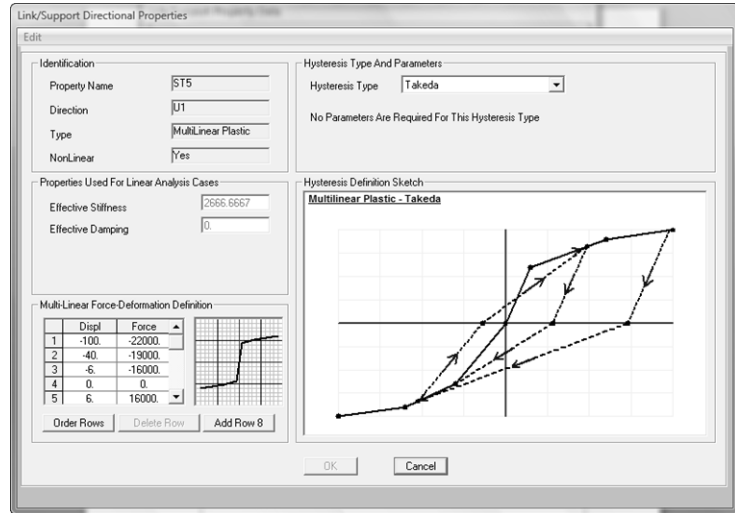


Figure 4.83: 2D model for nonlinear time history analysis and force-deformation input

Earthquake record selection conditions are explained in section 2.3.6 and Fahjan [13]. Fahjan [13] lists the earthquake records that are suitable for use with Turkish Earthquake code together with their scale factors. Earthquake records are simply multiplied by  $A_o$ , Importance Factor ( $I$ ), and scale factor given by Fahjan.

$$\text{Final Scale Factor to input} = A_o \cdot I \cdot \alpha_{ST} \quad (4.1)$$

Where  $\alpha_{ST}$  is given by Fahjan in Table 4.16

Table 4.16: Selected Earthquakes for Soil Class Z2 to be used in time history analysis.

EQ	Station	Record	Dis. to Fault	Fault Mech.	Scale Factor ( $\alpha_{ST}$ )
Imperial Valley	931 El Centro Array #12	H-E12230	18.20	SS	8.31
Imperial Valley	931 El Centro Array #12	H-E12140	18.20	SS	7.01
Superstittn Hills (B)	11369 Westmorland Fire Sta	B-WSM090	13.30	SS	5.10

Drift ratios for existing building for each storey obtained after time history analysis is shown in Figure 4.84. Envelope of three earthquakes were considered.

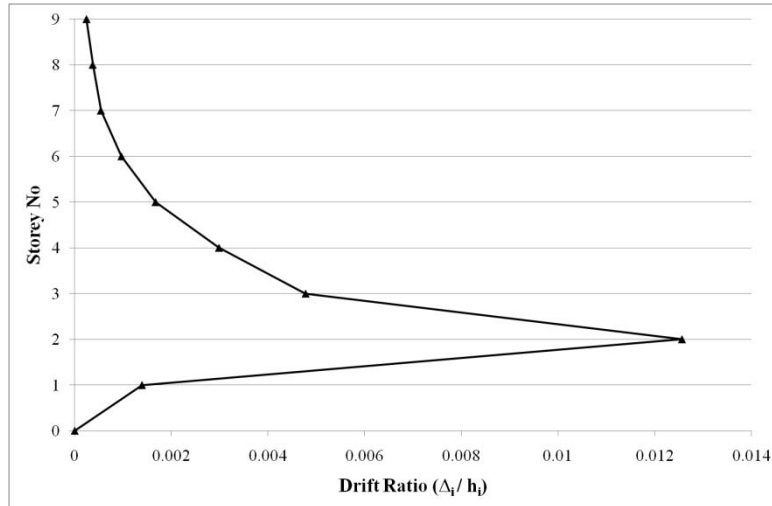


Figure 4.84: Envelope drift ratio demand for existing building at each storey after time history analysis.

Plastic rotations and internal forces were extracted using the drift demands above from each storey analysis model. Results from separate models were merged into a single set. Member by member assessment was performed according to TEC2007 regulations. Results are tabulated in Figures 4.85 – 4.120

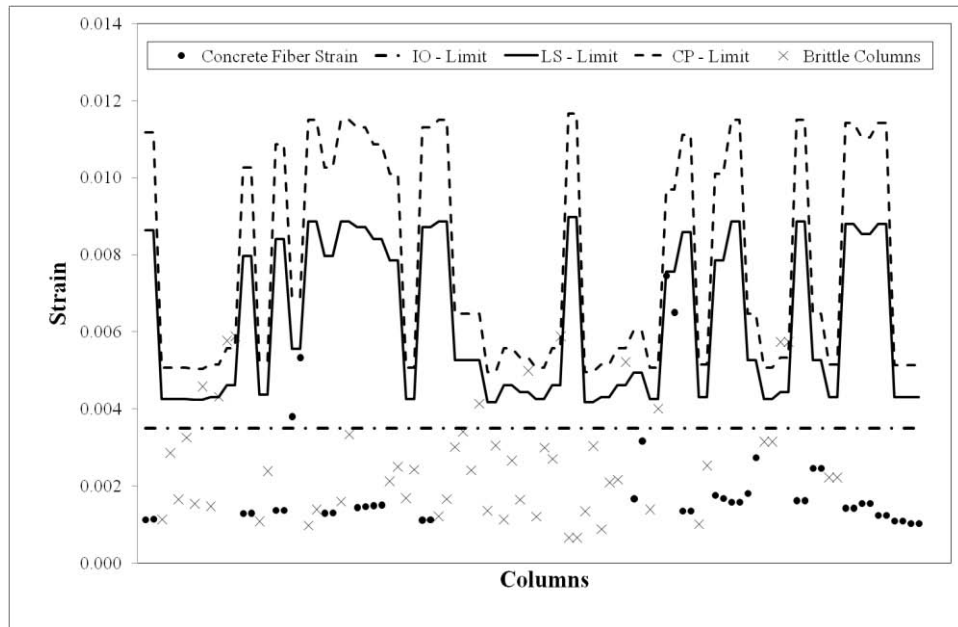


Figure 4.85: Existing Building: Concrete strains for basement storey columns

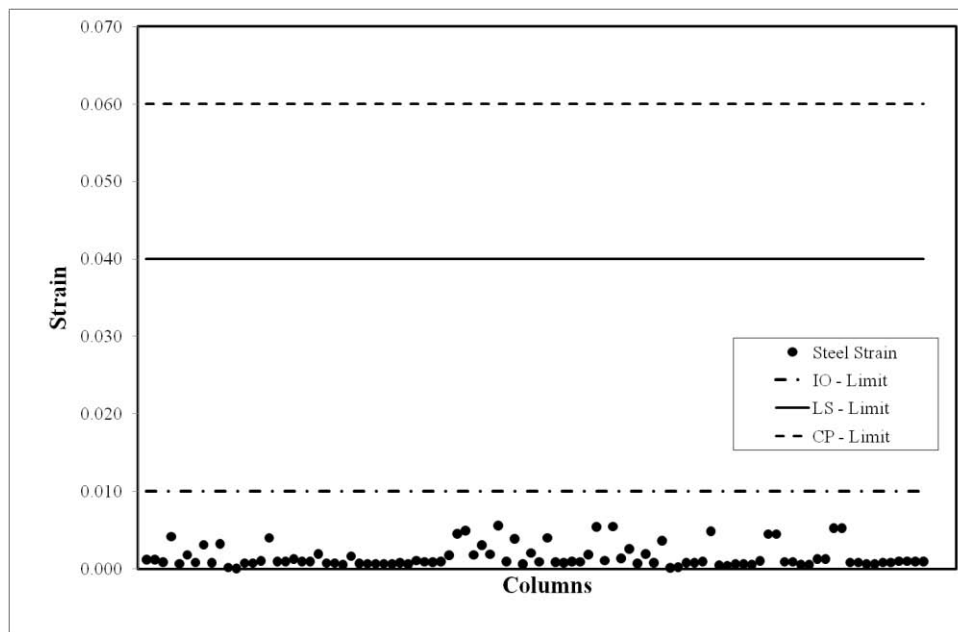


Figure 4.86: Existing Building: Steel strains for basement storey columns

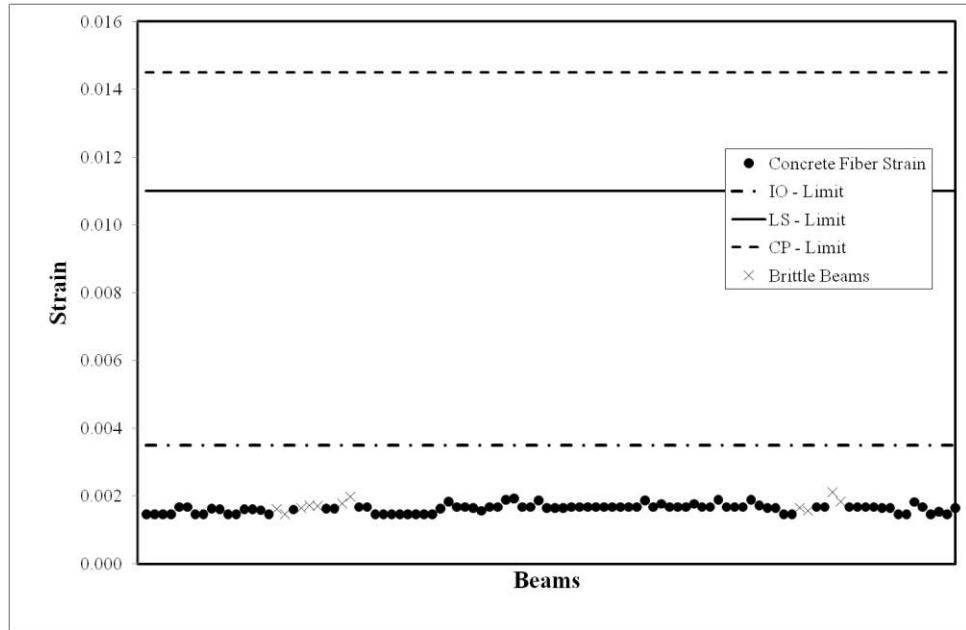


Figure 4.87: Existing Building, Concrete strains for basement storey beams

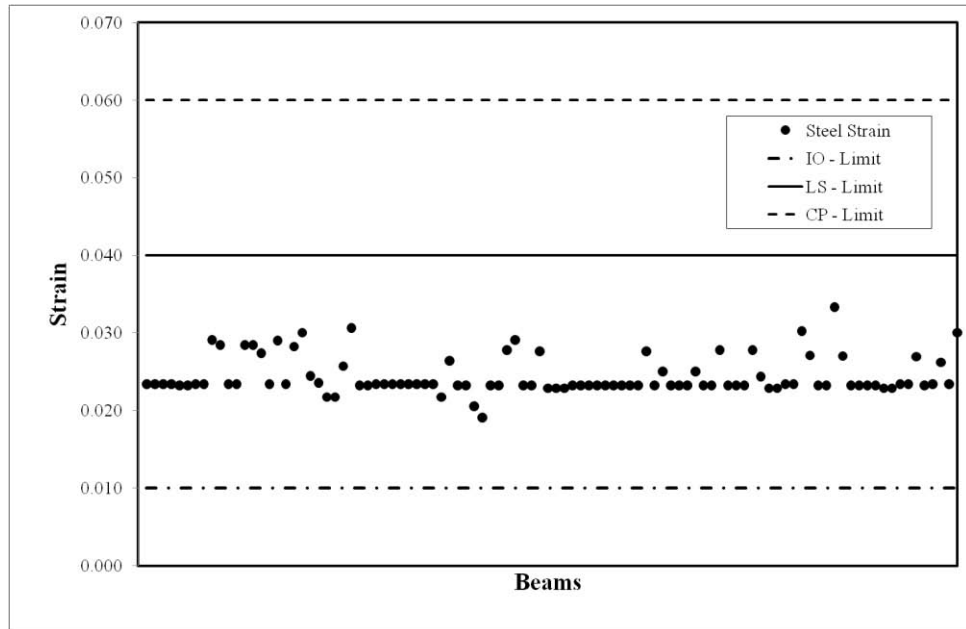


Figure 4.88: Existing Building, Steel strains for basement storey beams

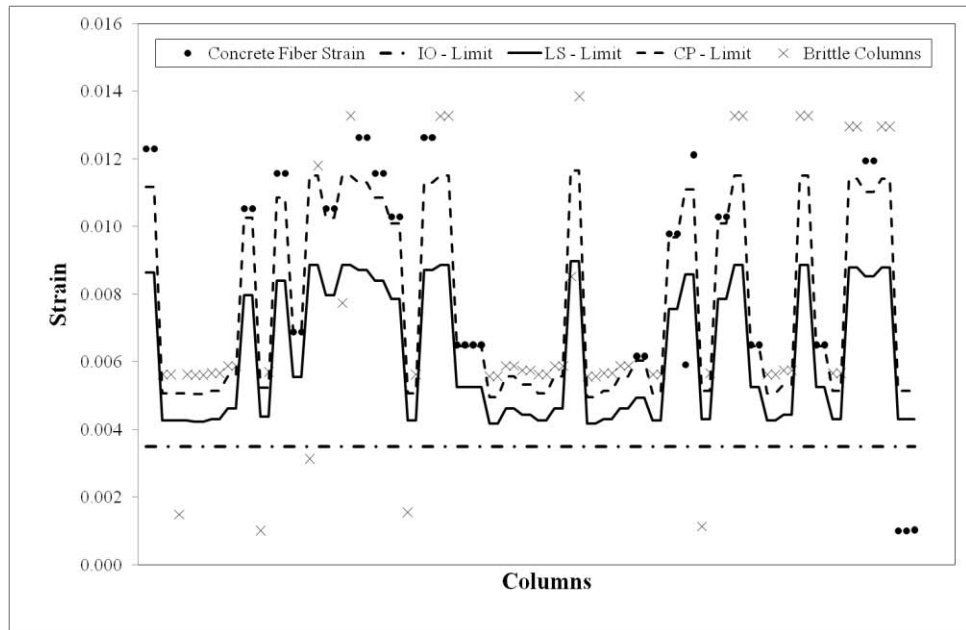


Figure 4.89: Existing Building, Concrete strains for ground storey columns

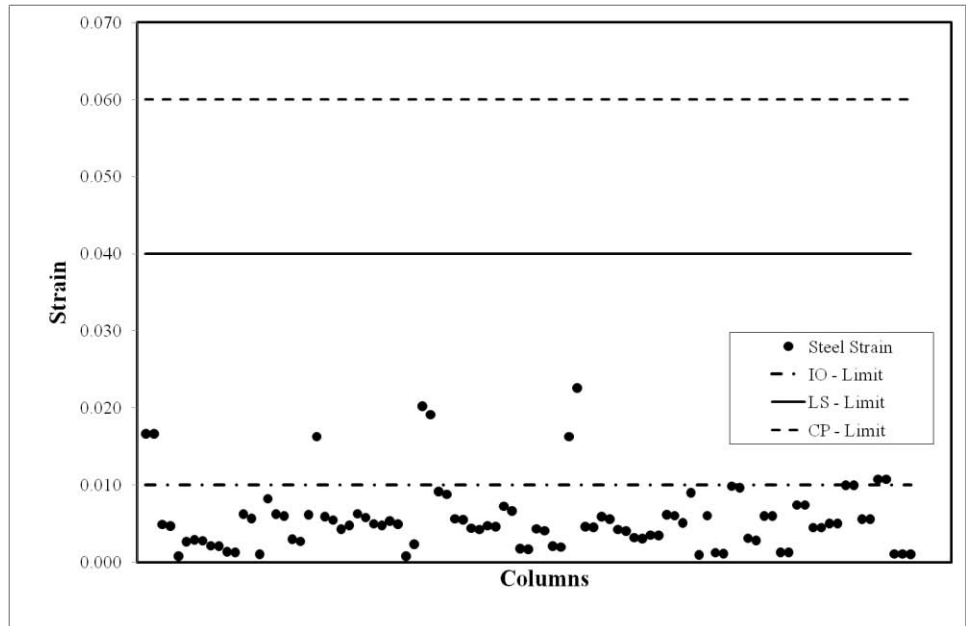


Figure 4.90: Existing Building, Steel strains for ground storey columns

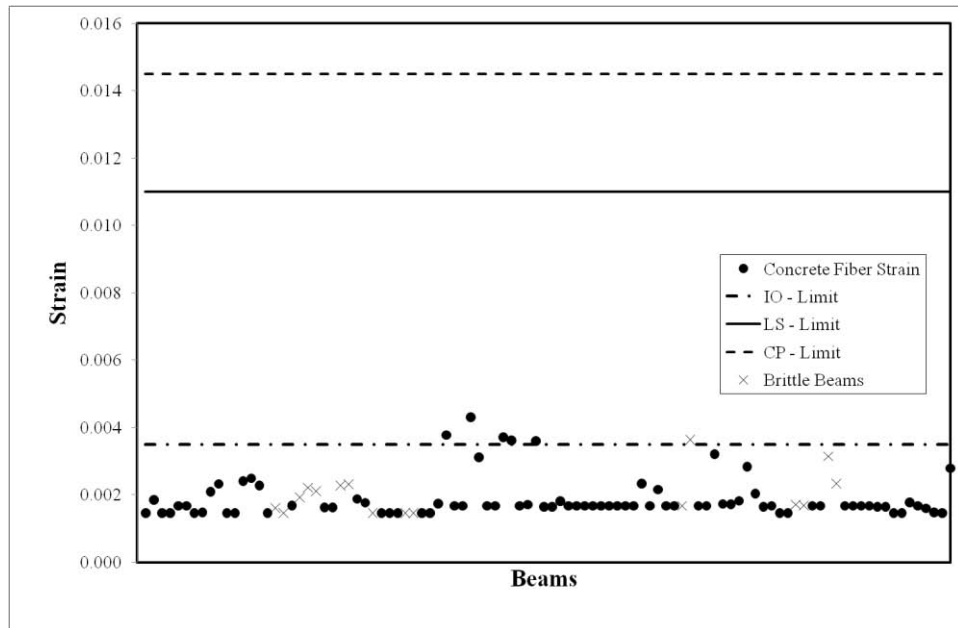


Figure 4.91: Existing Building Concrete strains for ground storey beams

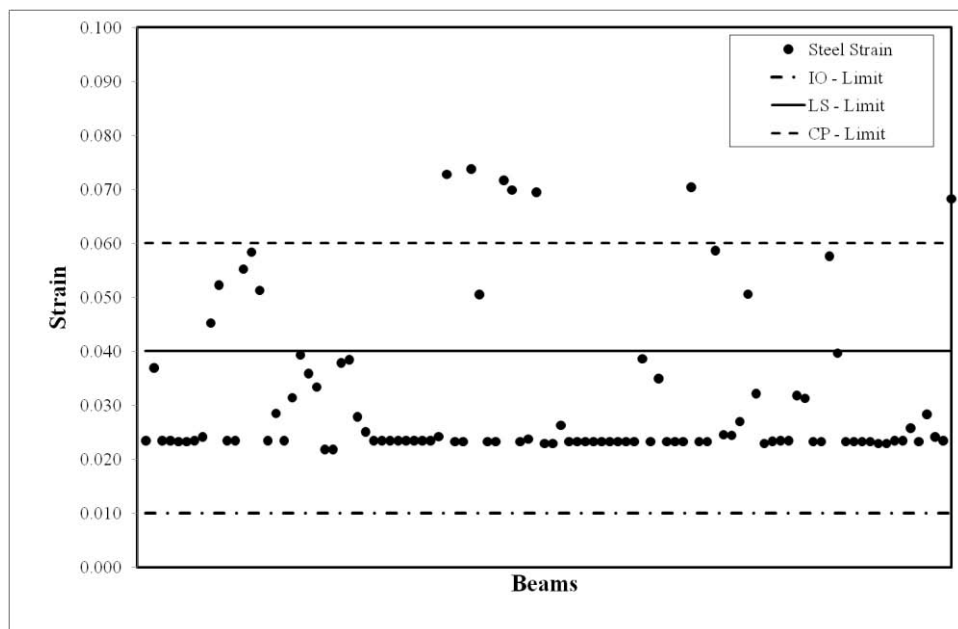


Figure 4.92: Existing Building Steel strains for ground storey beams

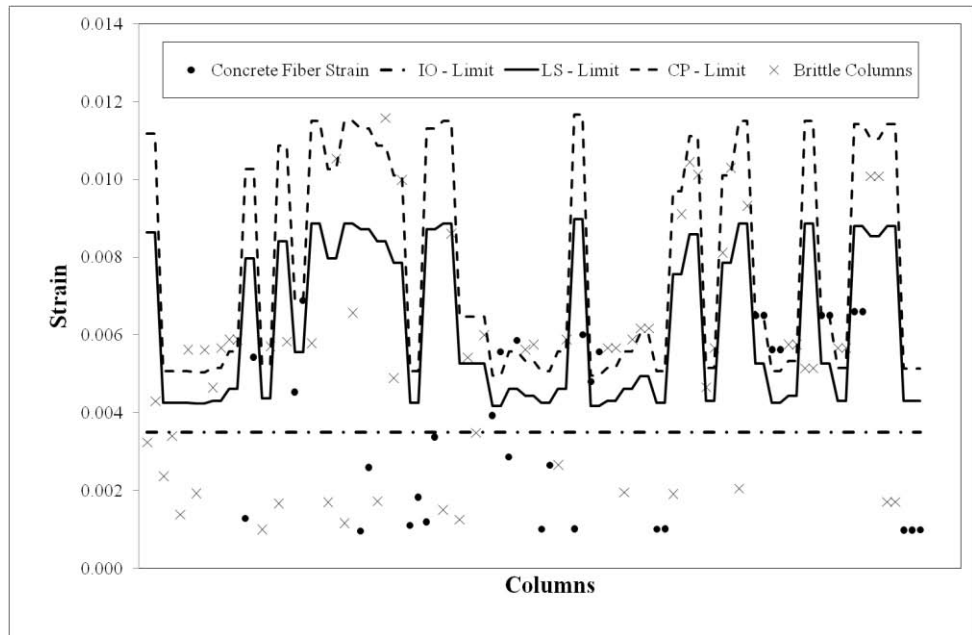


Figure 4.93: Existing Building Concrete strains for 1st storey columns

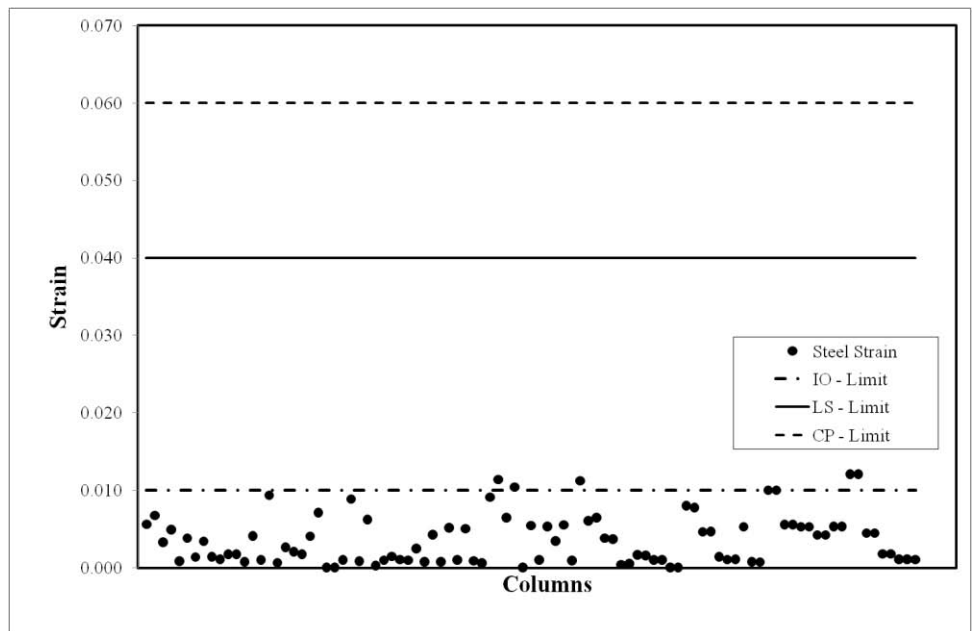


Figure 4.94: Existing Building Steel strains for 1st storey columns

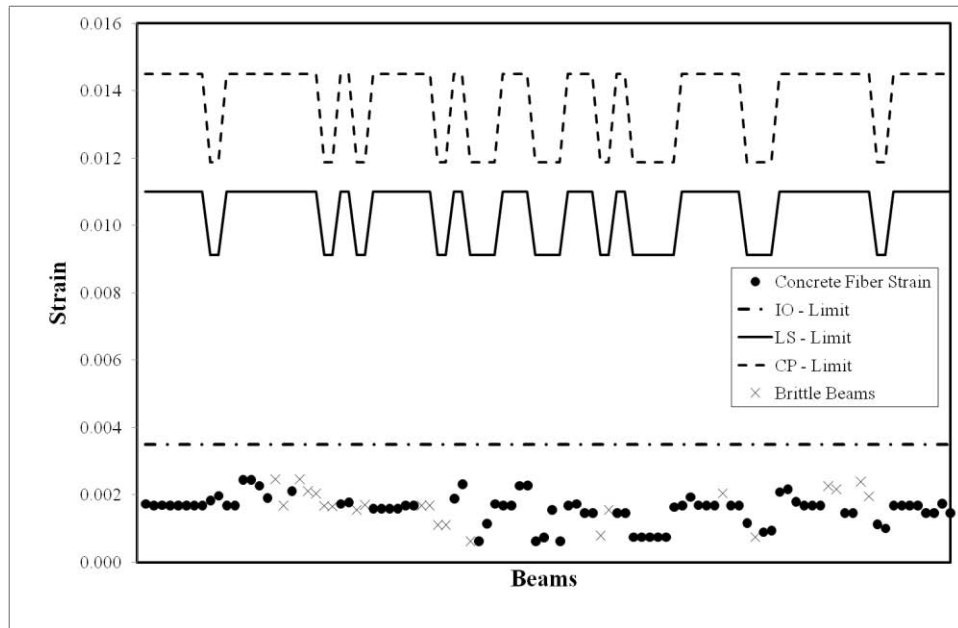


Figure 4.95: Existing Building Concrete strains for 1st storey beams

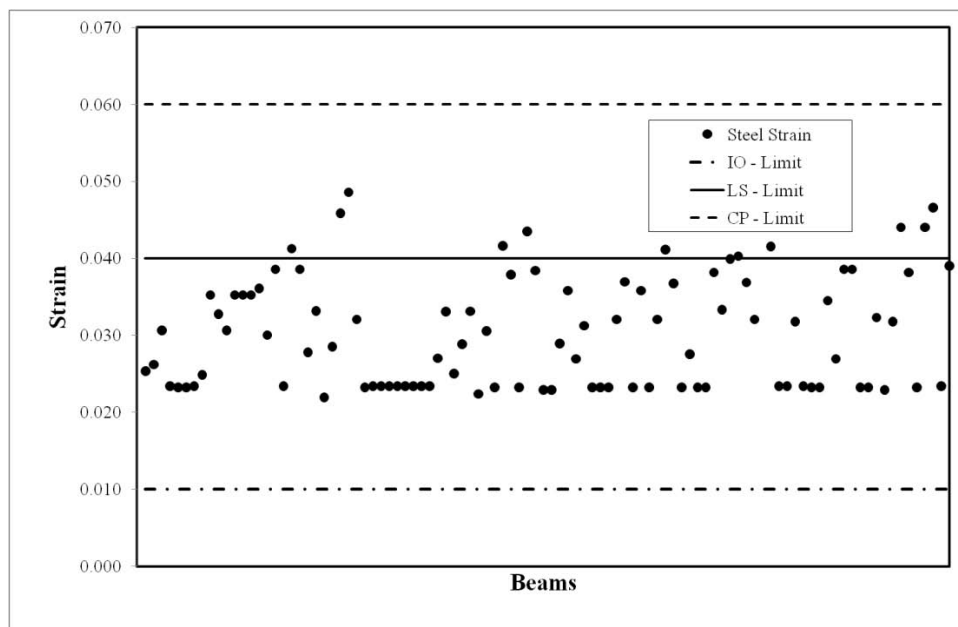


Figure 4.96: Existing Building Steel strains for 1st storey beams

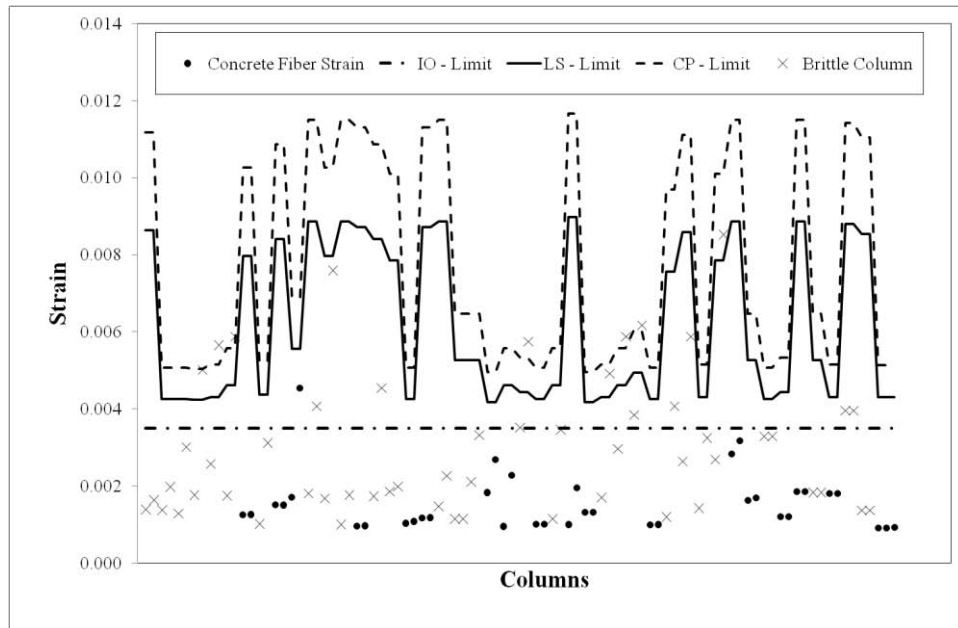


Figure 4.97: Existing Building Concrete strains for 2nd storey columns

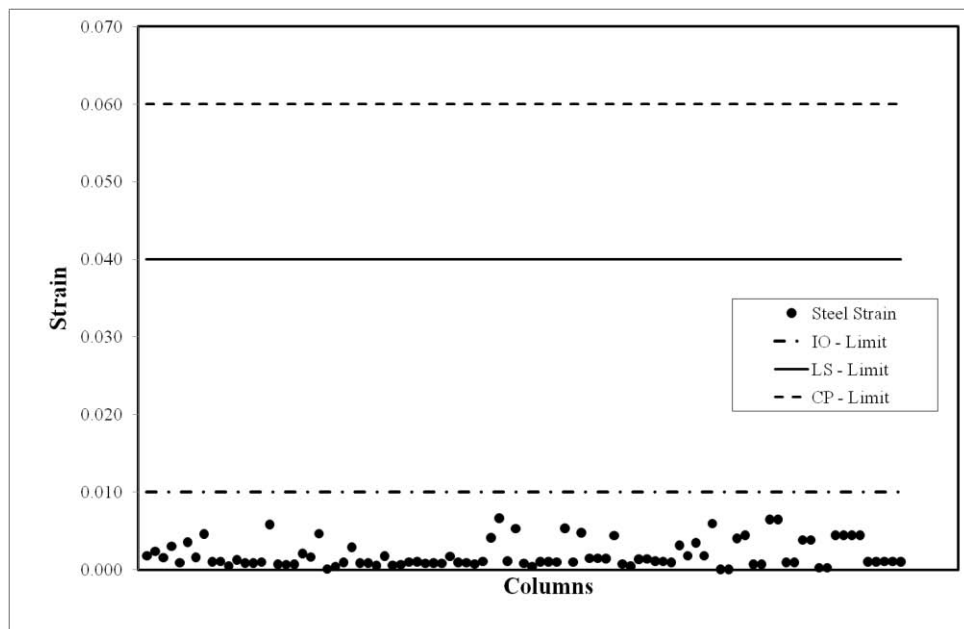


Figure 4.98: Existing Building Steel strains for 2nd storey columns

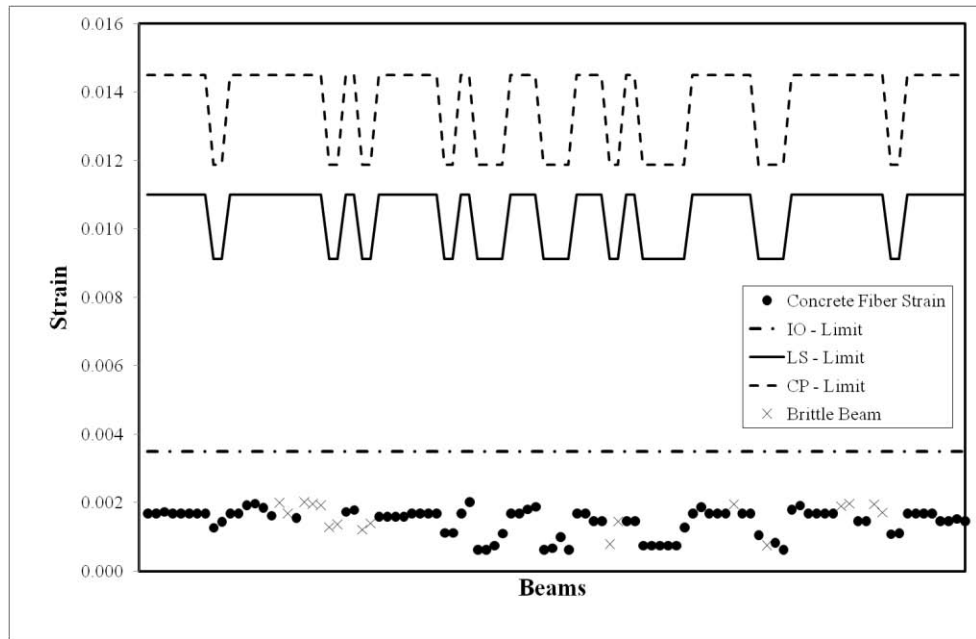


Figure 4.99: Existing Building Concrete strains for 2nd storey beams

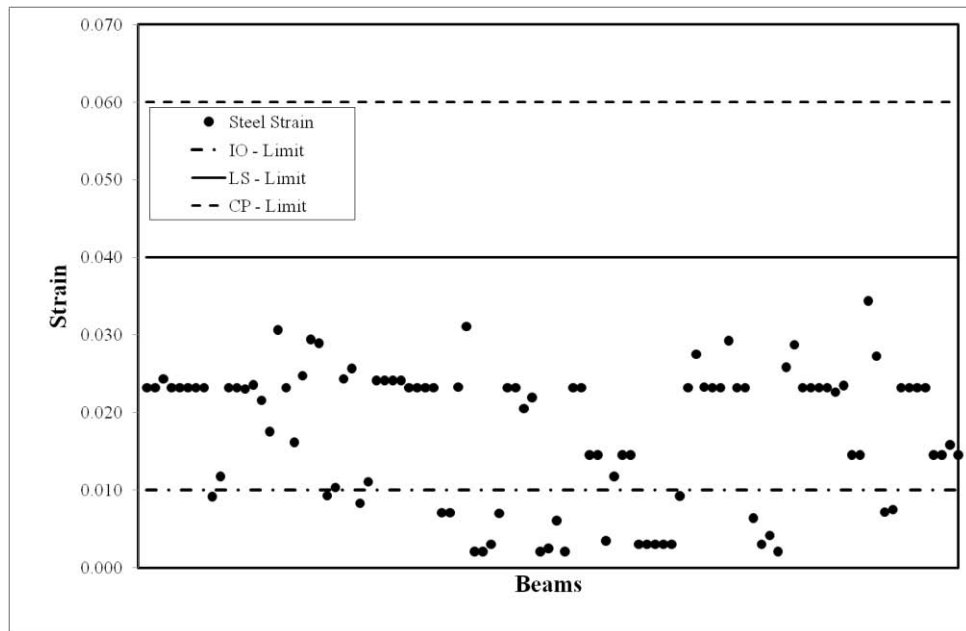


Figure 4.100: Existing Building Steel strains for 2nd storey beams

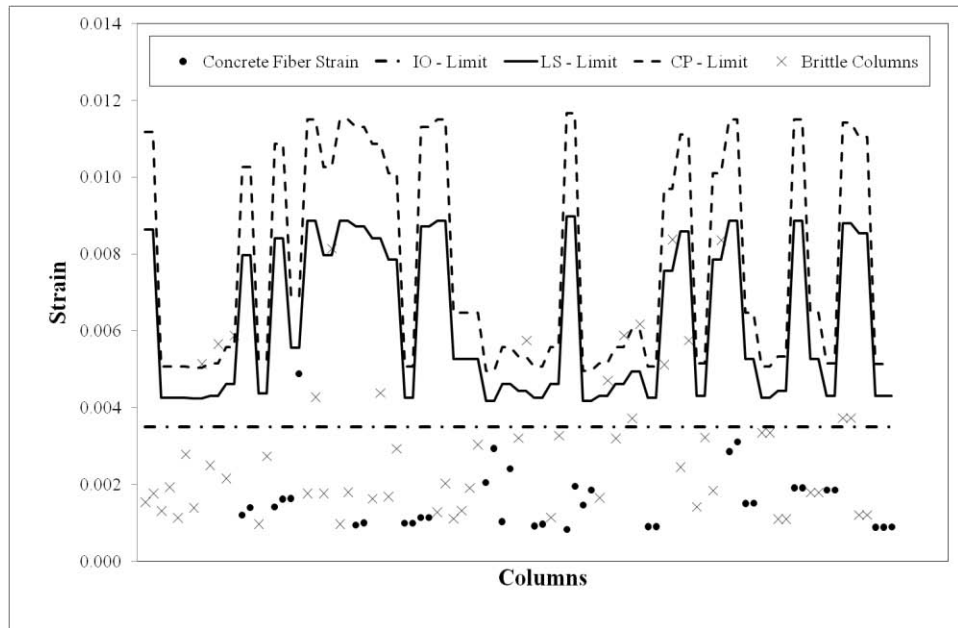


Figure 4.101: Existing Building Concrete strains for 3rd storey columns

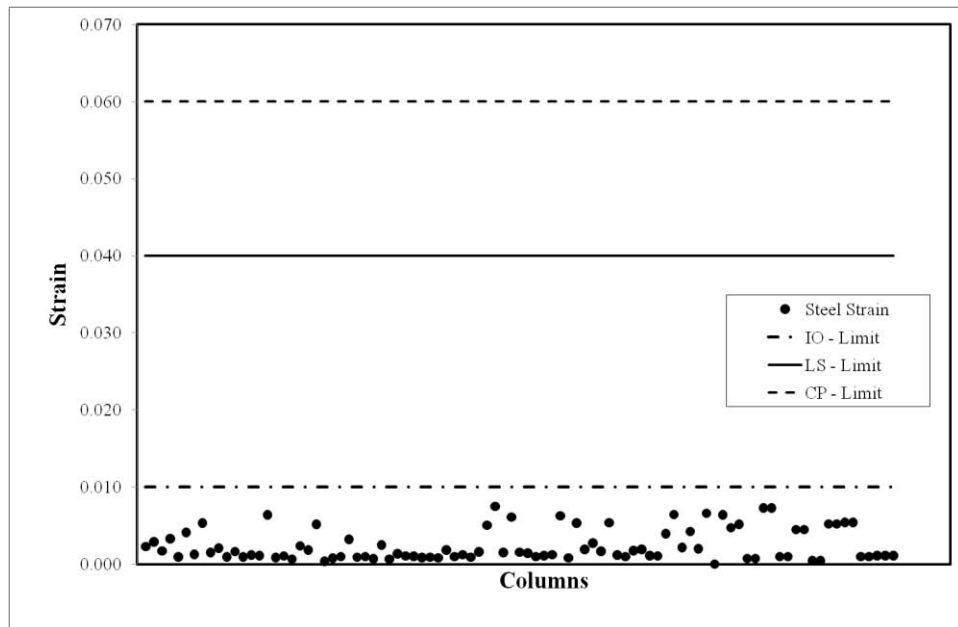


Figure 4.102: Existing Building Steel strains for 3rd storey columns

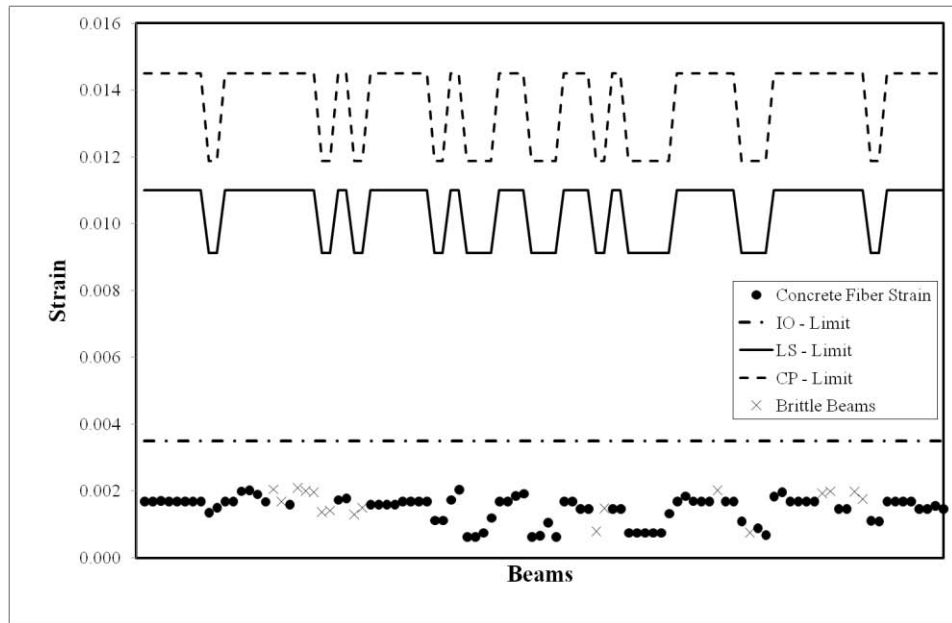


Figure 4.103: Existing Building Concrete strains for 3rd storey beams

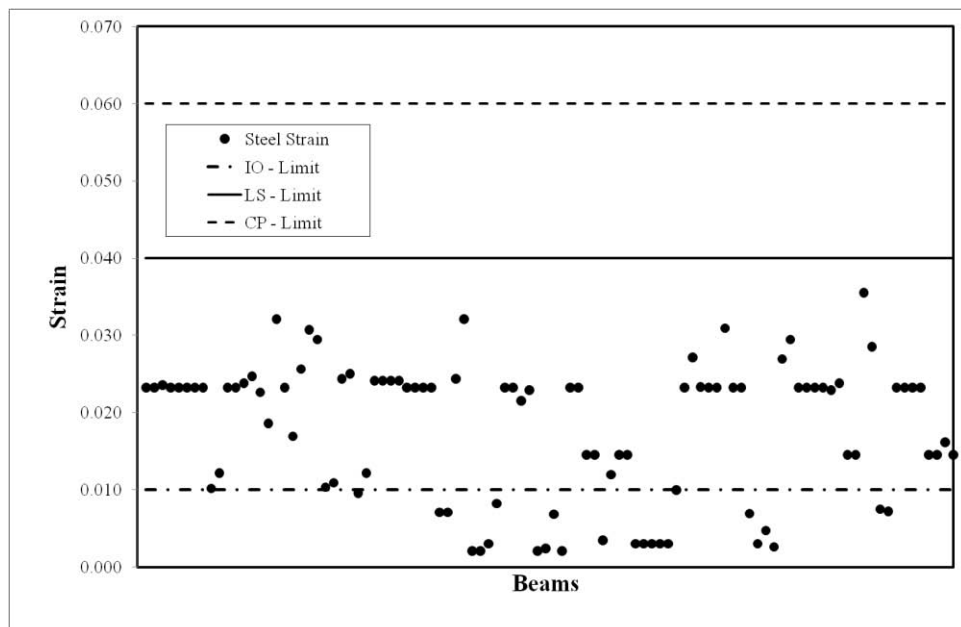


Figure 4.104: Existing Building Steel strains for 3rd storey beams

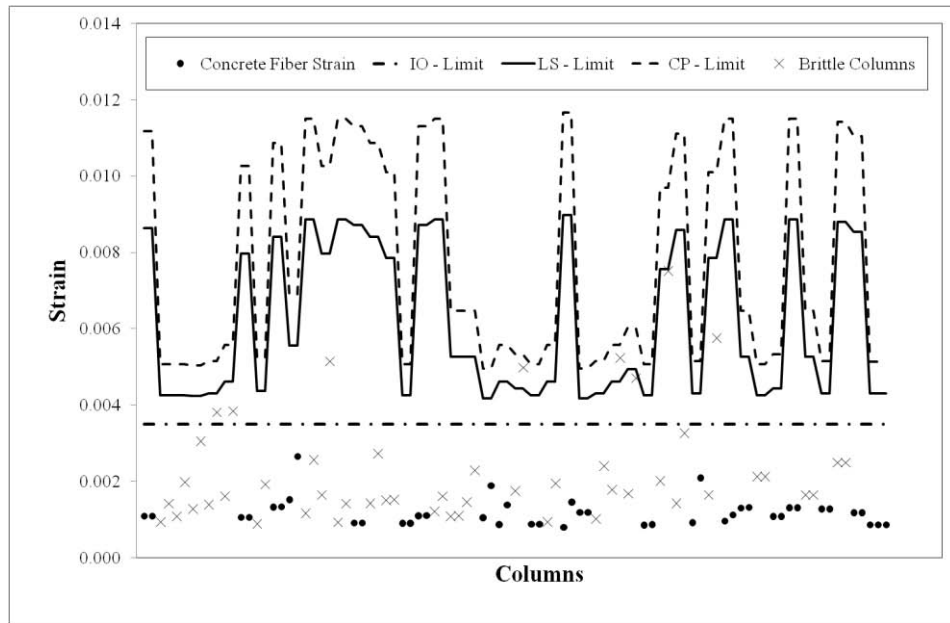


Figure 4.105: Existing Building Concrete strains for 4th storey columns

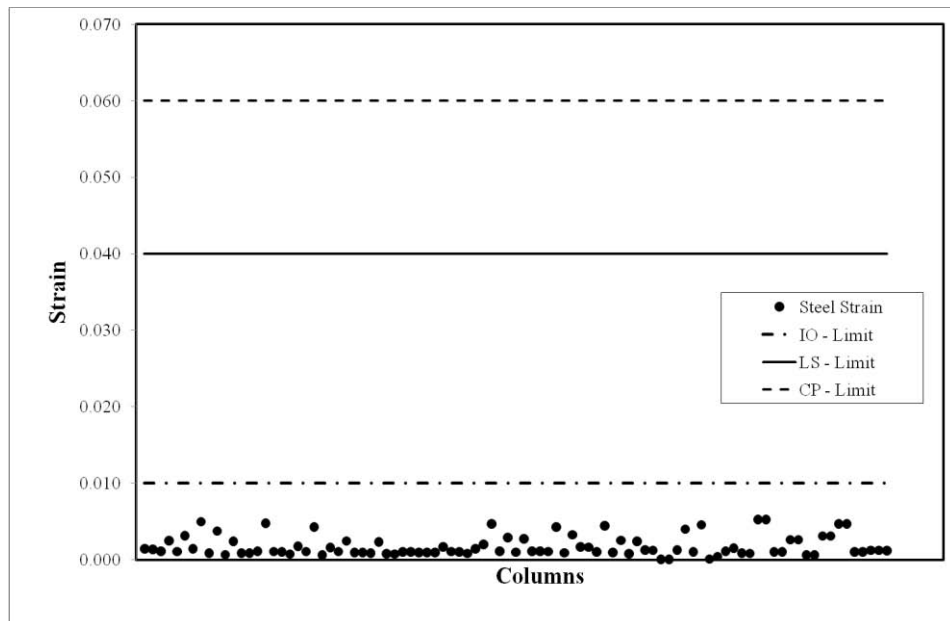


Figure 4.106: Existing Building Steel strains for 4th storey columns

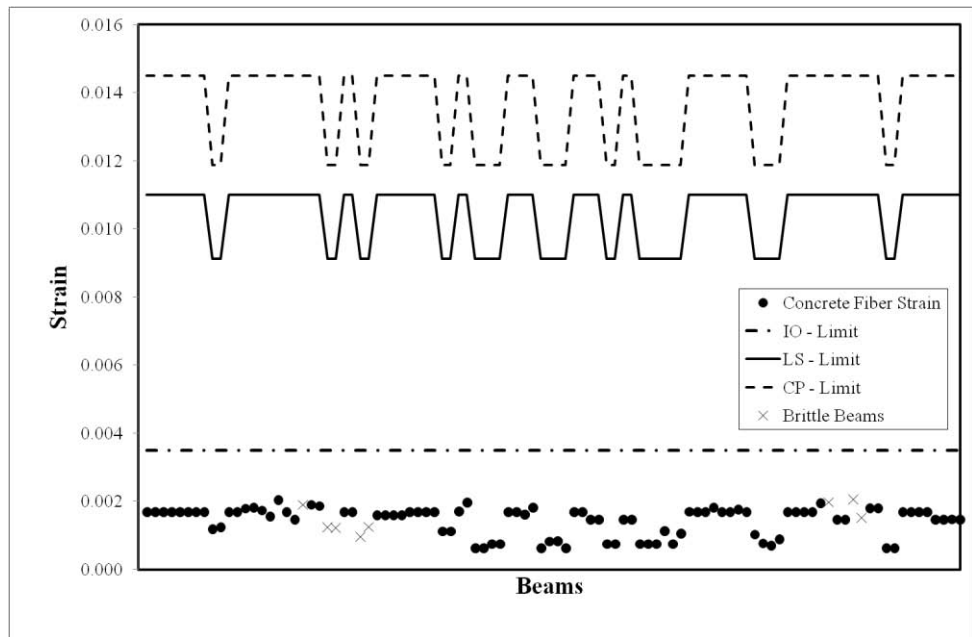


Figure 4.107: Existing Building Concrete strains for 4th storey beams

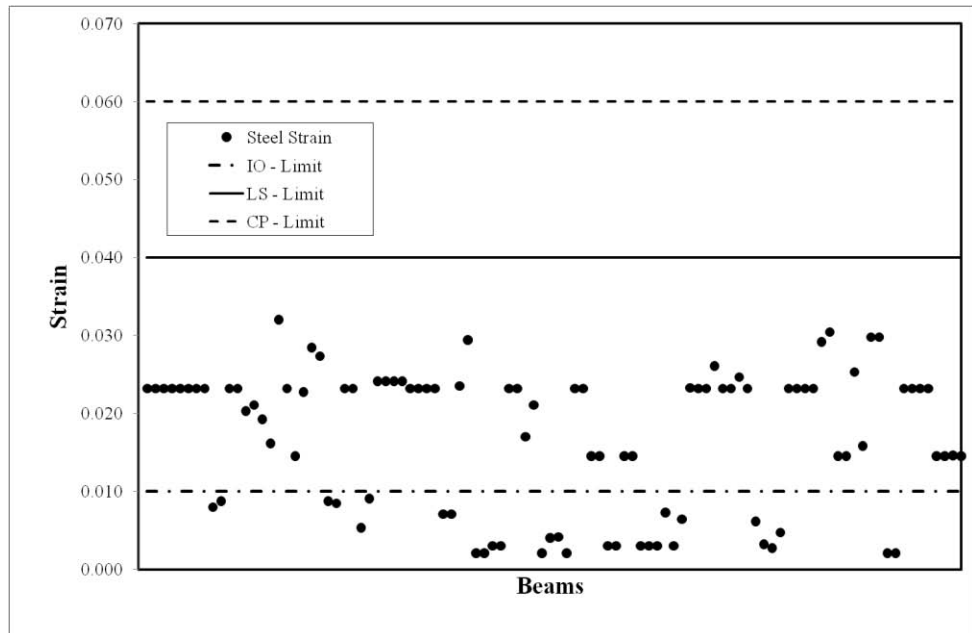


Figure 4.108: Existing Building Steel strains for 4th storey beams

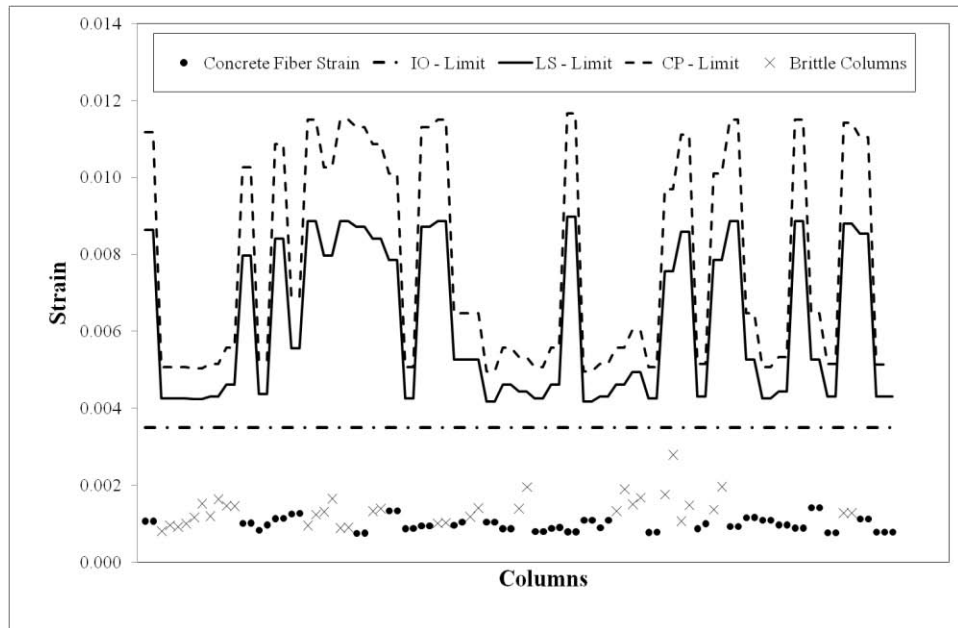


Figure 4.109: Existing Building Concrete strains for 5th storey columns

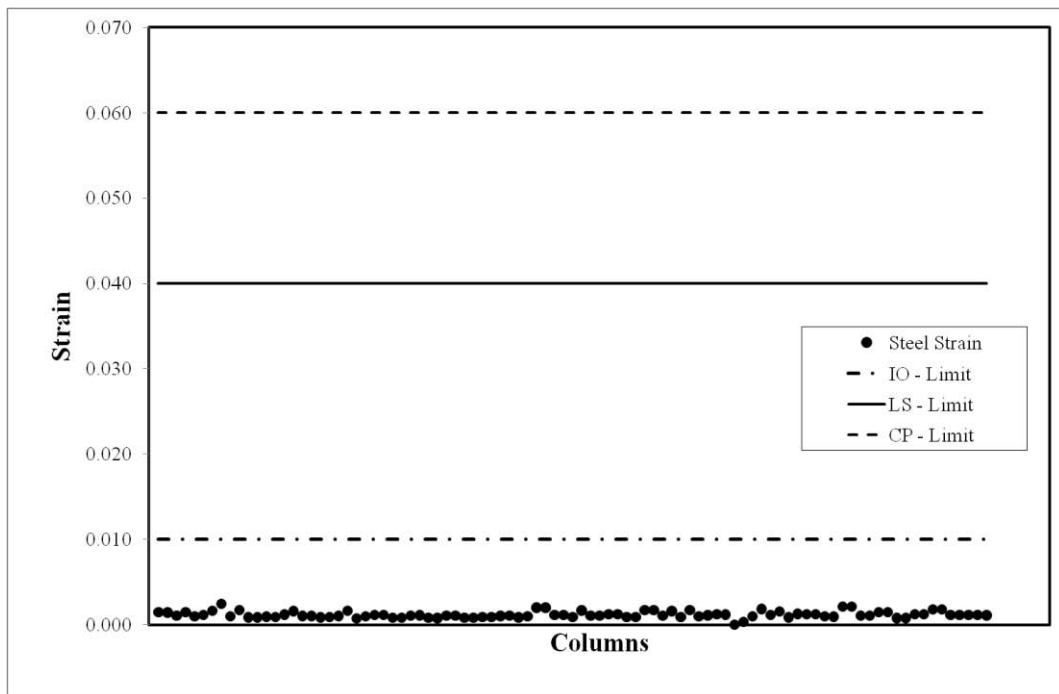


Figure 4.110: Existing Building Steel strains for 5th storey columns

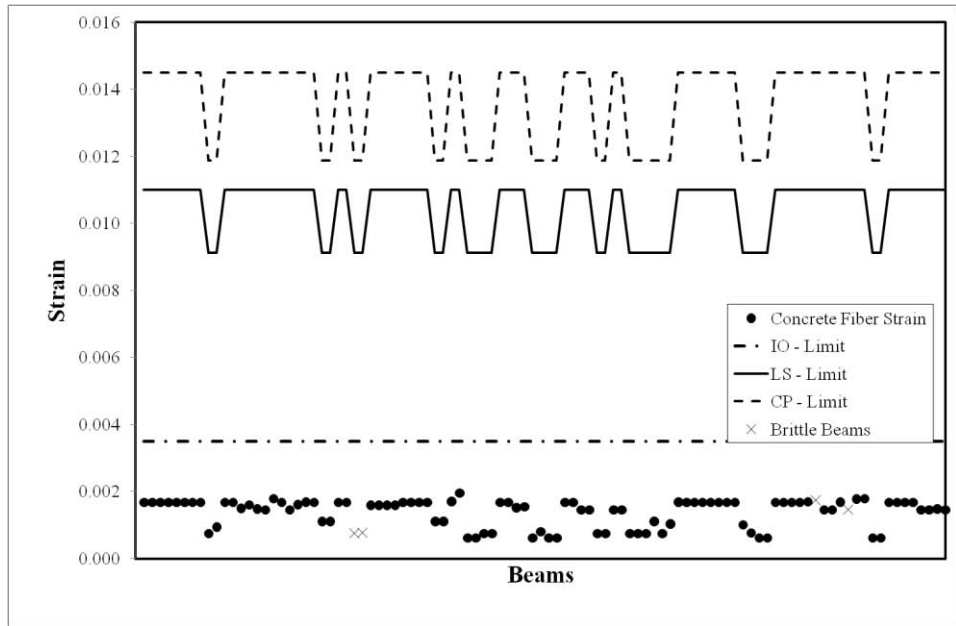


Figure 4.111: Existing Building Concrete strains for 5th storey beams

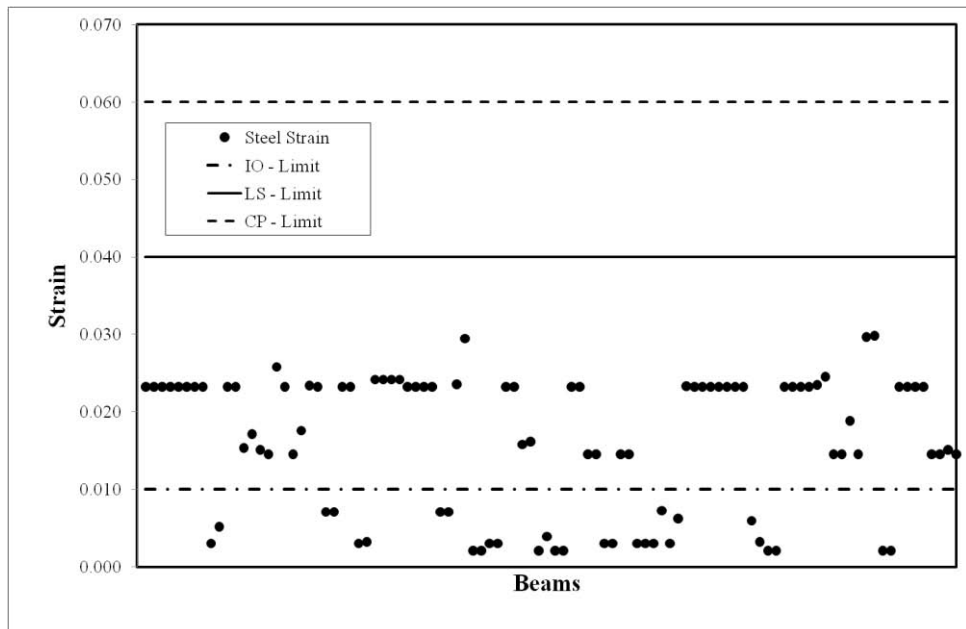


Figure 4.112: Existing Building Steel strains for 5th storey beams

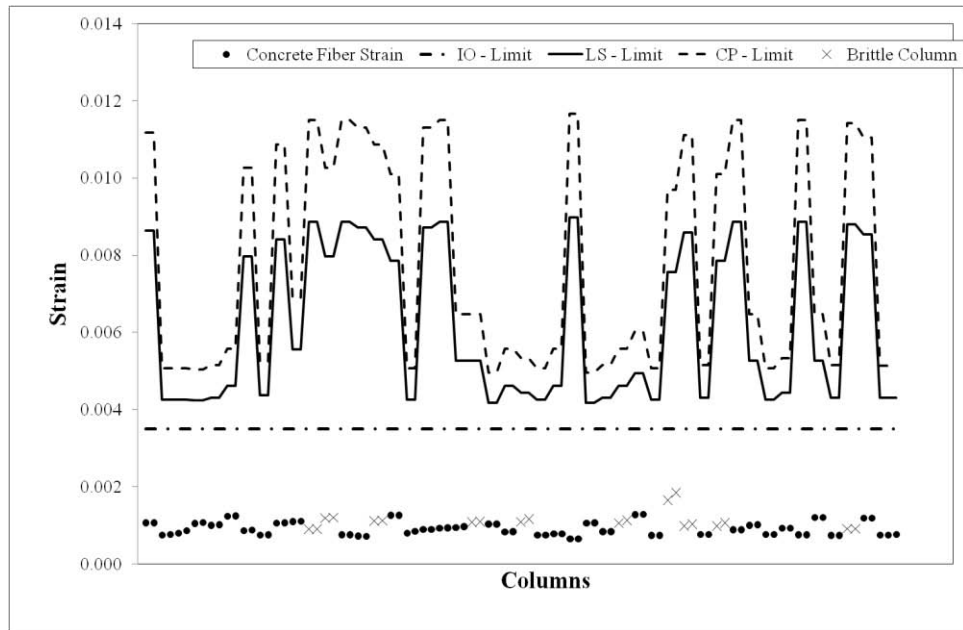


Figure 4.113: Existing Building Concrete strains for 6th storey columns

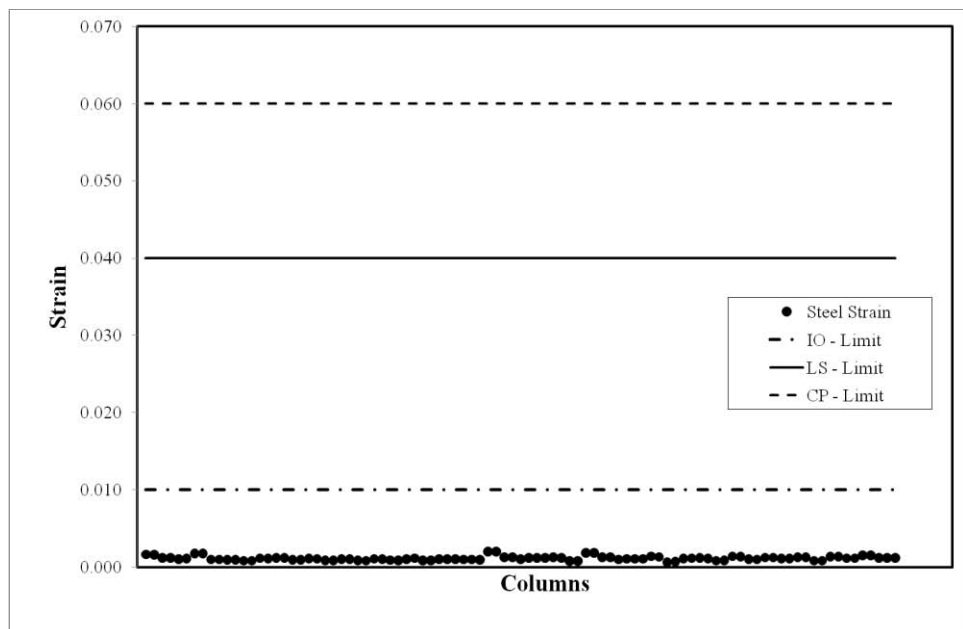


Figure 4.114: Existing Building Steel strains for 6th storey columns

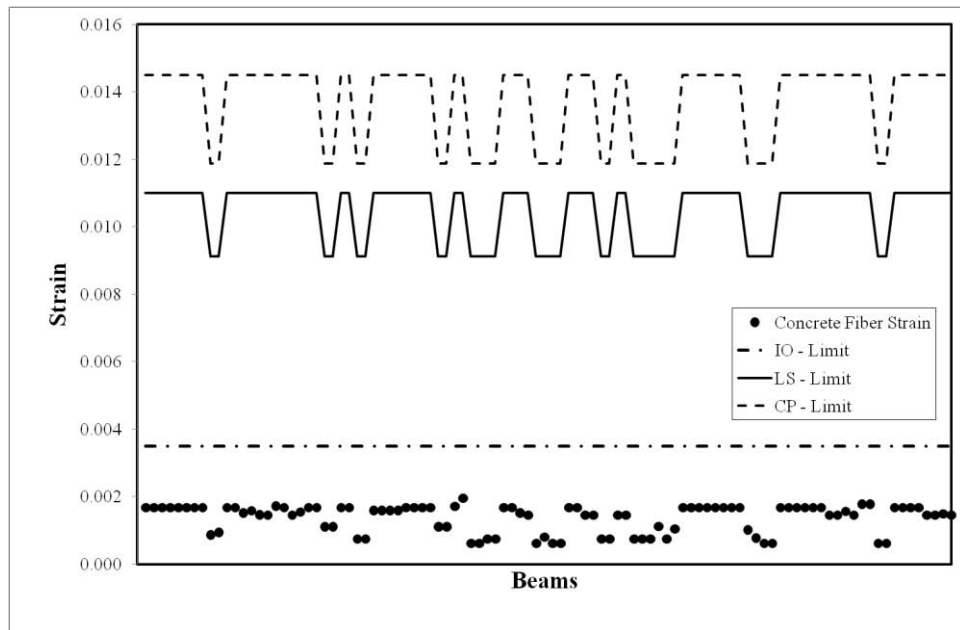


Figure 4.115: Existing Building Concrete strains for 6th storey beams

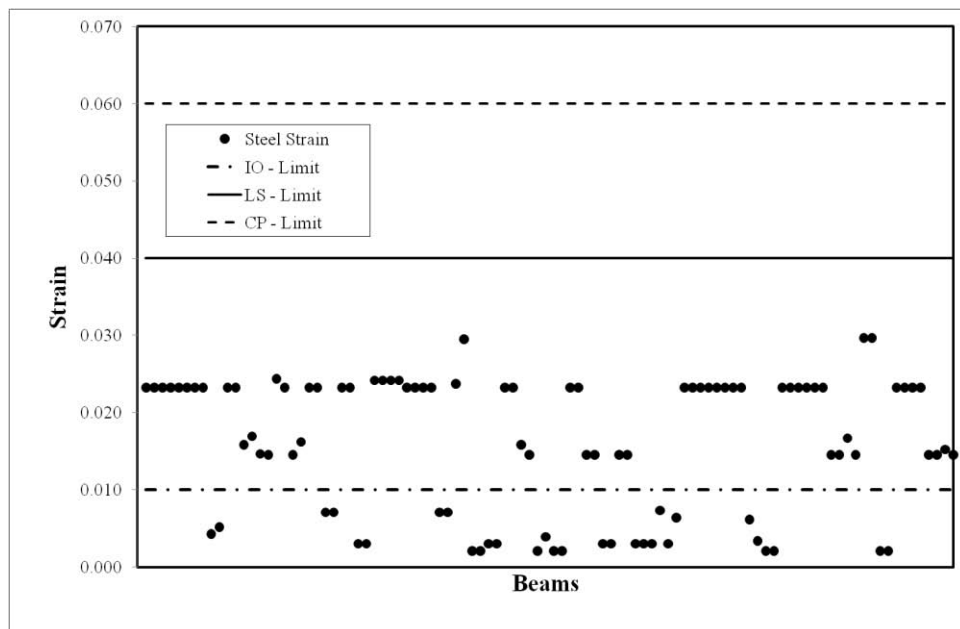


Figure 4.116: Existing Building Steel strains for 6th storey beams

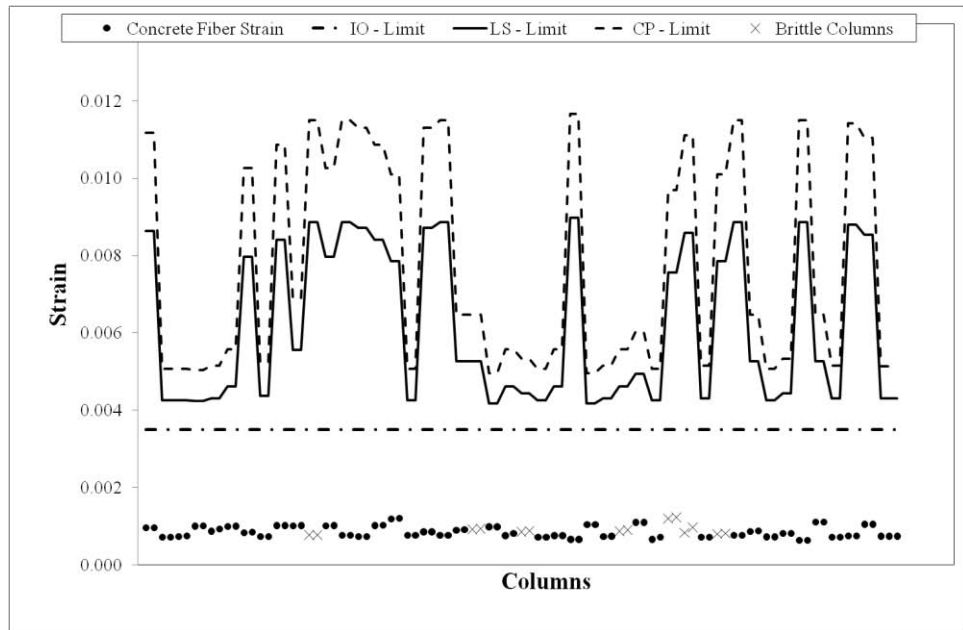


Figure 4.117: Existing Building Concrete strains for 7th storey columns

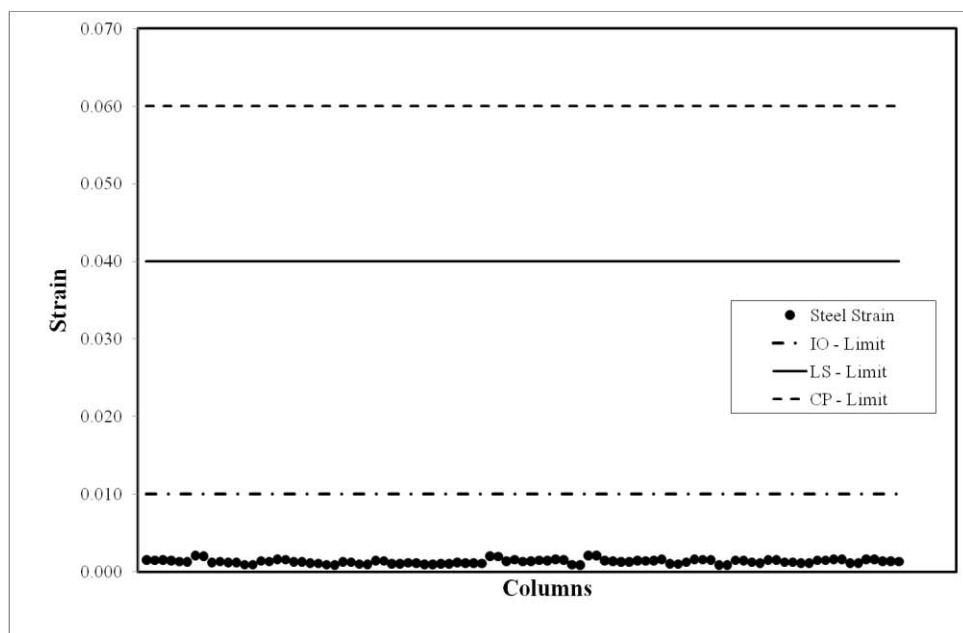


Figure 4.118: Existing Building Steel strains for 7th storey columns

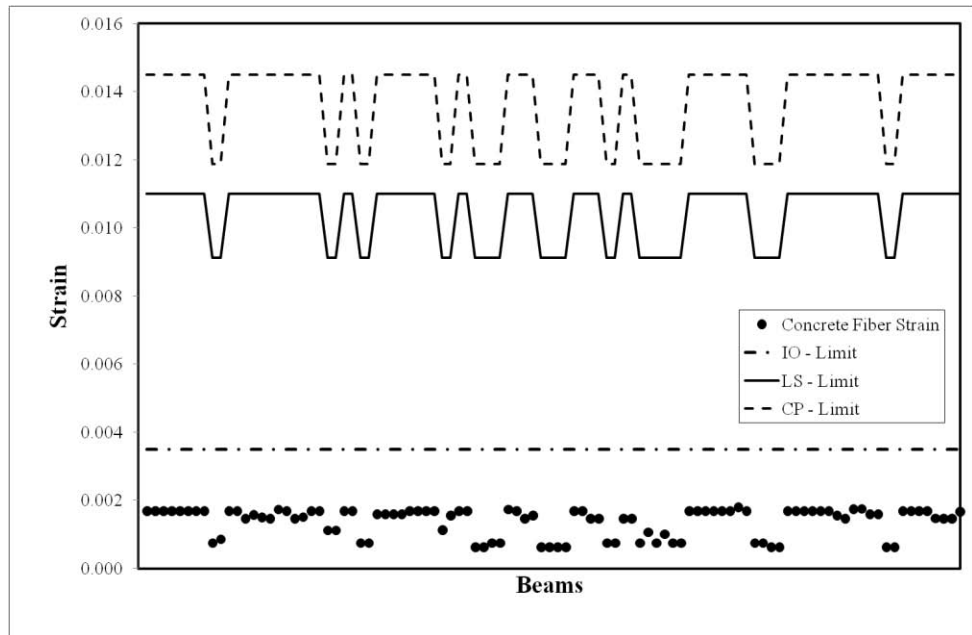


Figure 4.119: Existing Building Concrete strains for 7th storey beams

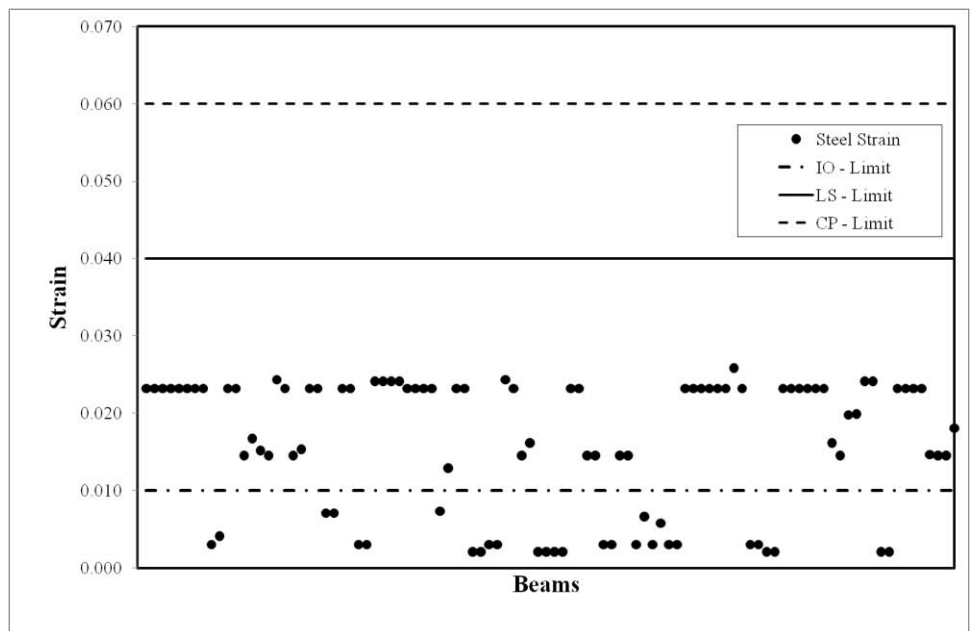


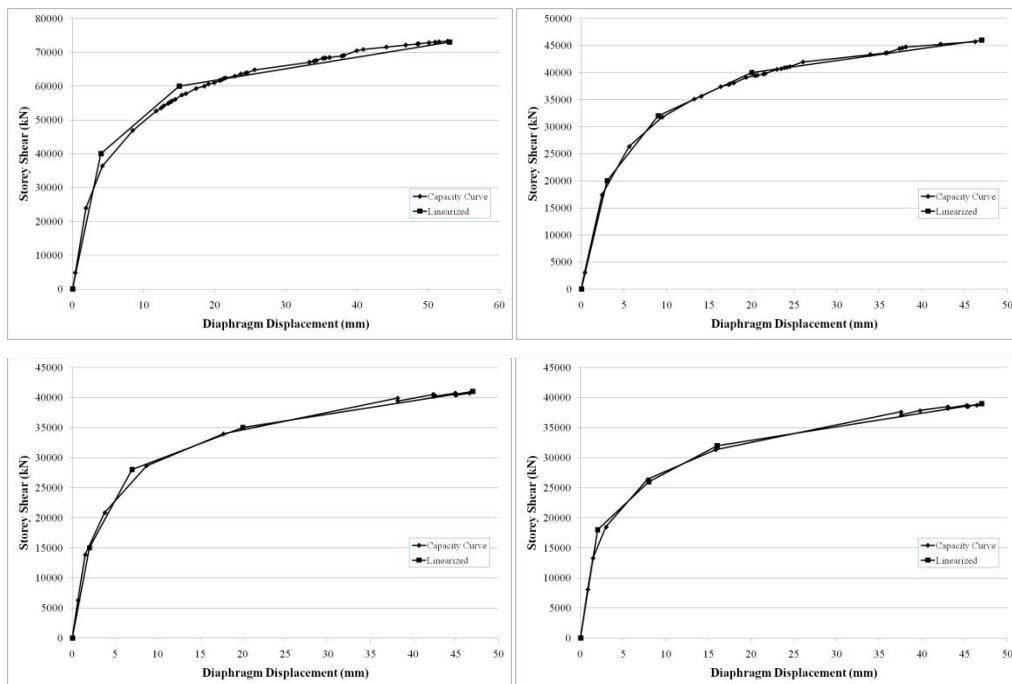
Figure 4.120: Existing Building Steel strains for 7th storey beams

Assessment results show that there are brittle members as well as ductile members over collapse prevention limit. Most of the beam strains (steel strain governs) are located in the life safety band which is quite a similar result obtained in modal pushover analysis. Since envelope drifts are concentrated at basement and ground storeys, the members located here seem to suffer more damage than any other storey. Hence, existing building does not satisfy the life safety requirements according to TEC 2007.

In this analysis, a unit load of 1 kN was applied in X and Y directions to obtain the force-deformation relationship of a specific storey. Application of a torsional moment may also be applicable in order to consider the softening effect of rotation.

#### 4.6.2 Retrofitted Building

Exactly the same procedure applied for the existing structure is repeated for retrofitted structure. Storey capacity curves are shown in Figure 4.121.



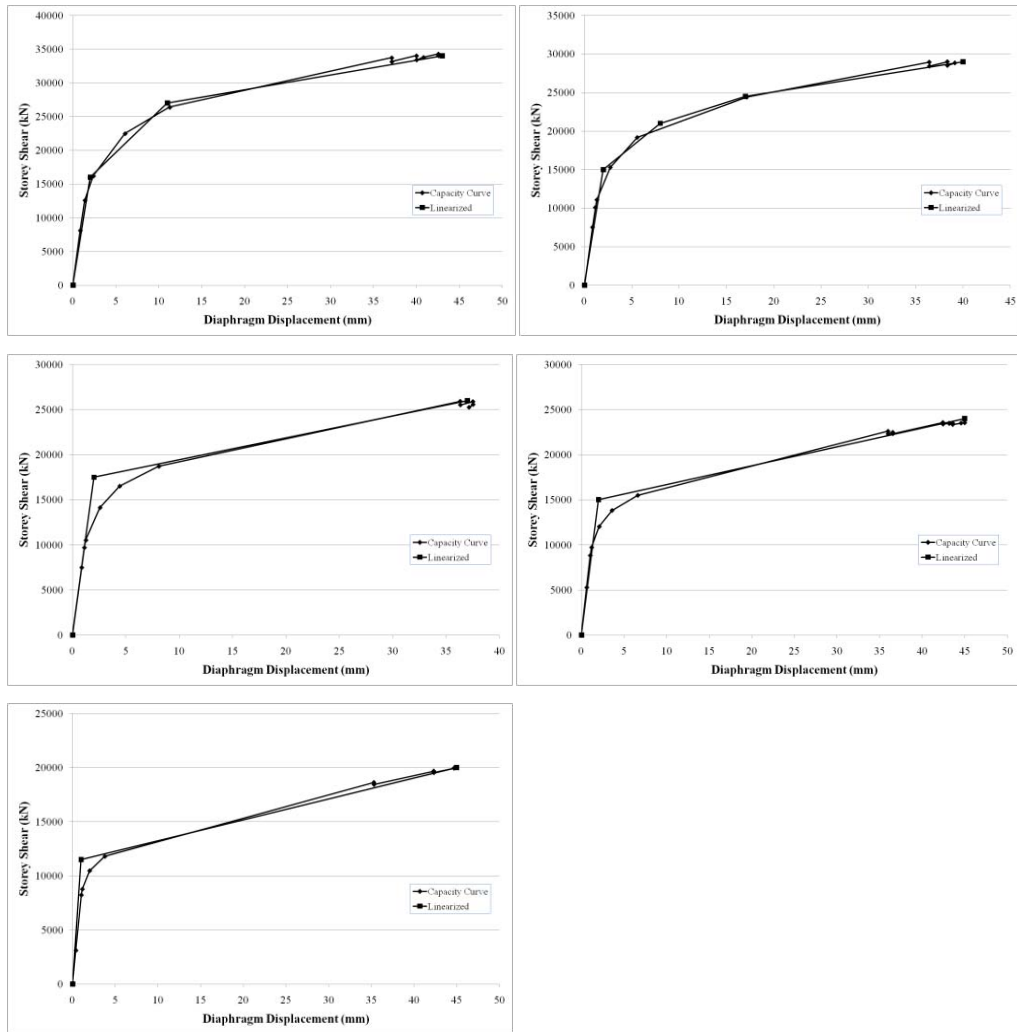


Figure 4.121: Storey capacity curves for retrofitted building.

Drift ratios for retrofitted building for each storey obtained after time history analysis is shown in Figure 4.122. Envelope of three earthquakes were considered.

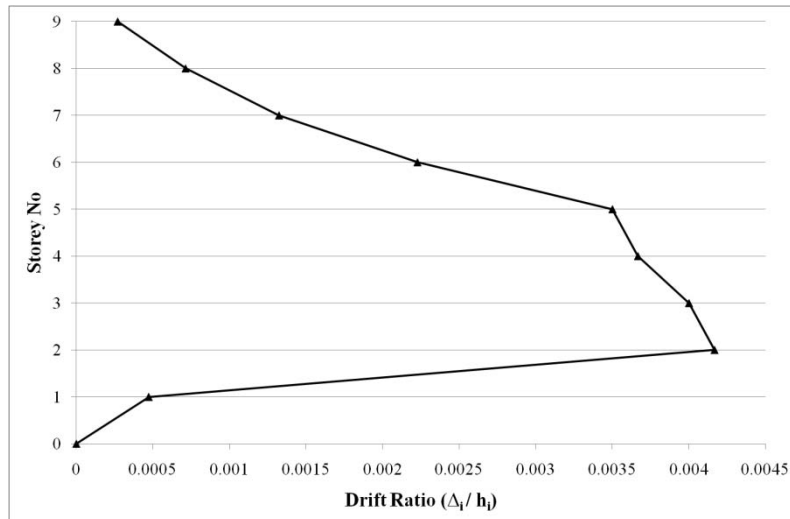


Figure 4.122: Envelope drift ratio demand for retrofitted building at each storey after time history analysis.

Plastic rotations and internal forces were extracted using the drift demands above from each storey analysis model. Results from separate models were merged into a single set. Member by member assessment was performed according to TEC2007 regulations. Results are tabulated in Figures 4.123 – 4.152

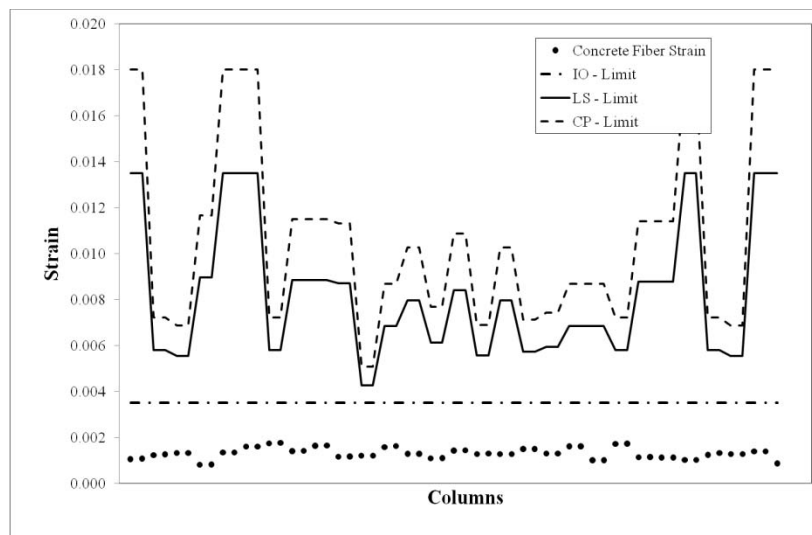


Figure 4.123: Retrofitted Building, Concrete strains for basement storey columns

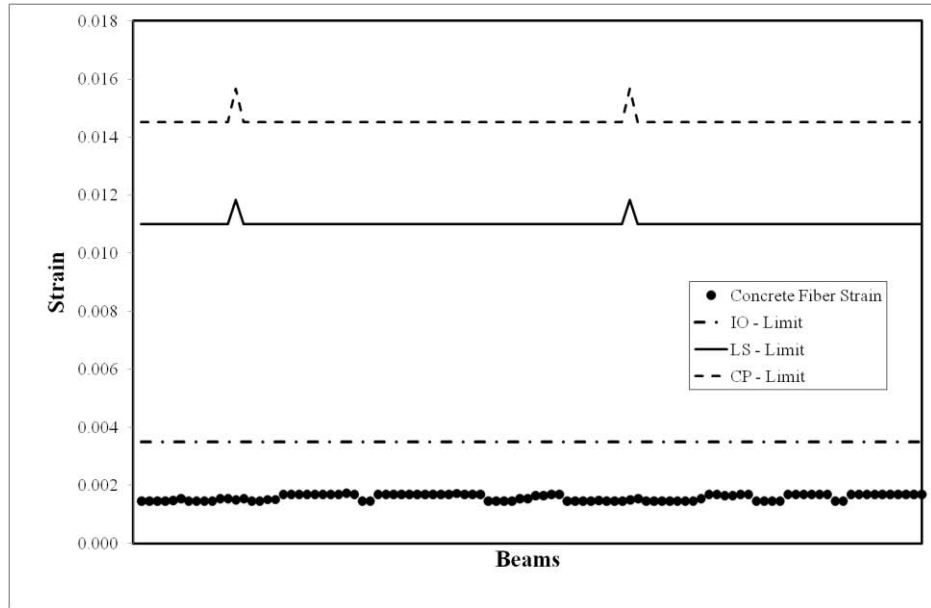


Figure 4.124: Retrofitted Building, Concrete strains for basement storey beams

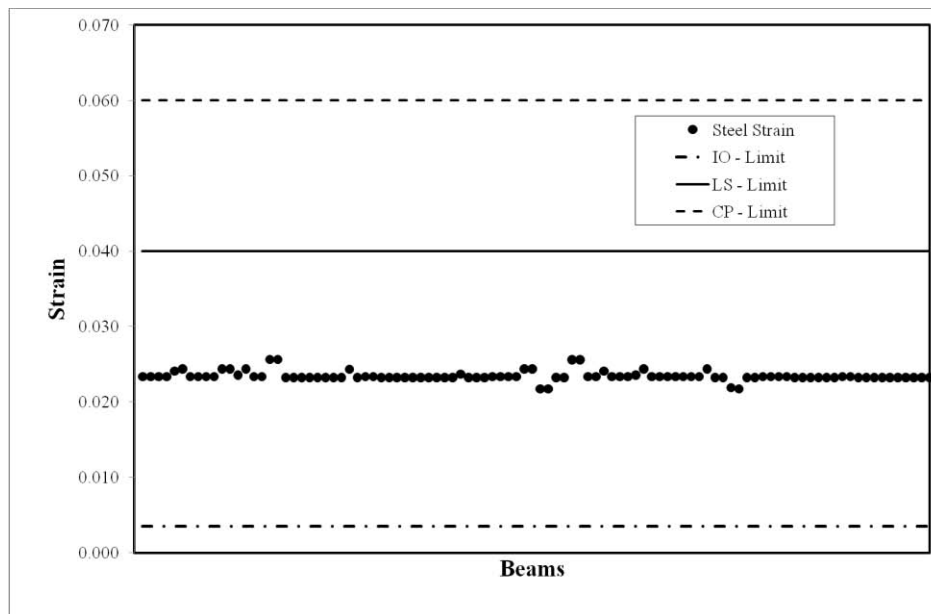


Figure 4.125: Retrofitted Building, Steel strains for basement storey beams

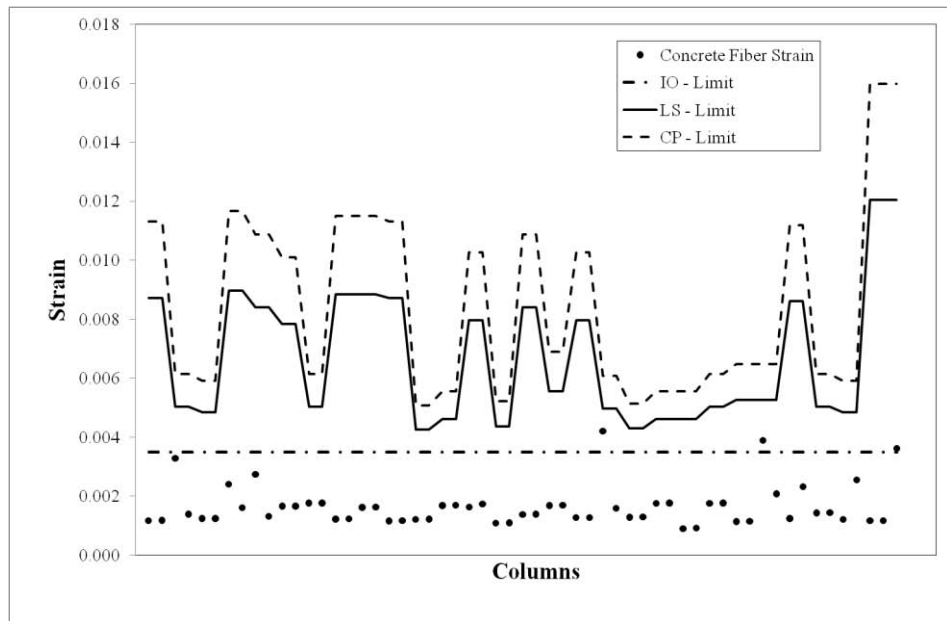


Figure 4.126: Retrofitted Building, Concrete strains for ground storey columns

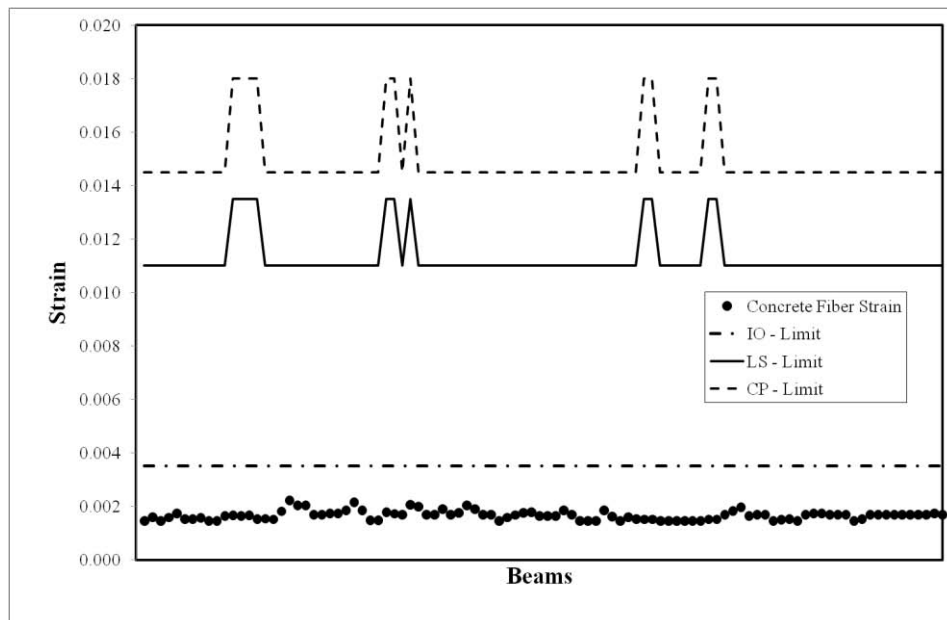


Figure 4.127: Retrofitted Building, Concrete strains for ground storey beams

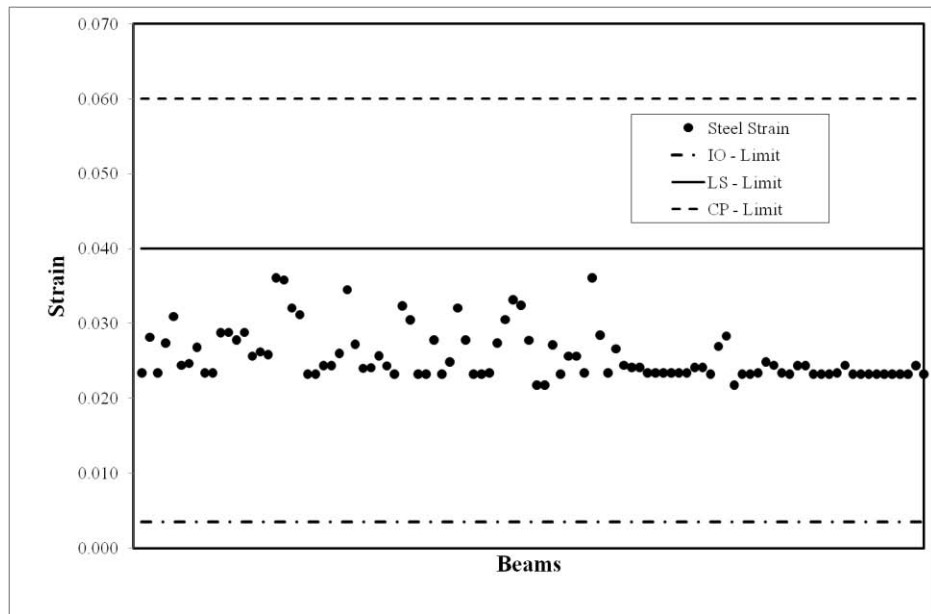


Figure 4.128: Retrofitted Building, Steel strains for ground storey beams

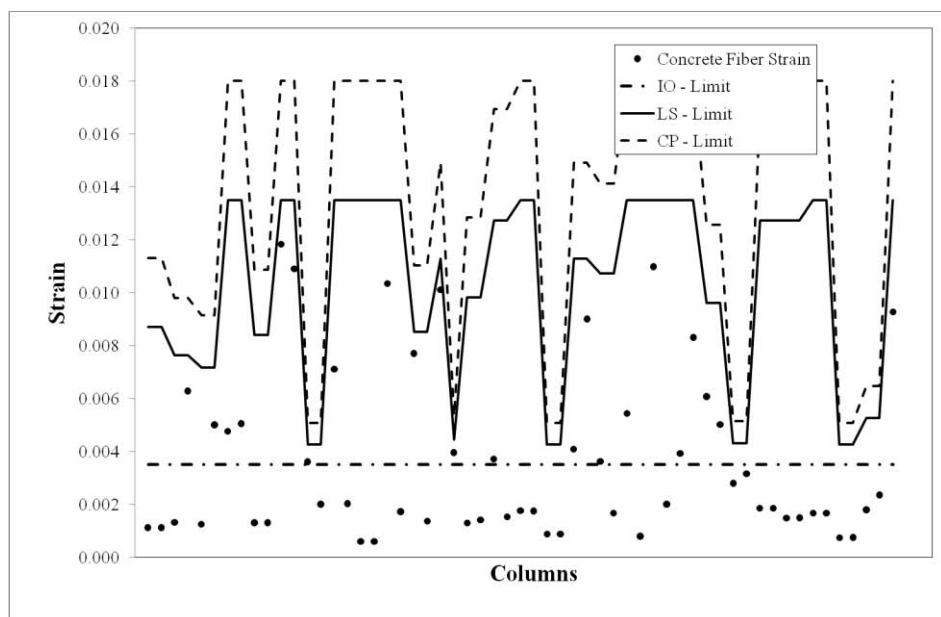


Figure 4.129: Retrofitted Building, Concrete strains for 1st storey columns

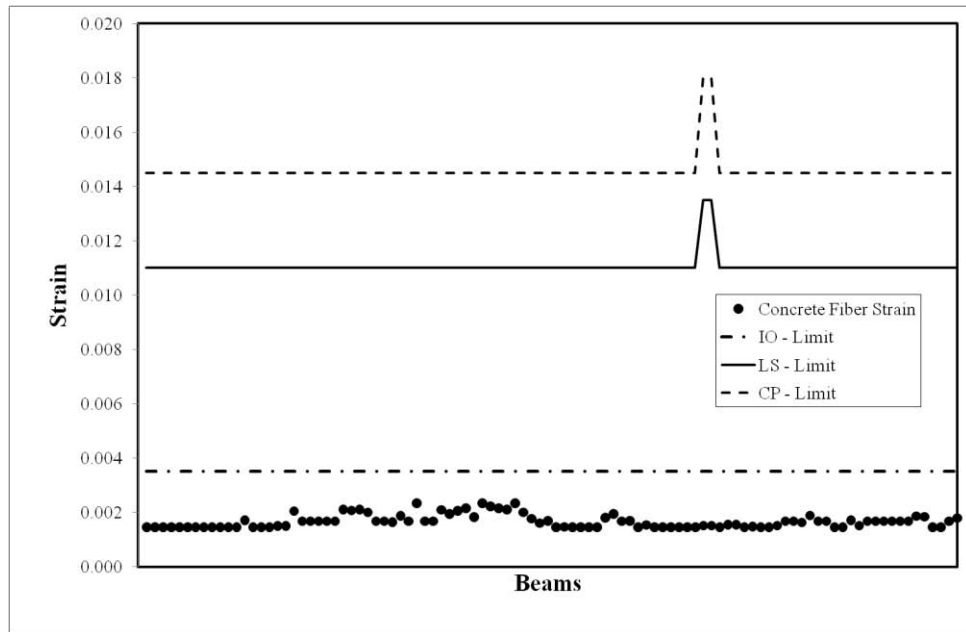


Figure 4.130: Retrofitted Building, Concrete strains for 1st storey beams

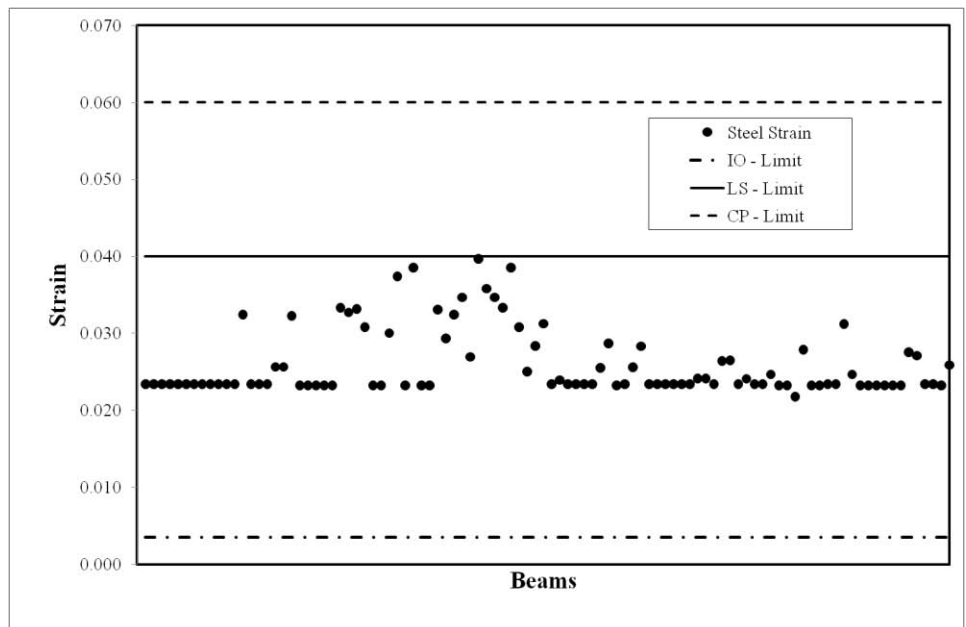


Figure 4.131: Retrofitted Building, Steel strains for 1st storey beams

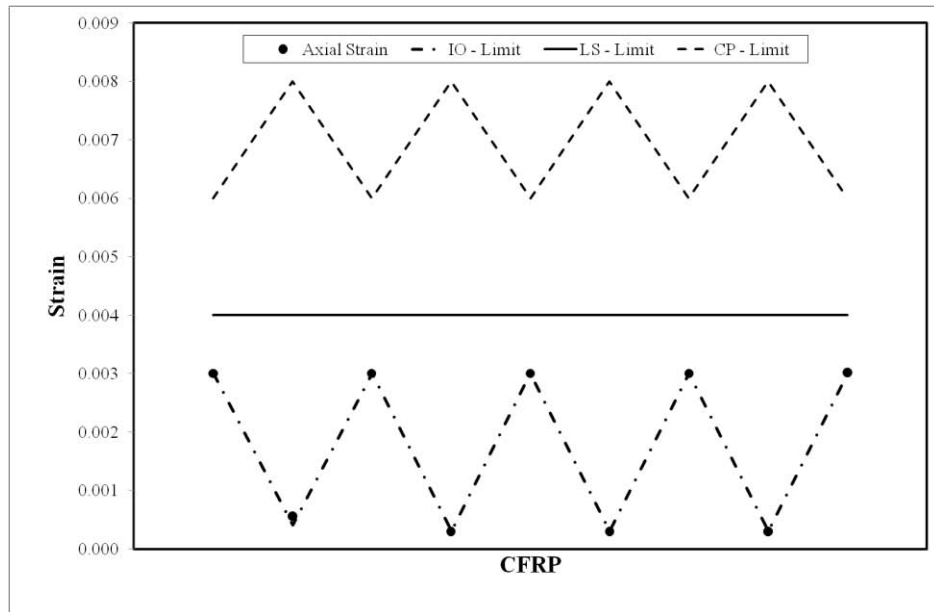


Figure 4.132: Retrofitted Building, Axial strains for 1st storey CFRP Walls

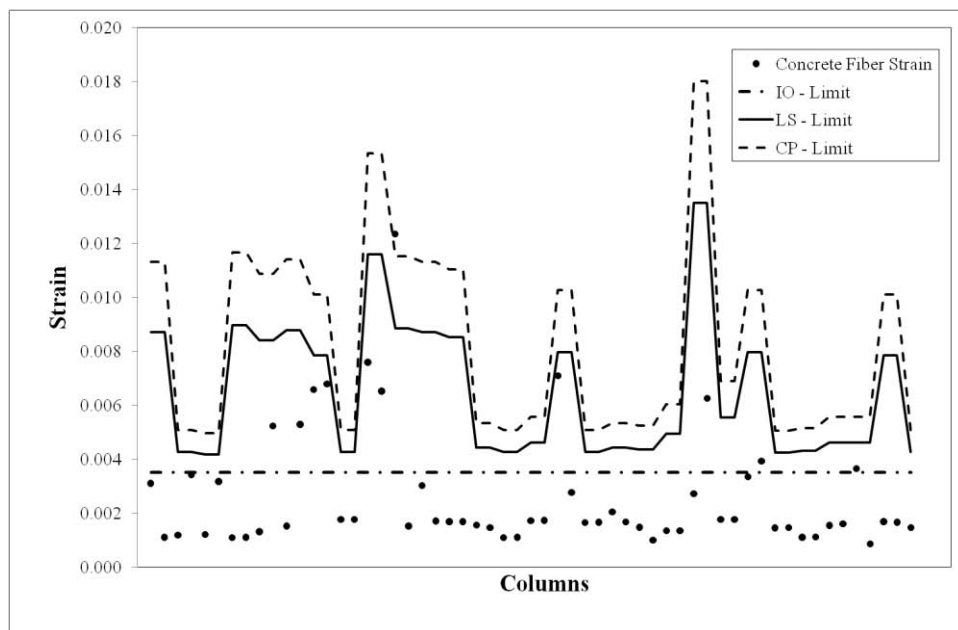


Figure 4.133: Retrofitted Building, Concrete strains for 2nd storey columns

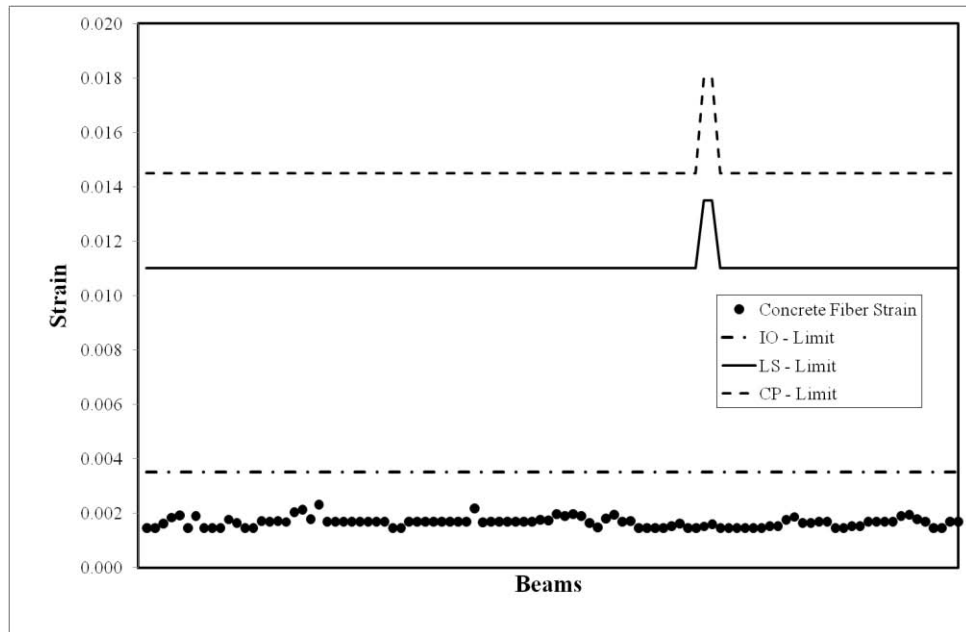


Figure 4.134: Retrofitted Building, Concrete strains for 2nd storey beams

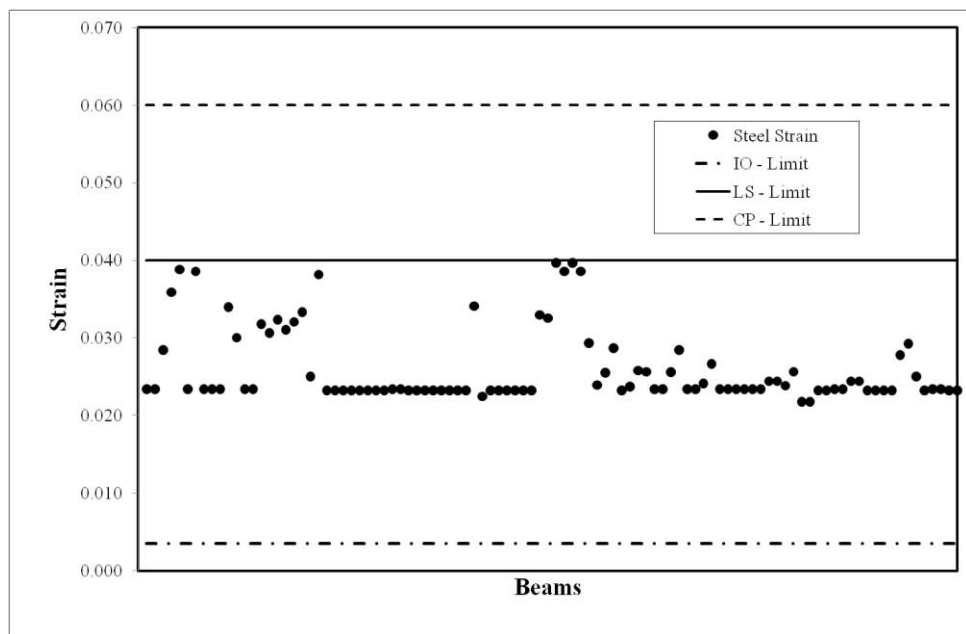


Figure 4.135: Retrofitted Building, Steel strains for 2nd storey beams

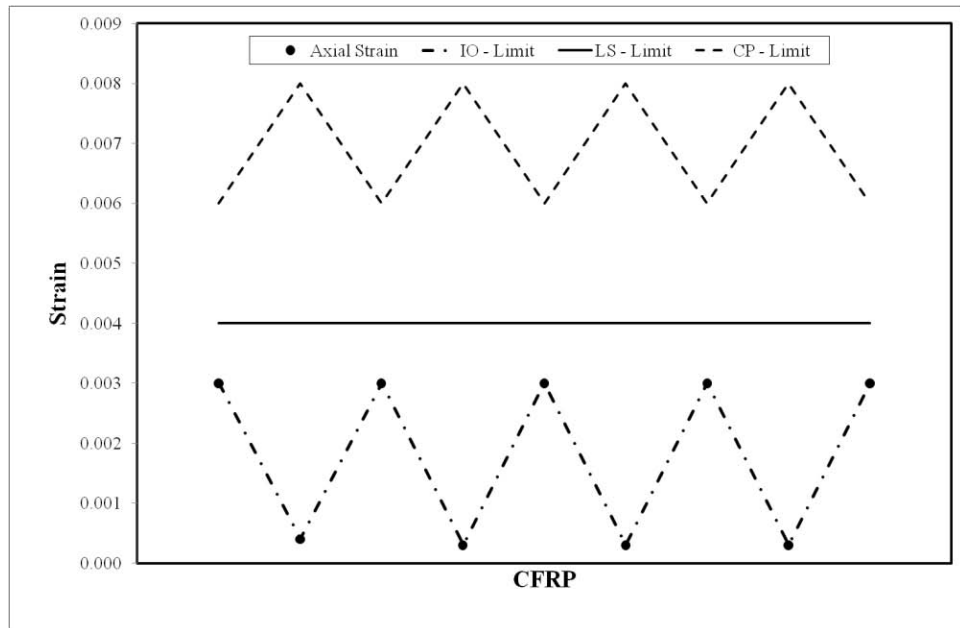


Figure 4.136: Retrofitted Building, Axial Strains for 2nd storey CFRP Walls

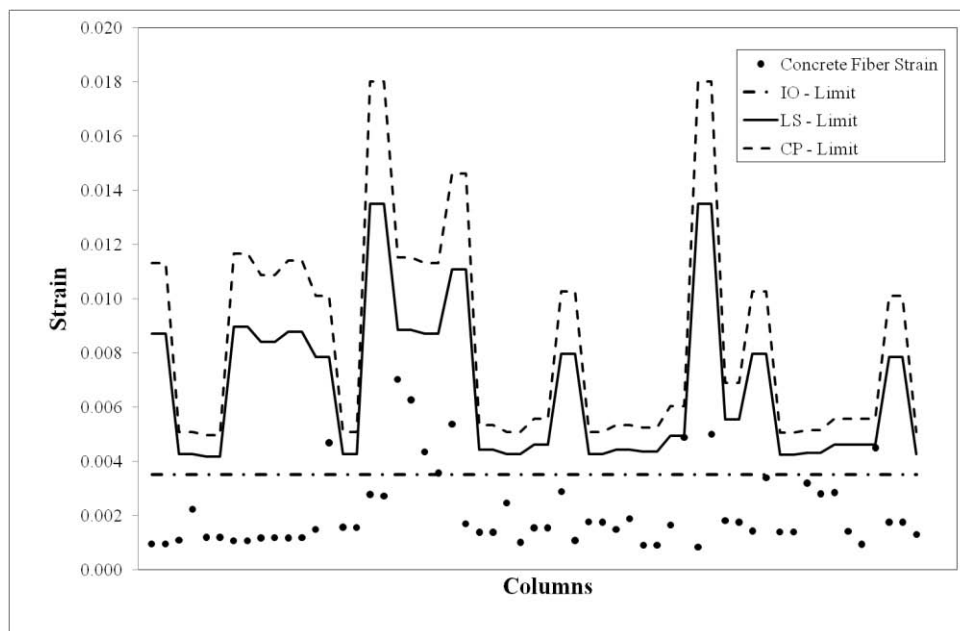


Figure 4.137: Retrofitted Building, Concrete Strains for 3rd storey columns

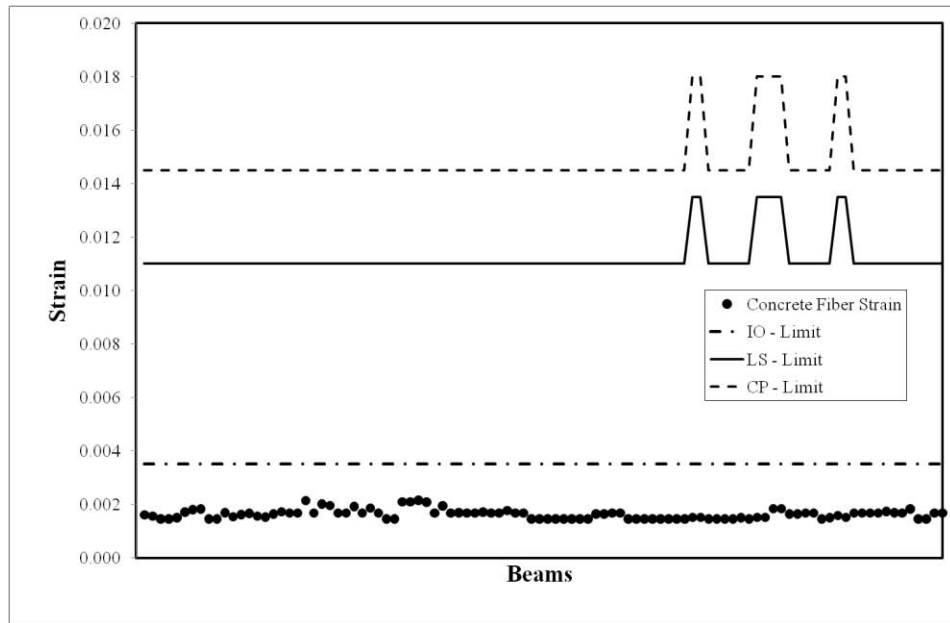


Figure 4.138: Retrofitted Building, Concrete Strains for 3rd storey beams

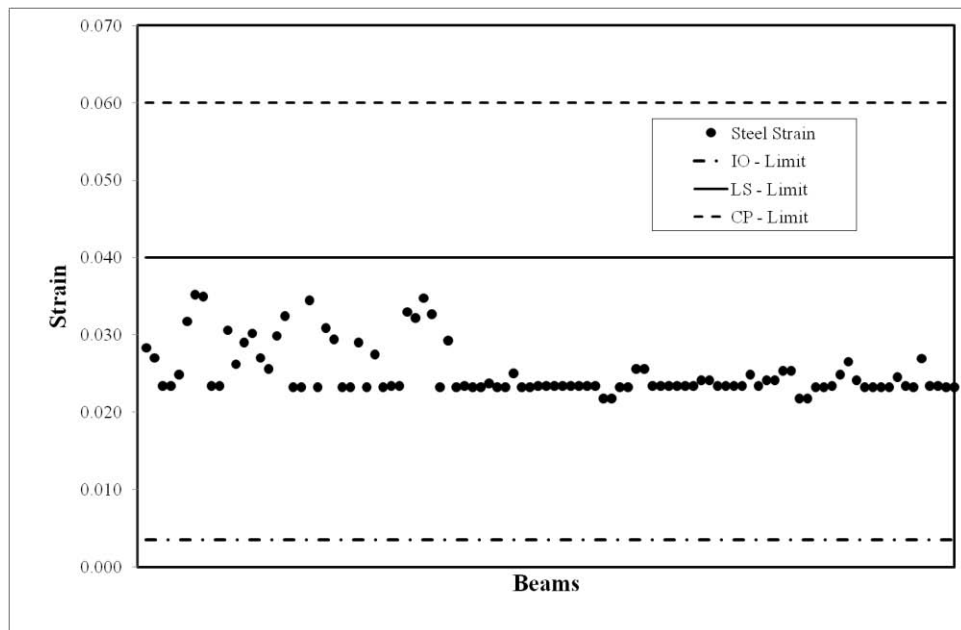


Figure 4.139: Retrofitted Building, Steel Strains for 3rd storey beams

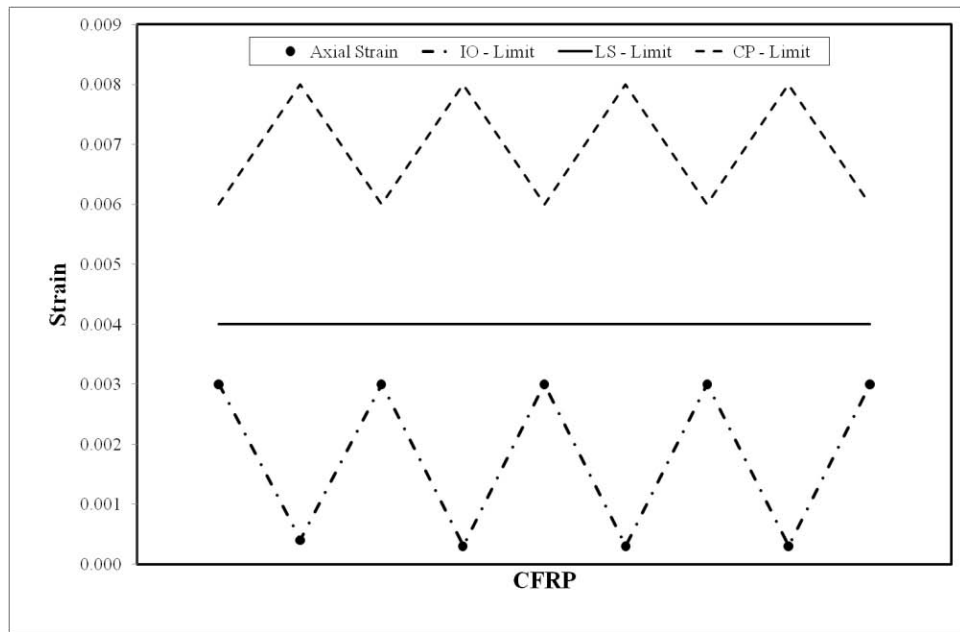


Figure 4.140: Retrofitted Building, Axial Strains for 3rd storey CFRP Walls

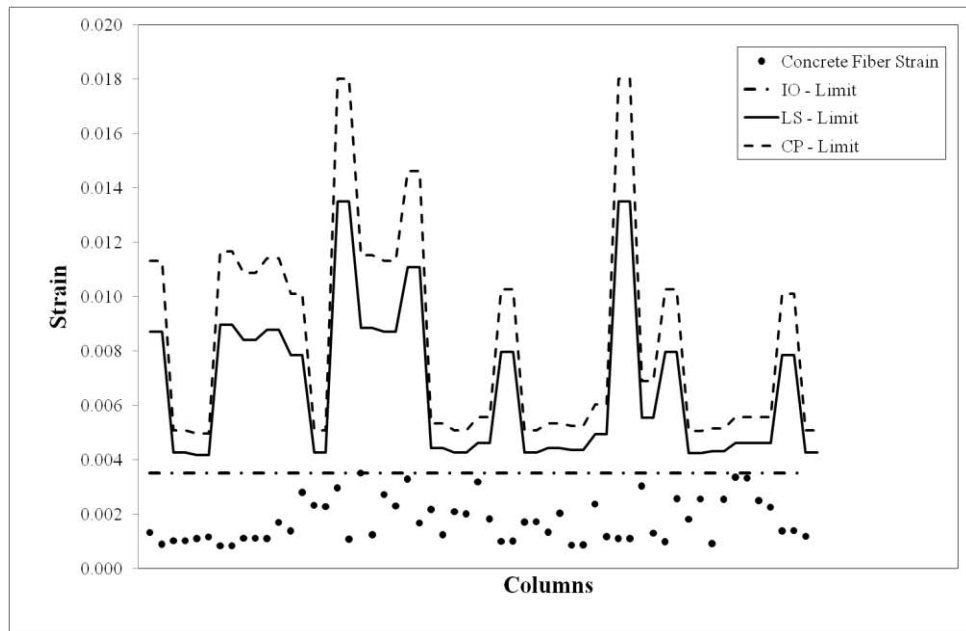


Figure 4.141: Retrofitted Building, Concrete Strains for 4th storey columns

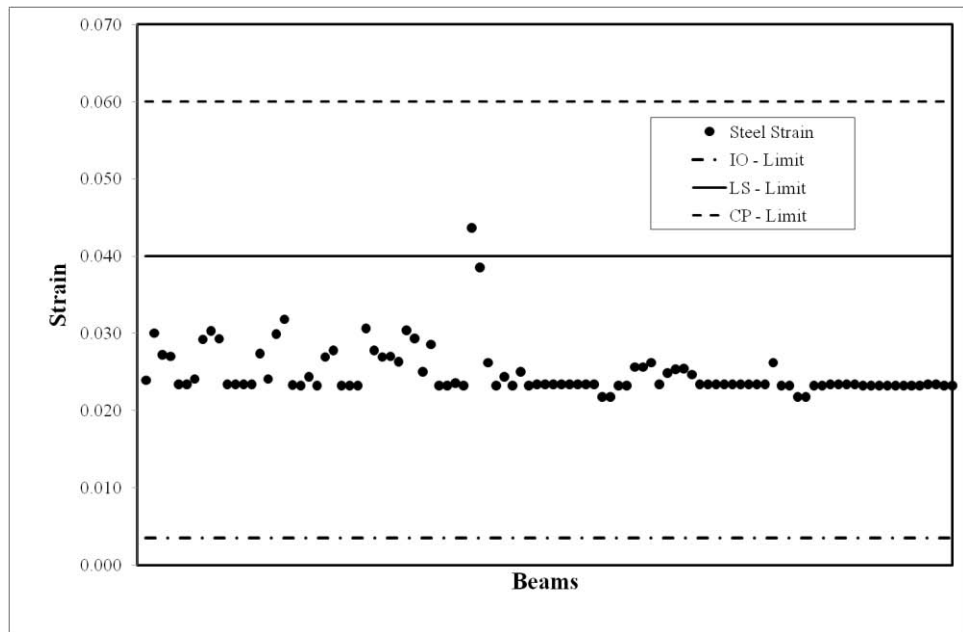


Figure 4.142: Retrofitted Building, Steel Strains for 4th storey beams

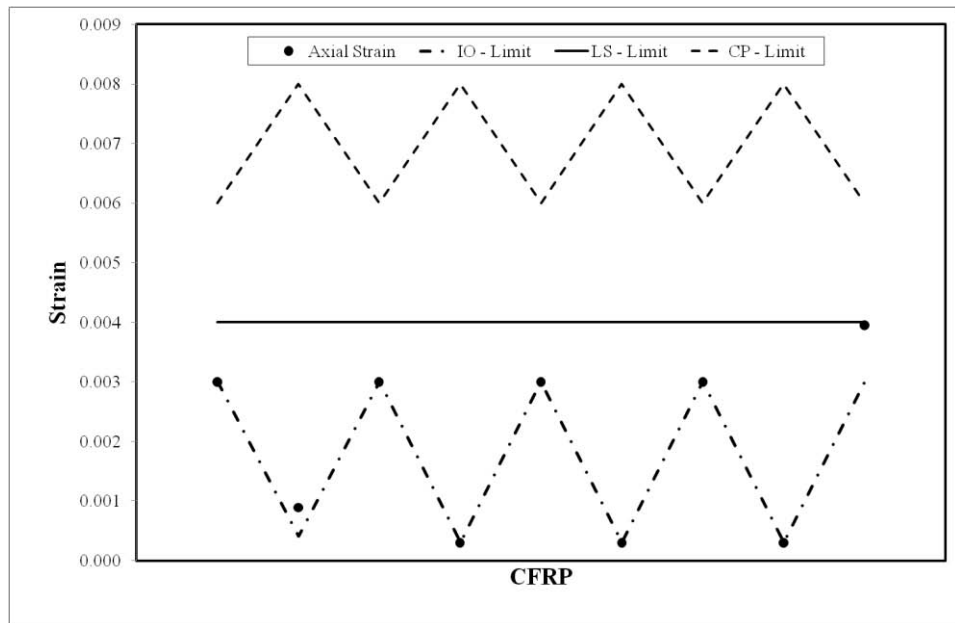


Figure 4.143: Retrofitted Building, Axial Strains for 4th storey CFRP

Walls

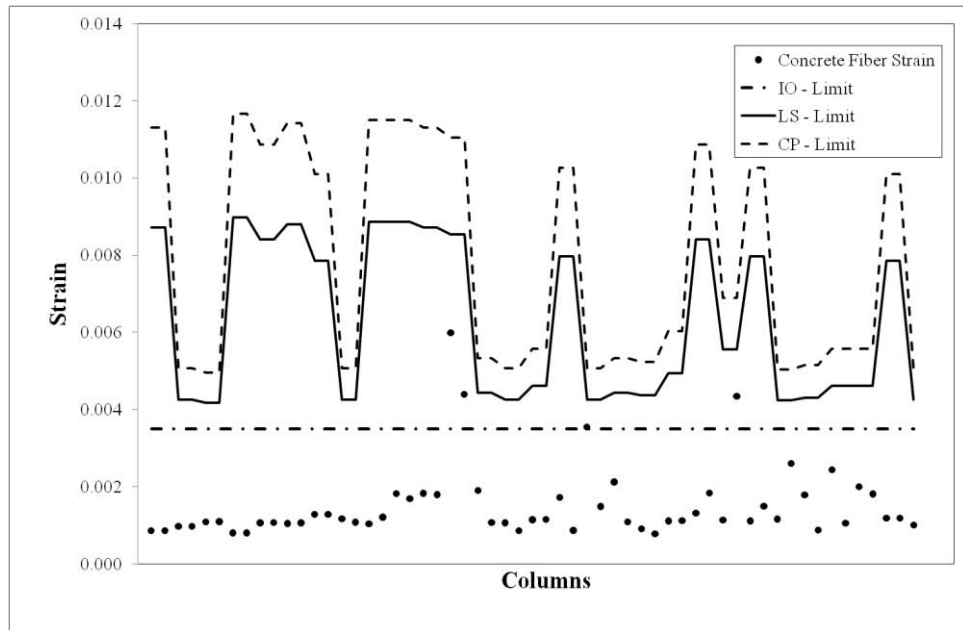


Figure 4.144: Retrofitted Building, Concrete Strains for 5th storey columns

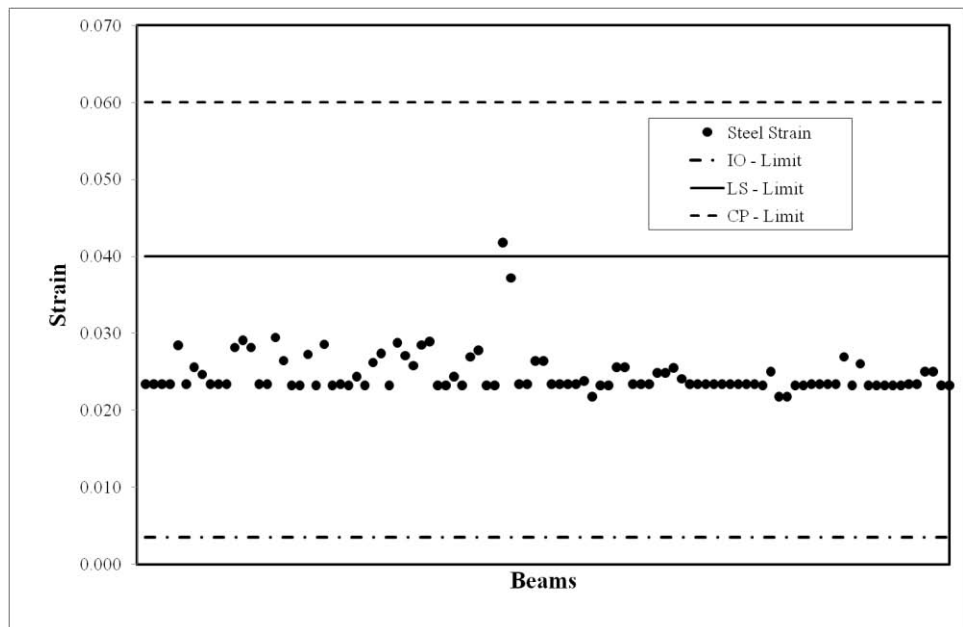


Figure 4.145: Retrofitted Building, Steel Strains for 5th storey beams

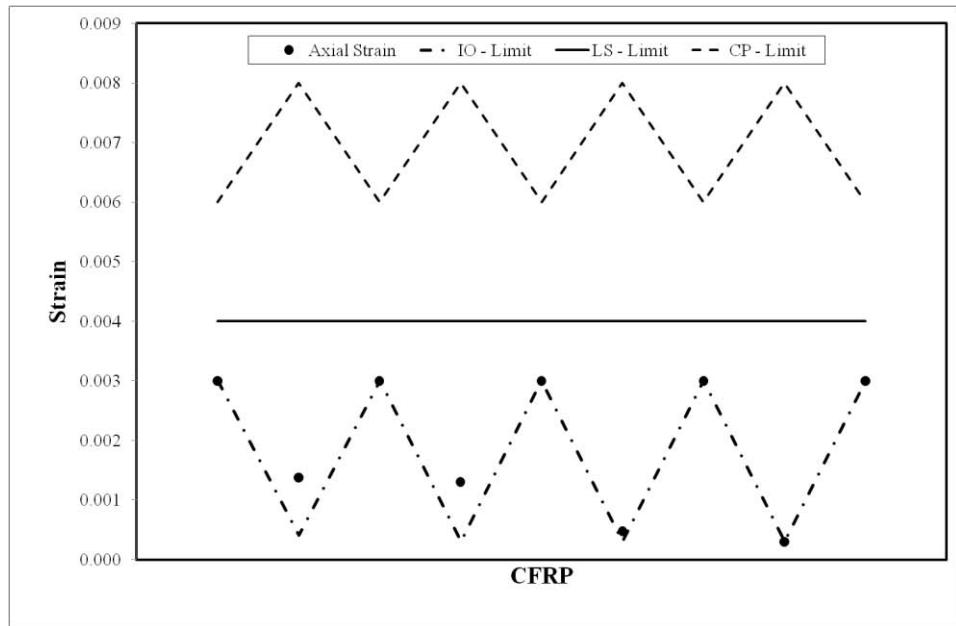


Figure 4.146: Retrofitted Building, Axial Strains for 5th storey CFRP Walls

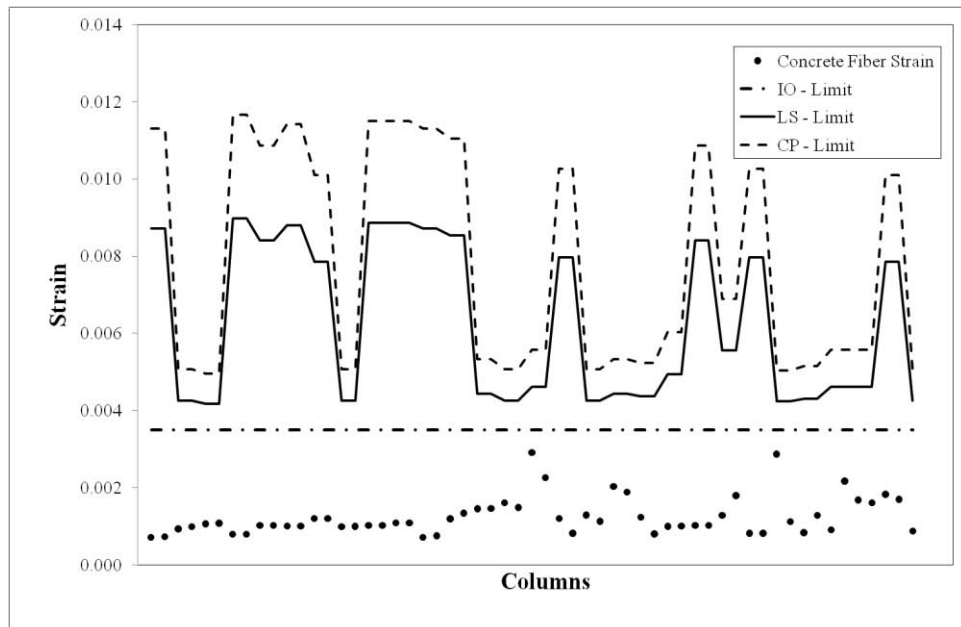


Figure 4.147: Retrofitted Building, Concrete Strains for 6th storey columns

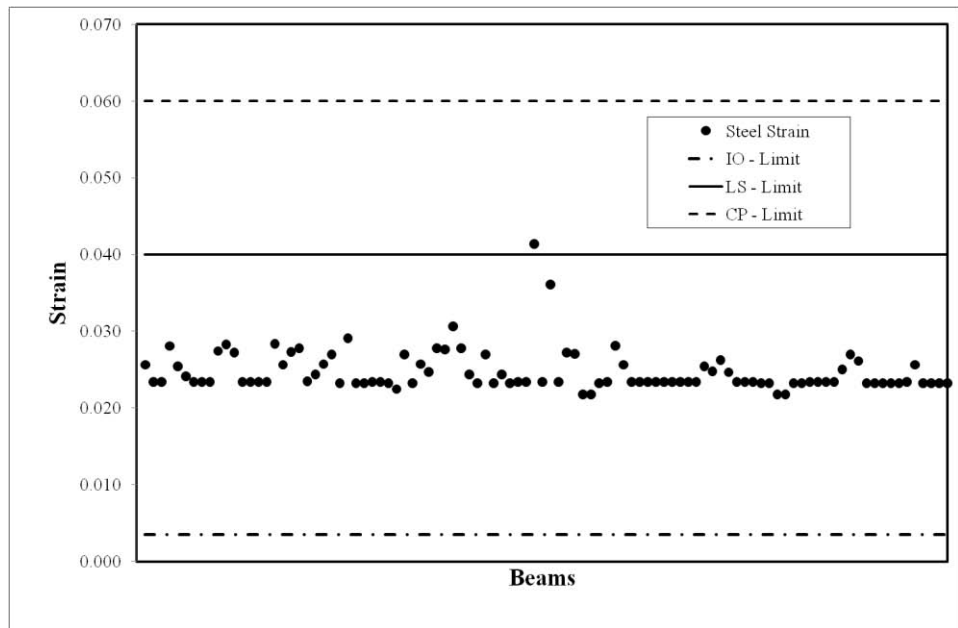


Figure 4.148: Retrofitted Building, Steel Strains for 6th storey beams

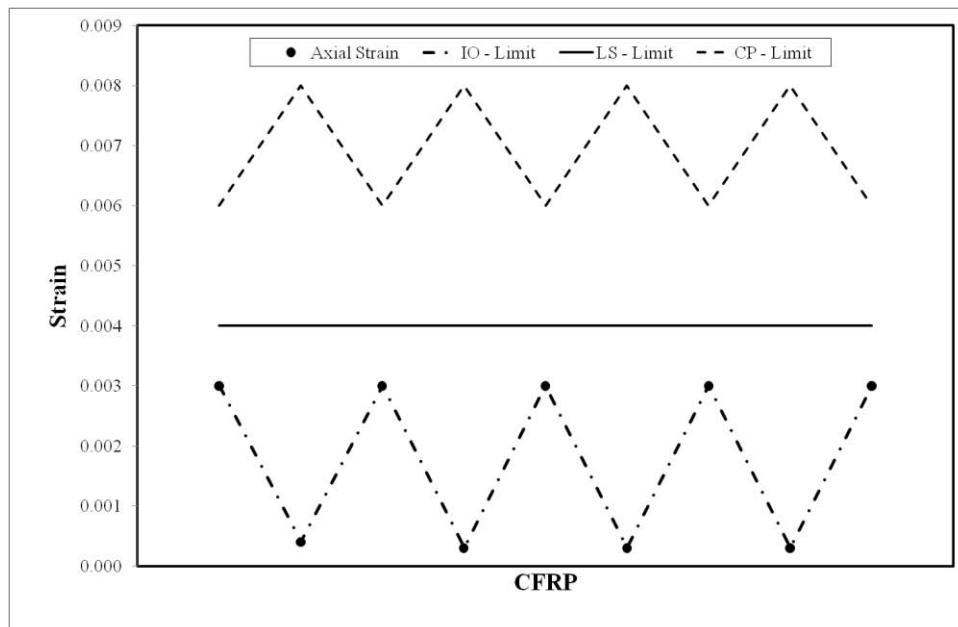


Figure 4.149: Retrofitted Building, Axial Strains for 6th storey CFRP

Walls

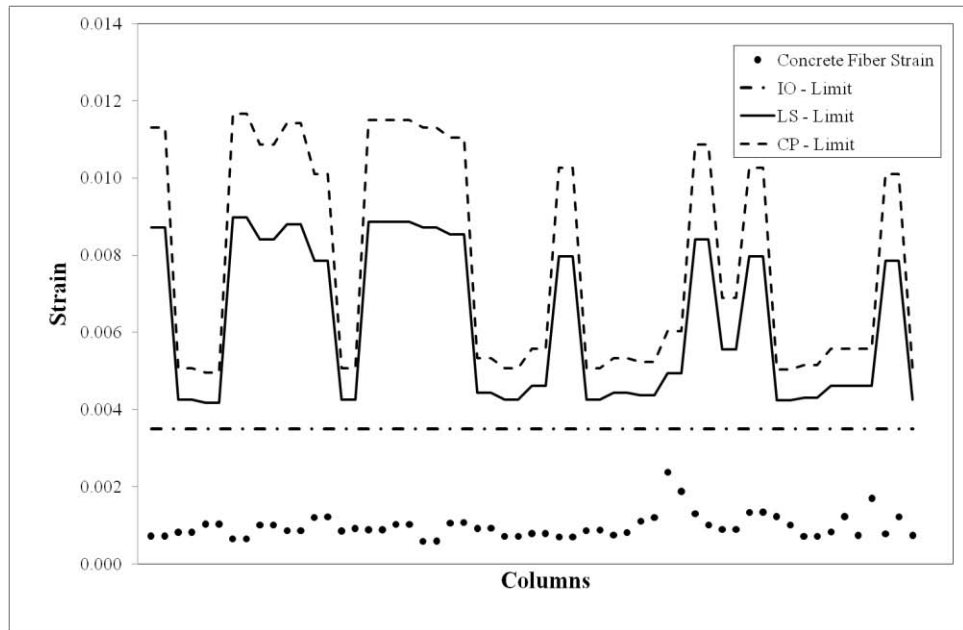


Figure 4.150: Retrofitted Building, Concrete Strains for 7th storey columns

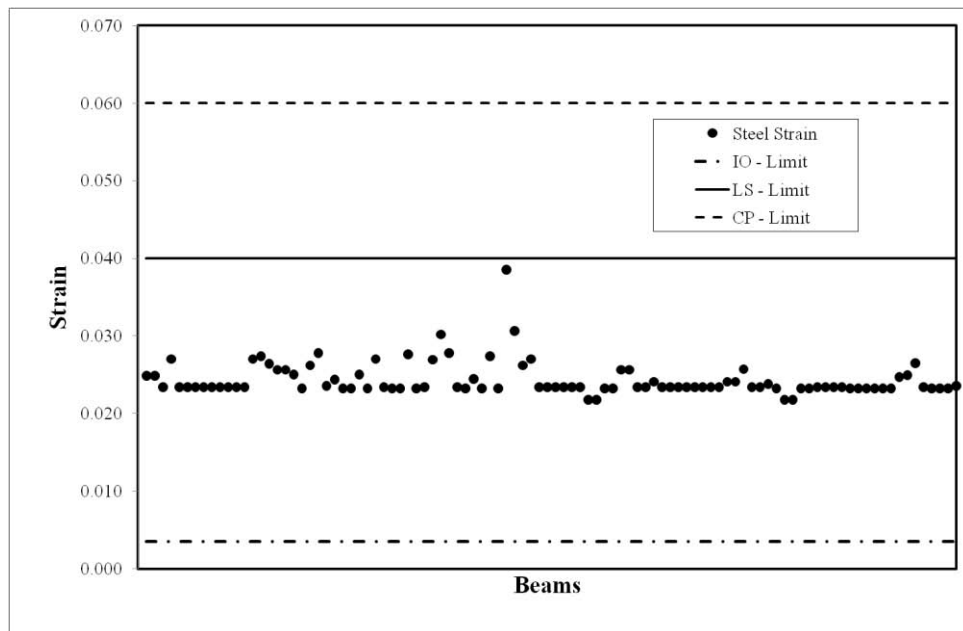


Figure 4.151: Retrofitted Building, Steel Strains for 7th storey beams

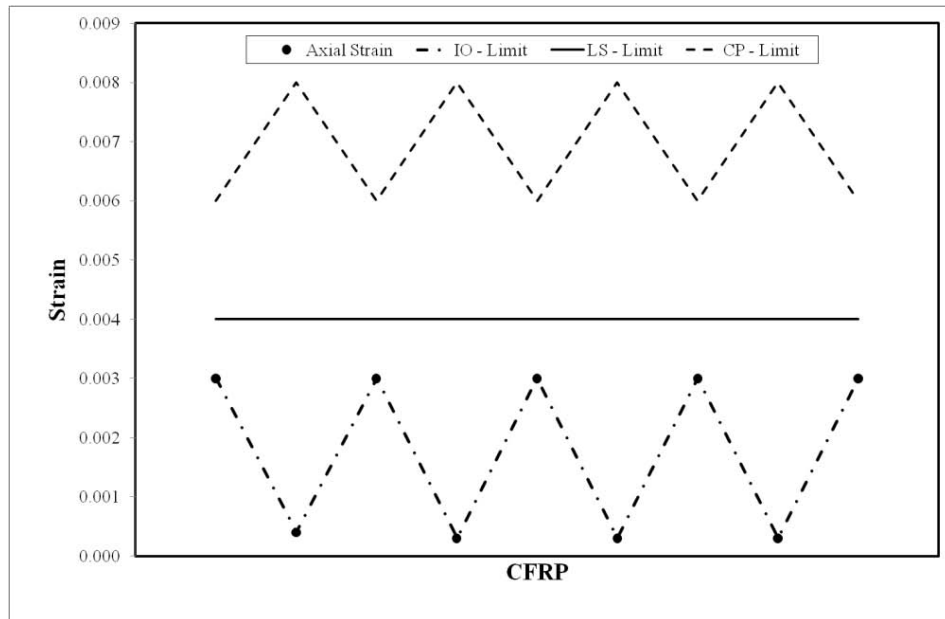


Figure 4.152: Retrofitted Building, Axial Strains for 7th storey CFRP Walls

Drift ratios satisfy the Life safety limit specified in TEC 2007. Also, the 0.0035 limit is satisfied for CFRP walls. Similar to modal pushover analysis, beams are located in the life safety band, rarely passing into collapse prevention region within the acceptable ratios specified in TEC2007.

Although more displacement demand is obtained in basement storey, this storey was held with inplane reinforced concrete shearwalls. CFRP walls start from 1st storey. Compression and tension struts are located in Life Safety and Immediate Occupancy regions. The performance check is performed using the axial strain limits explained in Chapter 3 since nonlinear hinges were used in accordance with Binici et. al. [8]

## CHAPTER 5

### SUMMARY AND CONCLUSION

The study presented here is a practical case that is being applied in real life. TEC 2007 obliges analysis and assessment techniques that will be widely used by design offices in Turkey. This study exemplifies the hybrid retrofitting of a mid-rise building located in EQ zone 1. CFRP strengthened masonry infill walls were used. Study combines the assessment techniques of TEC 2007 and CFRP diagonal strut models. It was seen that CFRP walls were effective in reducing the damage level of vertical load carrying members. Also it helps in situations where evacuation is difficult.

One of the methods used in this study was the “Elastic assessment method with Mode Superposition Analysis”. Demand forces were obtained under the combined effect of vertical and lateral loading. Member capacities under the demand axial loads were obtained and DCR values were calculated for each member failing either in ductile or brittle mode. These DCR values were compared with DCR-limit values specified by TEC 2007. Depending on the target performance level, percentage of members in different damage levels were obtained.

Since a single mode pushover analysis is not applicable for the building at hand, other analysis alternative in TEC2007 was Multi-Mode Pushover (IRSA: Incremental Response Spectrum Analysis) which is very difficult to perform practically. Thus it was held outside the current scope of the study.

Modal Pushover Analysis (MPA) proposed by Chopra [12] was one of the analysis alternatives. Briefly, separate static pushover analyses were performed for each mode loading and demands were found separately. Later on, the response quantities were combined by SRSS. Assumptions and limitations of this method was discussed in the study. As the authors of the method aim and state, it was

observed that the computational easiness was one of the advantages of this method. Retrofitted building at hand satisfied the TEC2007 life safety conditions after this analysis.

To avoid convergence problems and to estimate the drift demands, a simplified nonlinear time history analysis was utilised. Pushover curves for each storey were obtained by separate fixed-storey models. Then in a 2D nonlinear model, a time history analysis was performed to estimate the drift demands in X and Y direction. Although the rotational inertia of the storeys were calculated and input to model, this methods neglects the floor torsion while estimating the demands. However, results and drift demands obtained from this analysis seemed reasonable. One must not forget that, in this analysis, selection of earthquake records is quite important. In order to select an earthquake record that complies with TEC2007 criteria, Fahjan [13] was referred. Results are very dependent on the input accelerograms and the force deformation relationships used.

A comparison of drifts for elastic analysis, modal pushover analysis and time history analysis is given in Figure 5.1 and Figure 5.2.

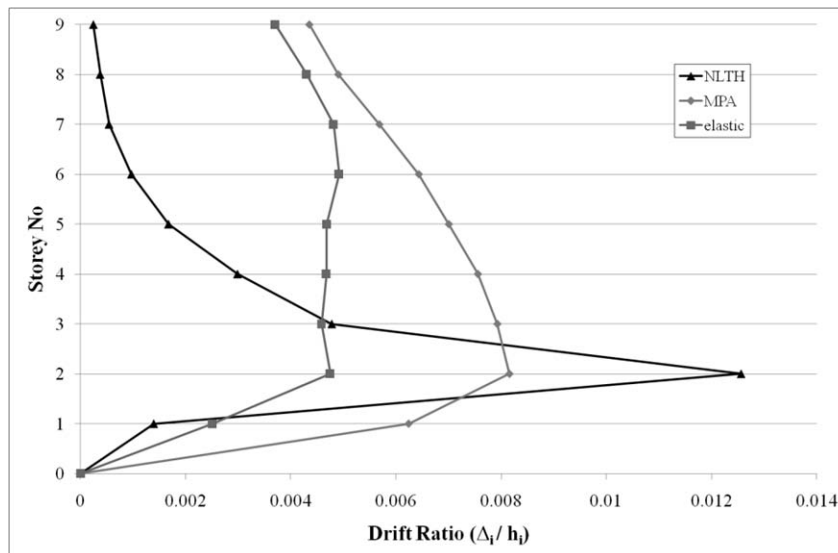


Figure 5.1: Comparison of drift demands for different analysis techniques for existing building.

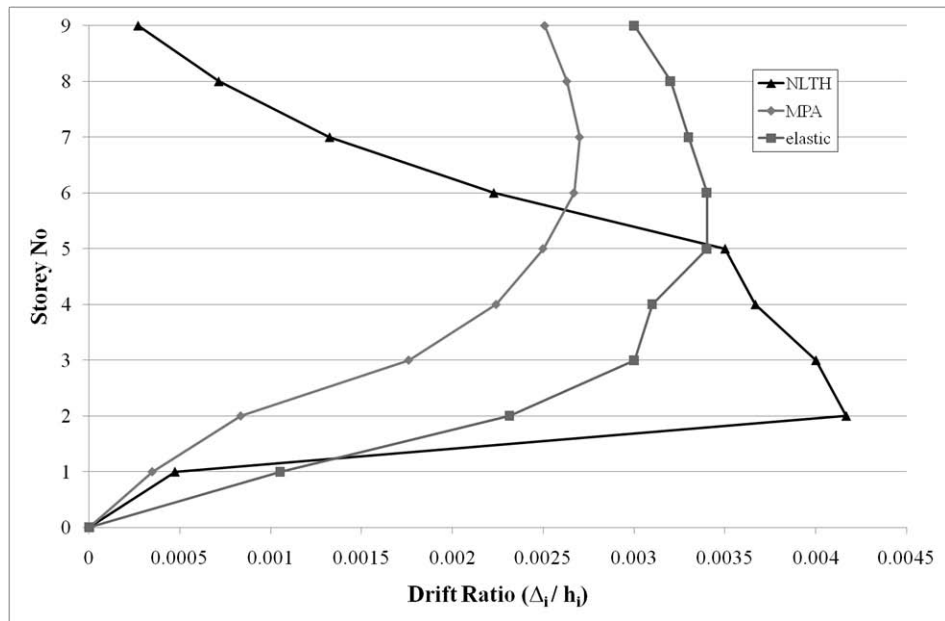


Figure 5.2: Comparison of drift demands for different analysis techniques for retrofitted building.

Elastic drift is less than the other two analysis because of the fact that elastic analysis does not take redistribution into consideration. Formation of plastic hinges obviously will soften the structure yielding a higher drift demand. Time history analysis demands are of envelope type. Ground storey and 1st storey seem to exhibit more drifts than other storeys. Ground storey is higher than the normal storeys. This difference may be due to the simplification process of 3D model into 2D where all demand is consumed by a single DOF (U1) only.

In Figure 5.3, variation of drift ratio with time is given for the critical ground storey for existing and retrofitted structures.

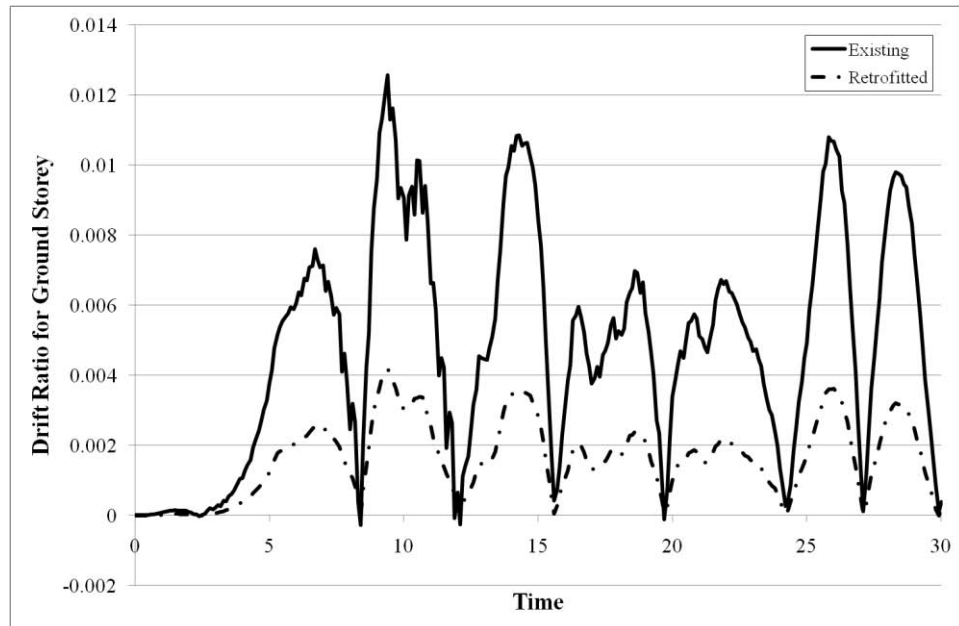


Figure 5.3: Variation of drift ratio of ground storey with respect to time.

A reduction in drift ratio is also observed after retrofitting. It is obvious that, although envelope of 3 earthquakes is considered, results will be dependent on the selected earthquakes and scale factor.

Nonlinear assessment technique in TEC2007 relies on the concrete and steel strains that takes place inside the section at the demand time. This bring additional computations and assumptions when converting back from plastic rotations to curvatures, and then to strains. This obliges very consistent section analysis calculations. The plastic hinge data entered at the beginning must be consistent with the data used during assessment (such as yield curvatures)

CFRP retrofitted masonry infill walls exhibit a favourable behaviour under the life safety level as shown by the results. For nonlinear analyses, axial compression and tension strains were compared with the values provided by Binici et.al [8]. Also, they satisfy the linear elastic assessment conditions. Example shop drawings for CFRP application are supplied in Chapter 3. In this study, CFRP application was thought as an auxiliary helper to reduce drift demands. Hence, a hybrid scheme was promoted.

Project is still being constructed in real life. Some pictures from construction is given in Appendix D.

## REFERENCES

1. Canbay, E., Ersoy, U., and Ozcebe, G., 2003, *Contribution of Reinforced Concrete Infills to Seismic Behavior of Structural Systems*, ACI Structural Journal September-October 2003, Title No. 100-S66
2. Turk, M., Ersoy, U., and Ozcebe, G., *Effect of Adding Reinforced Concrete Infill on Seismic Performance of Damaged Reinforced Concrete Frames*
3. Mehrabi, A.B., Shing, P.B., Schuller, M.P. & Noland, J.L., 1996, *Experimental Evaluation of Masonry-Infilled R/C Frames*, J. Struct. Engrg., ASCE, Vol. 122, pp. 228-237.
4. Negro, P. & Verzeletti, G., July, 1996, *Effect of Infills on the Global Behaviour of R/C Frames: Energy Considerations from Pseudo-synamic Tests*, Earthquake Engineering and Structural Dynamics, Vol. 25, No. 7, pp. 753-773.
5. Proenca, J., Oliviera, C.S., and Almeida, J.P., *Seismic Performance Assessment Of Reinforced Concrete Structures With Masonry Infilled Panels: The Case Of Block # 22 Of The Santa Maria Hospital In Lisbon*, ISET Journal of Earthquake Technology, Vol. 41, No. 2-4, June-December 2004, pp. 233-247.
6. Sayın, B., Yıldızlar, B. and Kaplan, S.A., *The Design Techniques of Infill Walls For Reinforced Concrete Structure Analyses*
7. Ozcebe, G., Binici, B., Ersoy, U., Tankut, T., Ozden, S., Karadogan, F., Yuksel, E., and Ilki, A., *Analysis of Infilled Reinforced Concrete Frames Strengthened with FRPs*
8. Binici, B., Ozcebe, G., *Analysis of Infilled Reinforced Concrete Frames Strengthened with FRPs*

9. Binici, B., Ozcebe, G., and Ozcelik, R., *Analysis and Design of FRPs for Seismic Retrofit of Infill Walls In Reinforced Concrete Frames*
10. Federal Emergency Management Agency (FEMA), 2000, *Prestandard and Commentary for the Seismic Rehabilitation of Buildings*, FEMA-356
11. *Turkish Earthquake Code: Specifications for the Buildings to be Constructed in Disaster Areas*, 2007, Ministry of Public Works and Settlement, Ankara, Turkey
12. Chopra, Anil K., and Goel, Rakesh K., *A Modal Pushover Analysis Procedure to Estimate Seismic Demands for Buildings: Theory and Preliminary Evaluation*, PEER 2001/03
13. Paret T.F., Sasaki K.K., Eilbeck D.H., and Freeman S.A., 1996, *Approximate inelastic procedures to identify failure mechanisms from higher mode effects*. Paper No. 966, Proceedings of 11<sup>th</sup> World Conference on Earthquake Engineering, Acapulco, Mexico.
14. Sasaki K.K., Freeman S.A., and Paret T.F., 1998, *Multi-Mode Ushover Procedure (MMP) – A Method to Identify the Effect Of Higher Modes in a Pushover Analysis*, Proceedings of 6<sup>th</sup> U.S. National Conference on Earthquake Engineering, Seattle, Washington
15. Fahjan, Y. M., *Selection and Scaling of Real Earthquake Accelerograms to Fit the Turkish Design Spectra*, Technical Bulletin of Chamber of Civil Engineering, 2008 4423-4444, Article No 292
16. Aydinoglu, M. Nuray, 2003, *An Incremental Response Spectrum Analysis Procedure Based on Inelastic Spectral Displacements for Multi-Mode Seismic Performance Evaluation*, Bulletin of Earthquake Engineering 1: 3-36
17. Turkish Standarts, TS-500, *Requirements For Design and Construction Of Reinforced Concrete Structures*, 2000

18. Oguz, Sermin, *Evaluation of Pushover Analysis Procedures for Frame Structures*, 2005, p.8, Master Thesis, Department of Civil Engineering, METU, ANKARA
19. Kent, D.C., and Park, R, *Flexural Members with Confined Concrete*, *Journal of the Structural Division*, ASCE, V.97, ST7, July 1971
20. Mander, J.B., Priestley, M.J.N., Park, R., 1988, *Theoretical Stress-Strain Model for Confined Concrete*, *Journal of Structural Division (ASCE)*, 114(8), 1804-1826
21. Priestley, M.J.N., 2003, *Myths and Fallacies in Earthquake Engineering, Revisited: The Malley-Milne Lecture*, Rose School, Collegio, Alessandro Volta, Pavia, Italy
22. Elnashai, A.S., 2002, *Do we really need inelastic dynamic analysis?*, *Journal of Earthquake Engineering* 6, 123-130
23. Antoniou, S., Rovithakis A., Pinho, R., 2002, *Development and Verification of a fully adaptive pushover procedure*, Paper No.822, Proceedings of 12<sup>th</sup> European Conference on Earthquake Engineering, London
24. Sengoz, Ali, 2007, *Quantitative Evaluation of Assessment Methods in the 2007 Turkish Earthquake Code*, Master Thesis, Department of Civil Engineering, METU, ANKARA
25. Altuntop, M.A., 2007, *Analysis of Building Structures with Soft Storeys*, Master Thesis, Department of Civil Engineering, Atılım University, ANKARA
26. Akguzel, Umut, 2003, *Seismic Retrofit Of Brick Infilled R/C Frames with Lap Splice Problem in Columns*, Master Thesis, Department of Civil Engineering, Bogazici University, ISTANBUL

## APPENDIX A

### STRESS-STRAIN DIAGRAM FOR CONCRETE

Moment Curvature calculation requires a concrete model that considers the effect of confinement in the section. In this study, Modified Kent&Park model is used. Model is described below.

Different curves are used for confined and unconfined regions of the section. Kent&Park defines the confined region as the region within the stirrup's outermost fiber.

Stress-strain diagrams shown in Figure A.1 are defined in two parts: parabolic curves and linear portions. They are formulized as follows.

Unconfined Concrete Parabolic Part

$$\sigma_c = f_c \left\{ \frac{2\varepsilon_c}{\varepsilon_{co}} - \left( \frac{\varepsilon_c}{\varepsilon_{co}} \right)^2 \right\} \quad (\text{A.1})$$

Unconfined Concrete Linear Part

$$\sigma_c = f_c (1 - Z_u (\varepsilon_c - \varepsilon_{co})) \quad (\text{A.2})$$

$$Z_u = \frac{0.5}{\varepsilon_{50u} - \varepsilon_{co}} \quad (\text{A.3})$$

$$\varepsilon_{50u} = \frac{3 + 0.285 f_c}{142 f_c - 1000} \geq \varepsilon_{co} \quad (\text{A.4})$$

Confined Concrete Parabolic Part

$$\sigma_c = f_{cc} \left\{ \frac{2\varepsilon_c}{\varepsilon_{coc}} - \left( \frac{\varepsilon_c}{\varepsilon_{coc}} \right)^2 \right\} \quad (\text{A.5})$$

$$\varepsilon_{coc} = \kappa \varepsilon_{co} \quad \kappa = 1 + \frac{\rho_s f_{ywk}}{f_c} \quad (\text{A.6})$$

$$\sigma_c = f_{cc} (1 - Z_u (\varepsilon_c - \varepsilon_{coc})) \geq 0.2 f_{cc} \quad (\text{A.7})$$

$$Z_u = \frac{0.5}{\varepsilon_{50u} + \varepsilon_{50h} - \varepsilon_{coc}} \quad (\text{A.8})$$

$$\varepsilon_{50h} = 0.75 \rho_s \left( \frac{b_k}{s} \right)^{0.5} \quad (\text{A.9})$$

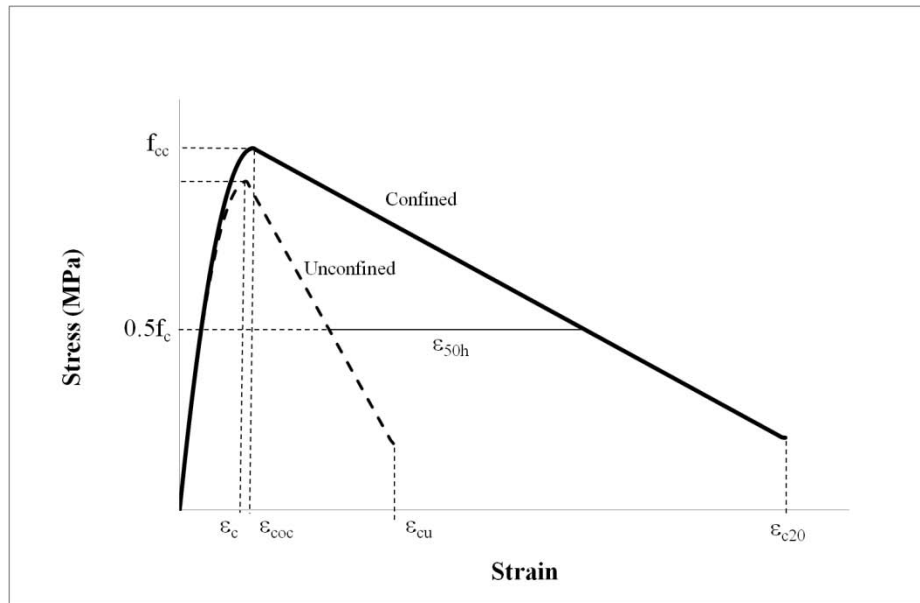


Figure A.1: Stress-Strain Curve

## APPENDIX B

### EXAMPLE CALCULATIONS FOR CFRP COMPRESSION AND TENSION TIES

#### B.1 Calculation of Elastic Properties According to TEC 2007

Summary of example calculation is given in Table B.1.

Table B.1: Example Calculation of Compression Strut and Tension Tie Properties according to TEC 2007

<b>Material</b>			
$f_{ck}$	10	MPa	Compressive strength of Existing Frame Concrete
$f_{wall}$	1	MPa	Compressive strength of infill material
$E_c$	24277.4	MPa	Elasticity modulus for existing frame concrete
$E_{wall}$	1000	MPa	Elasticity Modulus for infill material
<b>Geometry</b>			
$L$	2600	mm	Infill Wall Length
$h_{wall}$	2400	mm	Infill Wall Height
$t_{in}$	250	mm	Infill Wall Thickness
$t_p$	10	mm	Thickness of plaster
$R_{wall}$	3538.361	mm	Diagonal Length of the wall
$\theta$	42.70939	degrees	Inclination Angle of diagonal
$L/h_{wall}$	1.083333		<b>Wall can be retrofitted</b>
<b>Column</b>			
$b_k$	250	mm	
$h_k$	1300	mm	
$I_k$	4.58E+10	mm	

<b>Compression Strut</b>			
$\lambda_{duvar}$	0.000395		
$a_{wall}$	632.7084	mm	Width of compression strut
$t_{wall}$	260	mm	Thickness of compression strut
$k_{wall}$	46491.63	N/mm	Axial rigidity for compression strut
$A_{wall}$	164504.2	mm <sup>2</sup>	Area of compression strut
$P_f$	164.5042	kN	Compression strut capacity
<b>Tension Tie</b>			
$w_f$	650	mm	Width Of CFRP Layer
$t_f$	0.32	mm	Thickness of CFRP Layer
$E_f$	230000	MPa	Elasticity Modulus for CFRP
$A_f$	208	mm <sup>2</sup>	Effective Area of Tension Tie
$k_f$	13520.38	N/mm	Axial rigidity of Tension Tie
$T_f$	143.52	kN	Tensile Capacity of Tension Tie
$V_f$	105.459	kN	Shear Capacity

$$\lambda_{wall} = \left[ \frac{E_{wall} t_{wall} \sin 2\theta}{4E_c I_k h_{wall}} \right]^{\frac{1}{4}} = \left[ \frac{1000 \times 260 \times \sin(85.4)}{4 \times 24277 \times 4.58 \times 10^{10} \times 2400} \right]^{0.25}$$

$$= 0.000395$$

$$a_{wall} = 0.175 (\lambda_{wall} h_k)^{-0.4} r_{wall}$$

$$= 0.175 \times (0.000395 \times 1300)^{-0.4} \times 3538 = 632.7 \text{ mm}$$

$$k_{wall} = \frac{a_{wall} t_{wall} E_{wall}}{r_{wall}} = \frac{632.7 \times 260 \times 1000}{3538} = 46491 \text{ N/mm}$$

$$A_{wall} = a_{wall} t_{wall} = 632.7 \times 260 = 164504 \text{ mm}^2$$

$$P_f = A_{wall} f_{wall} = \frac{164504 \times 1}{1000} = 164.504 \text{ kN}$$

For the tension tie properties,  $w_f$  is chosen not to be smaller than  $a_{wall}$  that is calculated for compression strut. Hence,  $w_f = 650$  mm.

Thickness of a single layer CFRP is 0.16 mm. There are total of 2 layers, one on each side, thus total CFRP thickness,  $t_f = 0.32$  mm

Elasticity Modulus of CFRP material is  $E_f = 230000$  MPa.

Effective Area of Tension Tie,

$$A_f = w_f t_f = 650 \times 0.32 = 208 \text{ mm}^2$$

Axial Stiffness of Tension Tie,

$$k_f = \frac{A_f E_f}{r_{wall}} = \frac{208 \times 230000}{3538} = 13520 \text{ N/mm}$$

Tension Capacity of CFRP Tie,

$$T_f = 0.003 E_f w_f t_f = \frac{0.003 \times 230000 \times 650 \times 208}{1000} = 143.52 \text{ kN}$$

Shear capacity is the horizontal component of diagonal tension capacity

$$V_f = \frac{T_f L_{wall}}{r_{wall}} = \frac{143.52 \times 2600}{3538} = 105.429 \text{ kN}$$

## **B.2 Calculation of Nonlinear Hinge Properties Using Simplified Model**

### **B.2.1 Tension Tie**

Simplified design models for compression and tension ties were given in Figure 3.3. From previous calculations we know that;

Area of the tension tie,  $A_f = 208 \text{ mm}^2$

Ultimate tension stress of the nonlinear tension hinge,

$$\sigma_f = 0.003E_f = 0.003 \times 230000 = 690 \text{ MPa}$$

$$T_f = A_f \sigma_f = 690 \times 208 \times 10^{-3} = 143.52 \text{ kN}$$

Strain Limits as specified by the simplified model are;

$$\text{IO: } 0.003 \quad , \quad \text{LS: } 0.004 \quad , \quad \text{CP : } 0.006$$

Converting these strain limits into displacement, diagonal displacement limits can be obtained as follows,

$$d_{\text{IO}} = 0.003 R_{\text{wall}} = 0.003 \times 3538.61 = 10.61 \text{ mm}$$

$$d_{\text{LS}} = 0.004 R_{\text{wall}} = 0.004 \times 3538.61 = 14.15 \text{ mm}$$

$$d_{\text{CP}} = 0.006 R_{\text{wall}} = 0.006 \times 3538.61 = 21.23 \text{ mm}$$

## B.2.2 Compression Strut

Material properties of composite infill material,

$$f_{mc} = \frac{f_{in}t_{in} + f_m t_p}{t_{st}} = \frac{1 \times 250 + 1 \times 10}{260} = 1 \text{ MPa}$$

$$E_{sm} = \frac{E_{in}t_{in} + E_m t_p}{t_{st}} = \frac{1000 \times 250 + 1000 \times 10}{260} = 1000 \text{ MPa}$$

Properties of composite strut,

$$\alpha = \sqrt{\frac{2(M_{pj} + 0.2M_{pc})}{h^2 t_{st} f_{mc}}} = \sqrt{\frac{2(50000000 + 0.2 \times 150000000)}{2400^2 \times 260 \times 1}} = 0.327$$

$$w_s = \frac{(1 - \alpha)\alpha h}{\cos \theta} = \frac{(1 - 0.327) \times 0.327 \times 2400}{0.73} = 720 \text{ mm}$$

$$A_{st} = w_s t_{st} = 720 \times 260 = 186845 \text{ mm}^2$$

Sliding failure capacity,

$$V_{ss} = f_{mv} L t_{st} = 0.2 \times 2600 \times 260 = 135 \text{ kN}$$

Corner crushing failure,

$$V_{cc} = 250 t_{st} f_{mc} = 250 \times 260 \times 1 = 65 \text{ kN}$$

Ultimate capacity for composite strut,

$$V_{us} = \min(V_{ss}, V_{cc}) = 65 \text{ kN}$$

Ultimate Strength,

$$f_{us} = \frac{V_{us}}{A_{st}} = \frac{65000}{186845} = 0.3 \text{ MPa}$$

$$\varepsilon_{crs} = \frac{f_{us}}{E_{sm}} = \frac{0.3}{1000} = 0.0003$$

$$\varepsilon_{so} = 2 \cdot \varepsilon_{f,eff} = 2 \times 0.004 = 0.008$$

Where  $\varepsilon_{f,eff}$  is the strain at which FRP anchors fail or debonding occurs

Converting the stress and strain values to force and displacement units for compression strut,

$$d_{crs} = \varepsilon_{crs} \cdot R_{wall} = 0.0003 \times 3538.61 = 1.061 \text{ mm}$$

$$d_{so} = \varepsilon_{so} R_{wall} = 0.008 \times 3538.61 = 28.30 \text{ mm}$$

## APPENDIX C

### QUANTITY TAKE-OFF FOR CFRP

Estimated FRP usage is approximately 812 m<sup>2</sup> for the layout presented in section 4.4.3. Details of FRP quantity take-off is given in Tables C.1 to C.5

Table C.1: Quantity Take-off: CFRP strengthened wall D1X

<b>D1X</b>	wall thick. (mm)	anc. Depth (mm)	Anchor Width (mm)							
	260	150	100							
Storey	Diagonal Length (mm)	FRP Width (mm)	# Layer	Area (m <sup>2</sup> )	Anchor. Plate Area (m <sup>2</sup> )	# Anchor. Per Plate	# Anchor. Diagonal	Plate Anchor. Depth (mm)	Surface Anchor. Length (mm)	Anc. Area (m <sup>2</sup> )
1	4579.30	800.00	2	14.65	11.52	6	14	200.00	360.00	0.62
2	4579.30	800.00	2	14.65	11.52	6	14	200.00	360.00	0.62
3	4579.30	800.00	2	14.65	11.52	6	14	200.00	360.00	0.62
4	4579.30	800.00	2	14.65	11.52	6	14	200.00	360.00	0.62
5	4579.30	800.00	2	14.65	11.52	6	14	200.00	360.00	0.62
6	4579.30	800.00	2	14.65	11.52	6	14	200.00	360.00	0.62
7	4579.30	800.00	2	14.65	11.52	6	14	200.00	360.00	0.62
				102.58	80.64					4.368
<b>Total</b>	<b>187.58</b>	m <sup>2</sup>								

Table C.2: Quantity Take-off: CFRP strengthened wall D2X

<b>D2X</b>	wall thick. (mm)	anc. Depth (mm)	Anchor Width (mm)							
	110	150	100							
Storey	Diagonal Length (mm)	FRP Width (mm)	# Layer	Area (m <sup>2</sup> )	Anchor. Plate Area (m <sup>2</sup> )	# Anchor. Per Plate	# Anchor. Diagonal	Plate Anchor. Depth (mm)	Surface Anchor. Length (mm)	Anc. Area (m <sup>2</sup> )
1	3465.54	600.00	2	8.32	6.48	6	10	200.00	210.00	0.33
2	3465.54	600.00	2	8.32	6.48	6	10	200.00	210.00	0.33
3	3465.54	600.00	2	8.32	6.48	6	10	200.00	210.00	0.33
4	3465.54	600.00	2	8.32	6.48	6	10	200.00	210.00	0.33
5	3465.54	600.00	2	8.32	6.48	6	10	200.00	210.00	0.33
6	3465.54	600.00	2	8.32	6.48	6	10	200.00	210.00	0.33
7	3465.54	600.00	2	8.32	6.48	6	10	200.00	210.00	0.33
				58.22	45.36					2.31
<b>Total</b>	<b>105.89</b>	m <sup>2</sup>								

Table C.3: Quantity Take-off: CFRP strengthened wall D3X

<b>D3X</b>	wall thick. (mm)	anc. Depth (mm)	Anchor Width (mm)							
	110	150	100							
Storey	Diagonal Length (mm)	FRP Width (mm)	# Layer	Area (m <sup>2</sup> )	Anchor. Plate Area (m <sup>2</sup> )	# Anchor. Per Plate	# Anchor. Diagonal	Plate Anchor. Depth (mm)	Surface Anchor. Length (mm)	Anc. Area (m <sup>2</sup> )
1	2970.27	600.00	2	7.13	6.48	6	8	200.00	210.00	0.29
2	2970.27	600.00	2	7.13	6.48	6	8	200.00	210.00	0.29
3	2970.27	600.00	2	7.13	6.48	6	8	200.00	210.00	0.29
4	2970.27	600.00	2	7.13	6.48	6	8	200.00	210.00	0.29
5	2970.27	600.00	2	7.13	6.48	6	8	200.00	210.00	0.29
6	2970.27	600.00	2	7.13	6.48	6	8	200.00	210.00	0.29
7	2970.27	600.00	2	7.13	6.48	6	8	200.00	210.00	0.29
				49.90	45.36					2.016
<b>Total</b>	<b>97.28</b>	m <sup>2</sup>								

Table C.4: Quantity Take-off: CFRP strengthened wall D1Y

<b>D1Y</b>	wall thick. (mm)	anc. Depth (mm)	Anchor Width (mm)							
	110	150	100							
Storey	Diagonal Length (mm)	FRP Width (mm)	# Layer	Area (m <sup>2</sup> )	Anchor. Plate Area (m <sup>2</sup> )	# Anchor. Per Plate	# Anchor. Diagonal	Plate Anchor. Depth (mm)	Surface Anchor. Length (mm)	Anc. Area (m <sup>2</sup> )
1	3451.14	500.00	2	6.90	4.50	6	10	200.00	210.00	0.33
2	3451.14	500.00	2	6.90	4.50	6	10	200.00	210.00	0.33
3	3451.14	500.00	2	6.90	4.50	6	10	200.00	210.00	0.33
4	3451.14	500.00	2	6.90	4.50	6	10	200.00	210.00	0.33
5	3451.14	500.00	2	6.90	4.50	6	10	200.00	210.00	0.33
6	3451.14	500.00	2	6.90	4.50	6	10	200.00	210.00	0.33
7	3451.14	500.00	2	6.90	4.50	6	10	200.00	210.00	0.33
				48.32	31.5					2.31
<b>Total</b>	<b>82.13</b>	m <sup>2</sup>								

Table C.5: Quantity Take-off: CFRP strengthened wall D2Y

<b>D2Y</b>	wall thick. (mm)	anc. Depth (mm)	Anchor Width (mm)							
	110	150	100							
Storey	Diagonal Length (mm)	FRP Width (mm)	# Layer	Area (m <sup>2</sup> )	Anchor. Plate Area (m <sup>2</sup> )	# Anchor. Per Plate	# Anchor. Diagonal	Plate Anchor. Depth (mm)	Surface Anchor. Length (mm)	Anc. Area (m <sup>2</sup> )
1	3904.66	800.00	4	24.99	23.04	6	12	200.00	210.00	0.37
2	3904.66	800.00	4	24.99	23.04	6	12	200.00	210.00	0.37
3	3904.66	800.00	4	24.99	23.04	6	12	200.00	210.00	0.37
4	3904.66	800.00	4	24.99	23.04	6	12	200.00	210.00	0.37
5	3904.66	800.00	4	24.99	23.04	6	12	200.00	210.00	0.37
6	3904.66	800.00	4	24.99	23.04	6	12	200.00	210.00	0.37
7	3904.66	800.00	4	24.99	23.04	6	12	200.00	210.00	0.37
				174.93	161.28					2.604
<b>Total</b>	<b>338.81</b>	m <sup>2</sup>								

## APPENDIX D

### PHOTOGRAPHS

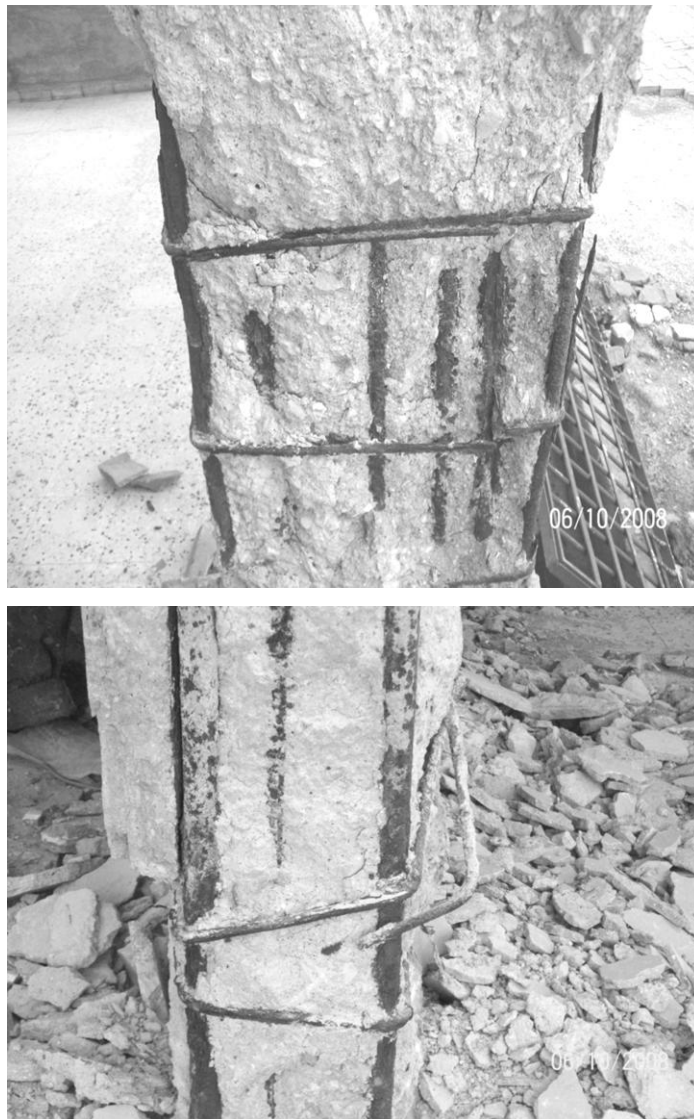


Figure D.1: Corroded reinforcements inside the ground storey column.

As shown in the picture, heavy corrosion is present in basement and ground storey columns. Regarding detailing, it can be seen that no 135 degrees hooks were used in column stirrups. Also no confinement region is present in support regions.

Corrosion damage needed an immediate repair action. Hence, all basement and ground storey columns were repaired against corrosion with special chemicals. After repair, all columns were wrapped with CFRP sheets. A repaired column is shown in Figure D.2.



Figure D.2: Column repaired against corrosion.



Figure D.3: CFRP Application on the masonry infill wall..



Figure D.4: Foundation excavation for eccentric reinforced concrete shearwalls



Figure D.5: Production of eccentric reinforced concrete shearwalls.



Figure D.6: Production of eccentric reinforced concrete shearwalls.



Figure D.7: Production of eccentric reinforced concrete shearwalls.